THE ROLE OF CYTOPLASMIC CHAPERONES IN THE BIOGENESIS, MATURATION, AND DEGRADATION OF CYTOPLASMIC AND INTEGRAL MEMBRANE PROTEINS

by

Annette Ahner

Doctor's License to Practice as Veterinarian, Justus-Liebig Universität, Gießen, Germany 1996

Submitted to the Graduate Faculty of

Arts and Sciences in partial fulfillment

of the requirements for the degree of

Doctor of Philosophy

University of Pittsburgh

2005

UNIVERSITY OF PITTSBURGH

FACULTY OF ARTS AND SCIENCES

This dissertation was presented

by

Annette Ahner

It was defended on

06.03.05

and approved by

Karen M. Arndt

Roger W. Hendrix

Jeffrey G. Lawrence

Martin C. Schmidt

Jeffrey L. Brodsky
Dissertation Director

THE ROLE OF CYTOPLASMIC CHAPERONES IN THE BIOGENESIS, MATURATION, AND DEGRADATION OF CYTOPLASMIC AND INTEGRAL MEMBRANE PROTEINS

Annette Ahner, PhD

University of Pittsburgh, 2005

I have characterized chaperone requirements for the biogenesis, maturation, and degradation of a cytosolic substrate, firefly luciferase (FFLux), in yeast, and of an integral membrane protein, cystic fibrosis transmembrane conductance regulator (CFTR), in yeast and in mammals.

It was previously demonstrated that the cytoplasmic Hsp40, Ydj1p, is required for efficient expression of FFLux in yeast. This raised the question whether two Ydj1p-interacting molecular chaperones, the yeast Hsp70, Ssa1p, and the yeast Hsp90, Hsp82, also impact FFLux expression. The possible influence of a nucleotide exchange factor for Ssa1p, Fes1p, was also investigated. I found that the chaperone requirements for FFLux biogenesis are distinct but overlapping. Whereas Ssa1p and Fes1p likely collaborate to fold FFLux, Ssa1p, independent of its nucleotide exchange factor, was necessary for stabilizing FFLux protein and message, and for efficient induction of FFLux mRNA. Therefore, Fes1p impacts only a subset of Ssa1p's actions. Although FFLux folding progresses independent of Hsp82, efficient expression of FFLux depends on Hsp82, mainly due to Hsp82's contribution to FFLux translation.

To identify the complete spectrum of chaperones that affect ER associated degradation (ERAD) of CFTR, I took a genomic approach in yeast. Transcriptional profiles between yeast expressing CFTR and control strains were examined by microarray analysis. Among the genes up-regulated in strains expressing CFTR was one encoding a small heat shock protein (sHsp), *HSP26*. Therefore, I investigated CFTR degradation in yeast strains lacking *HSP26* and found that the protein was stabilized; stabilization was enhanced in a strain lacking both *HSP26* and another sHsp-encoding gene, *HSP42*. In contrast, degradation of a soluble ERAD substrate and of another transmembrane protein proceeded with equal efficiency in wild type and in *hsp26hsp42* mutant yeast. Next, I examined whether sHsps regulate CFTR biogenesis in mammalian cells. I found that ΔF508-CFTR degradation was enhanced when αA-crystallin was over-expressed in HEK293 cells, although wild type CFTR biogenesis was unaffected. To examine why this sHsp accelerated degradation of ΔF508-CFTR, αA-crystallin was purified and I found that it was able to suppress aggregation of CFTR's first nucleotide binding domain. Together, these results suggest that sHsps increase ΔF508-CFTR's accessibility during proteasome-mediated degradation.

TABLE OF CONTENTS

LIST OF TABLES

LIST OF FIGURES

PREFACE

FOR MY PARENTS

I can’t express enough gratitude to my advisor, Dr. Jeff Brodsky, who let a veterinarian join his lab and turned her into a scientist. He served as an excellent mentor in every aspect of graduate school and was the perfect role model. I am grateful for all the guidance, motivation, and support, his constant availability, and care. I feel truly fortunate to have had such an outstanding scientist and friend as an advisor.

I also wish to thank all of the past and present members of the Brodsky laboratory for creating a fruitful and supportive working environment and for their friendship. Especially, I would like to thank Fadra White who performed the FFLux expression experiments in the *FES1* wild type and *fes1* deletion strain at 26°C (data not shown), and established the FFLux expression conditions for the *HSP82* wild type and *hsp82* mutant strains, Robert Youker for providing the purified NBD1, many exciting scientific discussions, and his friendship, Doug Placais who is starting to characterize a candidate from the microarray analysis, Robert Lee for helpful discussions, common night shifts, and his friendship. I owe many thanks to Jennifer Goeckeler who did not only get me started in the lab but was a constant source of inspiration and of helpful scientific discussions and a great friend.

I would also like to thank my dissertation committee, Drs. Karen Arndt, Roger Hendrix, Jeffrey Lawrence, and Martin Schmidt for their guidance and support throughout my graduate studies.

Additionally, thanks are owed to Tom Harper for his assistance in the preparation of posters and Cathy Barr for ensuring that all the deadlines and requirements were met for the graduate program as well as to maintain a legal status as international student.

I would also like to extend a sincere thank you to Dr. Raymond Frizzell for allowing me to conduct part of my research in his laboratory and Hui Zhang in his lab for introducing me to

the work with mammalian cell culture. I thank all the members of the Frizzell lab for their support and helpful discussions.

I also wish to thank all the members of the Arndt laboratory for advice and helpful discussion.

Finally, I owe a large debt of gratitude to my family, especially to my parents, for their enduring love, care, and support throughout my life and to my husband, Joachim Ahner, without whom I would not have undertaken this endeavor. His infinite love, support, and encouragement carried me through this venture.

1. INTRODUCTION

1.1. SECRETORY PATHWAY

Based on sequence analyses of eukaryotic genomes an estimated ~20% of all proteins reside in or traverse the secretory pathway (Lander *et al.*, 2001). The first committed step in this pathway is the translocation of newly synthesized polypeptides into the endoplasmic reticulum (ER). Protein import proceeds mainly co-translationally in mammals, but in yeast, it may occur co- or post-translationally. During co-translational translocation, the signal recognition particle (SRP) interacts with the signal peptide once it emerges from the ribosome. This process attenuates translation and the ribosome-polypeptide-SRP complex interacts with the SRP receptor at the ER-membrane. GTP-binding and hydrolysis liberate SRP, translation resumes and the polypeptide is released to the translocation machinery at the ER membrane (Johnson and van Waes, 1999; Keenan *et al.*, 2001; Luirink and Sinning, 2004). During post-translational translocation, the polypeptide is completely synthesized and discharged from the ribosome before associating with the translocation machinery at the ER (Rapoport *et al.*, 1999) and a key component of this machinery is the Sec61p translocation channel (Romisch, 1999). In both cases, Hsp70s and their co-factors are required for successful protein import in yeast (Chirico *et al.*,

1988; Deshaies *et al.*, 1988; Caplan *et al.*, 1992; Sanders *et al.*, 1992; Brodsky *et al.*, 1995; McClellan *et al.*, 1998; McClellan and Brodsky, 2000; Fewell *et al.*, 2001).

After folding in the ER and passing ER quality control (see below), secreted proteins are selectively incorporated into budding transport vesicles. These vesicles, which are coated with the COPII protein complex, collect the selected cargo from the ER and migrate to the ER-Golgi intermediate compartment or the Golgi complex (Barlowe *et al.*, 1994; Bonifacino and Glick, 2004). In contrast, retrograde transport back to the ER, which may be required to retain proteins in the ER, occurs via COPI coated vesicles (Letourneur *et al.*, 1994; Bonifacino and Glick, 2004). Further trafficking of protein substrates to the plasma membrane, the trans-Golgi network, and the endosome is supported by yet another pathway that utilizes clathrin coated vesicles (Bonifacino and Lippincott-Schwartz, 2003; Bonifacino and Traub, 2003).

Regardless of the acceptor organelle to which the vesicles are targeted, the coats must be shed and the vesicles must fuse with the acceptor membrane in order to deliver their cargo. Membrane fusion relies on complex formation between specific v-SNARE proteins of the transport vesicle with specific partner t-SNARE proteins on the target membrane (Chen and Scheller, 2001; Bonifacino and Glick, 2004). While different v-/t-SNARE complexes are able to convey some level of specificity to the process of membrane fusion, tethering factors provide additional target specificity prior to SNARE complex formation (Barr and Short, 2003; Bonifacino and Glick, 2004). Various steps of the vesicle budding, targeting, and fusion process are regulated and timed by different Rab proteins via GTP hydrolysis (Bonifacino and Glick, 2004). Therefore, the biogenesis of secretory proteins followed by their shuttling to the right destination within the cell

is highly regulated and complex; quality control check points at different steps along this journey prevent the cell from the fatal consequences that may arise from mistakes. One check point in the early secretory pathway is ER protein quality control.

1.2. ER PROTEIN QUALITY CONTROL

Protein maturation and folding in the ER are pre-requisites for subsequent transport through the secretory pathway because soluble and integral membrane proteins are subject to ER protein quality control (ERQC) (Ellgaard and Helenius, 2003). Proteins that are unable to fold or assemble into multi-protein complexes fail to pass the ERQC check-point and may be degraded, which unburdens the ER from housing aberrant proteins and eliminates the potential formation of toxic protein aggregates. ER proteins that are targeted for degradation are destroyed by the cytoplasmic proteasome. As a result, soluble proteins within this compartment must be re-exported, or "retro-translocated" to the cytoplasm, and the selection, targeting, and proteolysis of proteins residing in the ER or at the ER membrane has been referred to as ER associated protein degradation (ERAD) (Tsai *et al.*, 2002; Kostova and Wolf, 2003; McCracken and Brodsky, 2003). By definition, then, ERAD can be sub-divided into three stages: substrate recognition in or at the ER, targeting to the proteasome, and proteasome-mediated degradation.

1.2.1. The ubiquitin –proteasome pathway

Many ERAD substrates are ubiquitinated prior to their degradation via the 26S-proteasome. Conjugation of ubiquitin to the candidate protein requires three distinct steps (see Figure 1). First, the ubiquitin activating enzyme (E1) activates ubiquitin in an ATP-dependent manner through the formation of a high energy intermediate. Second, the activated ubiquitin is now passed on to a ubiquitin conjugating enzyme (E2). Finally, the ubiquitin moiety is transferred from the E2 to a lysine residue of the substrate that is bound to an ubiquitin ligase (E3), which catalyzes this reaction. Depending on the class of E3 involved, the attachment of the ubiquitin to the substrate proceeds either directly or indirectly (Glickman and Ciechanover, 2002; Pickart, 2004). While in most organisms only one E1 activates ubiquitin to transfer it to a range of E2s, many E3s exist. For example, the human genome encodes for more than 40 putative E2s and over 500 predicted E3s (Wong *et al.*, 2003). Sequentially appending ubiquitin onto substrates already containing ubiquitin creates a polyubiquitin chain. Once a minimum of 4 ubiquitins is in place, the ubiquitinated protein might then be identified by the 26S proteasome which degrades the substrate after deubiquitination by deubiquitinating enzymes (Thrower *et al.*, 2000; Glickman and Ciechanover, 2002). The 26S proteasome consists of 1 or 2 19S regulatory particles, also called the “cap” or PA 700, and a 20S catalytic core (see Figure 2). The 19S regulatory particle prevents proteins from aggregating, remodels polypeptide conformation, binds to ubiquitinated proteins, catalyzes retro-translocation of ERAD substrates out of the ER, and drives

Figure 1: Ubiquitin-proteasome pathway.

Ubiquitin is activated and covalently linked to an E1 in an ATP-dependent process. Activated ubiquitin is then transferred to an E2. An E3 facilitates the conjugation of ubiquitin via its C-terminal glycine to a lysine or a primary amine in the substrate. The polyubiquitinated substrate is recognized by the proteasome, deubiquitinated by Dubs and degraded. E1=ubiquitin activating enzyme, E2=ubiquitin conjugating enzyme, E3=ubiquitin ligase, Ubi=ubiquitin, Dub=deubiquitinating enzyme, G=glycine, K=lysine, magenta line=ERAD-substrate.

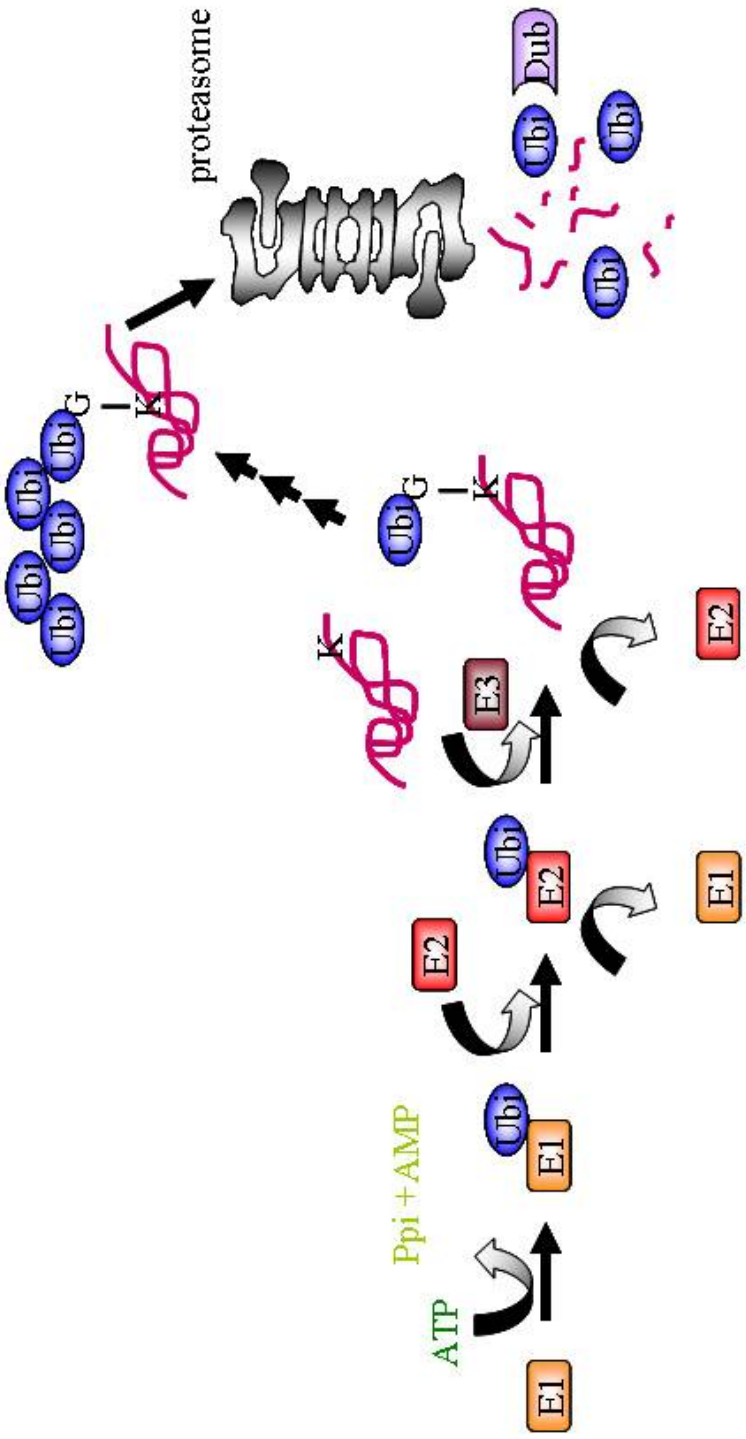

Figure 1: Ubiquitin-proteasome pathway.

Figure 2: Structure of the 26S proteasome.

The three-dimensional structure model is based on electron microscopy from *Drosophila* 26S proteasome and the crystal structure of *Thermoplasma* 20S proteasome. The 19S regulatory particles are represented in blue, the proteolytic 20S core particle is depicted in yellow.

(Adapted from Voges *et al.*, 1999).

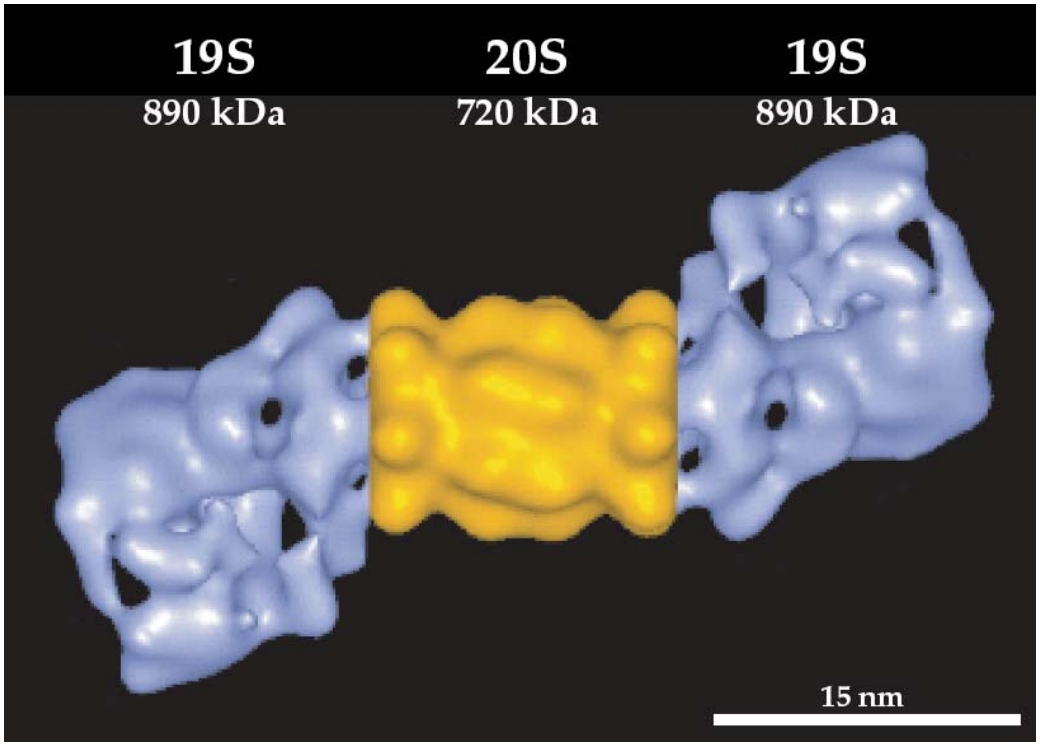

Figure 2: Structure of the 26S proteasome.

deubiquitinated substrates into the 20S core (Glickman *et al.*, 1998; Braun *et al.*, 1999; Strickland *et al.*, 2000; Verma *et al.*, 2000; Dai and Li, 2001; Lee *et al.*, 2001; Lam *et al.*, 2002; Liu *et al.*, 2002; Lee *et al.*, 2004). The 20S core harbors three distinct proteolytic activities that degrade substrates. The importance of the ubiquitin-proteasome pathway is emphasized by the plethora of substrates degraded and its implication in human diseases.

1.2.2. Distinct requirements for the degradation of ER-lumenal and transmembrane proteins

After they are selected for degradation in the ER, evidence suggests that soluble lumenal ERAD substrates, and at least some integral membrane substrates, are retro-translocated through the Sec61p translocation channel (Romisch, 1999); however, Sec61p function may be dispensable for the degradation of other membrane substrates (Walter *et al.*, 2001; Huyer *et al.*, 2004). In this case, the endopeptidase activity of the proteasome, or other proteases might clip cytoplasmic loops and directly extract the substrate (Walter *et al.*, 2001; Liu *et al.*, 2003), or a recently defined protein complex in the ER membrane might form a specific retro-translocation channel (Lilley and Ploegh, 2004; Ye *et al.*, 2004). In any event, many studies indicate that ERAD substrate retro-translocation from the ER and delivery to the proteasome is catalyzed by a multi-protein complex containing Cdc48p (also known as p97, or "Valosin-containing protein", VCP), Ufd1p, a factor isolated in a screen for ubiquitin fusion degradation mutants, and Npl4p, which is

encoded by a gene that, when mutated, leads to defects in nuclear protein localization (Bays and Hampton, 2002) (also see Table 1 for definitions). The Cdc48p-Ufd1p-Npl4p complex binds to the polypeptide backbone and then to the polyubiquitin conjugate on ERAD substrates that is appended through the action of E2s and E3s (see above); ATP hydrolysis by Cdc48p is required to complete retro-translocation (Ye *et al.*, 2003). In addition, the 19S "cap" (PA700) of the proteasome itself might facilitate the retro-translocation of some ERAD substrates (Lee *et al.*, 2004). Key mediators of ERAD substrate selection are ER resident lectins and molecular chaperones—such as the ER lumenal Hsp70, BiP—which facilitate folding but can then "decide" to target proteins for degradation (Fewell *et al.*, 2001; Ellgaard and Helenius, 2003); also see section 1.3. below). Lectins recognize glycans on secreted proteins. Specifically, calnexin and calreticulin bind and retain immature monoglucosylated glycoproteins ($Glc_1Man_9GlcNAc_2$, Glc is glucose, Man is mannose, GlcNAc is N-acetyl glucosamine) that have been trimmed by glucosidase. Removal of the remaining glucose frees the glycoprotein from the lectins so they can exit the ER. Prolonged ER retention results in mannose-trimming, and another lectin, known as EDEM, has been proposed to bind the Man_8-containing glycan and to target these glycoproteins for ERAD (Molinari *et al.*, 2003; Oda *et al.*, 2003). Although the calnexin and calreticulin cycles are absent in the yeast *S. cerevisiae*, the EDEM homologue known variably as Mnl1p or Htm1p also facilitates the proteolysis of glycosylated ERAD substrates (Jakob *et al.*, 2001; Nakatsukasa *et al.*, 2001). In contrast, Hsp70s, such as BiP, recognize peptides enriched in hydrophobic amino acids, and cycles of ATP binding, hydrolysis and ADP release are coupled with the association and dissociation of peptide substrates. Hsp40 co-chaperones enhance the ATPase activity of Hsp70s, and thus impact Hsp70-peptide capture. Together, Hsp70-Hsp40 chaperone pairs can retain aggregation-prone, misfolded proteins in solution (Fewell *et al.*,

Table 1: Partial list of factors required for ERAD, ERAD substrates, and description of constructs tested.

	Subcellular localization	Description
Hsp104	Cytosol	Yeast heat shock protein, 104 kD Involved in stress response, protein folding
Ssa1p	Cytosol	Yeast heat shock protein, 70 kD involved in protein translation, translocation, degradation, folding
Kar2p (mBiP homolog)	ER	Yeast heat shock protein, 78 kD involved in protein translocation, retro-translocation, folding degradation
Cwc23p	Cytosol	Yeast heat shock protein, 40 kD
Hlj1p	Cytosol, ER membrane anchored	Yeast heat shock protein, 40 kD Involved in protein folding
Jid1p	Transmembrane, ER	Yeast heat shock protein, 40 kD
Jem1p	ER	Yeast heat shock protein, 40 kD involved in protein folding
Scj1p	ER	Yeast heat shock protein, 40 kD involved in protein folding
Mnl1p = Htm1p	ER	Yeast lectin, man_8 binding, involved in ERQC
EDEM	ER	Mammalian lectin, man_8 binding, involved in ERQC
Sec61p	ER membrane	Yeast translocon
Cdc48p = p97 = Vcp	Cytosol	Yeast AAA-ATPase, involved in apoptosis, cell cycle, ER associated protein metabolism, vesicle fusion, ubiquitin dependent protein catabolism
Ufd1p	Cytosol	Yeast Cdc48p cofactor
Npl4p	Cytosol	Yeast Cdc48p cofactor
Der3p = Hrd1p	ER membrane	Ubiquitin ligase
Der1p (mDerlin-1 homolog)	ER membrane	Protein degradation (mDerlin, proposed component of dislocon machinery)
Hrd3p	ER membrane	Ubiquitin ligase
Doa10p	ER membrane	Ubiquitin ligase
Ubc1p	Cytosol	Ubiquitin conjugating enzyme
Ubc7p	Cytosol, ER membrane anchored	Ubiquitin conjugating enzyme
Wsc1p	Transmembrane, ER	Cell wall integrity and stress response component 1
KHN	ER lumen	yeast Kar2p signal sequence fused to simian virus 5 HA-Neuraminidase ectodomain
Ste6p	Transmembrane, plasmamembrane	Yeast plasma membrane mating factor transporter
Ste6p*	Transmembrane, ER	Mutated form of Ste6p

	Subcellular Localization	Description
KWW	Transmembrane, ER	KHN luminal domain/Wsc1p transmembrane domain/Wsc1p cytosolic domain
KSS	Transmembrane, ER	KHN luminal domain/Ste6p transmembrane domains/ Ste6-166p mutant cytosolic domain
KWS	Transmembrane, ER	KHN luminal domain/Wsc1p transmembrane domain/ Ste6-166p mutant cytosolic domain
CPY	Vacuole	Yeast carboxypeptidase Y
CPY*	Retained in ER	Mutated form of CPY
CT*	Transmembrane, ER	Membrane-bound CPY* lacking a cytosolic domain
CTG*	Transmembrane, ER	CT* with GFP as cytosolic domain
GFP	Cytosol	Green fluorescent protein
Vph1p	Transmembrane, plasmamembrane	Yeast vacuolar ATPase
CFTR	Transmembrane, plasmamembrane	Mammalian, cystic fibrosis transmembrane conductance regulator
A1PiZ	Retained in ER	Variant of mammalian α1-protease inhibitor, ERAD substrate
ΔG$p\alpha$F	Retained in ER	Mutant form of yeast mating factor, unglycosylated, ERAD substrate
ERAD		ER associated degradation
ERAD-L	ER lumen	ERAD upon checkpoint in the ER lumen
ERAD-C	Cytosol	ERAD upon checkpoint in the cytosol

(Table 1 continued)

2001). Not surprisingly, the release of BiP from ERAD substrates correlates with their degradation (Knittler *et al.*, 1995), and mutations in the gene encoding yeast BiP, *KAR2*, and/or deletion of BiP's Hsp40 partners, *JEM1* and *SCJ1*, slow the degradation of soluble ERAD substrates such as a mutated form of carboxypeptidase Y (CPY), which is denoted "CPY*", a nonglycosylated mating factor precursor known as pαF, and the Z variant of the human α1-protease inhibitor, A1PiZ, in yeast (Plemper *et al.*, 1997; Brodsky *et al.*, 1999; Nishikawa *et al.*, 2001; Kabani *et al.*, 2003). BiP is not required for the degradation of several integral membrane ERAD substrates in yeast, including CFTR (the cystic fibrosis transmembrane conductance regulator), Vph1p (a vacuolar ATPase), and a mutated form of a plasma membrane mating factor transporter, Ste6p, abbreviated as Ste6p*. Instead, their degradation requires a cytoplasmic Hsp70, Ssa1p (Hill and Cooper, 2000; Zhang *et al.*, 2001; Huyer *et al.*, 2004). Together, these data indicate the existence of at least two pathways for ERAD substrate selection—one that recognizes aberrant integral membrane proteins and another that recognizes ER lumenal soluble proteins. In addition, the molecules that select substrates in the two classes include both lectins that bind to specific glycan moieties and molecular chaperones that associate directly with the polypeptide.

Another apparent distinction between the ERAD pathways taken by soluble and membrane proteins is that soluble substrates can be transported to the Golgi and appear to be retrieved to the ER prior to degradation, whereas integral membrane ERAD substrates are retained in the ER (Caldwell *et al.*, 2001; Vashist *et al.*, 2001). Nevertheless, a discussion of "soluble" versus "membrane" ERAD substrate might be irrelevant: There could be varying requirements for the degradation of membrane proteins with different numbers of integral membrane domains or even

for one membrane protein with topologically distinct mutations. For example, the degradation of a membrane protein containing either a misfolded lumenal, transmembrane, or cytosolic domain might only require factors located in the same compartment as the aberrant domain. Although it is clear that ERAD is comprised of many different pathways, it has been difficult to unequivocally establish their existence. However, recent studies from the Ng and Wolf laboratories have better defined several distinctions between pathways taken by ERAD substrates *en route* to degradation (Taxis *et al.*, 2003; Vashist and Ng, 2004).

1.2.3. Protein sorting based on topology and localization of misfolded domains

The integral membrane substrates employed previously contained lesions located in the cytosolic domains, whereas misfolded domains in the soluble substrates resided exclusively in the ER lumen. This raised the possibility that the location of the lesion with respect to the ER membrane, rather than the residence of the protein (i.e., soluble versus membrane), determined the substrate's trafficking pattern. To examine this hypothesis, Vashist et al. designed protein chimeras with defined folded and misfolded domains and with different topologies (see Figure 3 and Table 1 for definitions of domains and proteins utilized), and then determined the requirements for their degradation by pulse-chase analysis in various wild type and mutant yeast strains (Vashist and Ng, 2004). The degradation of KHN, a soluble ERAD substrate consisting of a misfolded ER-lumenal domain was examined previously (Vashist *et al.*, 2001), and in the newer study a chimera denoted KWW was designed that also contained a misfolded ER-lumenal

Figure 3: A schematic representation of chimera ERAD substrates.

Three letter designations that describe the composition of the constructed ERAD substrates. The first, second, and third letters portray the lumenal, transmembrane, and cytosolic domains, respectively. KHN is depicted by blue stars, the Wsc1p transmembrane domain by red bars and the folded cytosolic and lumenal domains by red circles, and Ste6p* ("Ste6") is depicted by black bars/loops (transmembrane domain), black circles (folded cytosolic domain), and black stars (misfolded cytosolic domain). Also see the Table 1 for definitions of all proteins used to create these substrates.

(Adapted from Vashist and Ng, 2004).

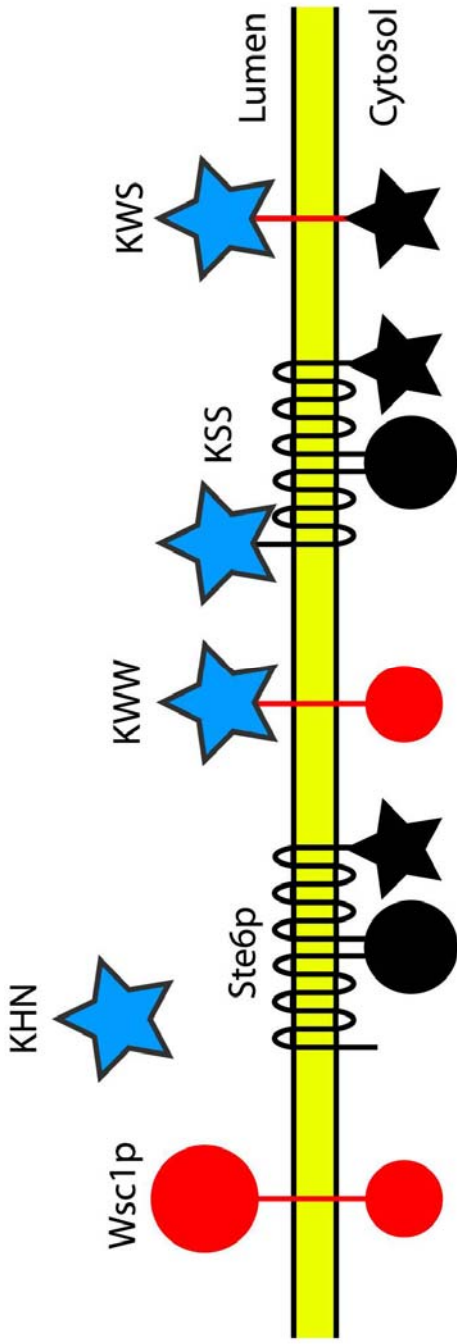

Figure 3: A schematic representation of chimera ERAD substrates.

domain but was anchored to the ER membrane by a single transmembrane domain (Figure 3). Using these substrates, the authors first re-investigated whether only soluble ERAD substrates appeared to be transported to the Golgi prior to their degradation (Caldwell *et al.*, 2001; Vashist *et al.*, 2001). If this were the case, KWW should be degraded independently of ER-to-Golgi transport, but Ng and colleagues discovered that membrane-bound KWW was degraded at a rate similar to soluble substrates and that a block in ER-to-Golgi transport stabilized KWW. Surprisingly, KWW degradation also required, Der1p, a protein so far known to facilitate only the degradation of lumenal substrates, and interestingly it is the yeast homologue of the putative retro-translocation channel (Knop *et al.*, 1996; Vashist *et al.*, 2001; Lilley and Ploegh, 2004; Ye *et al.*, 2004). Overall, one conclusion from this study is that the site of the lesion is the major determinant for this aspect of the ERAD pathway, and the authors proposed two surveillance mechanisms: ERAD-L (ERAD-Lumenal), which monitors the folded state of lumenal domains, and ERAD-C (ERAD-Cytosolic), which monitors the folded state of cytosolic domains (see Figure 4). Consistent with this distinction, only the ERAD-L pathway required the function of the yeast EDEM homologues, Mnl1p/Htm1p (see above) (Vashist and Ng, 2004).

To further define the relationship between ERAD-L and ERAD-C, Ng and co-workers next constructed a polytopic membrane protein with misfolded domains on both sides of the membrane (KSS; Figure 3). In principle, KSS should exhibit determinants for both the ERAD-L and ERAD-C pathways, but KSS instead exhibited characteristics only of an ERAD-C substrate: A short half-life, Der1p-independent degradation, no requirement for ER-to-Golgi transport, and dependence on the Doa10p ubiquitin ligase (E3; see section 1.2.1). Although it cannot be completely excluded that the magnitude of the folding defect in each domain differs, or that

Figure 4: Distinct ERAD pathways lead to degradation via the proteasome.

Black stars represent misfolded domains, and black triangles are N-linked core glycans. Whereas all ERAD substrates tested in vivo require the proteasome and probably the Cdc48-Ufd1p-Npl4p complex (A and B), there is significant variety and distinction concerning the rest of the ERAD machinery. For example, soluble substrates interact with lumenal chaperones to remain aggregation-free (A), whereas transmembrane proteins with prominent cytosolic domains require cytosolic chaperones (e.g. Ssa1p) for degradation (B). Misfolded ER lumenal proteins, and some transmembrane proteins with folding defects in the lumen, can be transported from the ER and appear to be retrieved from the Golgi before being degraded by the ERAD-L pathway. Their degradation requires Der1p (whose function is unknown), EDEM, and specific ubiquitin conjugating enzymes and ligases (A). In contrast, transmembrane proteins with misfolded domains in the cytosol, are retained in the ER and degraded by the ERAD-C pathway (B).

(Ahner and Brodsky, 2004).

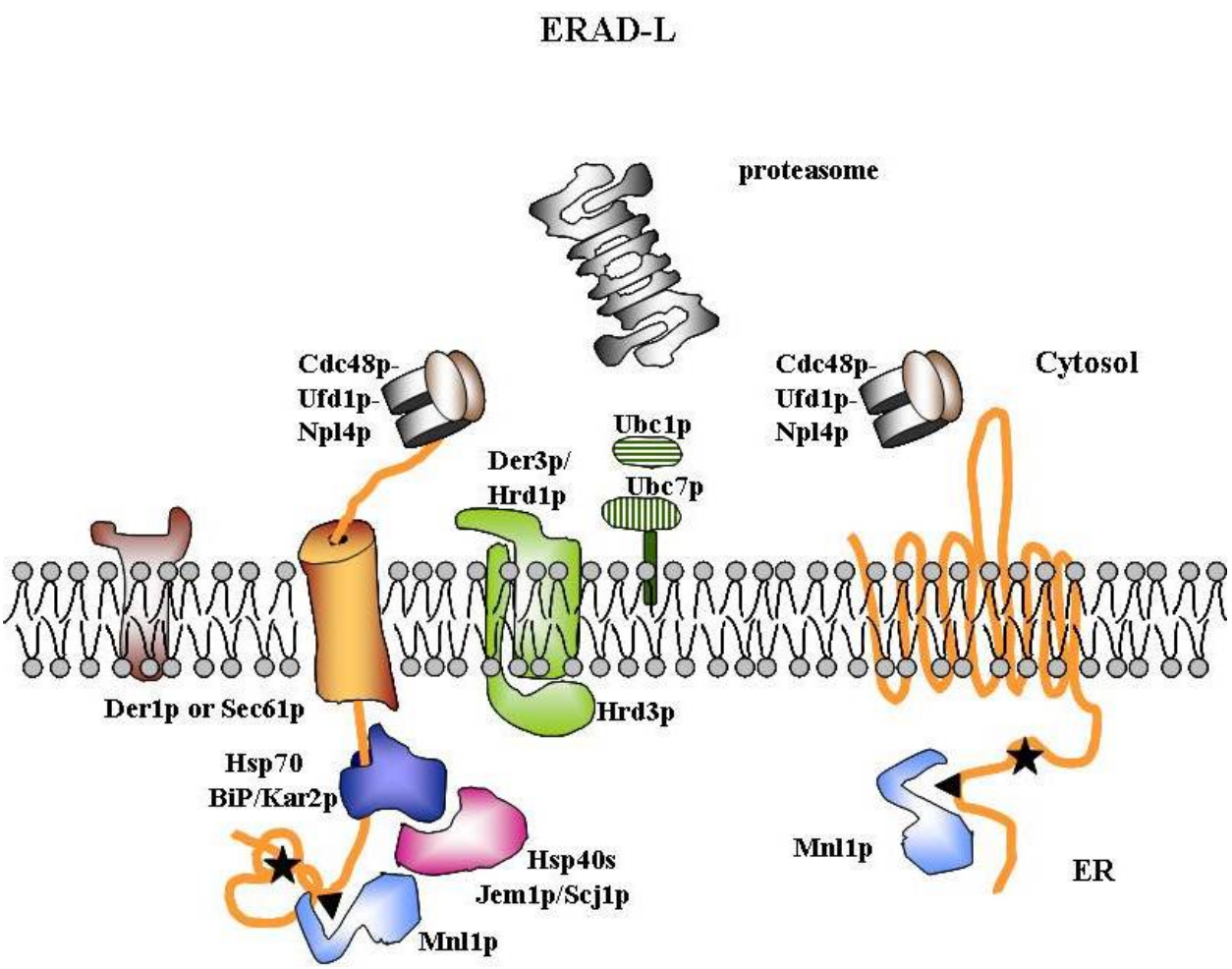

Figure 4.A: Distinct ERAD pathways lead to degradation via the proteasome.

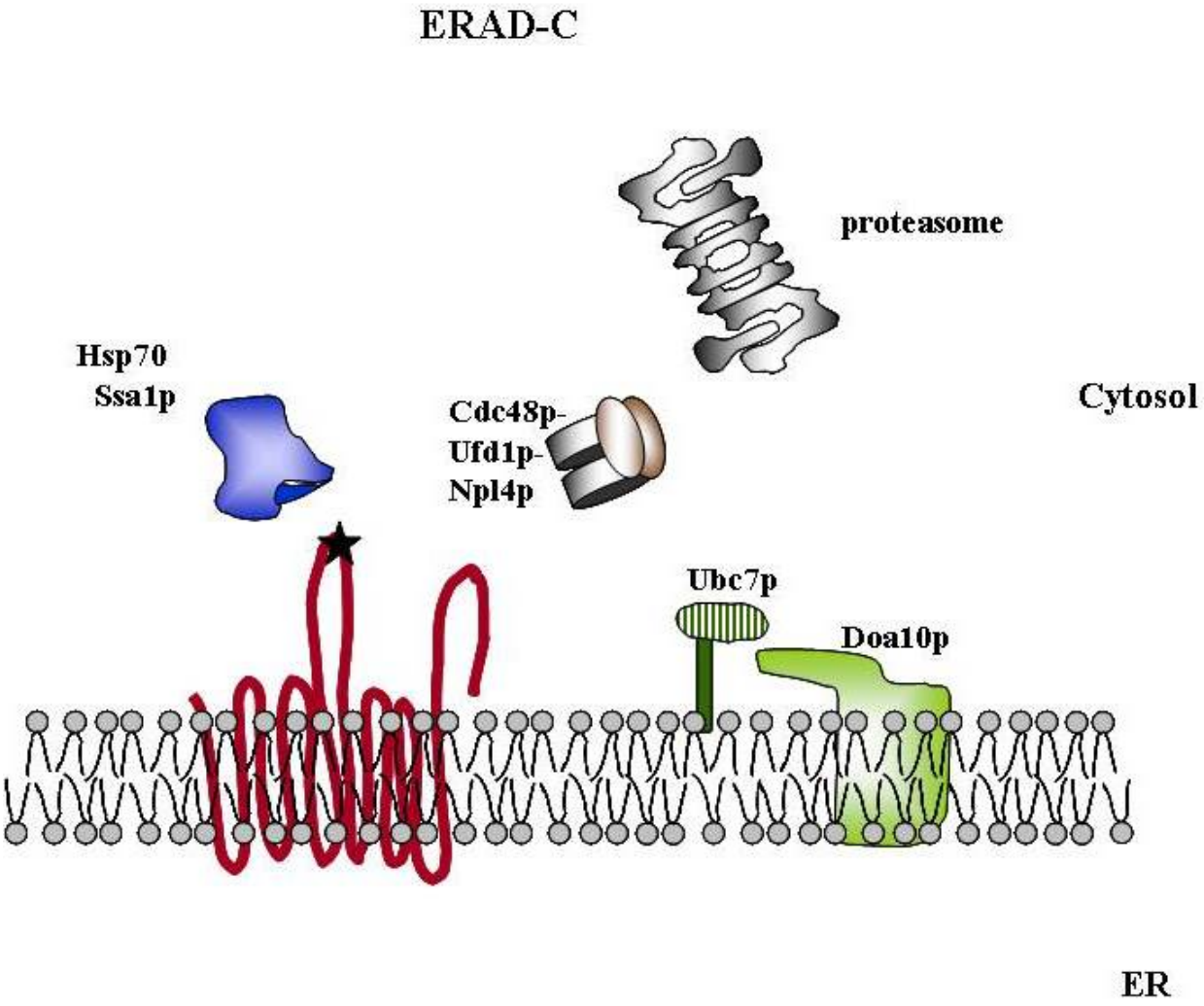

Figure 4.B: Distinct ERAD pathways lead to degradation via the proteasome.

domain accessibility to components of each machinery differs, these data strongly suggest that the ERAD-C check-point precedes the ERAD-L checkpoint.

1.2.4. Protein sorting based on membrane association and solubility

Taxis *et al.* (Taxis *et al.*, 2003) uncovered substrate-specific requirements of the ERAD machinery by similarly constructing and analyzing structurally different proteins, but each contained the same ER-lumenal ERAD substrate, CPY*. Thus, the degradation of CPY* was compared to CT*, which is a fusion protein containing CPY* anchored to the ER membrane via a single transmembrane domain, and CTG*, which is a chimera between GFP (Green Fluorescent Protein) in the cytoplasm and CT* (see also Table 1). Based on data from pulse-chase analyses in wild type and mutant yeast strains, the authors identified a core machinery required for the degradation of all three substrates, and that consists of the Der3p ubiquitin ligase (also known as Hrd1p), the ubiquitin-conjugating enzymes Ubc1p and Ubc7p, the Cdc48p-Ufd1p-Npl4p complex, and the proteasome (see Figure 4 and Table 1). But, the Der3p ubiquitin ligase was dispensable for KSS and Ste6-166p degradation, which depended instead on the Doa10p ligase (Vashist *et al.*, 2001). Therefore, ubiquitin ligases seem to exhibit specificity rather than being part of the general ERAD machinery.

According to the model by Vashist *et al.* (Vashist *et al.*, 2001), one would expect CT* and CTG* to be targeted to the ERAD-L pathway, like CPY*, since the aberrant domain in each substrate

resides in the lumen. Instead both CT* and CTG* were degraded independently of Der1p and ER-to-Golgi transport, suggesting that the membrane-spanning segment affects the ERAD pathway selection. In accordance with a previous observation, however, Wolf and colleagues found that CTG*, but neither CT* nor CPY*, was stabilized in strains mutated individually for the cytosolic Hsp70 chaperone, Ssa1p (see below) (Hill and Cooper, 2000; Zhang *et al.*, 2001). They also discovered that the cytoplasmic Hsp40 homologues Hlj1p, Cwc23, and Jid1p, and the Hsp104 chaperone modestly facilitate CTG* degradation. These data suggest that the GFP moiety in CTG*, which is properly folded, also influences ERAD, and one model to account for these data is that cytosolic chaperones help unfold GFP prior to proteasomal degradation. Overall the recent publications described indicate that ERAD substrates cannot simply be distinguished as being either lumenal or integral membrane proteins, and in Figure 4, I attempt to depict the requirements for the selection, targeting and degradation of model ERAD-C and ERAD-L substrates.

1.3. MOLECULAR CHAPERONES IN THE CYTOPLASM

Molecular chaperones, many of which were first identified as heat shock proteins (Hsps) are involved in a variety of cellular processes including protein folding and degradation, assembly and disassembly of protein oligomers, translocation of polypeptides across intracellular

membranes, refolding of denatured proteins, solubilization of protein aggregates, and activation of enzyme-catalyzed reactions (Frydman, 2001). Members of one Hsp class with a molecular mass of 70 kD, the Hsp70s, are highly conserved and are among the most abundant molecular chaperone sub-types. Hsp70s are composed of a conserved, ~44 kD N-terminal nucleotide binding site, followed by a ~18 kD peptide-binding domain, and a ~10 kD relatively non-conserved C-terminal lid region (Chappell *et al.*, 1987; Milarski and Morimoto, 1989; Flaherty *et al.*, 1990; Wang *et al.*, 1993; Zhu *et al.*, 1996). Hsp70s bind preferentially to substrate polypeptides containing stretches of amino acids with overall hydrophobic character (Flynn *et al.*, 1991; Blond-Elguindi *et al.*, 1993; Rudiger *et al.*, 2001). Polypeptide binding is driven by a conformational change and is nucleotide-dependent: In the ADP-bound state, the substrate affinity for Hsp70 is high and the kinetics of release are relatively slow, whereas fast cycling between polypeptide binding and release is observed in the ATP-bound state (Schmid *et al.*, 1994; McCarty *et al.*, 1995; Ziegelhoffer *et al.*, 1995).

The ATPase activity of Hsp70s, and thus their interaction with polypeptides, can be enhanced by Hsp40 molecular chaperones. Hsp40 interaction with Hsp70s requires the J-domain, a conserved ~70 amino acid domain that forms a four-helix bundle (Cyr *et al.*, 1992; Wall *et al.*, 1994; Cheetham and Caplan, 1998; Kelley, 1998; Qian *et al.*, 2002). After ATP hydrolysis, nucleotide exchange factors (NEFs), another class of Hsp70 cofactors, release ADP from Hsp70 and thus facilitate substrate dissociation from the chaperone. Therefore, NEFs enable Hsp70-mediated substrate binding and release, although whether they facilitate or inhibit protein folding has been a matter of debate (Brehmer *et al.*, 2001; Briknarova *et al.*, 2001; Sondermann *et al.*, 2001; Kabani *et al.*, 2002a; Kabani *et al.*, 2002b; Sondermann *et al.*, 2002).

Hsp110s comprise a subfamily of the Hsp70 family of chaperones with homology mostly in the N-terminal nucleotide-binding site (Easton *et al.*, 2000). In the yeast cytoplasm there are two members of the Hsp110 family of molecular chaperones: Sse1p and Sse2p (Mukai *et al.*, 1993; Shirayama *et al.*, 1993). Sse1p retains proteins in a folding competent conformation, and interacts with and is required for the function of the Hsp90 complex (Oh *et al.*, 1997; Brodsky *et al.*, 1999; Liu *et al.*, 1999; Goeckeler *et al.*, 2002). In contrast to the Hsp70s, the substrate specificity of this class of chaperones has not been characterized.

Hsp90 is one of the most abundant cytosolic proteins in the eukaryotic cell and is highly conserved (Caplan, 1999; Richter and Buchner, 2001). Unlike Hsp70, Hsp90 is able to bind ATP via an N-terminal domain as well as a C-terminal domain (though with lower affinity) (Grenert *et al.*, 1997; Prodromou *et al.*, 1997; Stebbins *et al.*, 1997; Marcu *et al.*, 2000; Garnier *et al.*, 2002; Soti *et al.*, 2002). Binding of ATP to the N-terminal domain facilitates Hsp90 dimerization, which then stimulates ATP hydrolysis (Prodromou *et al.*, 2000) and substrate dissociation (Young and Hartl, 2000). Many Hsp90-dependent functions—for example steroid hormone receptor activation—require the formation of an Hsp90 complex that may include Hsp70, Hsp40, the Hsp90 organizing protein (Hop), p23, the cyclophilins, and other proteins (Pratt and Toft, 2003).

Hsp70 and Hsp90 facilitate protein folding in mammalian cells but can “decide” to target substrates that are unable to fold for proteasome-mediated protein degradation. For example, mammalian Hsp70 and Hsp90 cooperate during the refolding of denatured firefly luciferase (FFLux), but addition of ansamycin antibiotics (geldanamycin, herbimycin A, radicicol) prevents

substrate dissociation from Hsp90 and redirects FFLux to the degradation pathway (Schneider *et al.*, 1996). In addition, the decision between folding and degradation can require Hsp70/Hs90 cofactors: Together with the J-domain-containing proteins, Hdj1/2 and the NEF HspBP1, Hsp70 facilitates the biosynthesis of the Cystic Fibrosis Transmembrane conductance Regulator (CFTR), the protein that when mutated gives rise to cystic fibrosis (CF) (see section 1.5. below); CFTR biogenesis is also facilitated by Hsp90 in mammalian cells (Strickland *et al.*, 1997; Meacham *et al.*, 1999; Choo-Kang and Zeitlin, 2001; Farinha *et al.*, 2002; Alberti *et al.*, 2004). However, when an Hsp70/Hsp90-interacting ubiquitin ligase, known as CHIP is recruited, there is a shift toward the degradation pathway (Connell *et al.*, 2001; Meacham *et al.*, 2001). The same is true during glucocorticoid receptor maturation and when the fate of heat-denatured FFLux was examined (Schneider *et al.*, 1996; Connell *et al.*, 2001). However, CHIP has also been reported to facilitate Hsp70-dependent folding when over-expressed (Kampinga *et al.*, 2003). One potential problem with these studies, which can give rise to the noted controversial conclusions, is the difficulty of specifically and rapidly disabling molecular chaperone function in mammalian cells. Particularly, administration of the ansamycin antibiotics can induce cell stress and chaperone or co-chaperone over-expression can initiate non-specific effects on cellular processes (Lawson *et al.*, 1998).

Table 2: Cytoplasmic chaperones and cofactors.

Yeast Hsp	Mammalian ortholog	Description
Sse1p	Hsp110	heat shock protein, ~110 kD, ribosome associated, member of the hsp90 complex, prevents protein aggregation
Hsp82	Hsp90	heat shock protein, ~90 kD, involved in protein maturation, prevents protein aggregation
Ssa1p	Hsp70	heat shock protein, 70 kD involved in protein translation, translocation, degradation, folding
Ydj1p	Hdj1/2	heat shock protein, 40 kD, Hsp70-cochaperone, involved in protein folding
Sis1p	Hsp40 ortholog	heat shock protein, 40 kD, involved in translation initiation
Hsp26	α-crystallin-like sHsp	heat shock protein, 26 kD, prevents protein aggregation
Hsp42	α-crystallin-like sHsp	heat shock protein, 42 kD, prevents protein aggregation
Fes1p	HspBP1	Nucleotide exchange factor for Ssa1/Hsp70
-	CHIP	Hsp70/Hsp90-interacting ubiquitin ligase
Sba1p	p23	Member of Hsp90 complex
Sti1p	Hop	Hsp90 organizing protein
Cprs	Cyclophilins	members of Hsp90 complex, prolyl-isomerases

1.4. SMALL HSPS

Small heat shock proteins (sHsps) constitute another, heterogeneous class of molecular chaperones that is so far rather ill-defined. sHsps share a conserved, ~80 amino acid "α-crystallin" domain at their C-terminus that is found in the best characterized member of this family, a protein mainly expressed in the eye-lens, α-crystallin (Caspers *et al.*, 1995; Horwitz, 2003). *Saccharomyces cerevisiae* encodes 2 members of the sHsp family, Hsp26 and Hsp42 (Geoffrey, 1997), while 10 human α-crystallin-related Hsps have been identified (Kappe *et al.*, 2003). All the proteins in this class examined so far oligomerize in vitro to form large complexes (de Jong *et al.*, 1998; Narberhaus, 2002). The oligomers may form hollow spheres with openings or cylinders (Haley *et al.*, 1998; Kim *et al.*, 1998a; Haslbeck *et al.*, 1999; Haley *et al.*, 2000; Van Montfort *et al.*, 2001a; van Montfort *et al.*, 2001b; Haslbeck *et al.*, 2004). For example, the crystal structure of *Methanococcus jannaschii* Hsp16.5 is shown in Figure 5. The spherical complex with octahedral symmetry consists of twenty four subunits and contains 14 openings. The monomers arrange into 10 β-strands, packed into 2 parallel sheets, and 2 short helices (Kim *et al.*, 1998a). Most α-crystallin-like Hsps consist mainly of β-sheets (Merck *et al.*, 1993; Leroux *et al.*, 1997; Muchowski *et al.*, 1997; Bova *et al.*, 1999; Shearstone and Baneyx, 1999; van Montfort *et al.*, 2001b; Narberhaus, 2002) as seen in the *Methanococcus jannaschii* (*Mj*) Hsp16.5, but the residues critical for monomer interaction may not be conserved. Also, the number of subunits within the oligomers seems to be exceptionally constant in *Mj* Hsp16.5 (Kim *et al.*, 1998a), but this does not appear to be true in every sHsp oligomer examined

Figure 5: Structure of *Mj* 16.5.

A: A space filling model of *Mj* Hsp16.5 oligomer arranged in a hollow sphere. Each color depicts one Hsp16.5 tetramer. Top right: ovals representing the 24 subunits, symmetry axes indicated by arrows; top left: schematic illustration of octahedral symmetry. B: The front one-third of the sphere is severed to expose the interior. View along the three-fold axis (left) and the four-fold axis (right). Each color depicts one Hsp16.5 tetramer. An octahedron in the same orientation as the corresponding sHsp is shown at the top.

(Kim *et al.*, 1998a).

A.

B.

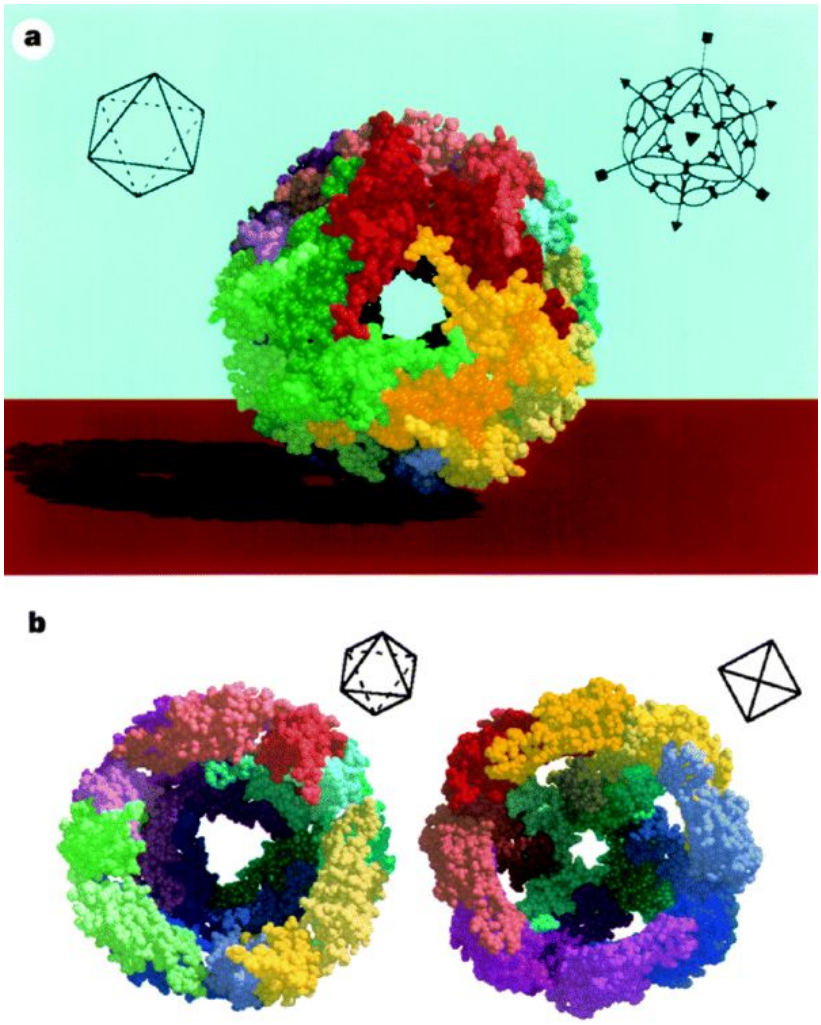

Figure 5: Structure of *Mj* Hsp16.5.

(Haley *et al.*, 1998; Ehrnsperger *et al.*, 1999; Haslbeck *et al.*, 1999; Shearstone and Baneyx, 1999; Haley *et al.*, 2000; Lindner *et al.*, 2000; Narberhaus, 2002). For comparison, Figure 6 represents a cryo-EM reconstruction of αB-crystallin and αB-crystallin with bound substrate, exhibiting a variable quaternary structure with a central cavity (Horwitz, 2003).

The significance of the assembly into oligomers for chaperone function is still controversial. While some sHsps exhibit chaperone activity in a dimeric or tetrameric state, others seem to lose function upon disassembly of the oligomer (Narberhaus, 2002). For example, the activity of the yeast Hsp26 depends on heat-shock induced dissociation into dimers (Haslbeck *et al.*, 1999). Overall, the predominance of β-sheets in the secondary structure and the tendency to oligomerize seems to be common among the family members of sHsp. In contrast, the subunit arrangement within the oligomers as well as the correlation between the chaperone activity and the state of the quaternary structure might differ between individual sHps.

Regardless of their exact oligomeric properties, sHsps have been demonstrated to associate with unfolded proteins and to prevent their aggregation (Horwitz, 1992; Jakob *et al.*, 1993; Ehrnsperger *et al.*, 1997; Lee *et al.*, 1997; Haslbeck *et al.*, 1999; Biswas and Das, 2004; Haslbeck *et al.*, 2004). In addition, α-crystallins have neuroprotective properties and confer resistance to apoptosis by negatively regulating tumor necrosis factor α and inhibiting caspase-3 activation (Kamradt *et al.*, 2001; Kamradt *et al.*, 2002; Kamradt *et al.*, 2005), as well as by preventing the translocation of Bax and Bcl-X_s into mitochondria (Mao *et al.*, 2004). Interestingly, the ERK and the p38 MAPK pathways are responsible for αB-crystallin

Figure 6: Cryo-EM reconstructions and models of recombinant αB-crystallin and αB-crystallin associated with α-lactalbumin.

A: A cryo-EM reconstruction of αB-crystallin illustrating the asymmetrical exterior of the αB-crystallin oligomer. B: A cropped view of the αB-crystallin reconstruction displaying the interior. Red denotes the strongest density and green the weakest. Blue depicts the surface. C: A cryo-EM reconstruction of αB-crystallin associated with α-lactalbumin. D: A model of αB-crystallin (magenta)/α- lactalbumin (red) complex. Scale bar = 100Å.

(Horwitz, 2003).

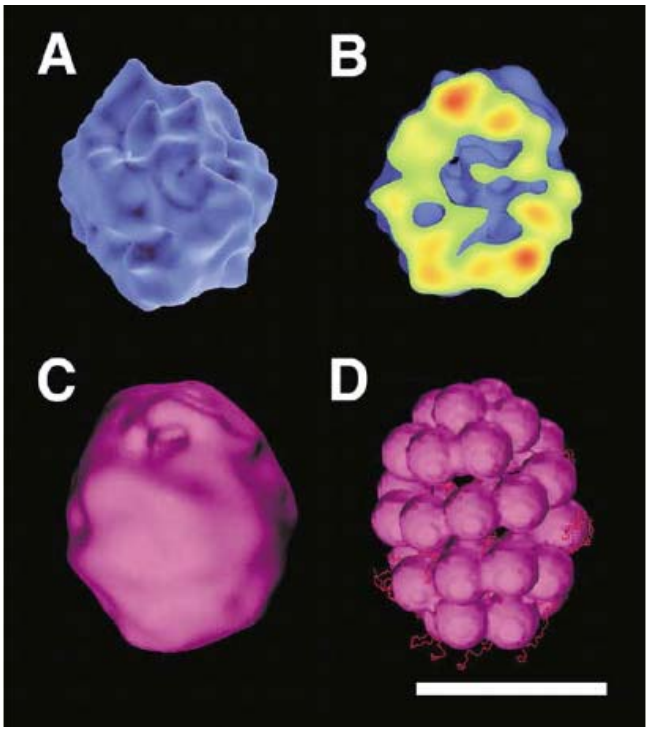

Figure 6: Cryo-EM reconstructions and models of recombinant αB-crystallin and αB-crystallin associated with α-lactalbumin.

phosphorylation on Ser-45 and Ser-59, respectively (Kato *et al.*, 1998; Hoover *et al.*, 2000; Eaton *et al.*, 2001). Phosphorylation on Ser-59 seems to be necessary and sufficient for protection of cardiac myocytes from apoptosis via caspase-3 inhibition (Morrison *et al.*, 2003).

Moreover, it has been shown in human lens epithelial cells that αB-crystallin prevents UVA-induced apoptosis by repressing UVA-induced activation of the RAF/MEK/ERK pathway, whereas αA-crystallin activates the PI3K/AKT pathway to promote survival under the same conditions (Liu *et al.*, 2004b). In addition, over-expression of αB-crystallin in vascular endothelial cells abrogates glucose-induced reactive oxygen species formation, activation of caspase-3, and therefore apoptosis (Liu *et al.*, 2004a). α-crystallins, as well as Hsp27, interact with various intermediate filaments and modulate their assembly and their interactions (Nicholl and Quinlan, 1994; Quinlan *et al.*, 1996; Perng *et al.*, 1999; Perng *et al.*, 2004). In addition, interactions between small Hsps and the actin cytoskeleton have been reported. (Miron *et al.*, 1991; Lavoie *et al.*, 1993a; Lavoie *et al.*, 1993b; Benndorf *et al.*, 1994; Iwaki *et al.*, 1994; Rahman *et al.*, 1995; Wang and Spector, 1996; Gu *et al.*, 1997; Piotrowicz and Levin, 1997; Wieske *et al.*, 2001; Verschuure *et al.*, 2002). In summary, sHsps seem to be able to regulate a plethora of signaling pathways to protect the cell under stress conditions.

sHsp function has also been linked to the ubiquitin-proteasome system, and physical interactions between sHsps and the 20S proteasome have been detected (Boelens *et al.*, 2001). While α-crystallin decreases peptide hydrolyzing activities for some substrates, it protects the trypsin-like activity of the proteasome against oxidative inactivation (Wagner and Margolis, 1995; Conconi *et al.*, 1998; Conconi *et al.*, 1999; Boelens *et al.*, 2001; Ito *et al.*, 2002). Hsp27 binds to the 26S

proteasome and to a polyubiquitinated substrate (Parcellier *et al.*, 2003). In addition, αB-crystallin may recruit the F-box protein, FBX4, an adaptor molecule for the ubiquitin ligase SCF, and promote substrate ubiquitination (den Engelsman *et al.*, 2003; den Engelsman *et al.*, 2004). Not surprisingly, then, specific diseases have been associated with mutations in α-crystallins (Litt *et al.*, 1998; Vicart *et al.*, 1998) and sHsps have been identified in glial inclusions in several tautopathies (Litt *et al.*, 1998; Vicart *et al.*, 1998; Dabir *et al.*, 2004; Richter-Landsberg and Bauer, 2004). Together, these data suggest an important role for the family of small heat shock proteins in protein folding, degradation, and protection against stress.

1.5. CFTR

The Cystic Fibrosis Transmembrane conductance Regulator (CFTR) gene encodes a 1480 amino acid membrane glycoprotein (Riordan *et al.*, 1989), and the protein belongs to the ATP-binding cassette (ABC) transporter superfamily (Higgins *et al.*, 1988; Higgins, 1989). CFTR functions as a cAMP regulated chloride channel in the apical membrane of epithelial cells, including those of airways, pancreas, intestine, and kidney (Jilling and Kirk, 1997; Stanton, 1997; Kopito, 1999; Riordan, 1999; Bertrand and Frizzell, 2003). CFTR is composed of two membrane-spanning domains (MSD1 and MSD2), each comprising six transmembrane segments, two nucleotide binding domains (NBD1 and NBD2), and a central regulatory (R) domain (see Figures 7 and 8).

Figure7: Schematic of CFTR domain topology.

N=N-terminus, C=C-terminus, MSD=Membrane spanning domain, NBD=Nucleotide binding domain, R=Regulatory domain

(adapted from McCarty, 2000).

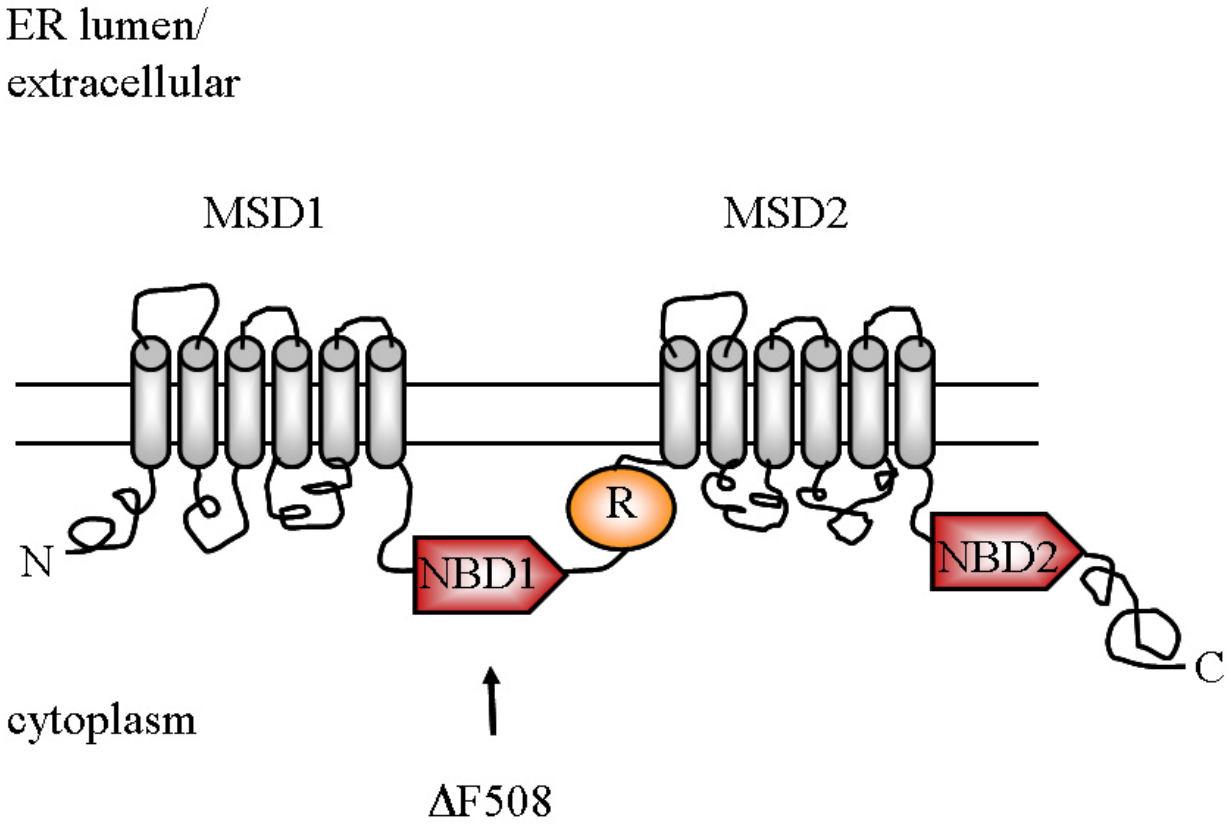

Figure 7: Schematic of CFTR domain topology.

Figure 8: Structural fold of mouse CFTR NBD1 with bound ATP.

This figure depicts the tertiary structure of the NBD1 of mouse CFTR bound to ATP. α-helices are represented in purple, extended β-sheets in yellow, turns in cyan, and coils in white. The position of the residue deleted in most cases of CF, F508, is illustrated in dark blue, and the position of ATP in red.

(Lewis *et al.*, 2004; modified with VMD (Visual Molecular Dynamics), Humphrey *et al.*, 1996).

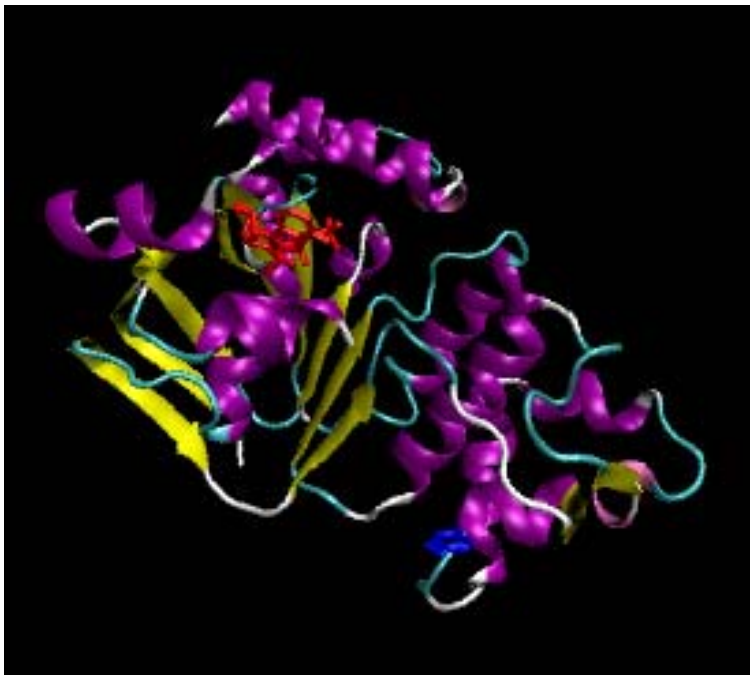

Figure 8: Structural fold of mouse CFTR NBD1**.**

CFTR channel gating depends on ATP binding to the NBDs (see Figure 8) and hydrolysis (Carson *et al.*, 1995; Gunderson and Kopito, 1995; Ikuma and Welsh, 2000; Vergani *et al.*, 2005). Mutations within the gene lead to cystic fibrosis (CF), one of the most frequent autosomal, recessive disorders in individuals of European descent. Although more than 1000 mutations in the gene encoding CFTR have been discovered (http://www.genet.sickkids.on.ca/cftr/), the deletion of the phenylalanine at position 508 within NBD1, "ΔF508-CFTR" (see Fig. 8) is the most common mutation associated with cystic fibrosis (Kerem *et al.*, 1989; Riordan *et al.*, 1989) and cells containing only this mutated variant lack the protein at the plasma membrane (Cheng *et al.*, 1990). During CFTR biogenesis, NBD1 is folded co-translationally while NBD2 undergoes a post-translational folding mechanism that depends on the folded NBD1 (Du *et al.*, 2005). After translocation into the ER, the folding of the core-glycosylated, endoH-sensitive, 140-kD precursor (referred to as band "B" on SDS-PAGE gels) is assisted by cytoplasmic and lumenal chaperones and monitored by ERQC. In mammalian cells, interactions with the Hsp40s Hdj1 or Hdj2 and the NEF HspBP1 facilitate the Hsp70-dependent biosynthesis of CFTR; CFTR biogenesis is also impacted by Hsp90 and CHIP E3 ligase (see above) in mammals (Strickland *et al.*, 1997; Meacham *et al.*, 1999; Choo-Kang and Zeitlin, 2001; Connell *et al.*, 2001; Meacham *et al.*, 2001; Farinha *et al.*, 2002; Alberti *et al.*, 2004). Yet another Hsp40, Csp1, stabilizes immature CFTR by binding to the N-terminus and regulatory domain of CFTR (Zhang *et al.*, 2002a). Finally, the ER localized chaperone, calnexin, interacts with the immature form of CFTR and ΔF508-CFTR (Pind *et al.*, 1994; Okiyoneda *et al.*, 2004). Together, these data indicate that molecular chaperones play an essential role in the biogenesis of CFTR (also see Table 3 for complete list of CFTR-interacting chaperones).

Table 3: CFTR interacting chaperones and chaperone-cofactors.

	Subcellular localization	Interaction with CFTR
Hsp70	Cytoplasm	Regulates CFTR maturation and degradation
Hdj1/2 (Hsp40)	Cytoplasm	Promotes CFTR maturation
Csp1 (Hsp40)	Cytoplasm	Stabilizes immature CFTR
CHIP (E3 ligase)	Cytoplasm	Promotes CFTR degradation
HspBP1 (NEF)	Cytoplasm	Promotes CFTR maturation
Hsp90	Cytoplasm	promotes CFTR maturation
Calnexin	ER	binds immature CFTR

The ΔF508-CFTR mutant fails to reside at the apical plasma membrane because its folding is severely impaired (Qu and Thomas, 1996; Qu *et al.*, 1997). This prevents ER export and leads to its degradation via ERAD (Cheng *et al.*, 1990; Kartner *et al.*, 1992; Yang *et al.*, 1993; Lukacs *et al.*, 1994; Ward and Kopito, 1994; Jensen *et al.*, 1995; Ward *et al.*, 1995; Kreda *et al.*, 2005). The folding of the wild type protein is also inefficient, leading to the degradation of ~80 % of the protein (Cheng *et al.*, 1990). However, it has been suggested that these values might be overly high and arise due to over-expression of CFTR in heterologous systems (Cheng *et al.*, 1990; Kalin *et al.*, 1999; Varga *et al.*, 2004). But, even in cell lines that synthesize endogenously low levels of CFTR a similarly inefficient maturation has been observed (Lukacs *et al.*, 1994; Ward and Kopito, 1994). Also, an effect of the immortalization of cell lines on maturation efficiency can't be excluded (Kopito, 1999). By comparison, the assembly of the acetylcholine receptor proceeds with high efficiency in a primary muscle cell culture, but it is severely hampered in established cell lines (Merlie and Lindstrom, 1983; Ross *et al.*, 1987), although, another member of the ABC transporter family, P-glycoprotein, matures with high efficiency in HEK293 cells (Loo and Clarke, 1997). Importantly, this issue may be finally settled because a very recent study on wild type CFTR and ΔF508-CFTR expression pattern in native tissues supports the hypothesis that defective protein processing is the major pathogenic mechanism in CF (Kreda *et al.*, 2005).

Regardless of the efficiency of wild type CFTR maturation, the ubiquitin-proteasome pathway has been identified as the degradative machinery responsible for proteolysis of wild type and ΔF508-CFTR in mammals (Denning *et al.*, 1992; Jensen *et al.*, 1995; Ward *et al.*, 1995; Xiong *et al.*, 1999; Zhang *et al.*, 2001; Gelman *et al.*, 2002; Lenk *et al.*, 2002; Younger *et al.*, 2004).

Export of properly folded CFTR from the ER and its transport to the Golgi in some cell lines may occur in a COPII-dependent fashion (Yoo *et al.*, 2002; Wang *et al.*, 2004), but only the wild type protein obtains the Golgi-specific modification of complex, endoH-resistant oligosaccharide chains, increasing its molecular weight to 160 kD (referred to as band "C" on SDS-PAGE gels, see Figure 9); however, ΔF508-CFTR never reaches this mature state under physiological conditions, indicating a block in ER exit (Lukacs *et al.*, 1994; Ward and Kopito, 1994). This block in ER exit can be partially suppressed by treating CFTR-expressing cells with chemical chaperones or by growth at lower temperatures (Denning *et al.*, 1992; Sato *et al.*, 1996). These data indicate that the deletion of F508 leads to a temperature-sensitive defect in the folding pathway of CFTR. The rescued mutant CFTR, though, exhibits a much shorter half life in post-Golgi compartments than the wild type protein due to increased susceptibility to ubiquitination and lysosomal degradation (Zhang *et al.*, 1998; Benharouga *et al.*, 2001; Sharma *et al.*, 2001; Sharma *et al.*, 2004). These results suggest that the misfolding and the complete absence of mutated CFTR from the plasma membrane in cystic fibrosis are major disease-causing defects. Therefore, facilitation of maturation and stabilization at the plasma membrane might be promising therapeutic targets.

It is important to note that CFTR residence at the plasma membrane is not sufficient for channel activity: Phosphorylation of the R-domain by protein kinase A (PKA) seems to be a prerequisite for CFTR channel activity and it is thought to render the protein sensitive to stimulation via ATP (Gadsby and Nairn, 1999; Riordan, 2005). CFTR chloride-conductance is also regulated by protein-protein interactions. At the apical plasma membrane, CFTR exists in a complex together with E3KARP or EBP50/NHERF1 and ezrin. This complex localizes PKA near the CFTR R-

Figure 9: Schematic of CFTR traversing the secretory pathway.

CFTR is co-translationally translocated into the ER and inserted into the ER membrane. In the ER, CFTR is core-glycosylated and folded. ER quality control may detect misfolded CFTR and target it for degradation via the 26S proteasome. If folding succeeds, CFTR is transported to the Golgi, where it matures to the C-form. CFTR then traffics to the plasma membrane. Wild type CFTR can be internalized into endosomes and may recycle back to the plasma membrane. However, plasma membrane quality control mechanisms might recognize misfolded CFTR at the endosome and subject it to degradation via the lysosome (Riordan, 2005). 26S=26S proteasome, B-form=immature, core glycosylated (ER) from of CFTR, C-form=maturely glycosylated CFTR. Blue lines denote CFTR at different stages during the secretory pathway, gray line represents CFTR mRNA. Membrane bound organelles are shown in beige and are specifically labeled within the figure, transport vesicles are depicted as beige circles.

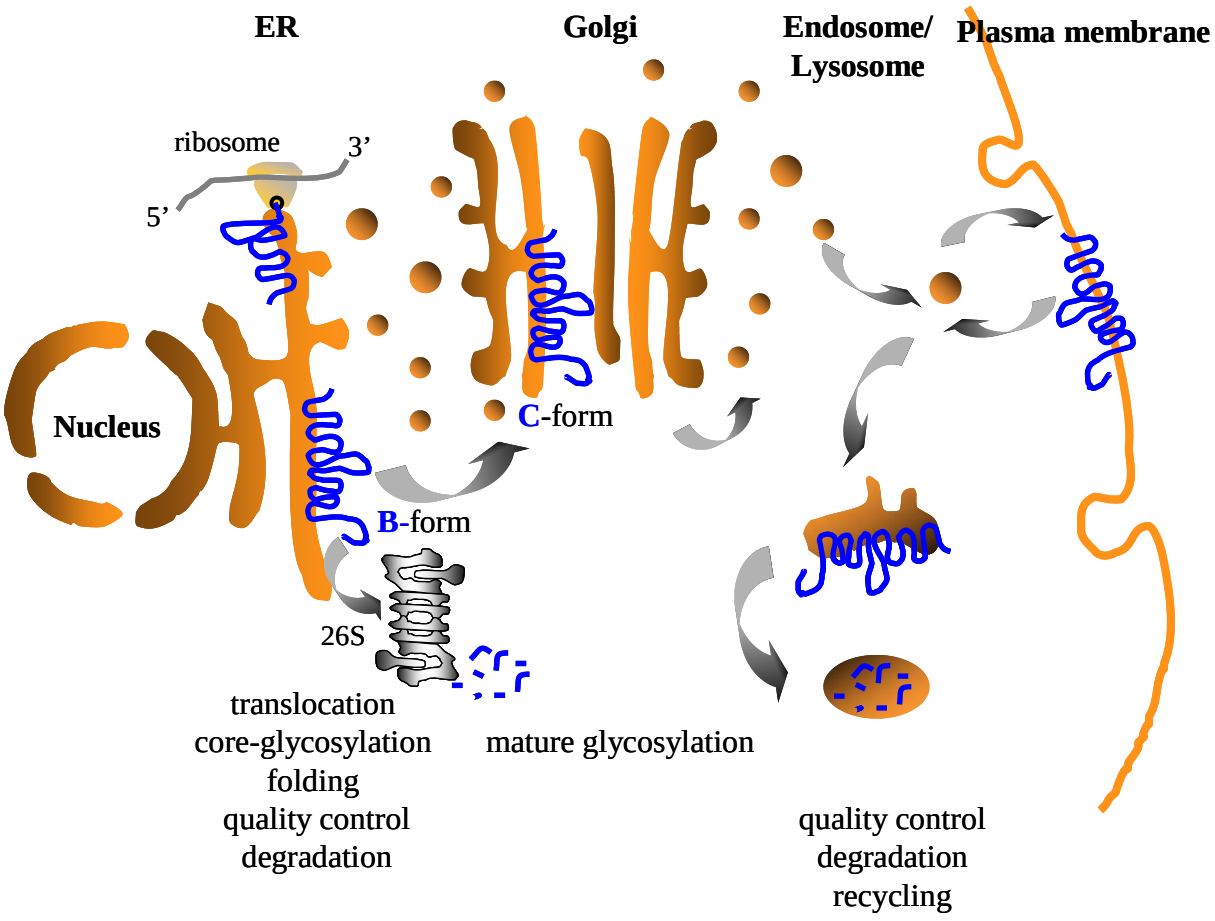

Figure 9: Schematic of CFTR traversing the secretory pathway.

domain, and connects CFTR to the cytoskeleton. This, in turn, contributes to the regulation of the channel activity and may stabilize CFTR at the apical plasma membrane (Dransfield *et al.*, 1997; Hall *et al.*, 1998; Short *et al.*, 1998; Wang *et al.*, 1998; Sun *et al.*, 2000a; Sun *et al.*, 2000b). These data indicate that the regulation of CFTR channel activity is complex and further suggests that a multi-factorial therapeutic approach might be required to successfully treat CF patients.

1.6. YEAST AS A MODEL SYSTEM

One drawback of the mammalian cell culture system is the inability to specifically and rapidly disable molecular chaperones. Methods common to investigate the chaperone requirements for cellular processes include administration of drugs to impact Hsp activity and over-expression of chaperones or their cofactors. Treatment with Hsp90 inhibiting ansamycin antibiotics, for example, can induce cell stress and chaperone or co-chaperone over-expression might lead to non-specific effects on cellular processes (Lawson *et al.*, 1998; Zou *et al.*, 1998). These pleiotropic effects can lead to controversial results. For example, the recruitment of the ubiquitin ligase CHIP shifts protein biogenesis toward the degradation pathway (Schneider *et al.*, 1996; Connell *et al.*, 2001; Meacham *et al.*, 2001); but CHIP has also been shown to promote Hsp70-dependent folding when over-expressed (Kampinga *et al.*, 2003). Also, inhibition of Hsp90 via administration of the ansamycin antibiotic geldanamycin leads to enhanced proteolysis of CFTR

in mammalian cell lines (Loo *et al.*, 1998), whereas the same drug caused stabilization of CFTR in an in vitro system (Fuller and Cuthbert, 2000).

Many aspects of protein synthesis, trafficking, and degradation are conserved between yeast and mammals. In addition, the budding yeast *Saccharomyces cerevisiae* offers a variety of genetic and biochemical tools enabling us to investigate the impact of chaperones on these pathways more specifically. In fact, the Brodsky laboratory showed that CFTR is an ERAD substrate in yeast as it is in mammals, and that the degradation of CFTR in yeast requires Ssa1p, a cytosolic Hsp70, and the function of one of two redundant cytosolic Hsp40 homologs, Ydj1 or Hlj1 (Zhang *et al.*, 2001; Youker *et al.*, 2004). Moreover, Youker *et al.* were able to address the conflicting reports on Hsp90 engagement in folding versus degradation by assessing CFTR stability in a yeast strain harboring a temperature sensitive mutation in a yeast Hsp90 ortholog upon shift to the non-permissive temperature. In agreement with Loo *et al.* (Loo *et al.*, 1998), they found that Hsp90 facilitates CFTR biogenesis (Youker *et al.*, 2004). Several other labs have also taken advantage of the yeast system and contributed to the further understanding of the mechanism of CFTR degradation (Kiser *et al.*, 2001; Fu and Sztul, 2003; Gnann *et al.*, 2004). Yeast have also been used to examine the biogenesis of other medically-relevant proteins (Coughlan and Brodsky, 2003). Together, these facts render yeast a useful model organism to study the conserved pathways of protein biogenesis, folding, and degradation.

1.7. THESIS OVERVIEW

Among other cellular processes, molecular chaperones are involved in protein biogenesis, folding, maturation, and degradation. Particularly, chaperone requirements for the folding and degradation of soluble, secretory proteins and integral membrane proteins have recently been compared and are distinct from each other (Strickland *et al.*, 1997; Meacham *et al.*, 1999; Hill and Cooper, 2000; Choo-Kang and Zeitlin, 2001; Meacham *et al.*, 2001; Zhang *et al.*, 2001; Farinha *et al.*, 2002; Kabani *et al.*, 2003; Taxis *et al.*, 2003; Alberti *et al.*, 2004; Huyer *et al.*, 2004; Youker *et al.*, 2004). In comparison, relatively few reports have addressed the chaperone requirements concerning the biogenesis, folding, and degradation of distinct polypeptides that reside in the cytoplasm (Schneider *et al.*, 1996; Brodsky *et al.*, 1998; Kim *et al.*, 1998b; Kampinga *et al.*, 2003).

In this work, I describe my characterization of the chaperone requirements for the biogenesis, maturation, and degradation of a cytosolic substrate, firefly luciferase, and of an integral membrane protein, the cystic fibrosis transmembrane conductance regulator, in yeast. I have also examined the role of one chaperone, αA-crystallin, on the biogenesis of CFTR in mammals.

2. DISTINCT BUT OVERLAPPING FUNCTIONS OF HSP70, HSP90, AND AN HSP70 NUCLEOTIDE EXCHANGE FACTOR DURING PROTEIN BIOGENESIS IN YEAST

2.1. INTRODUCTION

In addition to their catalysis of post-translational events, several lines of evidence indicate that Hsp70 and Hsp40 molecular chaperones also play critical roles during protein translation. First, two Hsp70 classes in yeast, Ssb and Ssz, and an Hsp40, known as Zuotin, form a stable complex and interact with ribosomes and nascent polypeptide chains; consistent with their role in translation, each of the individual mutant strains are hyper-sensitive to translation poisons, and over-expression of a putative elongation factor suppresses *ssb* temperature sensitivity (Nelson *et al.*, 1992; Pfund *et al.*, 1998; Yan *et al.*, 1998; Gautschi *et al.*, 2002; Hundley *et al.*, 2002). Second, another cytoplasmic Hsp40, Sis1p, associates with ribosomes, and deletion of the ribosomal proteins L35 and L39 rescues the temperature sensitivity of a *sis1* mutant; *sis1* mutants also exhibit aberrant polysome profiles (Zhong and Arndt, 1993). Third, deletion of *FES1*, a yeast NEF for Hsp70 that is the HspBP1 homolog, confers temperature-sensitive growth, aberrant polysome profiles, and sensitivity to a translation poison (Kabani *et al.*, 2002a). Fourth, the major Hsp70 in yeast, Ssa1p, associates with ribosomes and Sis1p (see above), and *ssa1* mutants exhibit a general translational defect (Horton *et al.*, 2001); consistent with these

data, Brodsky *et al.* showed that Ydj1p, which is an Hsp40 partner for Ssa1p and a member of the Hsp90 complex, is required for efficient translation of green fluorescent protein (GFP) and firefly luciferase (FFLux) in yeast (Brodsky *et al.*, 1998). And finally, it was also reported that Ssa1p associates with the poly(A)-binding protein (Pab1p), and that the association between Pab1p and the eIF4G translation initiation factor was reduced in the *ssa1* mutant (Horton *et al.*, 2001). However, because the eIF4E-eIF4G-Pab1p complex has been proposed to stabilize mRNAs by blocking the activity of the yeast mRNA de-capping enzyme (Schwartz and Parker, 2000; Vilela *et al.*, 2000), and because mammalian Hsp70 has been shown to bind to mRNA stabilization motifs (Henics *et al.*, 1999), the general *ssa1*-dependent translation defect might have arisen from a de-stabilization of untranslated messages.

Given the profound roles of Hsp70, Hsp90, and HspBP1 on protein maturation in mammals, it is surprising that the impact of Ssa1p (Hsp70), Hsp90, and the NEF for Ssa1p, Fes1p, during the biogenesis and maturation of specific proteins has not been examined in parallel in yeast. In this chapter, I show distinct but partially overlapping requirements for these factors during the biogenesis and degradation of FFLux. These studies were aided by the availability of specific mutations in the genes encoding each factor, and my data indicate the complexity with which chaperones and chaperone-partners mediated protein biogenesis.

2.2. MATERIALS AND METHODS

2.2.1. Yeast strains, plasmids, and molecular methods

The yeast strains used in this study were: *JN516* (referred to as wild type or *SSA1*), *MATα leu2-3, 112 his3-1 ura3-52 trp1Δ1 lys2 ssa2::LEU2 ssa3::TRP1 ssa4::LYS2; ssa1-45* (or Hsp70 mutant), *MATα leu2-3, 112 his3-1 ura3-52 trp1Δ1 lys2 ssa1-45 ssa2::LEU2 ssa3::TRP1 ssa4::LYS2* (Becker *et al.*, 1996); *RSY801* (referred to as wild type or *FES1*), *MATa ura3-52 leu2-3, 112 ade2-101; fes1Δ* (or Fes1p mutant*), MATa ura3-52 leu2-3, 112 ade2-101 fes1::KanMX4* (Kabani *et al.*, 2002a); *HSP82* (Hsp90 wild type) *MATa ade1-1 leu2-3,112 his3-11, 15 trp1-1 ura3-1 can1-100 hsc82::LEU2 hsp82::LEU2 pTGDHSP82 (TRP); hsp82* (referred to as Hsp90 mutant) *G313N MATa ade1-1 leu2-3, 112 his3-11, 15 trp1-1 ura3-1 can1-100 hsc82::LEU2 hsp82::LEU2 pTGDHSP82 G313N (TRP)* (Bohen and Yamamoto, 1993; Youker *et al.*, 2004); *W303* (referred to as *SSE1 and SIS1), MATα ade2-1 his3-11 leu2-3,112 ura3-1 trp1-1 can1-100; E0020* (referred to as *Δsse1*), *MATα his3 leu2 ura3 trp1 msi3::HIS3* (Shirayama *et al.*, 1993); *sis1-85* (Referred to as Sis1p mutant) *MATα ade2-1 his3-11 leu2-3,112 ura3-1 trp1-1 can1-100 sis1::HIS3 HA (C-term) sis1-85 (Leu/CEN)* (Zhong and Arndt, 1993).

Cells were grown either in complete medium (YP), synthetic complete medium lacking uracil (Sc-ura) but containing raffinose, glucose, or galactose at a final concentration of 2% as the

carbon sources at the indicated temperatures with vigorous shaking. The gene encoding firefly luciferase was in vitro transcribed from plasmid pGEM-luc (Promega). FFLux was expressed in yeast from a modified pRS316 CEN/ARS vector under the control of the GAL1-10 promoter (Brodsky *et al.*, 1998). Plasmids were introduced into host strains using lithium acetate-mediated transformation, and transformants were selected by growth on Sc-ura medium (Rose, 1990).

2.2.2. Preparation of cell extracts for luciferase assays and immunblot analysis, and of RNA for northern analysis, RT-PCR , and mRNA Decay assays

A ~50 ml yeast culture was grown at 26°C for 12 –16 h to an optical density at 600nm (OD) of 1-3 in Sc-ura supplemented with 2% raffinose. The cells were harvested, washed in double-distilled sterile water, and then re-suspended in the same medium at an initial OD of ~0.3. Cells were then re-grown to an OD of 1-3, harvested, washed twice with double-distilled sterile water, re-suspended at an initial OD of ~ 0.8 in the same medium but instead containing 2% galactose to induce FFLux expression. Finally, the yeast were grown in galactose at 30°C and processed at the indicated times.

For immunoblot and northern blot analyses, 60 ODs of cells were harvested and washed once with DEPC (Diethyl Pyrocarbonate; Sigma)-treated water, and the pellets were re-suspended in 200 μl of DEPC-treated water, split, and quick-frozen in liquid nitrogen.

For mRNA decay assays, cells were harvested after growth for 16 h in Sc-ura containing galactose at a final concentration of 2%, and then resuspended to a final OD of 10/mL in Sc-ura supplemented with glucose at a final concentration of 2% to repress FFLux transcription from the *GAL* promoter (Parker *et al.*, 1991). To ensure that transcription was inhibited, 1,10-phenanthroline was also added to a final concentration of 100 μg/ml (Parker *et al.*, 1991). At the indicated time points, duplicate 1ml aliquots of the culture were harvested and quick-frozen in liquid nitrogen. Total RNA was prepared as described above.

Protein extracts for immunoblot analysis were prepared as described previously (Brodsky *et al.*, 1998), and total RNA was isolated as published with minor modifications (Arndt *et al.*, 1995).

2.2.3. Luciferase activity assay

A total of 0.75 ODs of cells were assayed for light production upon incubation with luciferin in an Analytical Luminescence Laboratory (Ann Arbor, MI) Monolight 2010 Luminometer as described previously (Brodsky *et al.*, 1998). All assays were performed in triplicate.

2.2.4. Immunoblot analysis

Samples were loaded onto 12.5% SDS-polyacrylamide gels, and after electrophoresis, the proteins were transferred to nitrocellulose membranes (Schleicher and Schuell, pore diameter of 0.2μm). The antibodies used were raised against FFLux (Cortex Biochem, Inc.) and Sec61p (Stirling *et al.*, 1992). To detect the primary antibody either goat anti-rabbit horseradish peroxidase-conjugated secondary antibody (Amersham Life Sciences) was used, and the complex was visualized using the enhanced chemiluminescence detection kit (Pierce) or ^{125}I-labeled Protein A was added (Amersham Bioscience) and the complexes were detected by phosphorimager analysis. Data were quantified using Kodak 1D (v 3.6; Kodak) or Image Gauge (Fuji Film Science Lab) software.

2.2.5. Northern blot analysis

Total RNA was prepared from one aliquot of thawed cells (see above), and 40 μg were resolved on 0.8% agarose/formaldehyde gels, transferred to Gene Screen Plus membranes (NEN Life Science Products), and hybridized sequentially using ^{32}P-labeled, randomly primed full-length probes produced from a BamH1-Sac1 fragment removed from the gene encoding FFLux, and then a BamH1-HindIII fragment obtained from the *ACT1* gene that encodes yeast actin (obtained from K. Arndt, University of Pittsburgh). Filters were processed as previously described

(Ausubel, 1988), except that the high temperature wash was performed at 55°C for 10 min. Membranes were re-hybridized after the bound probe was removed from the filters by incubation in 0.1xSSC (20xSSC stock solution: 175.3g NaCl, 88.2g $CH_3COONa \cdot 3H_20$/l, adjusted to pH 7.0 with HCl), supplemented with an additional 15mM NaCl and containing 1% SDS for 20 min at 100°C. P-values were calculated via the program at http://faculty.vassar.edu/lowry/t_ind_stats.html.

2.2.6. RT-PCR

Total RNA (prepared as described above) was DNaseI-treated (Ambion) according to the manufacturer's specifications and the DNase and divalent cations were subsequently removed using DNA-free Kit (Ambion). First-strand cDNA synthesis was performed using 2.5 or 5 µg total RNA, M-MLV reverse transcriptase (GibcoBRL), and random primers (Roche) in a 10 µl reaction. A 1 µl aliquot of a 10-fold diluted reverse transcription reaction was amplified (20 cycles: 94°C for 1 min, 55°C for 1 min, 72°C for 1 min) with Taq-Polymerase (Promega) and trace-labeled with ^{32}P labeled dCTP. The primers for firefly luciferase were: 5'- GCCATTCTATCCTCTAGAGG and 3'- TTCACTGCATACGACGATTC. The primers corresponding to the *ACT1* gene were: 5'- GGATTCTGAGGTTGCTGCTT and 3'- CAGTTGGTGACAATACCGTG.

2.2.7. Pulse-chase immuno-precipitation

Pulse-chase immuno-precipitations from ^{35}S-metabolically labeled yeast were performed as published previously (Zhang *et al.*, 2001) using antibody raised against firefly luciferase (Cortex Biochem, Inc.) and Protein A Sepharose (Amersham).

2.2.8. In vitro transcription, mRNA capping, and decapping assay

To prepare the poly(A)-tailed, capped FFLux substrate for the decapping assay, the plasmid pGem-luc was linearized with Sal1 and in vitro transcribed utilizing SP6 MEGAscript™ (Ambion) according to the manufacturer's instructions, and a poly(A)-tail was added (Poly(A) Tailing Kit, Ambion). The quality of the transcript was assessed by agarose gel electrophoresis. The mRNA substrate was then capped with purified vaccinia virus capping enzyme (see below) in the presence of [α-^{32}P]GTP (NEN Life Science Products) and S-adenosylmethionine (Sigma) as described previously (Zhang *et al.*, 1999b). Cap-labeled mRNA was then separated from free nucleotide by G50 RNA spin columns (Roche) and stored at –70°C. The quality of the purified [α-^{32}P]m^{7}GpppN-RNA was confirmed by thin-layer chromatography (TLC) to show that the substrate was free of nucleotide, and the expected size was confirmed by agarose gel electrophoresis followed by phosphorimager analysis of the transferred fragment in relation to RNA standards (Millennium Markers™ –Formamide, Ambion).

Recombinant His-tag vaccinia virus capping enzyme (His_6- D1/D12) was purified from *E.coli* strain BL21 (DE3) provided by C. Wiluzs and S. Shuman (Luo *et al.*, 1995) (UMDNJ-Robert Wood Johnson Medical School and the Sloan-Kettering Institute, respectively) by Ni^{2+}-NTA chromatography and Heparin chromatography as described previously (Shuman, 1990; Zhang *et al.*, 1999b). The activity and thus fractionation of the enzyme was assessed by GMP-enzyme complex formation according to Guo and Moss (Guo and Moss, 1990) after each purification step.

To prepare extracts for the decapping assay, cells were grown in medium containing 2% raffinose as the sole carbon source to an OD_{600} of 0.7-1. The cultures were then switched to medium containing 2 % galactose, so that the growth conditions were identical to those used above, and grown to an OD_{600} of 0.7-1. Yeast cell extracts were prepared and the decapping reaction was performed as described previously (Zhang *et al.*, 1999b). In brief, 20 μg of yeast cell extract were incubated with [α-^{32}P]^{7m}GTP cap-labeled mRNA substrate for the indicated times at 37°C. The reaction products were analyzed by TLC and quantified by phosphorimager analysis using Image Gauge software (Fuji Film Science Lab).

2.3. RESULTS

2.3.1. Firefly luciferase enzymatic activity is compromised in *ssa1, hsp82,* and *fes1* mutant yeast

It was shown previously that the galactose-inducible expression of FFLux was slowed in yeast encoding a mutated form of the cytoplasmic Hsp40, Ydj1p (Brodsky *et al.*, 1998). Thus, I wished to determine whether two molecular chaperones known to interact with Ydj1p, Ssa1p (the primary yeast Hsp70), and Hsp82 (the yeast Hsp90), display a similar effect in FFLux expression after induction; I also examined whether the NEF for Ssa1p, Fes1p, impacted FFLux maturation (Cyr *et al.*, 1992; Kimura *et al.*, 1995; Becker *et al.*, 1996; Kabani *et al.*, 2002a). To this end, the gene encoding FFLux under the control of the same galactose-inducible yeast promoter was transformed into the temperature sensitive *hsp82 G313N* mutant strain, into the temperature sensitive *ssa1-45* mutant strain, and into a strain deleted for *FES1* (*fes1Δ),* as well as into the respective isogenic wild type strains. I chose to perform these assays at the semi-permissive temperature of 30°C because growth defects are not evident in the mutant strains relative to the isogenic wild types at this temperature (not shown). I first observed compromised luciferase activity in each mutant strain relative to wild type yeast after the carbon source had been switched from raffinose to galactose, and noted that the time-course of induction differed significantly in each set of wild type/mutant strains. For example, in the *ssa1-45* mutant, there was a more than 3-fold decrease in activity compared to the wild type 18h after galactose

induction (Figure 10A), and a 4- and 3.5-fold difference in enzymatic activity between the isogenic wild type strains and the *hsp82 G313N* mutant (8 h after FFLux induction) and *fes1Δ* yeast (6 h after FFLux induction), respectively (Figures 10B and C). By comparison, FFLux induction in the *ydj1* mutant previously used was reduced by 2-fold compared to the wild type 10 h after induction (Brodsky *et al.*, 1998).

2.3.2. Firefly luciferase expression is delayed in the *ssa1* mutant and more significantly in the *hsp82* mutant strain

I next wished to determine if the delayed increase and reduced levels of enzymatic activity in the chaperone mutant strains were caused by compromised translation, as observed in *ydj1* mutant yeast (Brodsky *et al.*, 1998), or by a defect in protein folding or another event. To this end, FFLux expression was monitored in the wild type and chaperone mutants by immunoblot analysis after the carbon source had been switched from raffinose to galactose. The levels of Sec61p, an integral ER membrane protein were examined in parallel and served as a loading control. I first monitored FFlux expression levels for 18 h after FFLux induction in the wild type and in the *ssa1-45* mutant strain and observed a delayed increase in FFlux induction in the mutant (Figure 11). At 18 h more than twice as much FFLux was present in wild type yeast compared to the *ssa1-45* mutant strain; the difference in FFLux enzymatic activity at this time point was approximately the same. However, at later time points a higher percentage of the protein synthesized in the wild type versus *ssa1-45* mutant strain was active (data not shown),

Figure 10: FFlux activity is delayed in the *ssa1* and *hsp82* mutant and in the *fes1* deletion strains. A. FFLux activity is indicated in relative light units (RLU), and data represent the means from 2 independent sets of experiments and are plotted as a function of time (h): *SSA1* wild type yeast, closed blue circles; *ssa1* mutant strain, open purple circles. B. FFLux activity is shown in relative light units (RLU) and the means from 3 independent sets of experiments are plotted as a function of time (h): *FES1* wild type yeast, closed blue circles; *fes1* deletion, open purple circles. Vertical bars indicate the standard error. C. FFLux activity is shown in relative light units (RLU) and the means from 3 independent sets of experiments are plotted as a function of time (h): *HSP82* wild type yeast, closed blue circles; *hsp82* mutant strain, open purple circles. Vertical bars indicate the standard error.

A

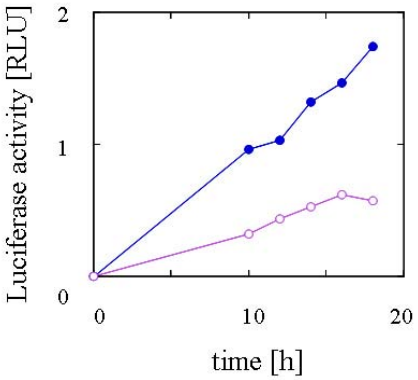

B

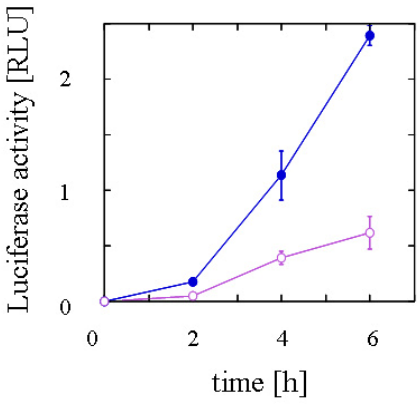

C

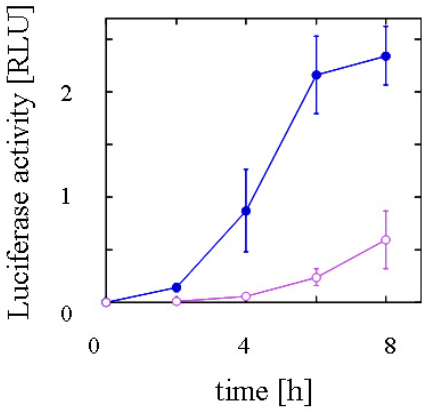

Figure 10: FFLux activity is delayed in the *ssa1* and *hsp82* mutant and the *fes1* deletion strain.

Figure 11: FFlux protein induction is delayed in *ssa1* mutant yeast. A. A western blot is shown depicting FFLux and Sec61p (as a control) protein levels in *SSA1* wild type yeast and in the *ssa1-45* mutant strain after growth in raffinose (repressing conditions, “R”), immediately after switch to galactose-containing medium (“G”), and at the indicated times (in h) after induction. B. The amounts of FFLux from 2 independent sets of experiments were plotted as a function of time (h). *SSA1* wild type yeast, closed blue circles; *ssa1-45* mutant strain, open purple circles.

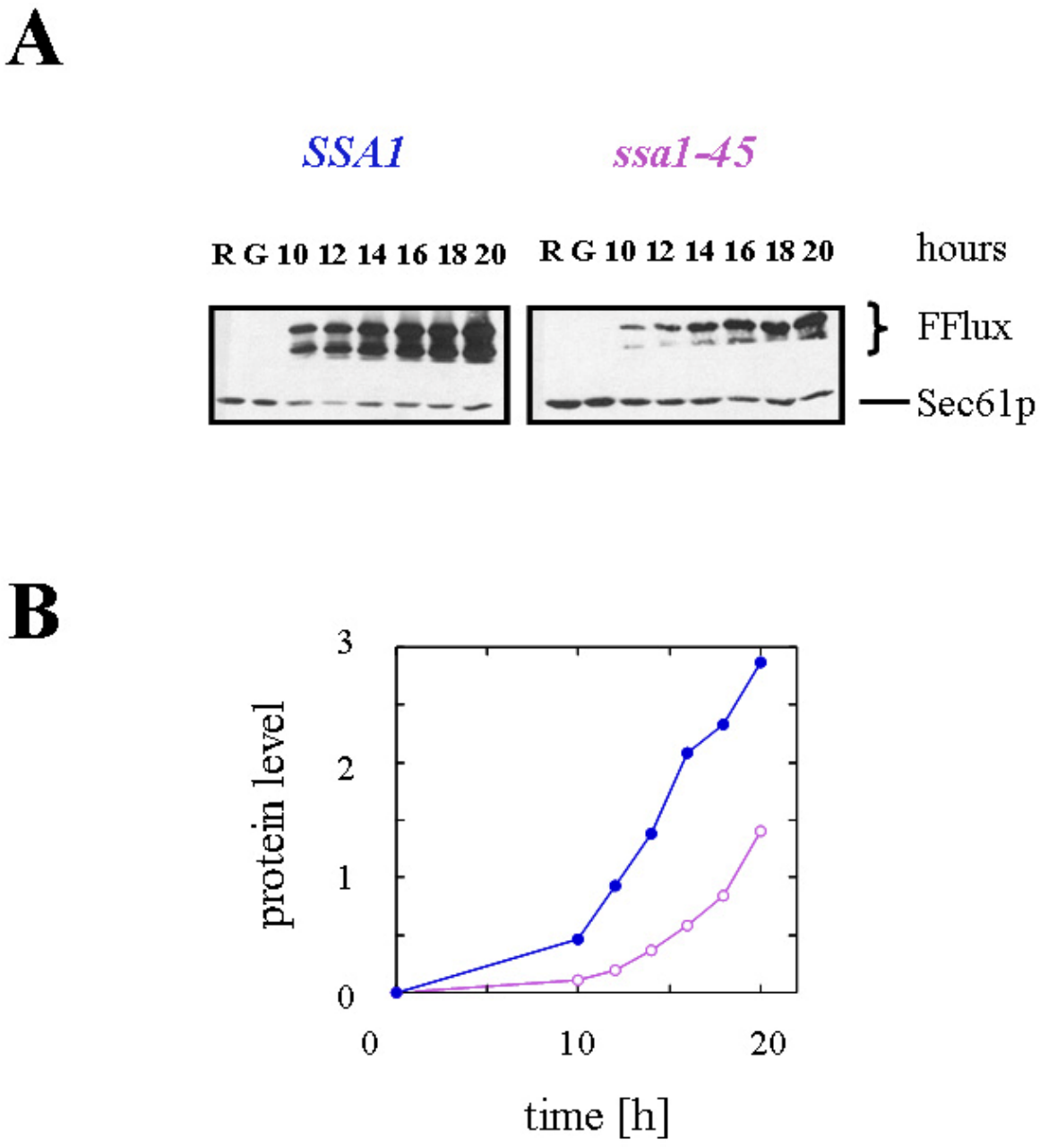

Figure 11: FFlux protein induction is delayed in *ssa1* mutant yeast**.**

suggesting that Ssa1p is important for FFLux protein folding. Overall, I concluded that Ssa1p plays a previously uncharacterized role in FFLux biosynthesis, as well as a role in protein folding, as previously described (Kim *et al.*, 1998b). In contrast, FFlux expression in the *fes1Δ* strain increased over time, even reaching a level somewhat higher than that in the wild type strain (Figure 12). This is in contrast to the decreased amount of FFLux activity observed in the *fes1Δ* strain (Figure 10B); therefore, these data indicate a role for the yeast Hsp70 NEF in protein folding, and are consistent with the finding that Ssa1p is required for maximal FFLux folding (see above). A recent report also indicates a role for Fes1p in protein folding in yeast (Shomura *et al.*, 2005). Similarly, several lines of evidence also support a role for mammalian NEFs in protein folding (Kanelakis *et al.*, 1999; Luders *et al.*, 2000; Alberti *et al.*, 2004). I also noted that a mild, general translation defect in *fes1Δ* yeast was observed in a previous study from the Brodsky laboratory (Kabani *et al.*, 2002a); however, this effect was not evident when FFLux synthesis was examined, suggesting that the translation defect might be protein-specific, as reported for the Ydj1p-dependence on protein translation (Brodsky *et al.*, 1998). The strongest defect in FFLux induction was observed in the *hsp82* mutant yeast strain: Only ~25% of FFLux was present in the mutant compared to wild type cells 8 h after induction (Figure 13). In this case, the difference in FFLux expression levels and in enzymatic activity between the *hsp82* mutant and the wild type strain are comparable, suggesting that yeast Hsp90 plays a significant role during FFLux synthesis, but a less profound role during the folding of newly translated FFLux. This second conclusion is consistent with observations in mammalian cells in which Hsp90 was shown to be involved in the refolding of denatured FFLux but not in the folding of newly synthesized FFLux (Schneider *et al.*, 1996).

Figure 12: FFlux protein induction is equally efficient in *FES1* wild type and *fes1* deletion strains. A. A western blot is shown that measures FFLux and Sec61p (as a control) protein levels in *FES1* wild type yeast and in the *fes1* deletion strain after the growth medium was switched to galactose. B. The amounts of FFLux from 3 independent sets of experiments were plotted as a function of time (h). *FES1* wild type yeast, closed blue circles; *fes1Δ* strain, open purple circles. Vertical bars indicate the standard error.

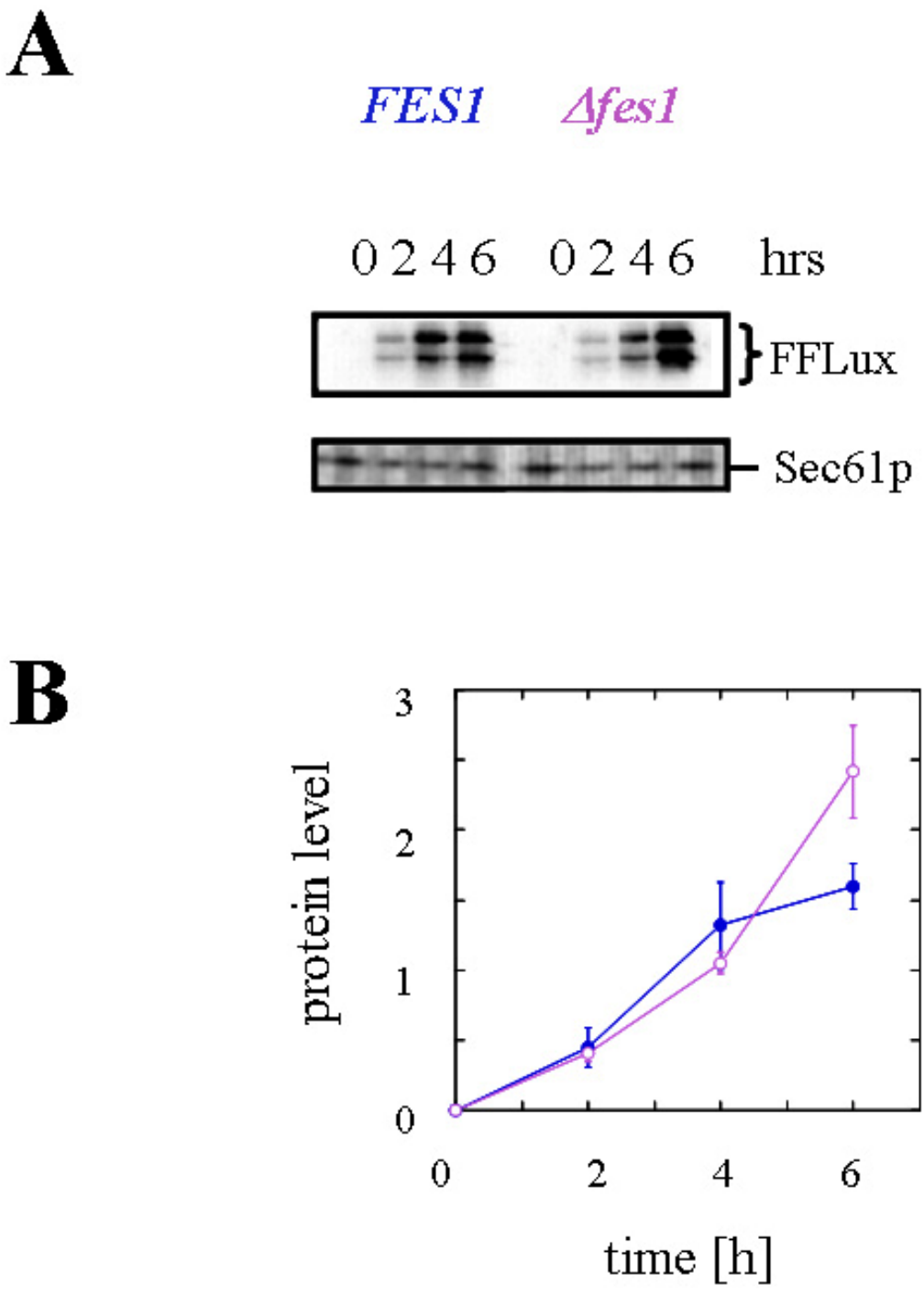

Figure 12: FFlux protein induction is equally efficient in *FES1* wild type and *fes1* deletion strains.

Figure 13: FFlux protein induction is delayed in *hsp82* mutant yeast. A. A western blot is shown that measures FFLux and Sec61p (as a control) protein levels in *HSP82* wild type yeast and in the *hsp82 G313N* mutant strain. B. The amounts of FFLux from 3 independent sets of experiments were plotted as a function of time (h). *HSP82* wild type yeast, closed blue circles; *hsp8*2 mutant strain, open purple circles. Vertical bars indicate the standard error.

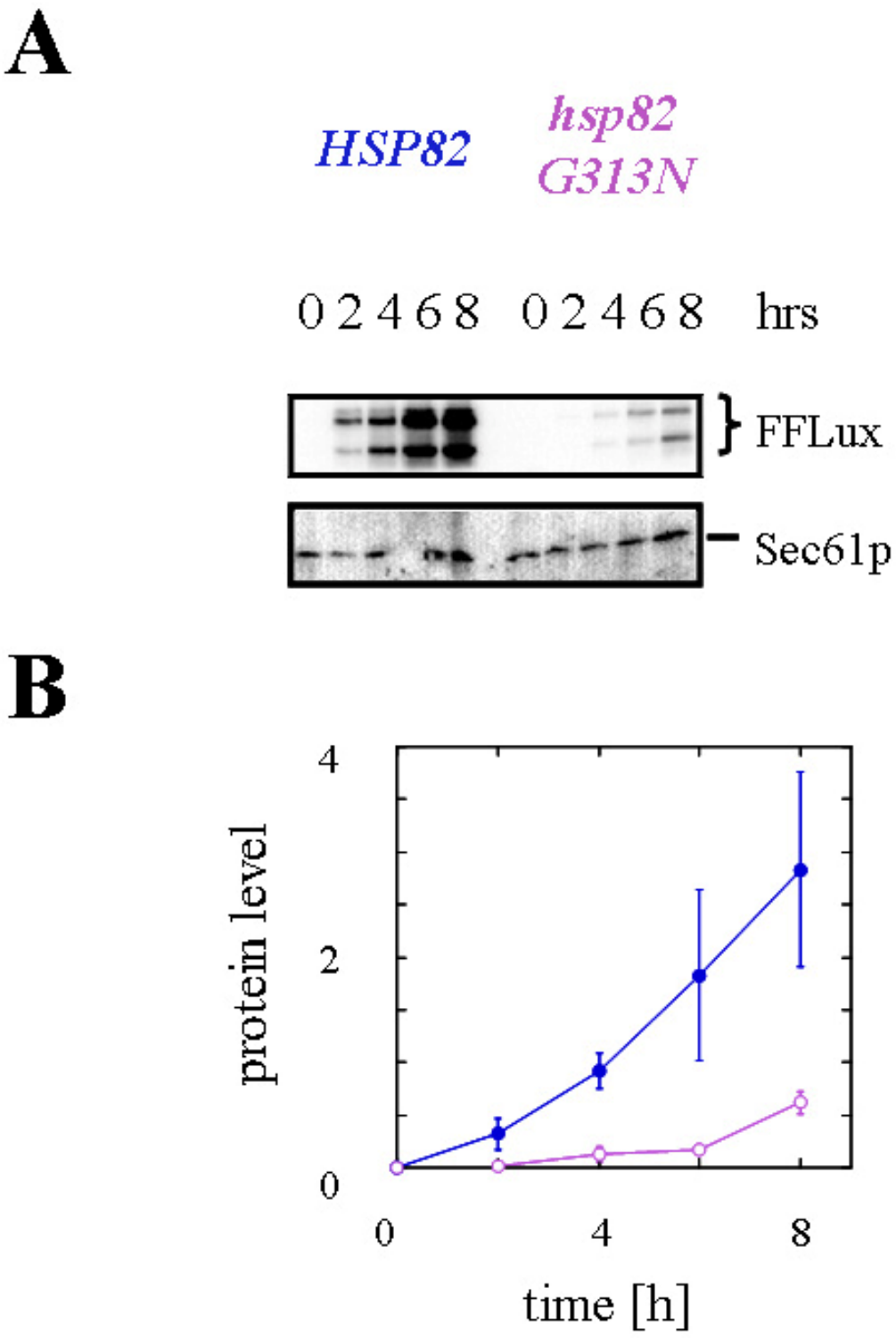

Figure 13: FFlux protein induction is delayed in *hsp82* mutant yeast.

I also tested whether cells mutated for two other chaperones affect FFLux expression: Sis1p is an Hsp40 involved in translation initiation that interacts with Ssa1p on the translating ribosome (Zhong and Arndt, 1993; Horton *et al.*, 2001), and Sse1p, a yeast Hsp110, interacts with Ydj1p and is a component of the Hsp90 complex (Kimura *et al.*, 1995; Goeckeler *et al.*, 2002). However, no effect was observed on FFLux enzymatic activity or induction in either the temperature sensitive *sis1* mutant or in *sse1Δ* cells (data not shown). These data suggest that the results described above were not due to global affects on chaperone function nor were they the result of incubating thermosensitive chaperone mutants at semi-permissive temperatures.

2.3.3. Firefly luciferase degradation is significantly accelerated in the *ssa1* mutant strain, but only modestly in *hsp82* mutant yeast

Hsp70s and Hsp90s have been implicated in the regulation of protein stability, and specifically, the rate of degradation of potentially mis-folded proteins changes in the *ssa1-45* and *hsp82 G313N* mutants (Schneider *et al.*, 1996; Strickland *et al.*, 1997; Imamura *et al.*, 1998; Loo *et al.*, 1998; Verma *et al.*, 2000; Connell *et al.*, 2001; Gusarova *et al.*, 2001; Meacham *et al.*, 2001; Murata *et al.*, 2001; Zhang *et al.*, 2001; Farinha *et al.*, 2002; Kampinga *et al.*, 2003; Huyer *et al.*, 2004; Youker *et al.*, 2004). Therefore, the decreased FFLux protein levels observed in these strains might have arisen in part from accelerated degradation. To determine whether FFLux is less stable in *ssa1-45* and *hsp82 G313N* yeast, the wild type and the mutant strains were transformed with the inducible FFLux gene and a pulse-chase analysis was performed at 30°C 16

and 6 h, respectively, after the carbon source had been switched from raffinose to galactose. As shown in Figure 14, FFLux is degraded significantly faster in the *ssa1-45* mutant strain compared to the wild type strain, with only 20 % of the protein remaining after a 90 min chase compared to ~85 % in wild type yeast. In contrast, FFLux was largely stable in both wild type and *fes1Δ* yeast (Figure 15). Similarly, the *hsp82 G313N* mutant yeast exhibited a minor decrease in FFLux stability, with ~70% protein remaining after 90 min while FFLux levels remained relatively unaltered in the wild type strain (Figure 16). From these results we conclude that FFLux is destabilized significantly only in the *ssa1-45* mutant, which further contributes to its decreased, steady-state expression (Figure 11).

2.3.4. Firefly luciferase mRNA induction is compromised in the *ssa1* mutant strain and in the *hsp82* mutant strain

To determine if defects in FFlux expression in the *ssa1-45* and *hsp82 G313N* mutant yeast result from lower levels of FFLux mRNA, I prepared total RNA from wild type yeast and the *ssa1-45* and *hsp82 G313N* mutants after galactose-mediated induction and performed northern blot and RT-PCR analyses to quantify FFLux mRNA levels over time (Figures 17 and 18). Whereas the wild type strains exhibited a pronounced increase in FFlux mRNA after galactose induction, whose time-courses were in-line with FFLux activity and protein levels, there was a 4-fold reduction in FFlux mRNA levels in the *ssa1-45* mutant versus the wild type (Figure 17B). In comparison, the difference in the FFLux mRNA levels between the *Hsp82* wild type and the

Figure 14: FFLux protein degradation is enhanced in the *ssa1-45* mutant strain. A. Rates of FFlux degradation were determined by pulse-chase immuno-precipitation in *SSA1* wild type yeast and the *ssa1-45* mutant strain after addition of cycloheximide. A. FFLux protein levels were quantified from 4 independent sets of experiments and averaged. All values were obtained after standardization to the levels detected directly after cycloheximide addition (0 min). Closed blue circles represent *SSA1* wild type protein levels, open purple circles represent *ssa1* mutant protein levels. Vertical bars indicate the standard error.

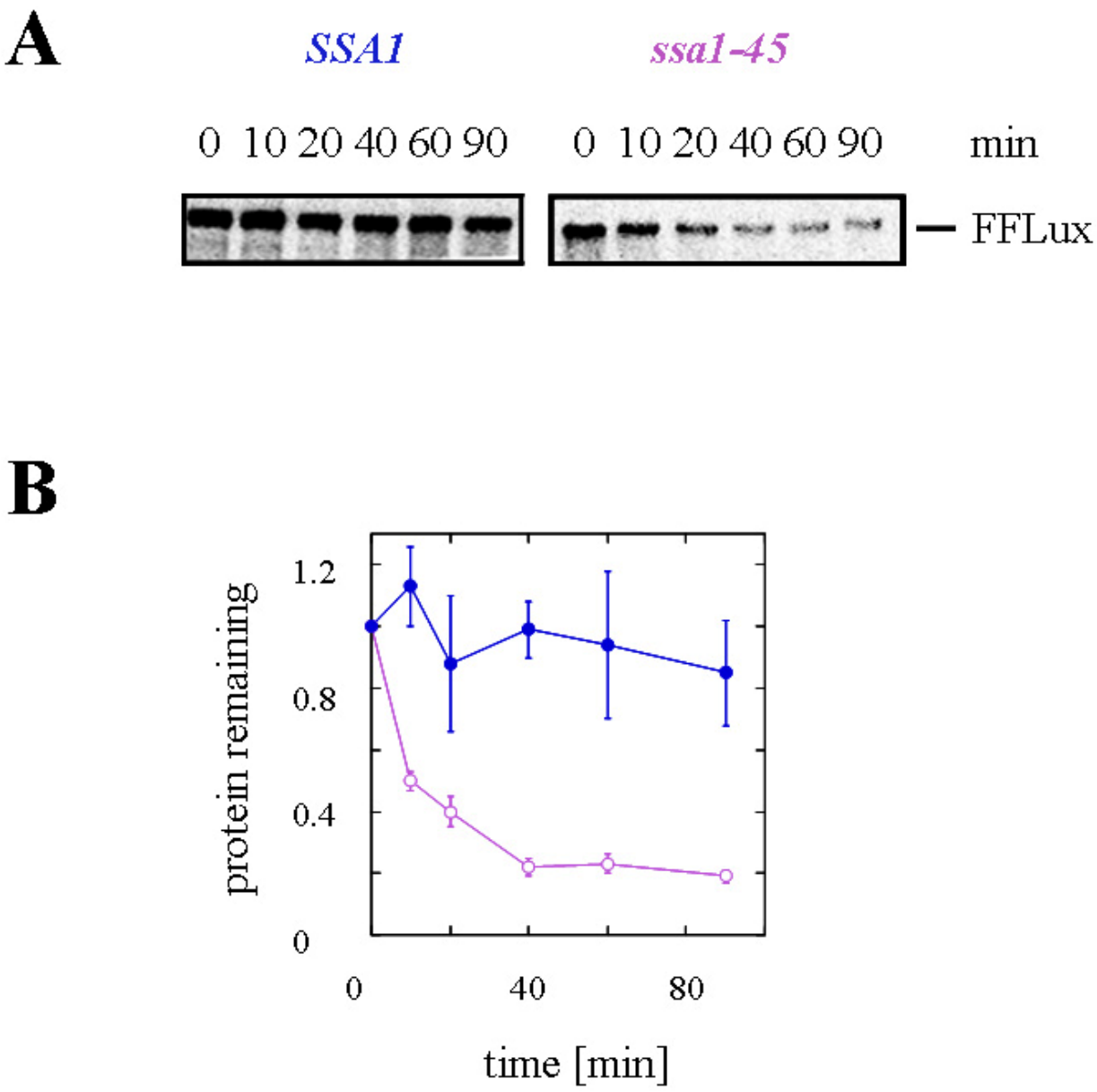

Figure 14: FFLux protein degradation is enhanced in the *ssa1-45* mutant strain.

Figure 15: FFLux protein is stable in wild type and *fes1Δ* yeast. A. Rates of FFlux degradation were determined by pulse-chase immuno-precipitation in wild type and *fes1Δ* yeast after addition of cycloheximide. Prior to the pulse-chase, FFLux protein was induced for 4h. B. FFLux protein levels were quantified, and each value corresponds to the level after standardization to the amount of protein obtained at 0 min. Data represent means of two independent experiments and vertical bars indicate the range in values. Closed blue circles represent *FES1* wild type protein levels, open purple circles represent *fes1* mutant protein levels.

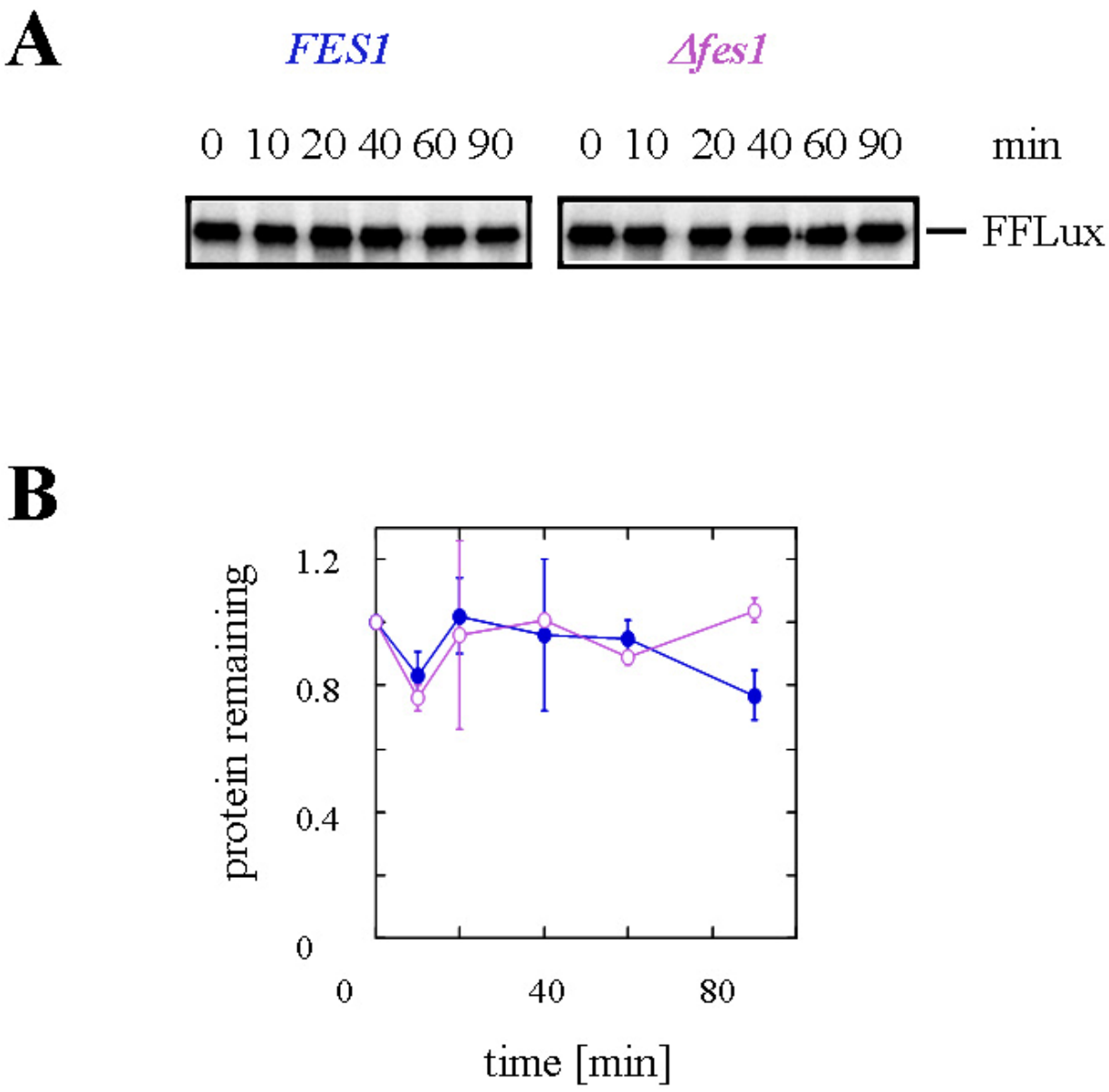

Figure 15: FFLux protein is stable in wild type and *fes1Δ* yeast.

Figure 16: FFLux protein degradation is enhanced in the *hsp82* mutant strain. A. Rates of FFlux degradation were determined by pulse-chase immuno-precipitation in *HSP82* wild type yeast and in the *hsp82 G313N* mutant strain after addition of cycloheximide. B. FFLux protein levels were quantified from 4 independent sets of experiments and averaged. All values were obtained after standardization to the levels detected directly after cycloheximide addition (0 min). Closed blue circles represent *HSP82* wild type protein levels, open purple circles represent *hsp82 G313N* mutant protein levels. Vertical bars indicate the standard error.

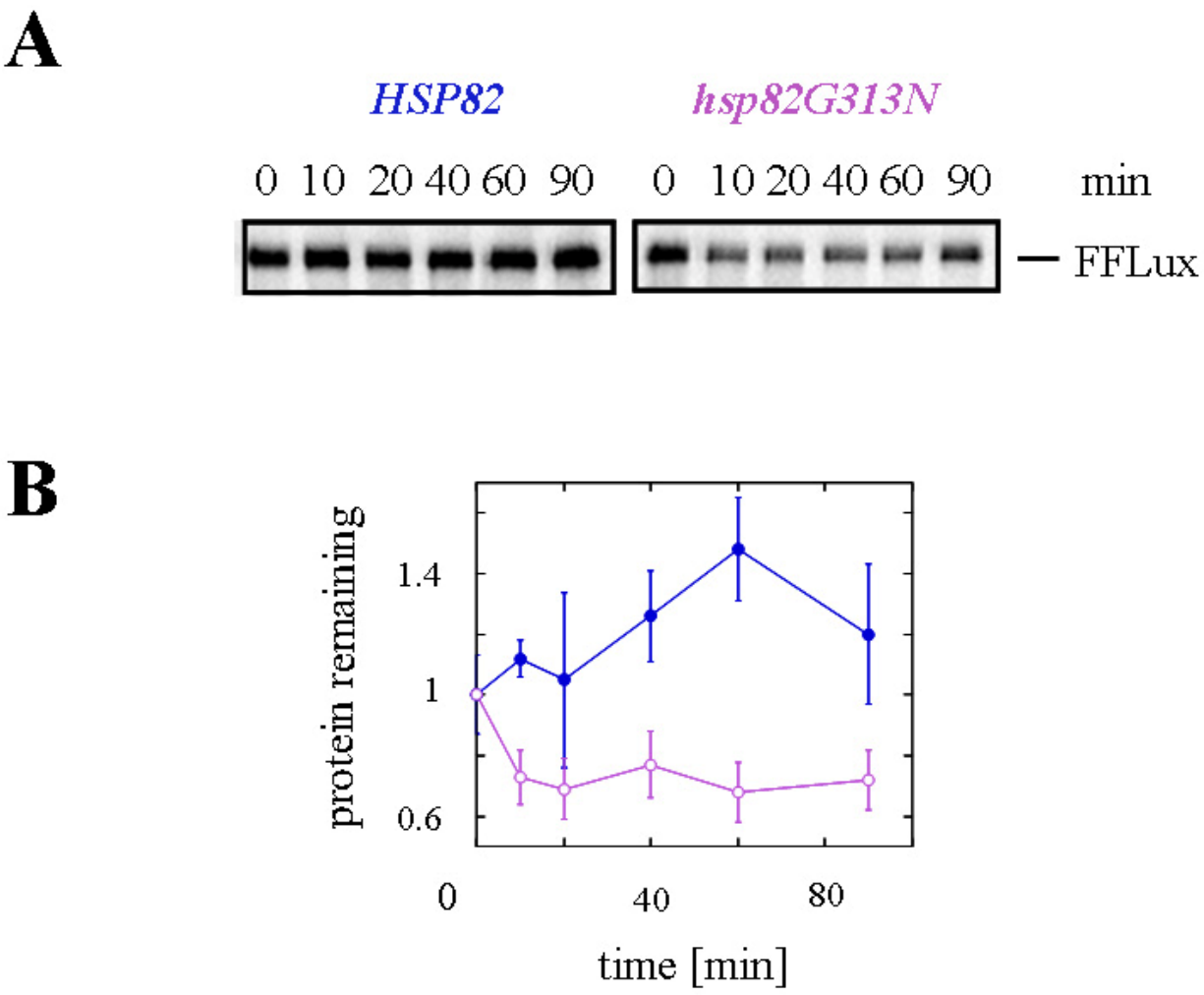

Figure 16: FFLux protein degradation is enhanced in the *hsp82* mutant strain.

Figure 17: Induction of FFlux mRNA is slowed in the *ssa1* mutant. A. FFLux mRNA was detected both by reverse-transcriptase (RT)-PCR and northern blot analysis from wild type and *ssa1-45* mutant yeast after the medium was switched from raffinose ("R") to galactose. B. FFLux mRNA levels were quantified from 2 independent sets of experiments and averaged. All values were obtained after standardization to the levels detected 20 h after induction. Closed blue symbols represent *SSA1* wild type mRNA levels, open purple symbols represent *ssa1* mutant mRNA levels. Circles correspond to data obtained from northern blot analysis, and triangles correspond to results from RT-PCR.

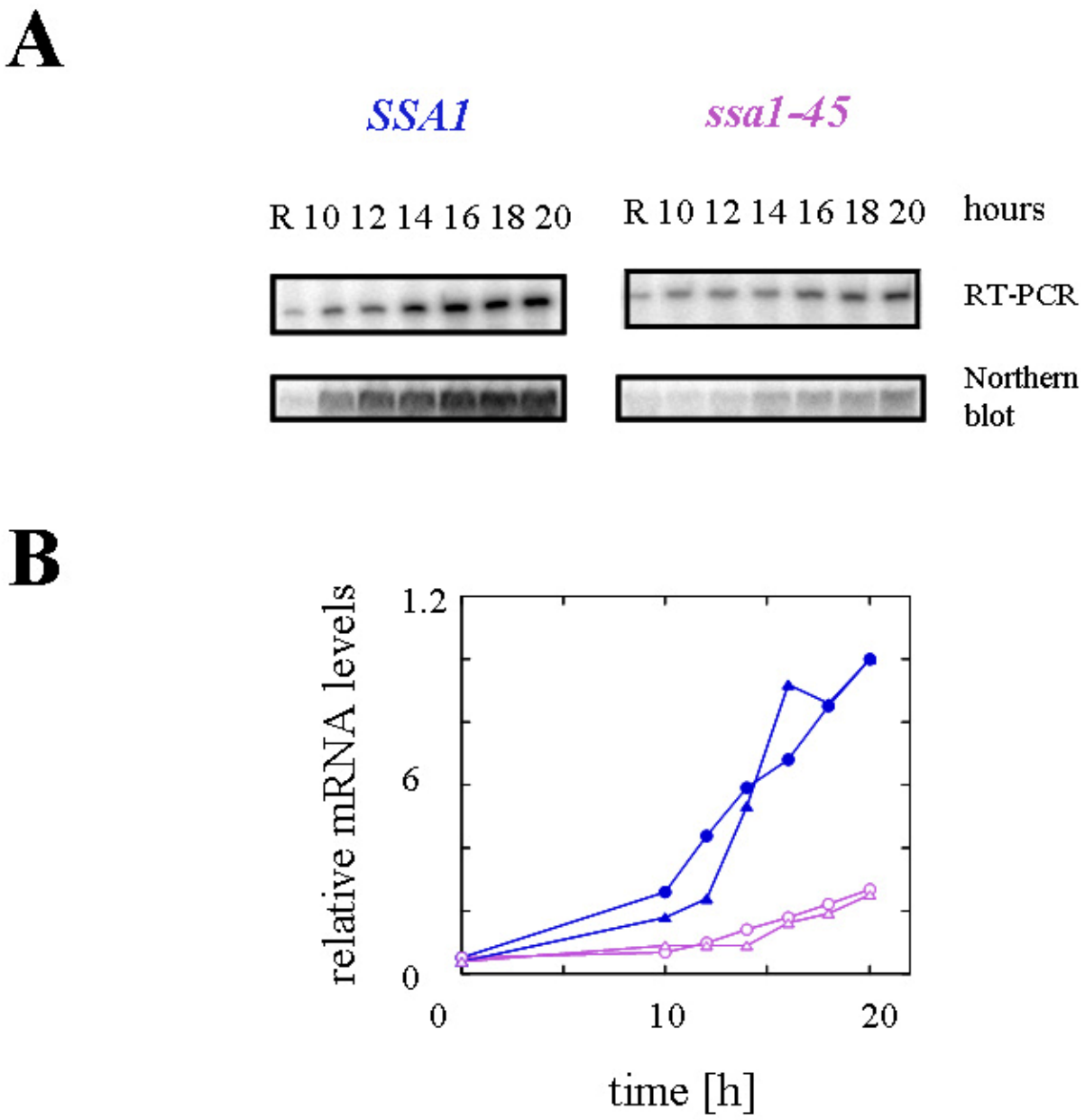

Figure 17: Induction of FFlux mRNA is slowed in the *ssa1* mutant.

Figure 18: Induction of FFlux mRNA is slowed in the *hsp82* mutant. A. FFLux mRNA was detected by northern blot analysis from wild type and *hsp82* mutant yeast after the medium was switched from raffinose to galactose. B. FFLux mRNA levels were quantified from 2 independent sets of experiments and averaged. All values were obtained after standardization to the levels detected 8 h after induction. Closed blue circles represent *HSP82* wild type mRNA levels, and open purple circles represent *hsp82* mutant mRNA levels.

A

B

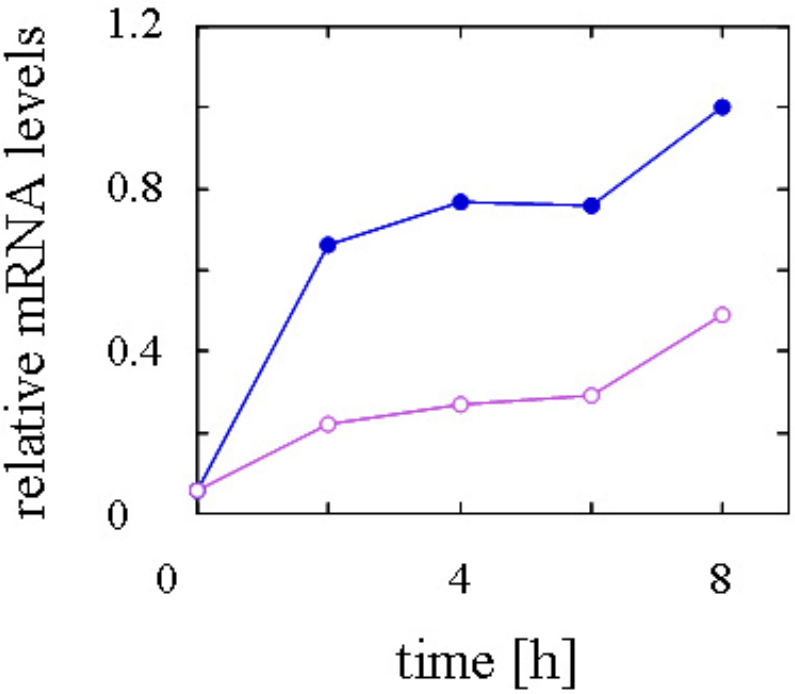

Figure 18: Induction of FFlux mRNA is slowed in the *hsp82* mutant.

hsp82 mutant was less pronounced (~2-fold) (Figure 18B). As a control, I found only subtle differences in actin (*ACT1*) mRNA levels between the wild type and mutant strains (data not shown). Moreover, I found that FFLux mRNA levels were ~20% higher in *fes1Δ* yeast as compared to wild type cells two hours after induction (data not shown), indicating that deletion of *FES1* does not slow FFLux-encoding mRNA accumulation.

2.3.5. Firefly luciferase mRNA degrades at a faster rate in the *ssa1-45* mutant strain

The decreased levels of FFlux mRNA in the *ssa1-45* mutant strain could be the result of a defect in transcription efficiency or the result of enhanced mRNA degradation in the mutant. Indeed, there is precedent that Hsp70 is involved in mRNA stability and decay. Mammalian Hsp70 as well as Hsp110 bind to AU-rich elements (AREs) in the 3'-untranslated region (3'UTR) of mRNAs, a region that mediates mRNA stability (Henics *et al.*, 1999). In contrast, the yeast Hsp70, Ssa1p, enhances ARE-regulated mRNA degradation (Duttagupta *et al.*, 2003). Consistent with a protective effect of Hsp70 on mRNAs, induction of Hsp70, down-regulation of the ubiquitin-proteasome network, or inactivation of the ubiquitin enzyme E1 each block decay of AU-rich mRNAs (Laroia *et al.*, 1999). Ssa1p was also proposed to be a regulatory factor of the decapping protein (Zhang *et al.*, 1999a), and Hsp70 may regulate the stability of its own mRNA (Kaarniranta *et al.*, 2000). Alternatively, a link between protein synthesis and mRNA stability has been established; *SSA1* and *SSA2*-mRNA degradation is enhanced when translation initiation

is limited (Barnes *et al.*, 1993; Barnes *et al.*, 1995; Barnes, 1998), and yeast strains defective in several translation initiation factors exhibit increased rates of mRNA decay, decapping, and deadenylation (Schwartz and Parker, 1999).

To decipher whether the FFLux message is less stable in *ssa1* mutant yeast compared to wild type cells, the strains containing the FFlux-inducible gene were grown in non-induction medium until mid-log phase and then switched to medium containing galactose and incubated at 30°C; these conditions were identical to those used to assess FFLux induction (see above). After 16 hours, the cells were harvested, resuspended in selective medium containing glucose to repress FFLux transcription and 1,10-phenanthroline was added to ensure that transcription was blocked (Parker *et al.*, 1991). Total RNA was prepared from cells removed from this reaction over time and FFlux and actin mRNA levels were measured. As shown in Figure 19, FFlux mRNA is degraded somewhat faster in the *ssa1-45* mutant strain. These results indicate that the difference in FFlux expression may be caused by a difference in mRNA stability. Because I was unable to detect the existence of AREs within the 3'UTR of the FFlux mRNA, I propose either that mRNA decapping activity is accelerated in the *ssa1-45* strain, leading to enhanced FFLux degradation, and/or that the attenuation of translation initiation (Horton *et al.*, 2001) de-protects the FFLux-encoding message, resulting in enhanced turnover of the mRNA.

Figure 19: FFlux mRNA decay rate is faster in *ssa1* mutant cells than in *SSA1* wild type yeast. mRNA degradation was measured using Northern blot analysis. Blotted mRNA levels represent relative amounts of Firefly Luciferase mRNA standardized to actin-1 mRNA levels. Closed blue circles represent *SSA1* wild type yeast, open purple circles symbolize *ssa1* mutant yeast. Vertical bars indicate the standard error. P-values are < 0.05, except were indicated: *< 0.1, ** < 0.15.

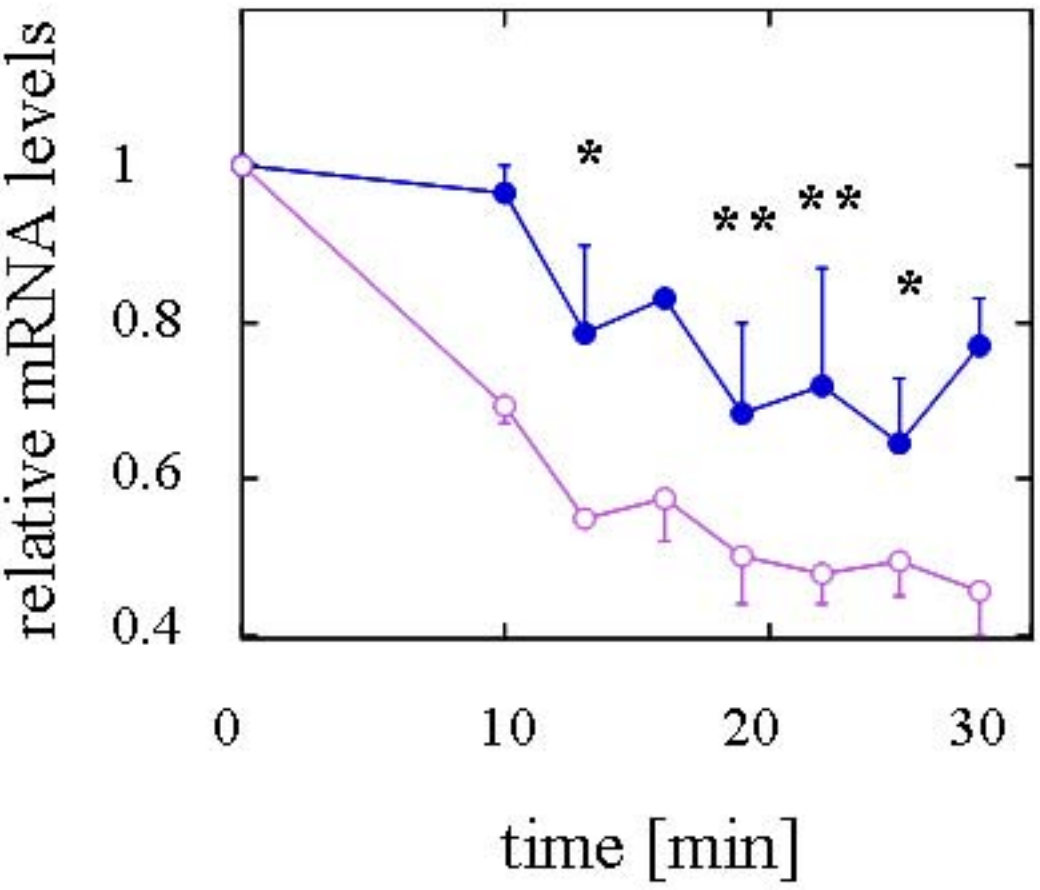

Figure 19: FFlux mRNA decay rate is faster in *ssa1* mutant cells than in *SSA1* wild type yeast.

2.3.6. Decapping of poly(A)-tailed firefly luciferase mRNA in the *SSA1* wild type and in the *ssa1-45* mutant strain occur at similar rates

The removal of the 5'-terminal cap structure (m^7G(5')ppp(5')N) is an important rate-limiting step in mRNA decay, and it had been shown previously that Ssa1p binds to the decapping enzyme (Dcp1p) and does so to a much higher level in strains mutated for genes encoding positive regulators of Dcp1p (Zhang *et al.*, 1999a). However, before examining whether decapping activity in *ssa1-45* mutant yeast was enhanced with respect to wild type cells, I needed to determine if firefly luciferase mRNA receives a poly(A)-tail in yeast. Thus, poly(A)-RNA was chromatographed from total RNA (see Materials and Methods) and the presence of poly-dT-bound FFLux mRNA was confirmed by Northern blot analysis. Next, to measure the decapping activity in wild type and *ssa1-45* mutant yeast, extracts were prepared and incubated with a poly(A)-tailed, capped FFLux-encoding mRNA. Aliquots were then removed over time and the amount of m^7GDP liberated from the capped mRNA was measured after phosphorimager analysis of TLC plates as described (Zhang *et al.*, 1999b). I first noted that decapping was magnesium-dependent, as anticipated (Zhang *et al.*, 1999b), because EDTA efficiently abolished decapping activity (Figure 20A). When I quantified the relative amounts of decapping activity in each extract I found no difference in the rates of decapping in the *SSA1* wild type and *ssa1-45* mutant strains (Figures 20A and 20B). Thus, I suggest that mutation of the *SSA1* gene might cause a defect in translation initiation that then leads to a shorter half-life of the firefly luciferase mRNA.

Figure 20: Decapping activities in *SSA1* wild type and *ssa1* mutant extract are identical.

A. The decapping products separated by thin-layer chromatography. B. Plotted decapping activity is shown as amount of m^7GDP represented as percentage of the capped substrate added to the decapping reaction. Closed blue circles represent *SSA1* wild type yeast, open purple circles symbolize *ssa1* mutant yeast. Vertical bars indicate the standard error.

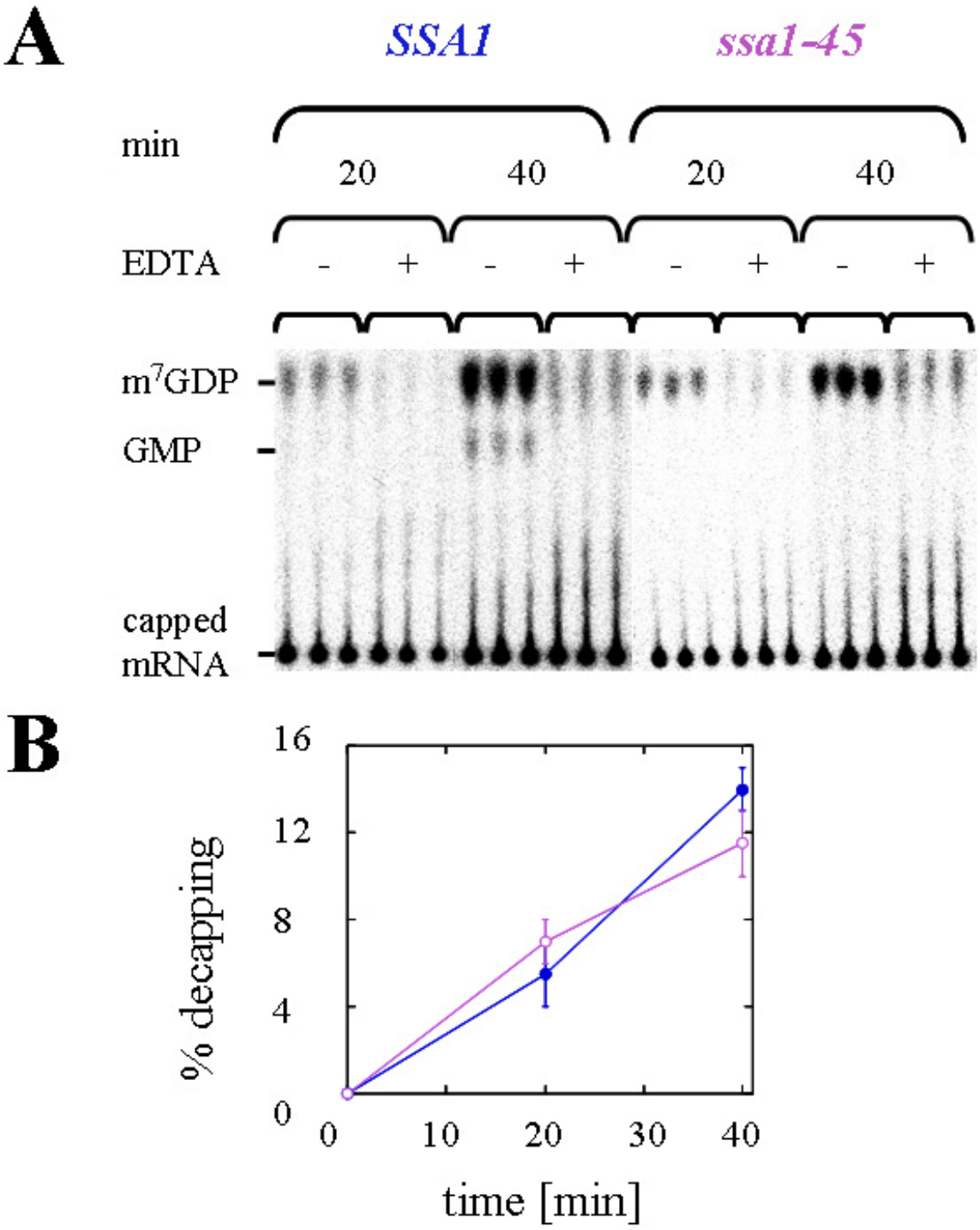

Figure 20: Decapping activities in SSA1 wild type and ssa1 mutant extract are identical.

2.4. DISCUSSION

The data presented in this chapter demonstrate that the expression of FFLux, a widely-used model reporter in both prokaryotes and eukaryotes, depends on a specific set of chaperones and a recently identified chaperone cofactor. I also find that the chaperone requirements during FFLux biosynthesis are distinct but overlapping. While Fes1p, an NEF for Ssa1p, and Ssa1p likely collaborate to fold FFLux, Ssa1p was also required to maintain the stability of FFLux protein, and for efficient induction of FFLux mRNA. These functions are Fes1p-independent because FFLux synthesis was robust in the *fes1* mutant. Together, the results suggest that the NEF impacts only a subset of Ssa1p's activities. In contrast, Hsp90 did not appear to be required for folding nascent FFLux but was essential for FFLux expression: Hsp90's contributions to protein stability and to FFLux mRNA induction were modest and can not explain the strong effect on FFLux protein expression noted in the *hsp82* mutant. Therefore, these data indicate that yeast Hsp90 plays an uncharacterized role in FFLux translation, and future efforts will be necessary to establish the molecular basis of this observation. In agreement with my discovery of a role for Fes1p in promoting FFLux folding, I also noted a requirement for its partner, Ssa1p, in folding. Fes1p facilitates the dissociation of ADP from Ssa1p and is thus predicted to aid in peptide release (Kabani *et al.*, 2002a). One can imagine that a defect in NEF function leads to prolonged Ssa1p-substrate binding, which would slow protein folding. Although the *ssa1-45* mutant strain also exhibits a delay in FFLux expression, I suggest that this does not arise mainly from a defect in folding or translation: FFLux degradation is significantly accelerated (~4-fold) in the *ssa1* mutant and FFLux mRNA induction is compromised ~4-fold. The impact of both defects should account for reduced FFLux protein levels (2-fold difference between wild type and mutant).

However, a general, mild translation defect was reported recently in *ssa1-45* mutant yeast (Horton *et al.*, 2001). In addition, it was observed that Ssa1p associates with ribosomes and with Sis1p (Zhong and Arndt, 1993; Horton *et al.*, 2001). Nevertheless, I note that the reported translation defect in the *ssa1* mutant was subtle and was examined at the restrictive temperature of 37°C, which arrests cell growth. In contrast, I examined the impact of Ssa1p in the mutant strain at the semi-permissive temperature of 30°C, at which no defect in cell growth is observed. Moreover, I note that neither FFLux induction nor enzymatic activity was compromised in a strain containing a temperature sensitive mutation in Sis1p, an Hsp40 that interacts with Ssa1p and functions in translation (not shown). I therefore conclude that Ssa1p has no major effect on FFLux translation *per se* and that it might rather impact FFLux translation efficiency indirectly by regulating the level of transcript.

The decreased levels of firefly luciferase mRNA in the *ssa1-45* mutant strain might have arisen at least in part from the relative instability of the FFLux-encoding mRNA in the *ssa1-45* mutant. My findings are consistent with previous reports denoting a role of Hsp70 in mRNA stability, and I suggest three models by which a defect in Ssa1p function might have led to FFLux mRNA destabilization.

First, mammalian Hsp70 binds to AREs in the 3'UTRs of mRNAs, elements which determine transcript decay rates by modulating the efficacy of poly(A)-tail-shortening (Wilson and Treisman, 1988; Greenberg *et al.*, 1990; Chen and Shyu, 1995; Henics *et al.*, 1999; Vasudevan and Peltz, 2001; Wilusz *et al.*, 2001; Duttagupta *et al.*, 2003). However, I was unable to identify AREs in the 3' UTR of FFLux (data not shown). Moreover, because mammalian Hsp110 also

binds to AREs (Henics *et al.*, 1999), I examined FFLux expression in yeast deleted for the *SSE1* gene, which encodes the constitutive Hsp110 protein in yeast (Mukai *et al.*, 1993; Shirayama *et al.*, 1993), but found that FFLux expression was proficient in this mutant. I suggest, therefore, that Ssa1p does not normally protect the FFLux message by binding to a putative ARE.

Second, the primary mRNA decay pathway in yeast occurs via deadenylation of the 3' poly(A) tail followed by removal of the 5' cap structure (m^7G(5')ppp(5')N) (Muhlrad *et al.*, 1994; Beelman *et al.*, 1996; LaGrandeur and Parker, 1998; Dunckley and Parker, 1999). The decapping enzyme competes with the eIF4F cap-binding translation initiation complex, which includes eIF4E, eIF4G (Schwartz and Parker, 1999, 2000; Vilela *et al.*, 2000). Thus, removal of the cap can represent a critical determinant between cap-dependent translation initiation and mRNA decay. This transition is proposed to occur after deadenylation through a rearrangement of a macromolecular complex associated with the cap, which includes Pab1p (Vilela *et al.*, 2000; Tharun and Parker, 2001; Ramirez *et al.*, 2002). Because Ssa1p has been found to bind to the Dcp1p decapping enzyme, and this interaction is enhanced in yeast mutated for one of two genes encoding positive regulators of Dcp1p, it has been proposed that Ssa1p acts as a negative regulator of Dcp1p and protects transcripts (Zhang *et al.*, 1999a). Alternatively, enhanced decay of FFLux mRNA in the *ssa1-45* mutant strain might originate from the presence of codons that are rarely used in yeast and could cause the ribosome to stall, as suggested by Brodsky *et al.* (1998). The low efficiency of translation could facilitate decapping and therefore degradation of the message. However, it is important to note that there is a second major pathway of mRNA decay where the transcript is degraded by the exosome in 3' to 5' direction without the requirement of prior decapping via DCP1 (Muhlrad and Parker, 1994; Muhlrad *et al.*, 1995;

Jacobs *et al.*, 1998; Butler, 2002). In accordance with these reports, I observed equal rates of decapping of the poly(A)-tailed firefly luciferase mRNA in the *SSA1* wild type and *ssa1-45* mutant strain. Therefore, my data suggest that Ssa1p is not a negative regulator of Dcp1p, although it is a member of a multi-protein complex that includes the initiation complex and Pab1p.

Third, the *ssa1* translation defect has been proposed to arise from compromised interaction between Pab1p and eIF4G at the initiation complex (Horton *et al.*, 2001). Ssa1p interacts with Pab1p, one of whose functions during translation initiation is to bring the 5'- and 3'-ends of the mRNA together, which in turn is mediated through Pab1p-eIF4G binding (Jacobson and Peltz, 1996; Tarun and Sachs, 1996; Gallie, 1998; Preiss and Hentze, 1998). Thus, Ssa1p might stabilize the translation initiation complex and prevent a nascent transcript from being degraded. Consistent with this view, Hsp70 appears to regulate the stability of its own message (Kaarniranta *et al.*, 2000) and Upf1p and Upf2p, proteins that regulate nonsense-mediated mRNA decay in yeast, have been demonstrated to engineer *SSA1*- and *SSA*2-mRNA degradation when translation initiation is inhibited (Barnes, 1998). I therefore propose that destabilization of the translation initiation complex in the *ssa1* mutant exposes FFLux mRNA, resulting in accelerated degradation.

Although I found that wild type and *ssa1* mutant extracts exhibited identical decapping activities for poly(A)-tailed FFlux message, I also found that the extent of decapping of FFLux mRNA lacking a poly(A)-tail was significantly higher in wild type extracts than in the *ssa1* mutant extracts (data not shown). Thus, Ssa1p may also regulate decapping activity at least for some

messages, as suggested (Zhang *et al.*, 1999a). The difference in decapping activities observed for poly(A) versus non-poly(A)-tailed substrates could be explained by a scenario in which the protective role of Ssa1p on the initiation complex is more dependent on the poly(A)-tail than its function in decapping; consequently, increased decapping is observed in the absence of polyadenylation in the wild type extract. Alternatively, the absence of the poly(A)-tail might preclude the association of regulatory factors that promote either stabilization or decapping of the substrate. Thus, it will be interesting to identify these modulators and to determine if Ssa1p's function in the transition state between translation initiation and decapping is of a direct or an indirect nature, and if this function applies to other messages.

In mammalian cells, the impact of Hsp90 and Hsp70 chaperones during protein biogenesis have been examined by treatment with ansamycin antibiotics, by over-expression of specific chaperones or co-chaperones, or by over-expression of a chaperone-associated E3 ubiquitin ligase that diverts proteins into the proteasome-mediated degradation pathway (Schneider *et al.*, 1996; Kanelakis *et al.*, 1999; Luders *et al.*, 2000; Connell *et al.*, 2001; Meacham *et al.*, 2001; Murata *et al.*, 2001; Farinha *et al.*, 2002). In my experiments, I employed specific mutant alleles of each gene that have been characterized for their effects on other cellular processes. Although I did not observe defects in cell growth, it is possible that some of the effects might have arisen from allele-specificity. However, the *fes1* mutant employed is a complete deletion of the *FES1* gene. Similarly, cellular levels of the *hsp82* mutant gene are significantly reduced relative to wild type cells (Fliss *et al.*, 2000). I therefore believe that it is unlikely that allele-specific effects account for my observations using the *fes1* and *hsp82* mutants. In contrast, the *ssa1-45* mutation lies in the peptide binding domain (Becker *et al.*, 1996) and could affect the binding kinetics

between the chaperone and the substrate. For example, extended periods of binding could target the substrate for degradation. However a biochemical analysis of Ssa1-45p has not been undertaken, and to date there is a dearth of rapid-acting *ssa1* mutants. I note that yeast lack a CHIP homologue, which in mammals interacts with the Hsp90 complex and regulates the decision between folding and degradation (Connell *et al.*, 2001; Murata *et al.*, 2001). CHIP also interacts with and regulates Hsp70-dependent decisions between the folding and degradation pathways (Meacham *et al.*, 2001). So far, it is not known which yeast E3 ubiquitin ligase(s) is/are impacted by Hsp90 and Hsp70 function, but this is a topic of ongoing studies in the Brodsky laboratory.

In summary, I have demonstrated in this chapter a high complexity of chaperone function in yeast. FFLux expression is facilitated by a specific set of chaperones and a chaperone cofactor, and the chaperone requirements are distinct but overlapping. While one chaperone can be involved in different steps of the biosynthesis of a substrate, its interacting factors might only collaborate for a subset of these functions. The choice of function may depend on the cofactor as well as on the polypeptide substrate. Characterization of the chaperone requirements for the biosynthesis of other substrates as well as an investigation of other chaperones and cofactors will hopefully reveal new features and interactions in the complex network of chaperone action.

3. REGULATION OF CFTR MATURATION AND DEGRADATION

3.1. INTRODUCTION

As mentioned in Chapter 1.5., cells containing only the most common mutant associated with cystic fibrosis, the deletion of the phenylalanine at position 508, "ΔF508-CFTR", (see Figure 8) lack the protein at the plasma membrane because its folding is severely impaired (Kerem *et al.*, 1989; Riordan *et al.*, 1989; Cheng *et al.*, 1990; Kartner *et al.*, 1992; Yang *et al.*, 1993; Lukacs *et al.*, 1994; Ward and Kopito, 1994; Jensen *et al.*, 1995; Ward *et al.*, 1995; Qu and Thomas, 1996; Qu *et al.*, 1997). This prevents ER export and leads to its degradation via ERAD (Cheng *et al.*, 1990; Kartner *et al.*, 1992; Yang *et al.*, 1993; Lukacs *et al.*, 1994; Ward and Kopito, 1994; Jensen *et al.*, 1995; Ward *et al.*, 1995). One very recent study on the wild type CFTR and ΔF508-CFTR expression patterns in native tissue corroborates the proposition that defective protein processing is the major pathogenic mechanism in CF (Kreda *et al.*, 2005). This translates into the necessity to characterize completely the molecular mechanism that enables the cell to distinguish ΔF508-CFTR from the wild type protein. The importance of this approach is further underscored by the fact that recent studies have been performed to identify drugs that activate CFTR channel activity. Drugs that stimulate the gating of the ΔF508 mutant were identified that are distinct from those that enhance the conductivity of the wild type channel (Ma *et al.*, 2002; Yang *et al.*,

2003). But more importantly, drug-induced activation of ΔF508-CFTR depended on conditions that allow ER exit and prevent degradation. This was accomplished by growing cells at decreased temperature (Ma *et al.*, 2002; Yang *et al.*, 2003). Therefore, a combinatorial therapy, correction of the processing defect as well as increasing channel gating, might prove vital.

Because yeast expressing CFTR grow as well as cells lacking the CFTR-expression vector (Zhang *et al.*, 2001), factors required for the ERAD of ΔF508-CFTR might be expressed at higher levels, which may counteract the accumulation of misfolded protein. Therefore, I utilized a genomic approach to identify components of the CFTR ERAD pathway that might have been up-regulated. In previous studies, two microarray analyses comparing gene expression levels in lung or in intestinal tissue between CFTR wild type mice and mice lacking CFTR detected an induction of the immune response (Xu *et al.*, 2003; Norkina *et al.*, 2004). The strong immune response elicited by CF in mammals might have masked the differential regulation of genes involved in recognition, trafficking, and degradation of CFTR. In contrast, because yeast lacks an immune response and because many aspects of CFTR degradation are conserved between yeast and mammals in general (see chapter 1.6.; Zhang *et al.*, 2001; Youker *et al.*, 2004), I used *S. cerevisiae* as a model system. Specifically, I identified genes that are differentially regulated in response to wild type CFTR expression in yeast by microarray analysis. I found that the protein product of one of the genes found to be up-regulated upon CFTR expression, *HSP26*, facilitates CFTR degradation in yeast, and that this sHsp and another sHsp, Hsp42, may be functionally redundant. In contrast, the turnover rates for a soluble and another integral membrane ERAD substrate were unaffected by deletion of the Hsp26 and Hsp42 encoding genes, suggesting client substrate specificity. I also found that a human ortholog of the sHsps,

αA-crystallin, enhances ΔF508-CFTR proteolysis in mammalian cells when over-expressed. Finally, purified recombinant αA-crystallin suppressed the aggregation of CFTR-NBD1. Together, these results provide new evidence for an involvement of sHsps in CFTR degradation.

3.2. MATERIAL AND METHODS

3.2.1. Yeast strains, plasmids, and molecular methods

The yeast strains used in this study were: *JN516* (referred to as wild type or *SSA1*), *MATα leu2-3, 112 his3-1 ura3-52 trp1Δ1 lys2 ssa2::LEU2 ssa3::TRP1 ssa4::LYS2; RSY368* (referred to as wild type or *HSP26) Matα can1-100 leu2-3,112 his3-11, 15 trp1-1 ura3-1 ade2-1; hsp26Δ* (or Hsp26 mutant) *Matα can1-100 leu2-3,112 his3-11, 15 trp1-1 ura3-1 ade2-1 hsp26::KanMX4; SEY6211* (referred to as wild type or *HSP26HSP42;* kindly provided by J. Buchner, Technical University Munich) *Mata ura3-52 leu2-3,112 his3-Δ200 trp1-Δ901 ade2-101 suc2-Δ9 GAL10; hsp26Δ* (or Hsp26 mutant*;* kindly provided by J. Buchner, Technical University Munich) *Mata ura3-52 leu2-3,112 his3-Δ200 trp1-Δ901 ade2-101 suc2-Δ9 GAL10 hsp26::HIS3; hsp42Δ* (or Hsp42 mutant*;* kindly provided by J. Buchner, Technical University Munich) *Mata ura3-52*

leu2-3,112 his3-Δ200 trp1-Δ901 ade2-101 suc2-Δ9 GAL10 hsp42::LEU2; hsp26Δhsp42Δ (or Hsp26 Hsp42 double mutant*;* kindly provided by J. Buchner, Technical University Munich) *Mat**a** ura3-52 leu2-3,112 his3-Δ200 trp1-Δ901 ade2-101 suc2-Δ9 GAL10 hsp26::HIS3 hsp42::LEU2* (*Robinson et al., 1988; Haslbeck et al., 2004)*; *BY4742* (referred to as wild type or *YBR075W*) *MAT**α** his3Δ1 leu2Δ0 lys2Δ0 uraΔ0; ybr075wΔ* (or Ybr075Wp mutant) *MAT**α** his3Δ1 leu2Δ0 lys2Δ0 uraΔ0 ybr075wΔC-term* (http://www.openbiosystems.com).

The *hsp26Δ* strain in the *RSY368* background was created using PCR-based gene disruption as described previously (Brachmann *et al.*, 1998). In brief, the *RSY368* wild type strain was transformed with an *hsp26::KanMX4* disruption cassette, generated by PCR from the template vector pRS400 (forward primer: GTGGTATTTCATAACAACGGTTCTTTTTC ACCCTTATTCCCTGTGCGGTATTTCACACCG; reverse primer: TGACATATGTTTCAA GCCATATGCAAGCAACAATGGTCCTAGATTGTACTGAGAGTGCAC). Transformants were selected by growth on complete medium supplemented with 2% glucose and G418 to a final concentration of 250 μl/ml (GibcoBRL). Correct insertion of the disruption cassette and the absence of the *HSP26* gene were confirmed by PCR utilizing primers up- and down-stream of the *HSP26* location in combination with primers within the sequence of the disruption cassette and *HSP26 (KAN* forward: ATTGATGTTGGACGAGTCGG; *KAN* reverse: ATCGCAGTGGTGAGTAACCA; *HSP26* up-stream, forward: GGATCGGAATAGTA ACCGTC; *HSP26* down-stream, reverse: GCCACATCCATAGAGATACC; *HSP26* coding, forward: CACCAAGACGTCAGT TAGCA; *HSP26* coding, reverse: TGTTGTCTGCATC CACACCT).

Cells were grown at the indicated temperatures with vigorous shaking in complete medium (YP) or synthetic complete medium lacking uracil Sc-ura but containing glucose at a final concentration of 2% as the carbon source. HA-tagged CFTR, CPY*, and Ste6p* were expressed in yeast from a 2μ plasmid containing *URA3* as the selectable marker under the control of the constitutive phosphoglycerate kinase promoter (Ng *et al.*, 2000; Zhang *et al.*, 2002b; Huyer *et al.*, 2004); yeast transformed with the 2μ plasmid pRS426 (Christianson *et al.*, 1992) without an insert served as controls, where indicated. Plasmids were introduced into host strains using lithium acetate-mediated transformation, and transformants were selected by growth on Sc-ura medium containing glucose (Rose, 1990).

Protein extracts from yeast for immunoblot analysis were prepared as described previously (Brodsky *et al.*, 1998).

3.2.2. Mammalian cell culture, plasmids, and transient transfection

HEK293 (human embryonic kidney) cells were cultured in Dulbecco's modified Eagel's medium (DMEM; Sigma) with 10% fetal bovine serum (Invitrogen), 4mM L-glutamine (Sigma), and penicillin-streptomycin (GibcoBRL) at 37°C in a humidified environment containing 5% CO_2.

To over-express chaperones, first, the αA-crystallin gene was removed from a pCIneo vector (kindly provided by U. Andley, Washington University) with SalI (3'), and XbaI (5'); the SalI

end was blunted with Klenow before the XbaI cut, and the gene was sub-cloned into pcDNA3.1 (kindly provided by R. Hughey, University of Pittsburgh) that had been cut with PmeI, blunted, and then cut with XbaI. The Hsp110 encoding gene was removed from a pBacPAKHis-1 vector (kindly provided by J.R. Subjeck, Roswell Park Cancer Institute, Buffalo, New York) with AccI (5'), this end was blunted using Klenow, and the second cut was made with KpnI (3'). The gene was then sub-cloned into pcDNA.3.1, which had been cut with HinDIII, blunted, and then cut with KpnI. The gene encoding Hsp70 was cut out of the pMSHSP70 vector (kindly provided by R.I. Morimoto, Northwestern University, Chicago) by first cutting with HinDIII, blunting this end, and then cutting with KpnI (5'), before it was sub-cloned into pcDNA3.1 that had been cut with XbaI, blunted, and cut with KpnI. XL10 Gold supercompetent cells (Stratagene) were transformed with one tenth (= 1 μl) of a ligation reaction and transformants were selected based on resistance to Ampicillin. Correct insertion and the DNA sequence of the insert were confirmed by sequence analysis. HspBPI in pcDNA3.1 was kindly provided by V. Guerriero, University of Arizona, and the CFTR and ΔF508-CFTR genes in pcDNA3.1 were kindly provided by R.A. Frizzell, University of Pittsburgh. For all experiments, HEK293 cells were grown in 60-mm dishes and transiently transfected with the indicated pcDNA3.1 expression plasmids aided by Lipofectamine 2000 (Invitrogen). After 24h, cells were subjected to pulse chase analysis or cell lysis as described previously (Zhang *et al.*, 2002a).

3.2.3. Immunoblot analysis

Samples were loaded onto 5% (CFTR detection in mammalian extracts), 10% (CFTR detection in yeast extracts), 15% (purified αA-crystallin), or 12.5% SDS-polyacrylamide gels. After electrophoresis, the proteins were transferred to PVDF (NEN) (to detect CFTR from mammalian cell extracts), or nitrocellulose (Schleicher and Schuell, pore diameter of 0.2μm). The antibodies used were raised against CFTR (M3A7, Upstate), αA-crystallin, Hsp90, Hsp70, Hsp110 (Stressgen), HspBP1 (kindly provided by V. Guerriero, University of Arizona), Kar2p (Brodsky and Schekman, 1993), or Sec61p (Stirling *et al.*, 1992). To detect the primary antibody, horse-radish peroxidase-conjugated secondary antibodies (anti-rabbit, anti-mouse, anti-rat (Amersham); anti-sheep (Jackson Immuno Research)) were used. The complexes were visualized using the enhanced chemiluminescence detection kit (Pierce) and quantified using Kodak 1D software (v3.6; Kodak).

3.2.4. Preparation of RNA for microarray and Northern blot analysis

A single yeast colony was inoculated into 4 ml of Sc-ura supplemented with 2% glucose and incubated over night at 30°C with vigorous shaking. The culture was diluted into 250 ml of the same media and grown to an OD_{600} of 0.37 at 30°C. Cells were harvested by centrifugation at 4000 rpm for 10 min in a Sorvall GSA rotor at 20°C. The pellet was resuspended in 25ml of

double distilled sterile H_2O and spun at 4000 rpm for 5 min at 20°C in a Sorvall SS 34 rotor. Pellets were snap frozen in liquid nitrogen and stored at -80°C. Yeast RNA was extracted with hot acid phenol (Sigma) as published in Current Protocols in Molecular Biology (Collart, 1993) with minor modifications. Specifically, the protocol was adjusted to isolate RNA from 250 ml of liquid yeast culture at a final OD_{600} of 0.37, and the RNA was extracted three times with acid phenol and twice with chloroform and subjected to RNeasy Midi Kit (Qiagen). RNA concentration and purity were determined spectrophotometrically by measuring the A_{260} and A_{280}. Only samples with a ratio of A_{260}/A_{280} higher than 1.8 were used. The integrity of total RNA was examined on a denaturing formaldehyde-agarose gel. Aliquots of all RNA samples were frozen and stored at -20°C.

3.2.5. Microarray analysis

Yeast 6.4K microarrays were obtained from the Ontario Cancer Institute Microarray Center (Toronto). Arrays were spotted with 6,240 yeast open reading frames plus control spots (6.4k total) in duplicate. cDNA probes were synthesized from 20 μg total yeast RNA (prepared as described above) and fluorescently labeled using the Atlas Glass Fluorescent Labeling Kit (Clontech) and Cy3 (CFTR expressing strain) and Cy5 (control strain) monofunctional reactive dyes (Amersham) according to the manufacturer's instructions. Labeled cDNA was concentrated with microcon YM-30 filters (Amicon) to a final volume of 36 μl, and 2 μl of 10 mg/ml salmon sperm DNA and 10 mg/ml of polyadenylic acid were added. The labeled probe, including carrier

DNA, was denatured at 90°C for 2 min and mixed with 40 μl pre-warmed (42°C) 2 x hybridization buffer (50% formamide in 10x SSC, and 0.2% SDS). The hybridization mixture was added under the lifter coverslip (Erie Scientific Company) covering the array, and the hybridization reaction was set-up in a humidified hybridization chamber and incubated for 16 h at 42°C. Arrays were washed for 5 min in: 0.2x SSC/0.1% SDS; 0.2x SSC; and 0.1x SSC. They were then quickly rinsed in 0.01x SSC and dried by centrifugation in a S2096 rotor in a Beckman CS-15R centrifuge at 1200 rpm for 5 minutes. Microarrays were scanned with a GMS 418 Array Scanner (Genetic Microsystems) and Signal intensities were measured with GenePix Pro 4.1 image analysis software (Axon Instruments). Data were normalized within an array by the ratio of total fluorescence. Statistical analysis was performed utilizing the program Significance Analysis of Microarrays (SAM). SAM employs a gene specific t-test and adds a small positive constant to the denominator to exclude genes with small differences between two examined conditions (Tusher *et al.*, 2001).

3.2.6. Northern blot analysis

Total RNA was prepared from one aliquot of thawed yeast (see above), and 20 μg were resolved on 1% agarose/formaldehyde gels, transferred to Gene Screen Plus membranes (NEN Life Science Products), and hybridized sequentially using ^{32}P-labeled, randomly primed probes produced from PCR fragments generated utilizing primers against *HSP26* (forward: CACCAAGACGTCAGTTAGCA, reverse: TGTTGTCTGCATCCACACCT), *FES1* (forward:

CTACAGCAGTTATTCGGTGG, reverse: ACTCTCGTCAGACAAGCACT), *YBR075W* (forward: CTTGAGTATACCGATTATGC, reverse: CACTGGACTCCGATATGGTA), *HSP82* (forward: AGAGAGCACCATTCGACTTG, reverse: AATTGACCAGTTCTGATAGC), and *SEC61* (forward: CCAACCGTGGTACTTTACTG, reverse: GTCCAGAAGAGCTTCGGATA). Filters were processed as previously described (Ausubel, 1988), except that the high temperature wash was performed at 55°C for 10 min. Membranes were re-hybridized after the bound probe was removed from the filters by incubation in 0.1x SSC, supplemented with an additional 15mM NaCl and containing 1% SDS for 20 min at 100°C.

3.2.7. ERAD assays

Yeast strains expressing HA-tagged CFTR were grown at 26°C over night in Sc-ura containing 2% glucose. Cultures were diluted to an OD_{600} of 0.15 in the same medium and grown to an OD_{600} of 0.4-0.6. Protein synthesis was inhibited by the addition of cycloheximide (50 μg/ml final concentration) and cells were shifted to 30°C. A total of 2.5 ODs of cells were harvested at the indicated time points, and proteins were extracted as described previously (Zhang *et al.*, 2002b). Samples were loaded onto 10% SDS-polyacrylamide gels, and after electrophoresis, the proteins were transferred to nitrocellulose membranes (Schleicher and Schuell, pore diameter of 0.2μm). Membranes were incubated with mouse monoclonal anti-HA antibody (12CA5, Roche Molecular Biochemicals) and rabbit polyclonal anti-Sec61p (Stirling *et al.*, 1992). To detect the primary antibody, horseradish peroxidase-conjugated secondary antiserum was used, and the

complex was visualized using the enhanced chemiluminescence detection kit (Pierce). Data were quantified using a Kodak 440CF Image Station and Kodak 1D (v 3.6; Kodak) software. The degradation of HA-tagged CPY* and HA-tagged Ste6p* were determined by pulse-chase immuno-precipitations from ^{35}S-metabolically labeled yeast as published previously (Zhang *et al.*, 2001) using mouse monoclonal anti-HA antibody (12CA5, Roche Molecular Biochemicals) and Protein A Sepharose (Amersham).

Wild type CFTR/ΔF508-CFTR degradation and maturation in HEK293 cells were assessed by pulse-chase immuno-precipitation as published previously (Zhang *et al.*, 2002a) with minor modifications. In brief, transfected HEK293 cells were incubated at 37°C and cells were starved for 30 min in cysteine- and methionine-free DMEM (GibcoBRL). Metabolic labeling was initiated with 140 μCi/ml Redivue Pro-mix L^{35}S (Amersham) for 30 min. The cells were then washed once with phosphate buffered saline (GibcoBRL), and directly either lysed in RIPA buffer (1x phosphate buffered saline pH 7.4, 1 % Triton X-100, 1 % sodium deoxycholate, 0.1 % SDS) containing protease inhibitors (protease inhibitor cocktail tablets (Roche), 1 tablet/50 ml) or incubated for the indicated times in DMEM. DNA was sheared by repeated pipetting through a 1 ml syringe with an 18G needle. Cell lysates containing ~6 μCi were treated with M3A7 anti-CFTR antibody (Upstate) or anti-αA-crystallin antibody (Stressgene) for 1 h at 4°C, and either Protein G- or Protein A-agarose (Invitrogen) was added, respectively. The mixture was incubated for 2 h at 4°C before the immuno-precipitates were isolated and washed three times with 1 ml RIPA buffer, resolved on 5 % SDS-PAGE, and analyzed by phosphorimager analysis using Image Gauge software (v3.45; Fuji Film Science Lab). P-values were calculated via the program at http://faculty.vassar.edu/lowry/t_ind_stats.html.

3.2.8. Purification of αA-crystallin and the NBD1 aggregation assay

αA-crystallin was expressed in *E.coli* BL21 DE from the pAED4 vector (kindly provided by K.P. Das, Bose Institute, Kolkata, India). One colony of the transformed bacteria was inoculated into 40 ml LB medium supplemented with Ampicillin (50 μg/ml final concentration) and grown at 37°C over night. The culture was diluted 1:10 in fresh media and grown for ~1.5 h. αA-crystallin expression was induced with isopropyl β-D-thiogalactoside (final concentration of 0.5mM) for ~4 h until an OD_{600} of ~1 was reached. Cells were harvested and the protein was purified as described previously (Biswas and Das, 2004) with minor modifications. In brief, cells were resuspended in 15 ml of buffer A (20mM Tris, pH 7.2, 0.5mM EDTA, 0.5mM DDT) containing protease inhibitors (protease inhibitor cocktail tablets, 1 tablet/50 ml (Roche) and PMSF at a final concentration of 1mM (Diagnostic Chemicals Incoorporated)), and the cells were frozen at -80°C and thawed before they were treated with lysozyme and sonicated. The lysate was cleared by centrifugation at 10,000 rpm for 20 min at 4°C in a SS34 rotor (Sorvall). The clarified lysate was then dialyzed against buffer A over night and applied to a DEAE-anion exchange column (Amersham) and proteins were eluted with a linear 0-0.5M NaCl gradient. Peak fractions containing αA-crystallin (as assessed by SDS-PAGE and Coomassie Brilliant Blue staining) were concentrated with centricon YM-10 filters (Amicon) and loaded onto a Sephacryl S300-HR (Amersham) size exclusion column (1 x 50 cm) and proteins were eluted with buffer A supplemented with 0.1M NaCl. Peak fractions containing αA-crystallin, determined as above, were dialyzed against buffer A, and the protein concentration was assessed by Bradford assay (Biorad). Aliquots were snap frozen in liquid nitrogen and stored at -80°C.

SDS-PAGE and Coomassie Brilliant Blue staining of the purified protein resulted in a band of ~18 kD (that was 95% pure) that was recognized by anti-αA-crystallin antibody (Stressgen) by immunoblot analysis. Molar concentration is always expressed in the text assuming that the protein is a monomer.

The ability of αA-crystallin to suppress the aggregation of NBD1 (kindly provided by R.T. Youker, University of Pittsburgh) was determined as described previously (Strickland *et al.*, 1997; Youker *et al.*, 2004).

3.3. RESULTS

3.3.1. Identification of genes up-regulated in response to CFTR expression in yeast

To identify genes up-regulated by the heterologous expression of CFTR in yeast, RNA was isolated from yeast strains transformed with either a plasmid synthesizing wild type CFTR under the control of a constitutive promoter or a vector control. Microarray analysis was performed with RNA from six pairs of independently transformed and grown yeast cultures. Exquisite care was taken to ensure that each yeast culture was grown and treated identically. Data from 6 Yeast

6.4K Microarrays (Ontario Cancer Institute) were normalized and statistical analysis was performed utilizing the program Significance Analysis of Microarrays (SAM) (Tusher *et al.*, 2001).

Allowing for a false discovery rate of 0.118 (the false discovery rate represents the median of the number of falsely identified genes divided by the number of genes termed significant), 359 genes were called significant, of these, 168 (~2.5% of the yeast genome) were up- and 191 (~2.9% of the yeast genome) were down-regulated (see Table 4 and 5). These changes in expression levels are most likely not due to Cl^- conductance because wild type CFTR does not exhibit channel activity in yeast (J.L. Brodsky, personal communication). For the time being, I focused on the genes with elevated expression levels, because factors directly involved in CFTR degradation would be expected to be up-regulated rather than down-regulated in the presence of CFTR. In agreement with published reports (Zhang *et al.*, 2001), genes typically up-regulated during cell stress responses or via the unfolded protein response (UPR) (e.g. *KAR2, JEM1, UBC7, DER1, FKB2, PDI, ERO1*; Chapman *et al.*, 1998; Travers *et al.*, 2000) did not exhibit an increase in mRNA levels as a result of CFTR expression in yeast. In fact, when I compared genes induced by CFTR expression in yeast with the genes listed as up-regulated during the UPR by Travers *et al*. (2000) and the UPR-induced genes screened by Palmer *et al*. (2003) there was no overlap. However, CFTR synthesis induced genes that might be involved in the proteolysis or maturation of the ion channel. These include the essential ubiquitin activating enzyme *UBA1*, a 26S proteasome subunit, *RPT2* (probably a spurious effect, since the mRNA level of other proteasomal subunits did not change), a putative deubiquitinating enzyme *UBP*8, and a regulator of vacuolar protein sorting, *VPS53*. Moreover, I detected amplification of the expression of three

cytoplasmic molecular chaperones, *HSP12*, a polypeptide engaged in plasma membrane protection (Sales *et al.*, 2000), *HSP26*, a member of the family of small Hsps or α-crystallin-like proteins (Narberhaus, 2002), and *SIS1*, an Hsp40 involved in translation initiation that acts in a complex with Ssa1p, Pab1p, and eIF4G (Zhong and Arndt, 1993; Horton *et al.*,2001). Although not every factor involved in translation initiation is up-regulated, different components of the complex might exhibit specific functions within this pathway so that the induction of one single factor might still modulate translation efficiency. In addition, *HAA1*, a transcriptional activator of the membrane stress response, was observed (Keller *et al.*, 2001). However, *HSP26* seems to be the most intriguing candidate of the three chaperones because members of the family of small Hsps have been implicated in a number of cellular processes, including the prevention of protein aggregation and of apoptosis, and the ubiquitin-proteasome pathway (see chapter 1.4, and Horwitz, 1992; Jakob *et al.*, 1993; Wagner and Margolis, 1995; Ehrnsperger *et al.*, 1997; Lee *et al.*, 1997; Conconi *et al.*, 1998; Conconi *et al.*, 1999; Haslbeck *et al.*, 1999; Boelens *et al.*, 2001; Kamradt *et al.*, 2001; Ito *et al.*, 2002; Kamradt *et al.*, 2002; Narberhaus, 2002; den Engelsman *et al.*, 2003; Morrison *et al.*, 2003; Parcellier *et al.*, 2003; Biswas and Das, 2004; den Engelsman *et al.*, 2004; Haslbeck *et al.*, 2004; Liu *et al.*, 2004a; Liu *et al.*, 2004b; Kamradt *et al.*, 2005). Several genes that are part of the trafficking machinery in the secretory pathway also exhibited elevated expression levels, including *APL4*, *ERP5*, and *GYP7*. In addition, 56 uncharacterized open reading frames (ORFs) were classified as significantly up-regulated, and computational analysis (http://www.incyte.com, http://www.ebi.ac.uk/InterProScan/, http://www.yeastgenome.org/) indicates that a subset of the corresponding polypeptides might impact CFTR degradation. For example, *YDR049W* encodes a protein associated with Cdc48p and Ufd2p, which, together with Npl4, catalyze ERAD substrate retro-translocation from the ER and delivery to the

proteasome (Bays and Hampton, 2002); the product of *YLR297W* interacts with the Cul3p ubiqitin ligase; *YBR062C* contains a ring finger motif and exhibits similarity to several ring finger E3 ligases; *YKL088W* is an ER resident flavoprotein, which could indicate a role in protein folding, and *YBL081W* encodes an ER localized protein; *YLL056C*, exhibits enhanced expression during cell stress and encodes most likely an integral membrane protein; the gene product of *YDR286C* has similarity to glutaredoxin-like and thioredoxin-like folds, which is suggestive of an involvement in protein folding; the gene product of *YAR028W*, is a ubiquitin-modified ER membrane protein; *YJL149W* encodes a protein containing a cyclin-like F-box that interacts with the E3 Skp-Cdc53-Hrt1 ubiquitin-ligase.

Accepting a false discovery rate of 0.218 (the false discovery rate represents the median of the number of falsely identified genes divided by the number of genes termed significant), 807 genes were called significant, of these, 324 (~4.9% of the yeast genome) were up- and 483 (~7.3% of the yeast genome) were down-regulated (see Table 6 and 7). From these induced candidates 3 are also up-regulated via the UPR (see above): *CLB2*, a G2-specific cyclin; *HMX1*, a heme-binding peroxidase; and *YOR385W*, which encodes a protein that interacts with the E3 ligase, Rsp5p (http://www.incyte.com, http://www.ebi.ac.uk/InterProScan/, http://www.yeastgenome.org/). Although the percentage of differentially regulated genes might seem high, it is important to note that, for example, the UPR induces ~5% of the yeast genome (Travers *et al.*, 2000), and that treatment of cultured human airway epithelia with keratinocyte growth factor induced the expression of 12.9% of the genes examined two-fold or higher (Prince *et al.*, 2001). Under these conditions, concurrent with published data, genes denoted as significantly up-regulated included *FES1* (referred to as *YBR101C* in Table 6), *HSP82*, and *NPL4*. Fes1p and its human ortholog,

HspBP1, serve as nucleotide exchange factors for the cytoplasmic Hsp70 (Kabani *et al.*, 2002a; Kabani *et al.*, 2002b). Moreover, HspBP1 facilitates the Hsp70-dependent biosynthesis of CFTR (Alberti *et al.*, 2004). Hsp82, as well as its mammalian ortholog, Hsp90, facilitate CFTR biogenesis (Loo *et al.*, 1998; Fuller and Cuthbert, 2000; Alberti *et al.*, 2004; Youker *et al.*, 2004). Npl4p complexes with Cdc48p and Ufd1p that together catalyze ERAD substrate retro-translocation from the ER and delivery to the proteasome (Bays and Hampton, 2002), and this complex has been shown to facilitate CFTR degradation in yeast (Gnann *et al.*, 2004). Additional genes with possible roles in CFTR degradation and maturation include *CIC1*, possibly involved in proteasome substrate specificity; *UBP16*, a potential ubiquitin-specific protease; *RPN2*, a proteasome subunit; *VPS28*, a component of the vacuolar protein sorting pathway; and CCT3, a component of the cytoplasmic chaperonin complex (http://www.yeastgenome.org/). Also, several genes implicated in protein trafficking, for example, *SEC22*, *SFB3*, and *ERP5* were up-regulated. An additional ORF, *YBR075W* encoding a putative metalloprotease that was only induced 1.24-fold will be discussed later (see Chapter 3.4).

To confirm the results of the microarray analysis, the mRNA levels for several of the genes identified to be induced as a result of CFTR expression in yeast were measured by northern blot analysis. For this purpose, RNA isolated from an independently transformed and propagated culture was extracted and probed using PCR-fragments specific for the tested genes (see section 3.2.6.). In agreement with the results presented in Table 4 and 6, *HSP26*, *HSP82*, *FES1*, and *YBR075W* exhibited elevated mRNA levels upon CFTR expression, whereas *SEC61*, which was chosen as a negative control, did not (see Figure 21).

Table 4: List of genes up-regulated with a false discovery rate of 0.118.

SAM analysis was performed using the one class response option. SAM score (d_i) is calculated as follows: $d_i = r_i/s_i+s_0$;

r_i is the average base 2 logarithm of the median of pixel-by-pixel ratio, s_i is the standard deviation, s_0 is a fixed value (Tusher *et al.*, 2001).

False discovery rate represents the median of the number of falsely identified genes divided by the number of genes termed significant.

The cut-off was set at 0.51133.

Candidates are represented in alphabetical order; genes that have not been assigned a name yet are positioned at the end ordered alphabetically according to their systematic gene name.

Table 4: List of genes up-regulated with a false discovery rate of 0.118.

Gene name	Gene ID	SAM score	Gene name	Gene ID	SAM score
ACE2	YLR131C	0.5354645	RVB1	YDR190C	0.6494475
ACS1	YAL054C	0.8154645	RVS167	YDR388W	0.6981901
AGE1	YDR524C	0.5252931	SAG1	YJR004C	0.7487353
ALG11	YNL048W	1.1179425	SAS4	YDR181C	0.5229334
ALG2	YGL065C	0.5721636	SHD7	YPL180W	0.6610702
AME1	YBR211C	1.1423313	SHE2	YKL130C	0.7677449
ANP1	YEL036C	0.7837898	SHS1	YDL225W	0.5385315
APL4	YPR029C	0.7323618	SIS1	YNL007C	0.6081705
ARD2	YOR253W	0.6415636	SKS1	YPL026C	0.6116995
ARO80	YDR421W	0.6274118	SKY1	YMR216C	0.7658334
BUD2	YKL092C	0.5996595	SLA1	YBL007C	0.8062825
CBK1	YNL161W	0.5514176	SPO12	YHR152W	0.6978559
CDC54	YPR019W	0.5814325	TBF1	YPL128C	0.7314996
CET1	YPL228W	1.0211773	TDP1	YBR223C	0.6222723
CIT2	YCR005C	0.6249329	TKL2	YBR117C	0.5700223
COQ3	YOL096C	0.6207772	UBA1	YKL210W	0.784157
DCP2	YNL118C	0.6408754	UBP8	YMR223W	0.8187045
ECO1	YFR027W	0.8466539	URE2	YNL229C	0.6458571
EMP70	YLR083C	0.5482601	VPS53	YJL029C	1.0312161
ENA1	YDR040C	0.610744	YAK1	YJL141C	0.5659178
ENP1	YBR247C	0.7467007	YAP1	YML007W	0.6273008
ERP5	YHR110W	0.5140957	YAT2	YER024W	0.8762284
FIT2	YOR382W	0.6383035	YHP1	YDR451C	0.6143564
FLM1	YLR368W	0.6957145	YNG2	YHR090C	0.6465669
FLO5	YHR211W	0.5217471	YSW1	YBR148W	0.7802424
FRE6	YLL051C	0.556788	ZPR1	YGR211W	0.7056389
FUN21	YAL031C	0.7113612	ZRT3	YKL175W	0.976345
FYV9	YDR140W	0.5946895		YAR028W	0.5264223
GAL2	YLR081W	0.5928116		YBL009W	1.1171276
GAP1	YKR039W	0.5305734		YBL077W	1.1505036
GDH3	YAL062W	1.8300928		YBL081W	0.5583936
GLG2	YJL137C	0.5441961		YBR028C	0.7959197
GPI1	YGR216C	0.7576396		YBR062C	0.584843
GYP7	YDL234C	0.7388224		YBR063C	0.526655
HAA1	YPR008W	0.7521704		YBR134W	0.8298711
HAP4	YKL109W	0.5258314		YBR184W	0.718524
HMG1	YML075C	0.6846509		YBR220C	0.5587535
HOC1	YJR075W	0.9413915		YBR285W	0.6422557
HSP12	YFL014W	0.650576		YCL003W	0.5255249
HSP26	YBR072W	0.5148915		YCR023C	0.5113346
HST1	YOL068C	0.5313157		YCR100C	0.5217153
ISR1	YPR106W	0.5350464		YCRX01W	0.57279
KEL3	YPL263C	0.609486		YDL233W	0.5877314
LAG1	YHL003C	0.5536525		YDL238C	0.8471742
LAG2	YOL025W	0.6741755		YDR049W	0.7098481
LIN1	YHR156C	1.4123377		YDR109C	0.5260415
LYS7	YMR038C	0.7775951		YDR286C	0.5326126
MCM1	YMR043W	1.0563949		YDR357C	0.6599726

(Table 4 continued)

Gene name	Gene ID	SAM score	Gene name	Gene ID	SAM score
MDJ1	YFL016C	0.8767176		YDR396W	0.5475443
MED2	YDL005C	0.8481425		YDR458C	0.5410779
MEF1	YLR069C	0.5835699		YFL011W-A	0.713291
MET1	YKR069W	1.0066376		YFL-TYA	0.5267725
MMM2	YGL219C	0.5696961		YGL232W	0.650455
MNT4	YNR059W	0.764895		YGR126W	0.6925856
MOT1	YPL082C	0.8080344		YGR146C	0.6053002
MOT3	YMR070W	0.8633962		YHR029C	0.7135
MRPL3	YMR024W	0.6409642		YHR202W	0.7325546
MRPL49	YJL096W	0.5153423		YIL105C	0.6368369
MRS6	YOR370C	0.5719788		YJL010C	0.7446528
NEJ1	YLR265C	0.5374652		YJL144W	0.5987485
OKP1	YGR179C	0.5733336		YJL149W	0.5218521
OSH7	YHR001W	0.8259891		YJR039W	0.5434616
OXA1	YER154W	0.6362773		YKL088W	0.6878349
PAN3	YKL025C	0.6046646		YKL121W	1.0225889
PDR3	YBL005W	1.0103331		YKR023W	0.6001399
PDX1	YGR193C	0.5239218		YKR064W	0.5756685
PEX12	YMR026C	0.8941366		YLL056C	0.5821999
PEX18	YHR160C	0.8099402		YLR077W	0.6787384
PHO2	YDL106C	0.5846557		YLR101C	0.7894003
PHO4	YFR034C	0.6298684		YLR254C	0.5953134
POL32	YJR043C	0.8113145		YLR297W	0.5761218
PZF1	YPR186C	0.8591886		YLR408C	0.5486848
RAD27	YKL113C	0.7898438		YLR456W	0.6293983
RAD7	YJR052W	0.9807294		YML040W	0.5194019
REF2	YDR195W	0.9020187		YMR074C	0.6414522
RFC1	YOR217W	0.8815917		YMR245W	0.7909302
RPT2	YDL007W	0.5529343		YNL134C	0.5959392
RRP3	YHR065C	0.5396577		YNL152W	0.7092224
RRP4	YHR069C	0.5888745		YNL182C	0.5128074
RRP9	YPR137W	0.5724691		YOL154W	0.5207258
RSA3	YLR221C	0.6675734		YOR238W	0.6505084
RSC9	YML127W	0.7431848		YOR243C	0.5551412
RSM23	YGL129C	0.6523725		YOR315W	0.59822
RTT106	YNL206C	0.8869165		YOR338W	0.5131982

Table 5: List of genes down-regulated with a false discovery rate of 0.118.

SAM analysis was performed using the one class response option. SAM score (d_i) is calculated as follows: $d_i = r_i/s_i+s_0$;

r_i is the average base 2 logarithm of the median of pixel-by-pixel ratio, s_i is the standard deviation, s_0 is a fixed value (Tusher *et al.*, 2001).

False discovery rate represents the median of the number of falsely identified genes divided by the number of genes termed significant.

The cut-off was set at -0.48842.

Candidates are represented in alphabetical order; genes that have not been assigned a name yet are positioned at the end ordered alphabetically according to their systematic gene name.

Table 5: List of genes down-regulated with a false discovery rate of 0.118.

Gene name	Gene ID	Sam score	Gene name	Gene ID	Sam score
ADE5,7	YGL234W	-0.5638618	SIS2	YKR072C	-0.8281534
ANB1	YJR047C	-0.8771838	SKI2	YLR398C	-0.7773624
APL3	YBL037W	-0.5059574	SML1	YML058W	-0.5947792
ARP2	YDL029W	-0.4893178	SOM1	YEL059C-A	-1.0830485
ASK10	YGR097W	-0.5582381	SPC72	YAL047C	-0.5990846
ATM1	YMR301C	-0.6166013	SPS2	YDR522C	-0.8421081
ATP16	YDL004W	-0.5071484	SPT15	YER148W	-0.5132295
BCK2	YER167W	-0.6621884	SSU1	YPL092W	-0.5578112
CAF20	YOR276W	-0.489803	SSY5	YJL156C	-0.7555033
CAP2	YIL034C	-0.5786572	SWI1	YPL016W	-0.7993155
CCW12	YLR110C	-0.5080126	TFC3	YAL001C	-1.2722991
CDC123	YLR215C	-0.5222616	THR1	YHR025W	-0.51672
CGR1	YGL029W	-0.617686	TIF6	YPR016C	-0.4912277
CIN1	YOR349W	-0.4919311	TLG2	YOL018C	-0.5442128
CMK1	YFR014C	-0.8771254	TOS1	YBR162C	-0.5127822
CPR3	YML078W	-0.5880611	TPI1	YDR050C	-0.5763772
CTP1	YBR291C	-0.5741348	TPO4	YOR273C	-0.6887964
CUP5	YEL027W	-0.5461762	TRM1	YDR120C	-1.1159056
CUS2	YNL286W	-0.5565059	URA3	YEL021W	-2.0327624
CYR1	YJL005W	-0.770266	URK1	YNR012W	-0.8347968
DDC1	YPL194W	-0.4921074	VRG4	YGL225W	-0.6518238
DDI1	YER143W	-1.0672786	VTI1	YMR197C	-0.5099446
ECM14	YHR132C	-0.6296432	WSC2	YNL283C	-0.5242826
EDC1	YGL222C	-0.6915139	YHB1	YGR234W	-0.7115812
ELP3	YPL086C	-0.7761648	YHM1	YDL198C	-0.5821653
ERG24	YNL280C	-0.6583339	YKT9	YKL199C	-0.8987017
ESS1	YJR017C	-0.5154189	YPS1	YLR120C	-0.667331
EXG1	YLR300W	-0.5039264	ZUO1	YGR285C	-0.6367788
EXG2	YDR261C	-0.7857579		YAL061W	-0.7721073
GFD1	YMR255W	-0.6508879		YBR096W	-0.539775
GSH1	YJL101C	-0.6910685		YBR161W	-0.5394987
GTT2	YLL060C	-0.5307255		YBR210W	-0.5882846
GUP2	YPL189W	-0.6164146		YBR273C	-0.555588
GUT1	YHL032C	-0.9843011		YCL049C	-0.7209117
HBS1	YKR084C	-0.653613		YCR015C	0.6548429
HDR1	YBR138C	-0.7184401		YCR051W	-0.8402798
HIS1	YER055C	-0.5840717		YCRX09C	-0.7433812
HIS3	YOR202W	-0.9051203		YDL211C	-0.5418984
HKR1	YDR420W	-0.6411346		YDR153C	-0.7638346
HMT1	YBR034C	-0.5356794		YDR266C	-0.595464
HOM2	YDR158W	-0.7588959		YDR267C	-0.5616636
HTA2	YBL003C	-0.5267023		YDR417C	-0.5829851
HYP2	YEL034W	-0.7604866		YDR474C	-0.8745562
ICY2	YPL250C	-0.7400547		YFL065C	-0.9317297
IDP2	YLR174W	-1.0389159		YFR017C	-0.6100714
KRE5	YOR336W	-0.753278		YGL088W	-0.7943729
KRR1	YCL059C	-0.7553605		YGL117W	-0.5636607
KTR7	YIL085C	-1.5423158		YGL157W	-0.7236745

(Table 5 continued)

Gene name	Gene ID	Sam score	Gene name	Gene ID	Sam score
LSM5	YER146W	-0.6257448		YGL231C	-0.5223212
MCD1	YDL003W	-0.8430706		YGR272C	-0.6552175
MDN1	YLR106C	-0.5197688		YGR291C	-0.5283463
MET31	YPL038W	-0.9244627		YHR048W	-0.5585158
MMP1	YLL061W	-0.7514018		YIL083C	-0.5263372
MNN5	YJL186W	-0.9352424		YJL120W	-0.8680117
MPM1	YJL066C	-0.6837316		YJL162C	-0.8677083
MTR3	YGR158C	-0.7688142		YJR141W	-0.6508222
MUS81	YDR386W	-0.7542717		YKL206C	-0.4993421
NAF1	YNL124W	-0.5031403		YKR015C	-0.5973333
NAT3	YPR131C	-0.6452392		YKR100C	-0.5733185
NCE102	YPR149W	-0.6372099		YLL023C	-0.5178149
NOC2	YOR206W	-0.7384881		YLL047W	-0.8169775
NTF2	YER009W	-0.5201889		YLL049W	-0.6211896
PAC2	YER007W	-0.6327443		YLL067C	-0.5901414
PER1	YCR044C	-0.4920325		YLR020C	-0.556217
PET111	YMR257C	-0.542882		YLR023C	-1.0143902
PEX2	YJL210W	-0.7291338		YLR047C	-0.5013212
PEX7	YDR142C	-0.9158877		YLR050C	-0.5232866
PGK1	YCR012W	-0.7175373		YLR162W	-1.2259172
PHM6	YDR281C	-0.6125406		YLR331C	-0.7910865
PMP3	YDR276C	-0.5436216		YLR346C	-0.5909111
PRS2	YER099C	-0.7096873		YLR391W	-0.5701325
PSP2	YML017W	-0.5065558		YLR407W	-0.6437377
PTA1	YAL043C	-0.5121358		YLR454W	-0.7141599
PUT4	YOR348C	-0.5628027		YML002W	-0.5965356
PXR1	YGR280C	-0.8210194		YML108W	-0.8036918
REC102	YLR329W	-0.9538199		YMR103C	-0.7063822
RER2	YBR002C	-0.5960078		YMR124W	-0.7289924
RHR2	YIL053W	-0.6780381		YMR157C	-0.6056594
RIB2	YOL066C	-0.9407293		YMR252C	-0.5955838
RIC1	YLR039C	-0.7041078		YMR313C	-1.0197925
RIM15	YFL033C	-0.7190081		YMR321C	-0.4905542
RPB7	YDR404C	-0.4981934		YNL035C	-0.5544527
RPL16B	YNL069C	-0.6626343		YNL058C	-0.4910254
RPL30	YGL030W	-0.6581788		YNL338W	-0.557514
RPL38	YLR325C	-0.5820594		YOL015W	-0.764133
RPL4A	YBR031W	-0.5264042		YOL073C	-0.9509722
RPL9A	YGL147C	-0.4916093		YOR051C	-0.7200898
RPL9B	YNL067W	-0.5893585		YOR073W	-0.9731931
RRB1	YMR131C	-0.5777884		YOR155C	-0.5105856
SAH1	YER043C	-0.6114601		YOR164C	-0.8285988
SAP190	YKR028W	-0.4884243		YOR205C	-0.5148132
SCS2	YER120W	-0.493586		YOR291W	-0.6694206
SED1	YDR077W	-0.5088592		YOR322C	-0.5010336
SER3	YER081W	-0.5556438		YPL276W	-0.5134629
SFL1	YOR140W	-0.6625662		YPR012W	-1.4859598
SHC1	YER096W	-0.6328324			

Table 6: List of genes up-regulated with a false discovery rate of 0.219.

Candidates already represented in Table 4 are excluded.

SAM analysis was performed using the one class response option. SAM score (d_i) is calculated as follows: $d_i = r_i/s_i+s_0$;

r_i is the average base 2 logarithm of the median of pixel-by-pixel ratio, s_i is the standard deviation, s_0 is a fixed value (Tusher *et al.*, 2001).

False discovery rate represents the median of the number of falsely identified genes divided by the number of genes termed significant.

The cut-off was set at 0.37478.

Candidates are represented in alphabetical order; genes that have not been assigned a name yet are positioned at the end ordered alphabetically according to their systematic gene name.

Table 6: List of genes up-regulated with a false discovery rate of 0.219.

Gene name	Gene ID	Sam score	Gene name	Gene ID	Sam score
ADH4	YGL256W	0.493342	SHG1	YBR258C	0.4388417
ALG8	YOR067C	0.4240654	SMD2	YLR275W	0.4354625
ARN2	YHL047C	0.3837193	SNM1	YDR478W	0.3931462
ASF1	YJL115W	0.4411638	SPP1	YPL138C	0.479571
ASH1	YKL185W	0.4146571	SUR1	YPL057C	0.4417018
BFR2	YDR299W	0.4938719	TAF12	YDR145W	0.4463338
BNA4	YBL098W	0.49472	TFA1	YKL028W	0.3804029
BRF1	YGR246C	0.4217324	TFB3	YDR460W	0.4405711
CCT3	YJL014W	0.3787599	TFG2	YGR005C	0.4261854
CDC50	YCR094W	0.5026724	TOS7	YOL019W	0.5041942
CFT1	YDR301W	0.4775833	TPK2	YPL203W	0.4754099
CHK1	YBR274W	0.4044078	UBP16	YPL072W	0.3747842
CIC1	YHR052W	0.3857037	URA4	YLR420W	0.4791495
CKI1	YLR133W	0.4340565	VPS28	YPL065W	0.3902836
CLB2	YPR119W	0.4784397	XYL2	YLR070C	0.4965696
CLF1	YLR117C	0.4255446	YAP1801	YHR161C	0.3779147
COT1	YOR316C	0.468054	YAP6	YDR259C	0.4737717
CRS5	YOR031W	0.4379941	YSC83	YHR017W	0.444902
CUP1-1	YHR053C	0.4451074	YTA6	YPL074W	0.4415857
CUP1-2	YHR055C	0.4257587	ZDS1	YMR273C	0.5027629
CYC8	YBR112C	0.416638		YBL005W-B	0.376432
DAT1	YML113W	0.4202432		YBL101W-A	0.5079474
DEM1	YBR163W	0.4654022		YBL107C	0.4520141
DOP1	YDR141C	0.452437		YBR101C	0.4538358
DUO1	YGL061C	0.4662963		YBR168W	0.3758019
ENB1	YOL158C	0.466643		YBR204C	0.407345
ERG5	YMR015C	0.4108163		YBR235W	0.4125767
FAT1	YBR041W	0.3808455		YBR259W	0.4039933
FET3	YMR058W	0.3881147		YCL042W	0.4579868
FHL1	YPR104C	0.4635475		YCRX15W	0.4940827
FRE4	YNR060W	0.386091		YDR221W	0.4255089
FUN26	YAL022C	0.4726588		YDR340W	0.4134746
FUN31	YAL017W	0.3819605		YFL063W	0.4429495
FYV1	YDR024W	0.3751428		YFR008W	0.4372755
GDI1	YER136W	0.3888266		YGL042C	0.4946791
GRE2	YOL151W	0.4536828		YGL168W	0.4158372
HAM1	YJR069C	0.4436346		YGR111W	0.4546116
HGH1	YGR187C	0.4903233		YGR125W	0.4332553
HMX1	YLR205C	0.4340485		YHL010C	0.398237
HSP82	YPL240C	0.3911802		YHL026C	0.4835794
IMD1	YAR073W	0.3997759		YHR145C	0.3752084
ISC1	YER019W	0.3959086		YHR149C	0.4488217
IXR1	YKL032C	0.4673089		YIL121W	0.4180313
LPD1	YFL018C	0.4855592		YIL127C	0.4767312
LSM7	YNL147W	0.462476		YJL132W	0.4524199
MAL33	YBR297W	0.4738088		YJL160C	0.4018974
MDH3	YDL078C	0.4212906		YJR070C	0.3860262
MRPL13	YKR006C	0.4755724		YJR088C	0.4143578

(Table 6 continued)

Gene name	Gene ID	Sam score	Gene name	Gene ID	Sam score
MTR2	YKL186C	0.4854254		YJR115W	0.4815571
MUM2	YBR057C	0.4122139		YKL133C	0.456663
NDD1	YOR372C	0.4155453		YKL137W	0.3857732
NIT3	YLR351C	0.420616		YKR018C	0.4738795
NPL4	YBR170C	0.4178502		YKR038C	0.4344144
NUP57	YGR119C	0.4166915		YKR060W	0.37544
OCA1	YNL099C	0.3795482		YKR089C	0.4004008
PAN5	YHR063C	0.4844171		YLR137W	0.4527801
PCD1	YLR151C	0.391998		YLR294C	0.4068739
PCL9	YDL179W	0.411219		YLR412W	0.4862919
PDR12	YPL058C	0.4022537		YLR440C	0.3999926
PIN2	YOR104W	0.4431754		YMR046C	0.4332095
POP5	YAL033W	0.4052184		YMR160W	0.4188163
POS5	YPL188W	0.3863893		YMR192W	0.4010943
PPE1	YHR075C	0.4666037		YMR215W	0.5003371
PRD1	YCL057W	0.3780508		YMR304C-A	0.3919877
PRP6	YBR055C	0.431794		YNL129W	0.4092399
PUB1	YNL016W	0.4109086		YNL191W	0.4789758
RDH54	YBR073W	0.5091566		YOL045W	0.4700731
RGS2	YOR107W	0.4344168		YOL054W	0.3849798
RHO5	YNL180C	0.4391915		YOR072W	0.3905673
RPN2	YIL075C	0.4152061		YOR256C	0.3955263
RRM3	YHR031C	0.425695		YOR292C	0.4235329
RSC1	YGR056W	0.4634058		YOR320C	0.3773285
RSM18	YER050C	0.3989076		YOR385W	0.3773067
RSM22	YKL155C	0.3960271		YOR391C	0.459942
RUB1	YDR139C	0.4684762		YPL103C	0.4416011
SAE2	YGL175C	0.5091157		YPL146C	0.5055029
SEC22	YLR268W	0.3783762		YPL184C	0.477432
SFB3	YHR098C	0.4625626		YPR157W	0.399345

Table 7: List of genes down-regulated with a false discovery rate of 0.219.

Candidates already represented in Table 5 are excluded.

SAM analysis was performed using the one class response option. SAM score (d_i) is calculated as follows: $d_i = r_i/s_i+s_0$;

r_i is the average base 2 logarithm of the median of pixel-by-pixel ratio, s_i is the standard deviation, s_0 is a fixed value (Tusher *et al.*, 2001).

False discovery rate represents the median of the number of falsely identified genes divided by the number of genes termed significant.

The cut-off was set at -0.31966.

Candidates are represented in alphabetical order; genes that have not been assigned a name yet are positioned at the end ordered alphabetically according to their systematic gene name.

Table 7: List of genes down-regulated with a false discovery rate of 0.219.

Gene name	Gene ID	Sam score	Gene name	Gene ID	Sam score
ABF2	YMR072W	-0.4035166	SES1	YDR023W	-0.3600553
ACC1	YNR016C	-0.3420976	SFB2	YNL049C	-0.4538388
ADO1	YJR105W	-0.3707425	SGT1	YOR057W	-0.3761106
AFG2	YLR397C	-0.3329074	SHE9	YDR393W	-0.4006388
AMD2	YDR242W	-0.4076542	SHM2	YLR058C	-0.359617
APS1	YLR170C	-0.3764075	SHR3	YDL212W	-0.3340474
ARC18	YLR370C	-0.4082286	SKI6	YGR195W	-0.3644783
ARG1	YOL058W	-0.4850193	SLY1	YDR189W	-0.3882459
ARG3	YJL088W	-0.4815167	SNQ2	YDR011W	-0.3944842
ARG8	YOL140W	-0.3700517	SPT4	YGR063C	-0.3951073
ARO3	YDR035W	-0.4793793	SRL3	YKR091W	-0.3718807
ARO4	YBR249C	-0.3196622	SSE2	YBR169C	-0.3791994
AUT10	YFR021W	-0.4339836	SSH1	YBR283C	-0.3570308
AUT4	YCL038C	-0.3925144	STB5	YHR178W	-0.3308338
AUT7	YBL078C	-0.4702483	STE11	YLR362W	-0.4685999
BUD23	YCR047C	-0.3968652	STE4	YOR212W	-0.3306096
BUR6	YER159C	-0.3416653	STM1	YLR150W	-0.3555988
CBF5	YLR175W	-0.3959819	STP2	YHR006W	-0.4209888
CDC31	YOR257W	-0.328109	STT4	YLR305C	-0.4463394
CHO2	YGR157W	-0.3951097	SUB2	YDL084W	-0.4008951
CHS7	YHR142W	-0.4781038	SUR4	YLR372W	-0.3223841
CLC1	YGR167W	-0.3337671	SWD1	YAR003W	-0.3924043
CMD1	YBR109C	-0.3692843	SWI6	YLR182W	-0.4243125
CNE1	YAL058W	-0.4369845	SYS1	YJL004C	-0.460956
COS8	YHL048W	-0.3936434	TAL1	YLR354C	-0.4253518
COX11	YPL132W	-0.4546737	TCP1	YDR212W	-0.3371377
CRD1	YDL142C	-0.3546696	TEF1	YPR080W	-0.3272715
CTR2	YHR175W	-0.3914934	TIF2	YJL138C	-0.4349815
CWP1	YKL096W	-0.4165249	TIF3	YPR163C	-0.3229135
CYB5	YNL111C	-0.3535774	TOA2	YKL058W	-0.3836746
CYC3	YAL039C	-0.3449293	TOM22	YNL131W	-0.4323298
DAK1	YML070W	-0.342392	TRS33	YOR115C	-0.3838477
DBP2	YNL112W	-0.4736917	TRX1	YLR043C	-0.3708407
DFR1	YOR236W	-0.3230952	TUB2	YFL037W	-0.4213864
DIA2	YOR080W	-0.3868678	TUP1	YCR084C	-0.4541179
DIT1	YDR403W	-0.3911024	UGP1	YKL035W	-0.3435169
DRE3	YIL003W	-0.3253628	UME1	YPL139C	-0.4306439
DYS1	YHR068W	-0.4366676	UTP4	YDR324C	-0.462796
EAF3	YPR023C	-0.4476286	VID24	YBR105C	-0.4702607
ECM1	YAL059W	-0.4064597	VID31	YKL054C	-0.4033984
ECM17	YJR137C	-0.3389033	VPS25	YJR102C	-0.3335088
ECM4	YKR076W	-0.3227636	VPS5	YOR069W	-0.4378908
EDS1	YBR033W	-0.339196	VPS73	YGL104C	-0.4550529
ELG1	YOR144C	-0.3221461	YBT1	YLL048C	-0.4126298
ENA2	YDR039C	-0.3642974	YCF1	YDR135C	-0.4251066
ERG10	YPL028W	-0.3614997	YMD8	YML038C	-0.4534763
ERG13	YML126C	-0.3832324	YNK1	YKL067W	-0.3339919
ERG28	YER044C	-0.4361113	YPK2	YMR104C	-0.3663585

(Table 7 continued)

Gene name	Gene ID	Sam score	Gene name	Gene ID	Sam score
ERG3	YLR056W	-0.3638514	YRB1	YDR002W	-0.4585467
ERG9	YHR190W	-0.3291244	YRF1-2	YER190W	-0.4130435
ERV1	YGR029W	-0.4027255	YRF1-5	YLR467W	-0.4021749
FAP7	YDL166C	-0.3776291	ZMS1	YJR127C	-0.3693425
FCY2	YER056C	-0.3587603	ZRT2	YLR130C	-0.3791246
FKS1	YLR342W	-0.452844		YAL011W	-0.3294305
FLO10	YKR102W	-0.3920069		YAR066W	-0.449276
FPR1	YNL135C	-0.4237143		YBL004W	-0.4840155
FUN19	YAL034C	-0.3212891		YBL029W	-0.4104987
GFD2	YCL036W	-0.4244291		YBL060W	-0.3252889
GOT1	YMR292W	-0.3286361		YBR090C-A	-0.3441699
GPA1	YHR005C	-0.3446049		YBR280C	-0.3667338
GSC2	YGR032W	-0.3890059		YCR029C	-0.3990985
GSF2	YML048W	-0.3807991		YDL193W	-0.372173
GTT1	YIR038C	-0.4071764		YDL206W	-0.3958075
GUP1	YGL084C	-0.3773532		YDR026C	-0.3529741
HAP3	YBL021C	-0.3492004		YDR031W	-0.4032447
HEM1	YDR232W	-0.3861053		YDR061W	-0.3509296
HEM15	YOR176W	-0.376219		YDR112W	-0.4508237
HEM2	YGL040C	-0.4616791		YDR133C	-0.4015184
HHF1	YBR009C	-0.3834597		YDR134C	-0.3656822
HIF1	YLL022C	-0.4138735		YDR185C	-0.3779283
HIS4	YCL030C	-0.3359354		YDR233C	-0.3961261
HSP30	YCR021C	-0.4314327		YDR445C	-0.4780046
HTB2	YBL002W	-0.481522		YEL072W	-0.340726
HXT15	YDL245C	-0.4569976		YER087C-A	-0.3921715
IDH2	YOR136W	-0.4205422		YER160C	-0.3224668
IFM1	YOL023W	-0.4194741		YFR035C	-0.3601227
ILV2	YMR108W	-0.3684969		YFR039C	-0.3580471
ILV3	YJR016C	-0.4218617		YFR041C	-0.4061667
IPP1	YBR011C	-0.4496889		YFR042W	-0.4286775
IRA1	YBR140C	-0.4615404		YGL020C	-0.4025
ISU2	YOR226C	-0.430773		YGL039W	-0.3362466
ISY1	YJR050W	-0.3472745		YGL057C	-0.330754
JNM1	YMR294W	-0.3600522		YGL101W	-0.4246622
KIN2	YLR096W	-0.3285851		YGL107C	-0.4338464
KRE2	YDR483W	-0.419801		YGR093W	-0.4369948
KRE25	YNL296W	-0.467667		YGR117C	-0.3424121
LOT6	YLR011W	-0.4304672		YGR257C	-0.3347576
LRG1	YDL240W	-0.41597		YGR273C	-0.4209733
LYS1	YIR034C	-0.3282855		YHR209W	-0.4612944
LYS12	YIL094C	-0.4510331		YIL039W	-0.4699887
LYS20	YDL182W	-0.4232446		YIL088C	-0.4183268
MAK3	YPR051W	-0.4197246		YIL165C	-0.3762928
MAK31	YCR020C-A	-0.4274004		YIR043C	-0.3542488
MET10	YFR030W	-0.4541879		YJL070C	-0.4207034
MET16	YPR167C	-0.4223595		YJL131C	-0.4707061
MMF1	YIL051C	-0.4551257		YJL163C	-0.3985463
MRPL35	YDR322W	-0.3519177		YJL206C-A	-0.3344618
MRPS18	YNL306W	-0.3211355		YKL036C	-0.4372884
MUB1	YMR100W	-0.3270531		YKL083W	-0.3848484
MUP3	YHL036W	-0.4547943		YKL084W	-0.456032

(Table 7 continued)

Gene name	Gene ID	Sam score	Gene name	Gene ID	Sam score
NAP1	YKR048C	-0.4645902		YKL097W-A	-0.3776041
NDE2	YDL085W	-0.3846987		YKL224C	-0.4424214
NFI1	YOR156C	-0.357053		YKR040C	-0.3895782
NFS1	YCL017C	-0.4689462		YKR046C	-0.3365784
NGL1	YOL042W	-0.4264941		YKR049C	-0.3210018
NOG1	YPL093W	-0.3275348		YLL055W	-0.3756343
NOP13	YNL175C	-0.3727326		YLL058W	-0.3289342
NOP58	YOR310C	-0.3563652		YLR022C	-0.3676946
PAB1	YER165W	-0.468184		YLR041W	-0.4331768
PAN6	YIL145C	-0.4333445		YLR063W	-0.428873
PCL5	YHR071W	-0.3940985		YLR072W	-0.3555556
PDA1	YER178W	-0.4519567		YLR179C	-0.3322725
PEP3	YLR148W	-0.3334164		YLR184W	-0.3385824
PET123	YOR158W	-0.4424146		YLR326W	-0.3826544
PFK2	YMR205C	-0.3931861		YLR392C	-0.4856061
POP6	YGR030C	-0.4367696		YLR445W	-0.4410903
PRI1	YIR008C	-0.4818085		YML005W	-0.4287361
PRP19	YLL036C	-0.3493669		YML018C	-0.3480285
PRP22	YER013W	-0.3380746		YML082W	-0.4455778
PRS5	YOL061W	-0.4454714		YML089C	-0.3282588
PYC2	YBR218C	-0.328169		YML117W-A	-0.4611421
RAD50	YNL250W	-0.3503908		YMR086W	-0.4689234
RHO1	YPR165W	-0.3917889		YMR196W	-0.3671669
RIF1	YBR275C	-0.3502153		YMR291W	-0.4341237
RPG1	YBR079C	-0.4307518		YMR315W	-0.3596854
RPL16A	YIL133C	-0.4616214		YNL047C	-0.3834452
RPL23A	YBL087C	-0.355134		YNL056W	-0.3715618
RPL7B	YPL198W	-0.3467297		YNL089C	-0.3583673
RPS27A	YKL156W	-0.4004054		YNL119W	-0.4648008
RPT5	YOR117W	-0.4241453		YNL136W	-0.4635686
RRN3	YKL125W	-0.3589719		YNL227C	-0.4216299
RRP12	YPL012W	-0.4791035		YNL254C	-0.3218216
RRP5	YMR229C	-0.4263711		YNR025C	-0.3445592
RRP8	YDR083W	-0.3881478		YNR036C	-0.3283297
RSN1	YMR266W	-0.372745		YNR063W	-0.4398687
RSR1	YGR152C	-0.4058296		YOR108W	-0.3519813
SAC7	YDR389W	-0.391687		YOR112W	-0.3856989
SAM1	YLR180W	-0.349022		YOR282W	-0.3346497
SAM2	YDR502C	-0.3503821		YOR296W	-0.3203675
SAM3	YPL274W	-0.3710006		YOR304C-A	-0.4436558
SAR1	YPL218W	-0.3747223		YOR352W	-0.3688478
SDC1	YDR469W	-0.352773		YPL044C	-0.4033875
SEC11	YIR022W	-0.4198859		YPL230W	-0.3219021
SEC9	YGR009C	-0.3620644		YPR003C	-0.3629078
SEH1	YGL100W	-0.45741		YPR099C	-0.4398538

Figure 21: *HSP26, HSP82, FES1,* and *YBR075W* mRNA levels are elevated in yeast expressing CFTR.

HSP26, HSP82, FES1, YBR075W, and *SEC61* mRNAs were detected by northern blot analysis from yeast transformed with a plasmid expressing CFTR under the control of a constitutive promoter ("+") and yeast transformed with a vector control ("-"). The fold up-regulation upon CFTR expression as determined by northern blot analysis was: *HSP26*: 1.7; *HSP82*: 1.4; *FES1*: 1.3; *YBR075W*: 1.24.

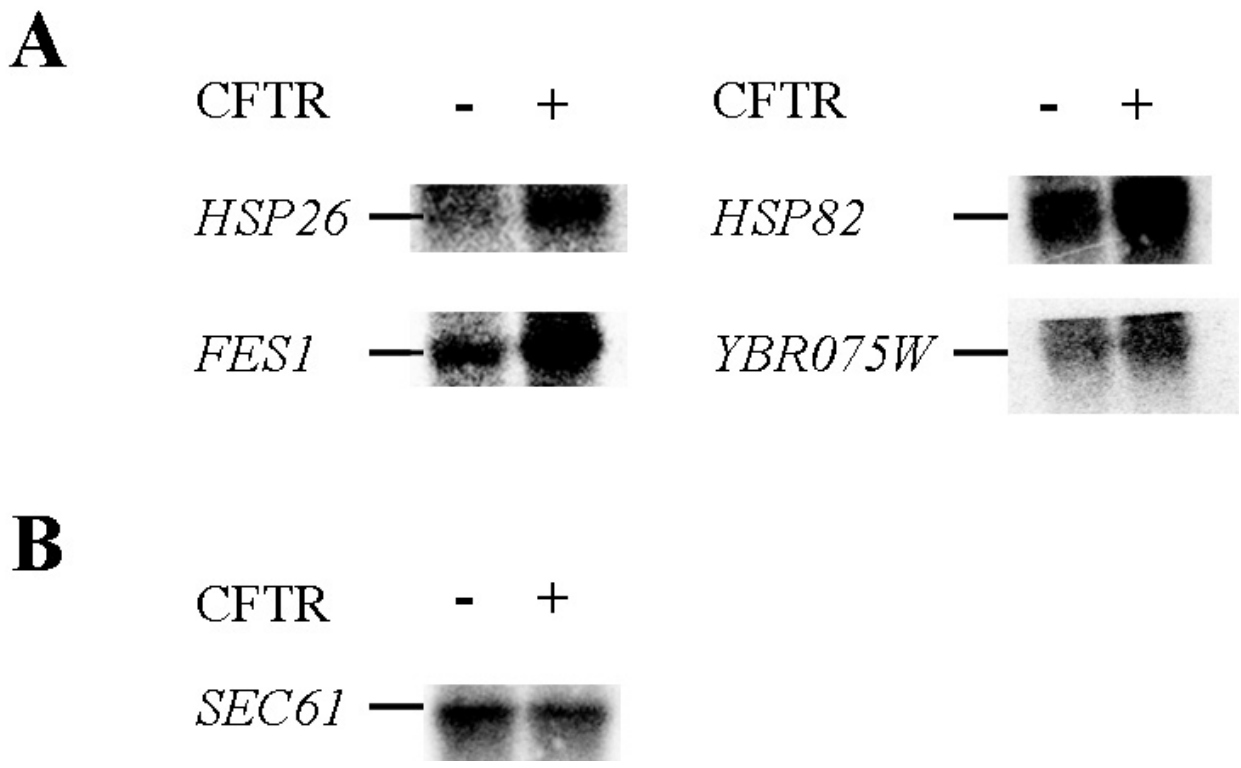

Figure 21: *HSP26*, *HSP82*, *FES1*, and *YBR075W* mRNA levels are elevated in yeast expressing CFTR.

Taken together, the microarray analysis of gene expression levels in response to heterologous synthesis of CFTR in yeast identified several genes already shown to impact CFTR biogenesis, but also revealed a number of putative factors that might regulate CFTR degradation and maturation in yeast, many of which are conserved in mammals.

3.3.2. Small Hsps facilitate specifically the degradation of CFTR in yeast

As mentioned above, one of the molecular chaperones exhibiting induced mRNA levels upon CFTR expression in yeast was *HSP26*, a member of the small Hsp family. Hsp26 and other sHsps have been shown to prevent proteins from aggregating. Mammalian sHsps also inhibit apoptosis when up-regulated and two family members have been linked to the ubiquitin-proteasome pathway (see Chapter 1.4, and Narberhaus, 2002). Therefore, I wanted to assess whether Hsp26 plays a role in CFTR degradation or maturation. To this end, I expressed an HA-epitope-tagged form of wild type CFTR under the control of a constitutive promoter in a wild type yeast strain and in an *hsp26* deletion strain that I generated via one-step gene-replacement. The rate of CFTR degradation was then determined by cycloheximide chase analysis at 30°C (see Materials and Methods). The levels of Sec61p, an integral ER membrane protein, were measured as well, and provided a loading control. I found that the proteolysis of CFTR was reduced in the *hsp26Δ* mutant compared to the wild type yeast: ~50% of the protein remained 90 min after cycloheximide addition in the *hsp26Δ* strain and only ~25% of the CFTR remained in the wild type strain at this point (see Figure 22A and B).

Figure 22: CFTR degradation is slowed in the *hsp26* deletion mutant.

A. Rates of CFTR degradation were determined by cycloheximide chase experiments in *HSP26* wild type yeast and in the *hsp26Δ* deletion mutant strain after addition of cycloheximide. Sec61p serves as a loading control. B. CFTR protein levels were quantified from 3 independent sets of experiments and averaged. All values were obtained after standardization to the levels detected directly after cycloheximide addition (0 min). Closed blue circles represent the CFTR protein levels in *HSP26* wild type yeast, open purple circles represent the CFTR protein levels in the *hsp26Δ* mutant. Vertical bars indicate the standard errors of the mean. P-values for 40, 60, and 90 minutes after cycloheximide addition are 0.0112, 0.0222, and 0.0625, respectively.

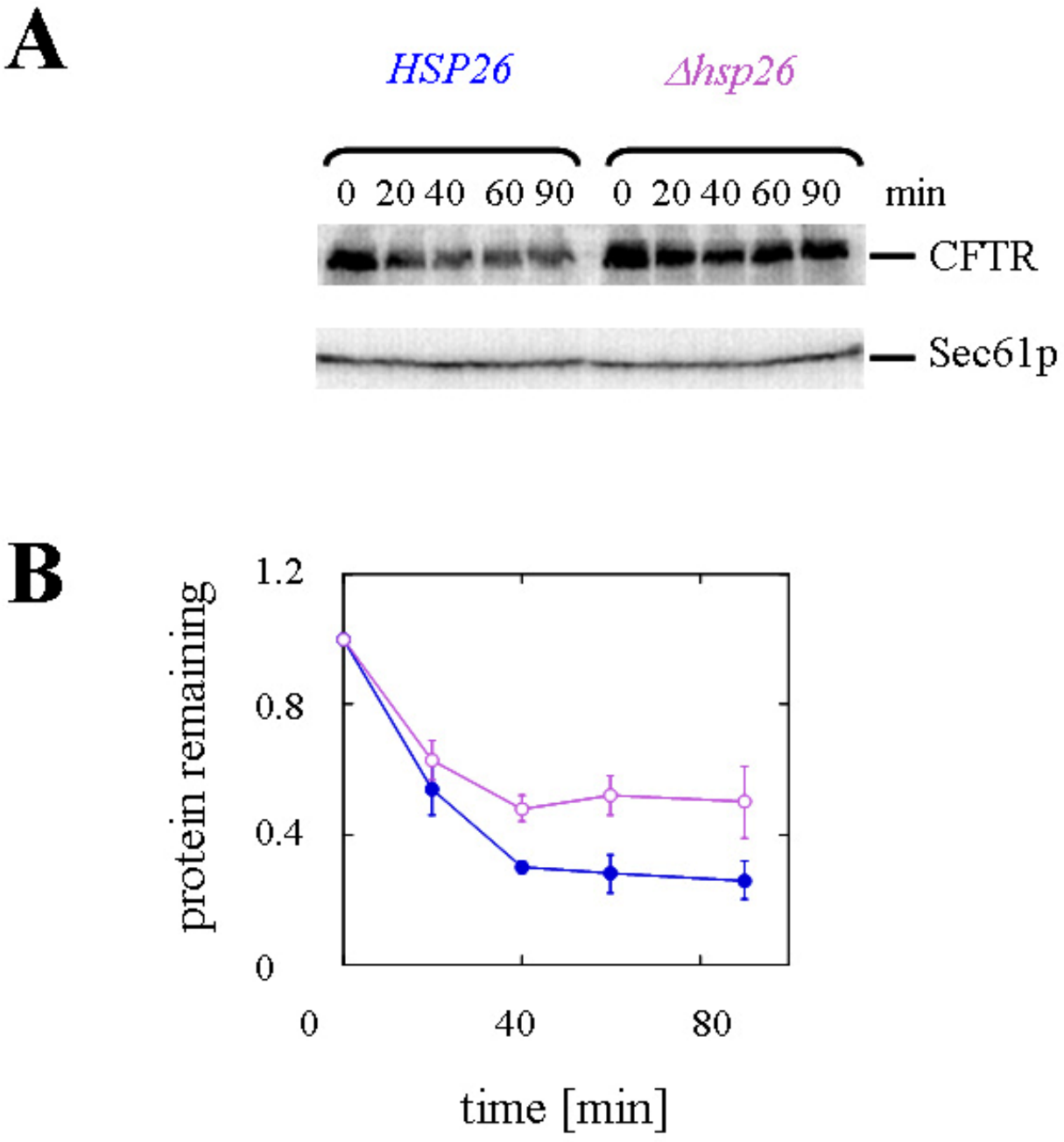

Figure 22: CFTR degradation is slowed in the *hsp26* deletion mutant.

As mentioned in Chapter 1.3, different ERAD substrates require distinct factors for their degradation, depending on solubility, membrane association, and localization of the lesion (Plemper *et al.*, 1997; Brodsky *et al.*, 1999; Hill and Cooper, 2000; Fewell *et al.*, 2001; Nishikawa *et al.*, 2001; Vashist *et al.*, 2001; Zhang *et al.*, 2001; Kabani *et al.*, 2003; Taxis *et al.*, 2003; Ahner and Brodsky, 2004; Huyer *et al.*, 2004; Vashist and Ng, 2004). Hence, I wished to establish if Hsp26 contributes to the degradation of every ERAD substrate. If such an effect were observed it might arise from a general stress response in the deletion strain, and may simply be an artifact. To exclude this possibility I transformed the corresponding wild type and *hsp26Δ* strains with a vector expressing CPY*, a soluble ERAD substrate (Hiller *et al.*, 1996), under the control of a constitutive promoter, and CPY* degradation was measured by pulse-chase immuno-precipitation at 30°C. In agreement with published results on the effects of other molecular chaperones on soluble ERAD substrates versus integral membrane proteins, I observed that the effects of deleting *HSP26* on CFTR and CPY* were distinct: proteolysis of the soluble ERAD substrate was slightly enhanced in the *hsp26Δ* mutant (see Figure 23).

Saccharomyces cerevisiae encodes 2 α-crystallin domain-containing members of the sHsp family, Hsp26 and Hsp42 (Geoffrey, 1997). Whereas Hsp42 seems to be a general sHsp, Hsp26 can be induced by cell stress, even though, the two homologs share ~90% of their client proteins (Haslbeck *et al.*, 2004). This suggested that Hsp42 may also impact CFTR degradation. To resolve this proposition, CFTR was expressed in strains containing a different genetic background (see Materials and Methods in subsection 3.2.1.), and that were deleted for *HSP26*, *HSP42*, or both genes. Cycloheximide chase experiments were performed at 30°C in these strains and in the isogenic wild type strain and the amount of CFTR remaining over time was

Figure23: CPY* protein degradation is not attenuated in *hsp26Δ* yeast.

A. The rates of CPY* degradation were determined by pulse-chase immuno-precipitation experiments in *HSP26* wild type yeast and in the *hsp26Δ* mutant strain after addition of cycloheximide. B. CPY* protein levels were quantified from 3 independent sets of experiments and averaged. All values were obtained after standardization to the levels detected directly after cycloheximide addition (0 min). Closed blue circles represent the CPY* protein levels in *HSP26* wild type yeast, open purple circles represent the CPY* protein levels in the *hsp26Δ* mutant. Vertical bars indicate the standard errors of the means.

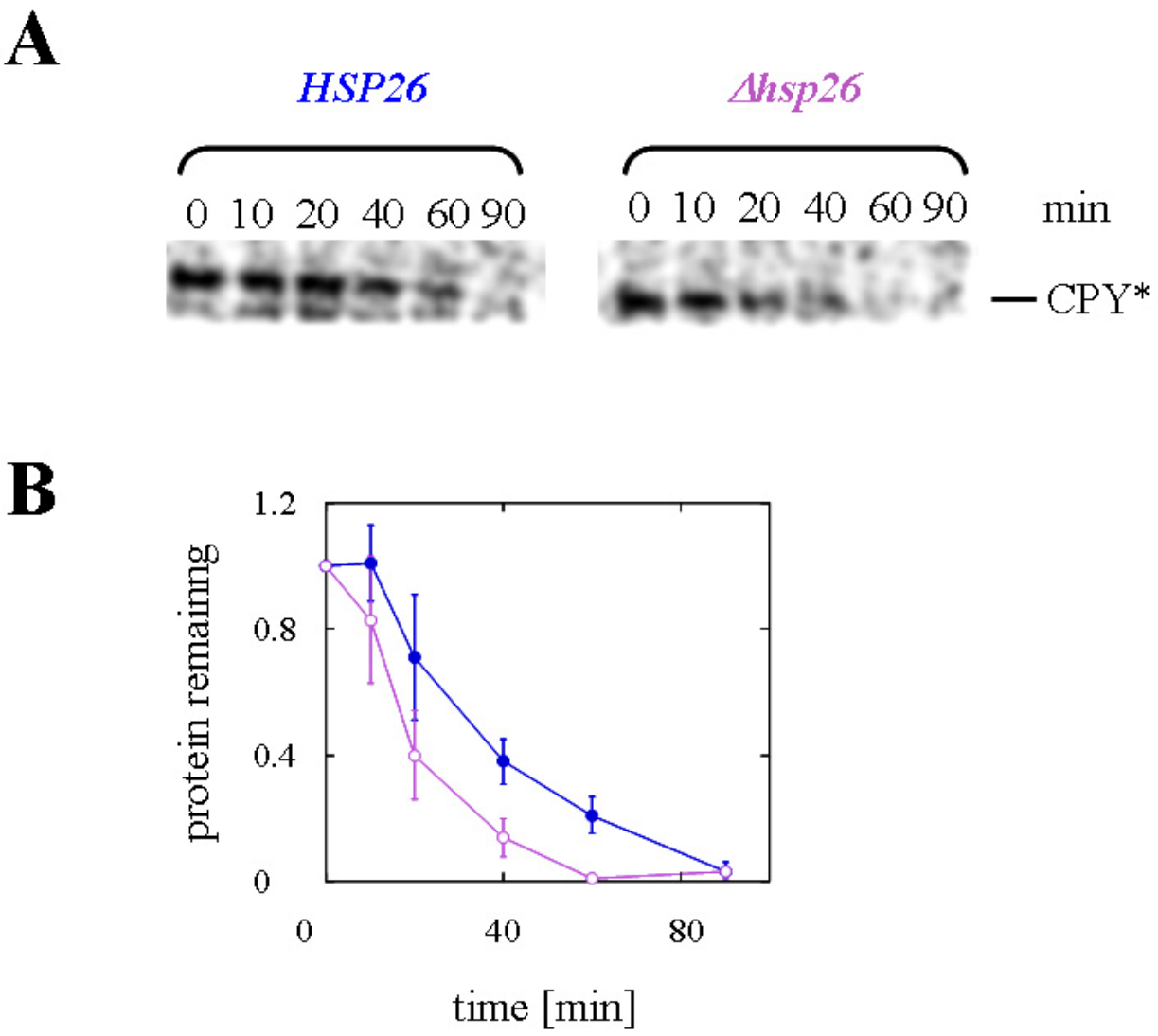

Figure 23: CPY* protein degradation is not attenuated in the *hsp26Δ* yeast.

measured. Sec61p served again as a loading control (data not shown). While neither the *hsp26Δ* mutant nor the *hsp42Δ* mutant showed a robust stabilization of CFTR, in this strain background, ~90% of the protein remained stable after the 90 min chase period in the *hsp26Δhsp42Δ* double mutant compared to only 30% in the wild type strain (see Figure 24). These results indicate that Hsp26 and Hsp42 both facilitate CFTR degradation and suggest that they compensate for each other in the single deletion strains. This functional redundancy is consistent with the observation, noted above, that the two sHsps in yeast share ~90% of their substrates (Haslbeck *et al.*, 2004). However, the degree of compensation appears to be dependent on the genetic background because CFTR was degraded at a faster rate in the isogenic wild type yeast compared to the *hsp26Δ* mutant in the first background utilized (see Fig.ure 22). Moreover, the stabilization observed in the single mutants shown in Figure 24 is less prominent than in the first experiment. Such background-specific chaperone-dependent effects are not without precedence (Caplan and Douglas, 1991; Atencio and Yaffe, 1992).

To evaluate whether cells lacking both, Hsp26 and Hsp42 are able to degrade a soluble ERAD substrate, I transformed the isogenic wild type strain and the *hsp26Δ hsp42Δ* double mutant with the vector expressing CPY* and degradation was measured by pulse-chase immuno-precipitation at 30°C. In accordance with the ERAD substrate specificity of other chaperones (see above) there was no difference between the rate of CPY* proteolysis between the wild type yeast and the *hsp26Δ hsp42Δ* double mutant (see Figure 25). This indicates that neither of these sHsps in yeast assists in the ERAD of a misfolded, soluble ER protein, whereas they are required for the degradation of the integral membrane protein, CFTR. These data also preclude the possibility

Figure 24: CFTR degradation is slowed in the *hsp26Δhsp42Δ* double mutant.

A. Rates of CFTR degradation were determined by cycloheximide chase experiments in *HSP26HSP42* wild type yeast, in the *hsp26Δ* deletion mutant and the *hsp42Δ* deletion mutant, and in the *hsp26Δhsp42Δ* double mutant strain after addition of cycloheximide. Sec61p levels served as a loading control (data not shown). B. CFTR protein levels were quantified from 4 independent sets of experiments and averaged. All values were obtained after standardization to the levels detected directly after cycloheximide addition (0 min). Closed blue circles represent the levels of CFTR in *HSP26HSP42* wild type cells, and open purple triangles represent CFTR levels in the *hsp26Δ* mutant. Closed red circles triangles CFTR remaining in the *hsp42Δ* mutant, and open yellow circles depict experiments in the *hsp26Δhsp42Δ* double mutant. Vertical bars indicate the standard errors of the means. Comparison of CFTR protein levels between the wild type yeast and the *hsp26Δhsp42Δ* double mutant strain at 60 and 90 minutes after cycloheximide addition yielded p-values < 0.03.

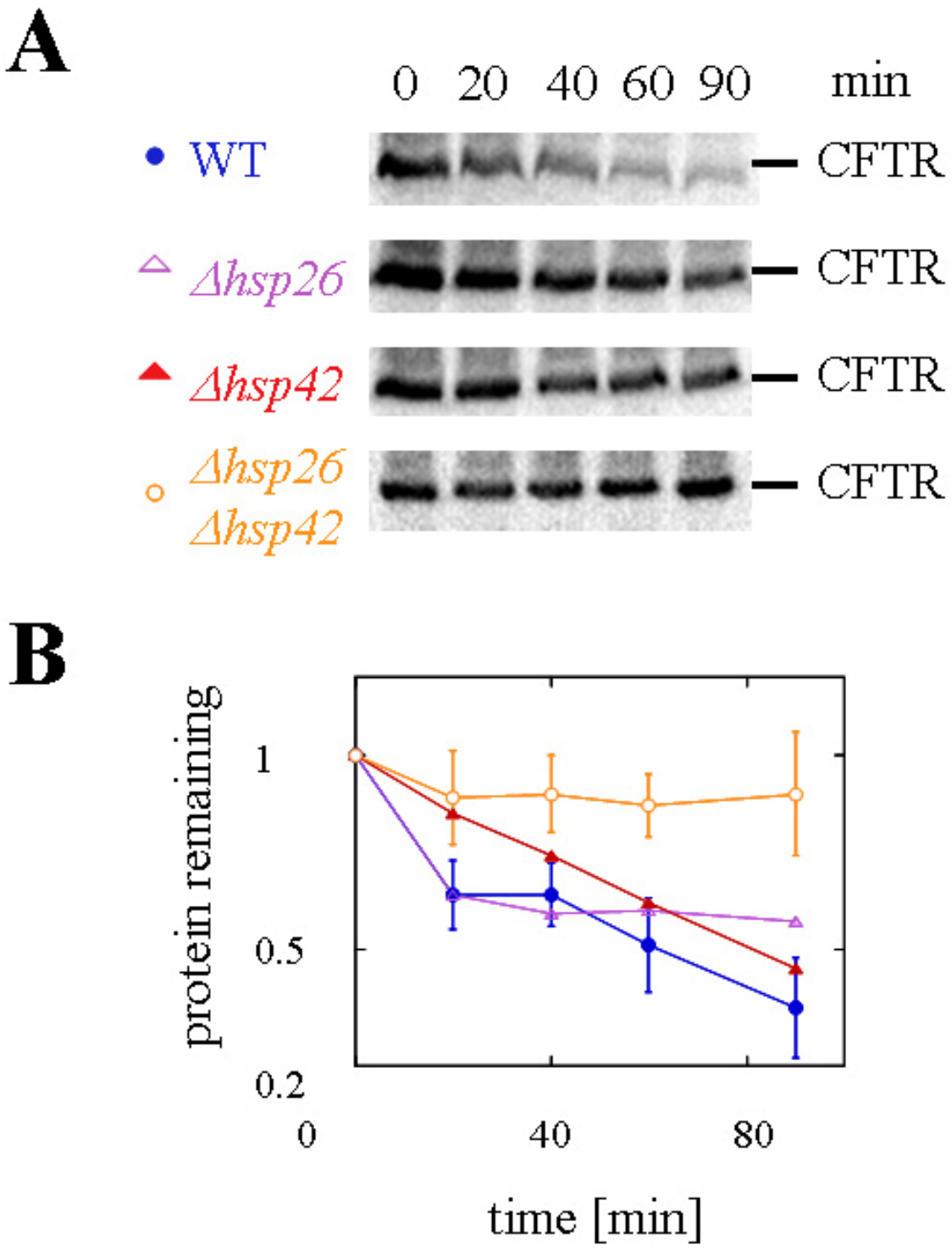

Figure 24: CFTR degradation is slowed in the *hsp26Δhsp42Δ* double mutant.

Figure 25: CPY* protein degradation is equally efficient in the *HSP26HSP42* wild type and *hsp26Δhsp42Δ* double mutant strains.

A. Rates of CPY* degradation were determined by pulse-chase immuno-precipitation experiments in *HSP26HSP42* wild type yeast and in the *hsp26Δhsp42Δ* double mutant strain after addition of cycloheximide. B. CPY* protein levels were quantified from 2 independent sets of experiments and averaged. All values were obtained after standardization to the levels detected directly after cycloheximide addition (0 min). Closed blue circles represent CPY* protein levels in *HSP26* wild type yeast, and open yellow circles represent CPY* protein levels in the *hsp26Δhsp42Δ* double mutant. Vertical bars indicate the range of the data.

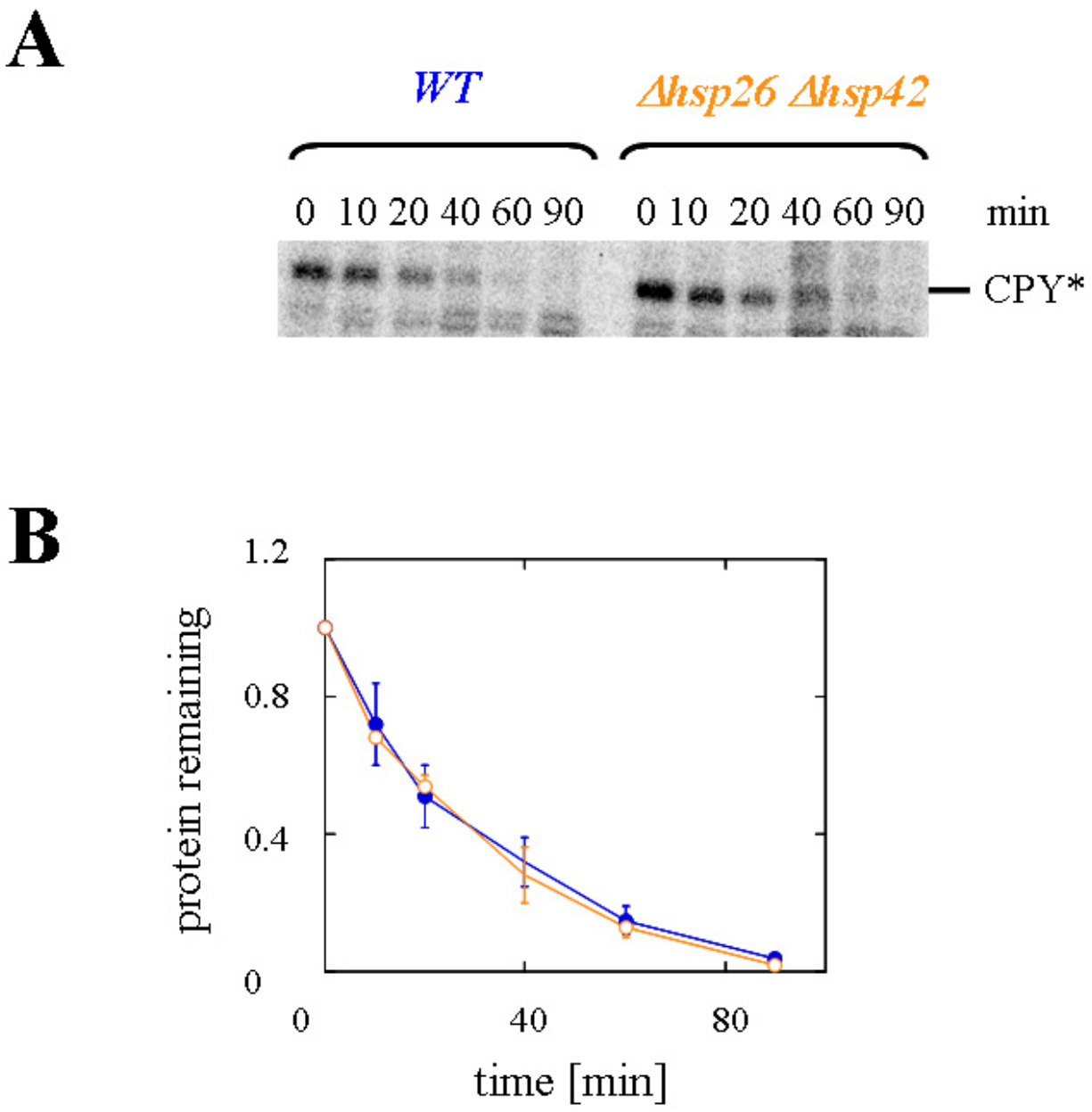

Figure 25: CPY* protein degradation is equally efficient in the *HSP26HSP42* wild type and *hsp26Δhsp42Δ* double mutant strains.

that the observed effect is due to a non-specific stress or growth response that arises from the deletion of the *sHSPs.*

Kar2p is the ER resident Hsp70 that is up-regulated by the UPR, which arises from the accumulation of unfolded or misfolded proteins in the ER (Gething, 1999). To further confirm that the stress response was not induced in the *hsp26Δ hsp42Δ* double mutant, I assessed Kar2p levels in the wild type strain and the double mutant by immuno-precipitation. There was no elevation of Kar2p levels (see Figure 26) in the mutant relative to the wild type strain, suggesting again that the observed defects are due to deletion of the sHsps rather than to a nonspecific up-regulation of stress inducible genes.

To further determine the substrate specificity of the sHsps during ERAD we explored their effect on the degradation of another misfolded integral membrane protein in yeast. Ste6p is the yeast **a**-mating factor pheromone transporter, an ABC transporter with structural similarity to CFTR, the sequence similarity between the two transporters is low and restricted to the NBDs (NBD1: ~26% identical, NBD2 ~31% identical; http://www.ncbi.nlm.nihgov/BLAST/Blast.cgi) (Kuchler *et al.*, 1989). Deletion of the C-terminal 52 amino acids, instigates ER retention of the mutated protein, denoted Ste6p*, and prompts its degradation via ERAD (Loayza *et al.*, 1998). Notably, a recent study reported identical requirements for the ERAD of CFTR and Ste6p* in yeast (Huyer *et al.,* 2004). To examine if the sHsps are also involved in Ste6p* degradation, I transformed the *hsp26Δ hsp42Δ* double mutant and the isogenic wild type strain with a vector expressing Ste6p* under the control of a constitutive promoter and Ste6p* degradation was measured by pulse-chase immuno-precipitation experiments at 30°C. Surprisingly, the *hsp26Δ*

Figure 26: The UPR is not induced in the *hsp26Δhsp42Δ* mutant.

Kar2p and Sec61p protein levels in the *HSP26HSP42* wild type and *hsp26Δhsp42Δ* double mutant strains were determined by immuno-precipitation. Results of two independent experiments are displayed. The *HSP26* wild type protein is denoted as "*WT"* in blue, *hsp26Δhsp42Δ* double mutant protein as "*Δ*" in yellow.

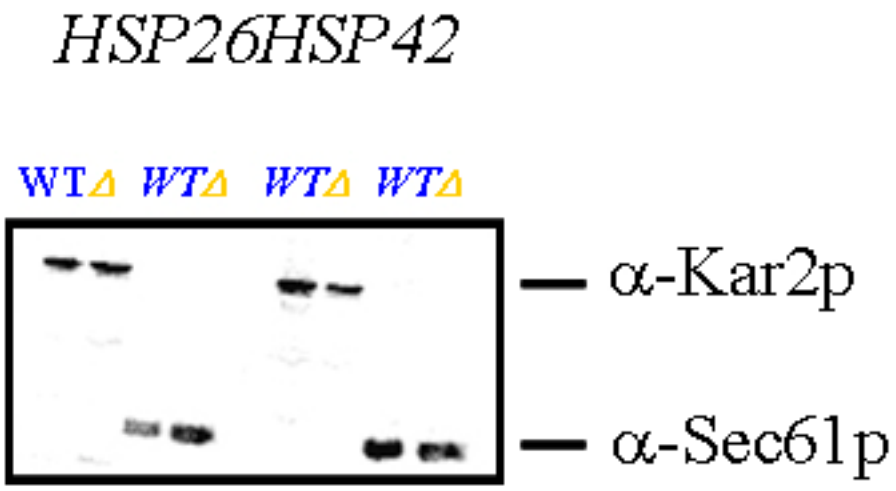

Figure 26: The UPR is not induced in the *hsp26Δhsp42Δ deletion* mutant.

hsp42Δ double mutant proficiently degraded Ste6p* compared to the wild type strain (Figure 27). This indicates that Hsp26 and Hsp42 are able to distinguish between two similar membrane proteins. This could be attributable to differences between CFTR and Ste6p or to the difference in the nature of the defects that make each protein an ERAD substrate. Whereas wild type CFTR is an ERAD substrate in yeast, Ste6p* is distinguished from the wild type protein by a C-terminal deletion. One can envision that the nature or degree of the misfolding between the two ERAD substrates might differ significantly, and so they might present distinct accessibility for interacting proteins. Also, one can not exclude the possibility that the sHsps might require the C-terminus of the ABC transporters in order to impact their half life.

3.3.3. Over-expression of the human sHsp, αA-crystallin, facilitates ΔF508-CFTR degradation in HEK293 cells

I next wanted to establish if sHsp function in mammals is important for CFTR degradation. αA-crystallin is one of 10 members of the small Hsps or α-crystallin-like proteins in humans (Kappe *et al.*, 2003), and it has been demonstrated to associate with unfolded proteins and to prevent their aggregation (Horwitz, 1992; Jakob *et al.*, 1993; Biswas and Das, 2004) and to prevent apoptosis when over-expressed (Liu *et al.*, 2004b). Therefore, I transiently co-transfected HEK293 cells with vectors over-expressing wild type CFTR and either an empty vector or a vector expressing αA-crystallin. Also, I co-transfected the cells with CFTR and Csp1 (mHsp40),

Figure 27: Ste6p* is degraded with equal efficiency in the *HSP26HSP42* wild type and *hsp26Δhsp42Δ* mutant strains.

A. Rates of Ste6p* degradation were determined by pulse-chase immuno-precipitation experiments in *HSP26HSP42* wild type yeast and in the *hsp26Δhsp42Δ* double mutant strain after addition of cycloheximide. B. Ste6p* protein levels were quantified from 2 independent sets of experiments and averaged. All values were obtained after standardization to the levels detected directly after cycloheximide addition (0 min). Closed blue circles represent the levels of Ste6p* in *HSP26* wild type cells, and open yellow circles represent Ste6p* levels in the *hsp26Δhsp42Δ* double mutant. Vertical bars indicate the range of the data.

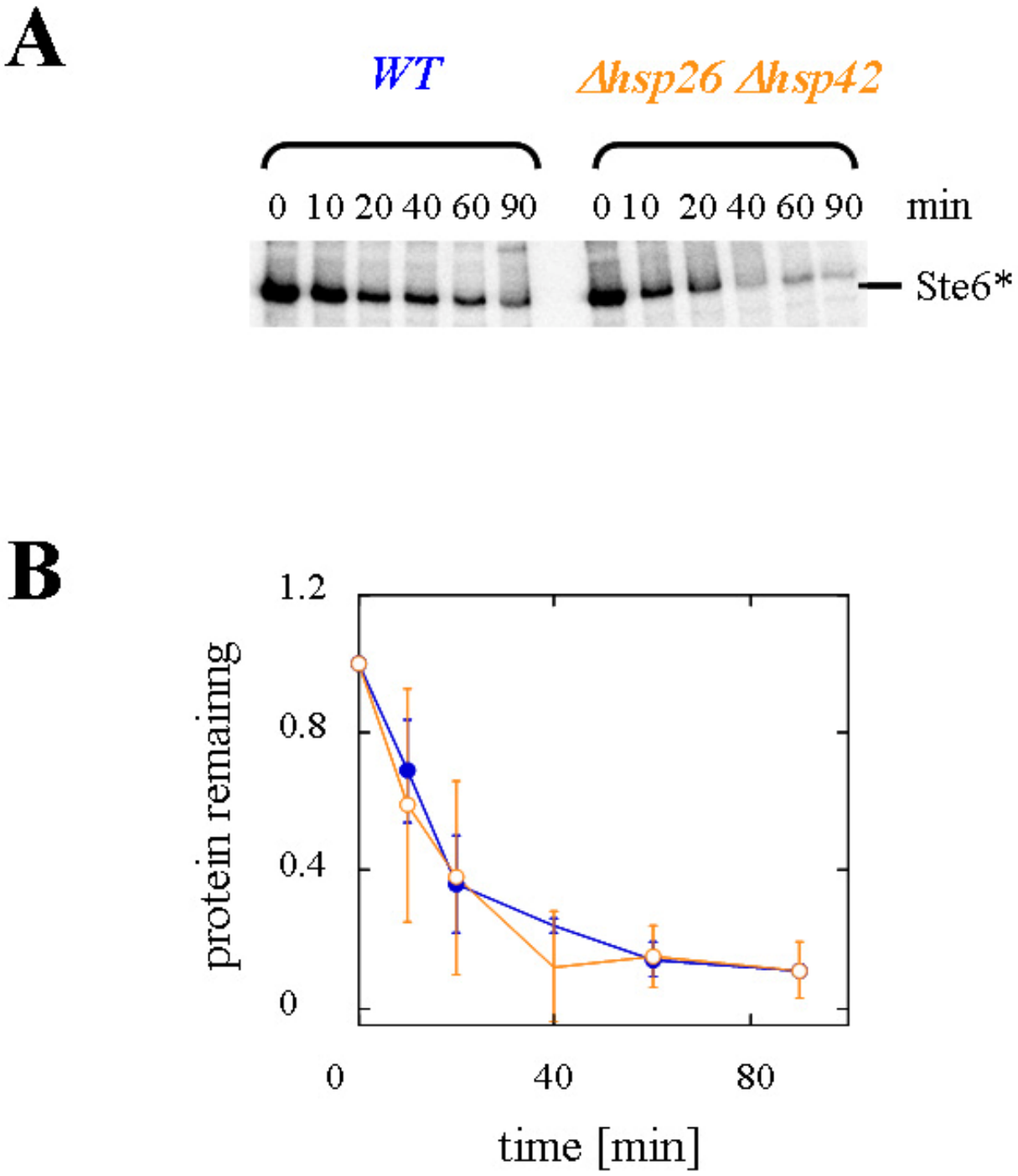

Figure 27: Ste6p* is degraded with equal efficiency in the *HSP26HSP42* wild type and *hsp26Δhsp42Δ* mutant strains.

Hsp110, Hsp70, or HspBP1 (NEF for Hsp70) expression vectors, so that I could compare the effects of αA-crystallin to the impact of other chaperones and chaperone cofactors (see Materials and Methods). Initially, CFTR levels were assessed by western blot analysis (see Figure 28A). Hsp90 served as loading control and its expression levels remained essentially unchanged upon over-expression of CFTR in combination with different chaperones and chaperone cofactors (see Figure 28A). Successful over-expression of the chaperones, which varied considerably, was confirmed by western blot analysis (see Figure 28B). A lower molecular weight band of unknown identity was detected in addition to the expected signal at about 110 kD with the anti-Hsp110 antibody. In accordance with previous reports, Csp1 prevented CFTR from maturating to the complex glycosylated form "band C" (Zhang *et al.*, 2002a), and levels of CFTR were reduced about 3.5 fold (average of 2 independent experiments) upon Hsp70 over-expression, consistent with reports demonstrating an involvement of Hsp70 in CFTR degradation (Meacham *et al.*, 2001; Zhang *et al.*, 2001). The preliminary data also suggested that over-expression of Hsp110, HspBP1, and αA-crystallin did not lead to a robust change in wild type CFTR maturation (see Figure 28), although upon Hsp70 and αA-crystallin over-expression, the amount of immature CFTR (B-band) was reduced below detection level. This observation could be explained by an increase in the degradation of the immature form, but since the B-band signal was very low, no conclusions can be drawn with confidence.

Since the deletion of *HSP26* and *HSP42* in yeast caused a stabilization of CFTR, I desired to investigate more carefully if the conserved human ortholog, αA-crystallin, plays a role in CFTR degradation. Two mammalian homologs of the family of small Hsps have been linked to the ubiquitin-preoteasome system (Wagner and Margolis, 1995; Conconi *et al.*, 1998; Conconi *et al.*,

Figure 28: Steady-state expression levels of CFTR are decreased upon over-expression of Hsp70, and unchanged upon over-expression of Hsp110, αA-crystallin, and HspBP1.

A. A western blot depicting CFTR and Hsp90 (as a loading control) protein levels in HEK293 cells and HEK293 cells co-transfected with CFTR (1.5 μg) and a vector control or containing either CSP1, HSP110, HSP70, αA-crystallin, or HspBP1, (1.5 μg for each) is shown. B. Western blots are shown that measure Hsp110, Hsp70, αA-crystallin, and HspBP1 protein levels.

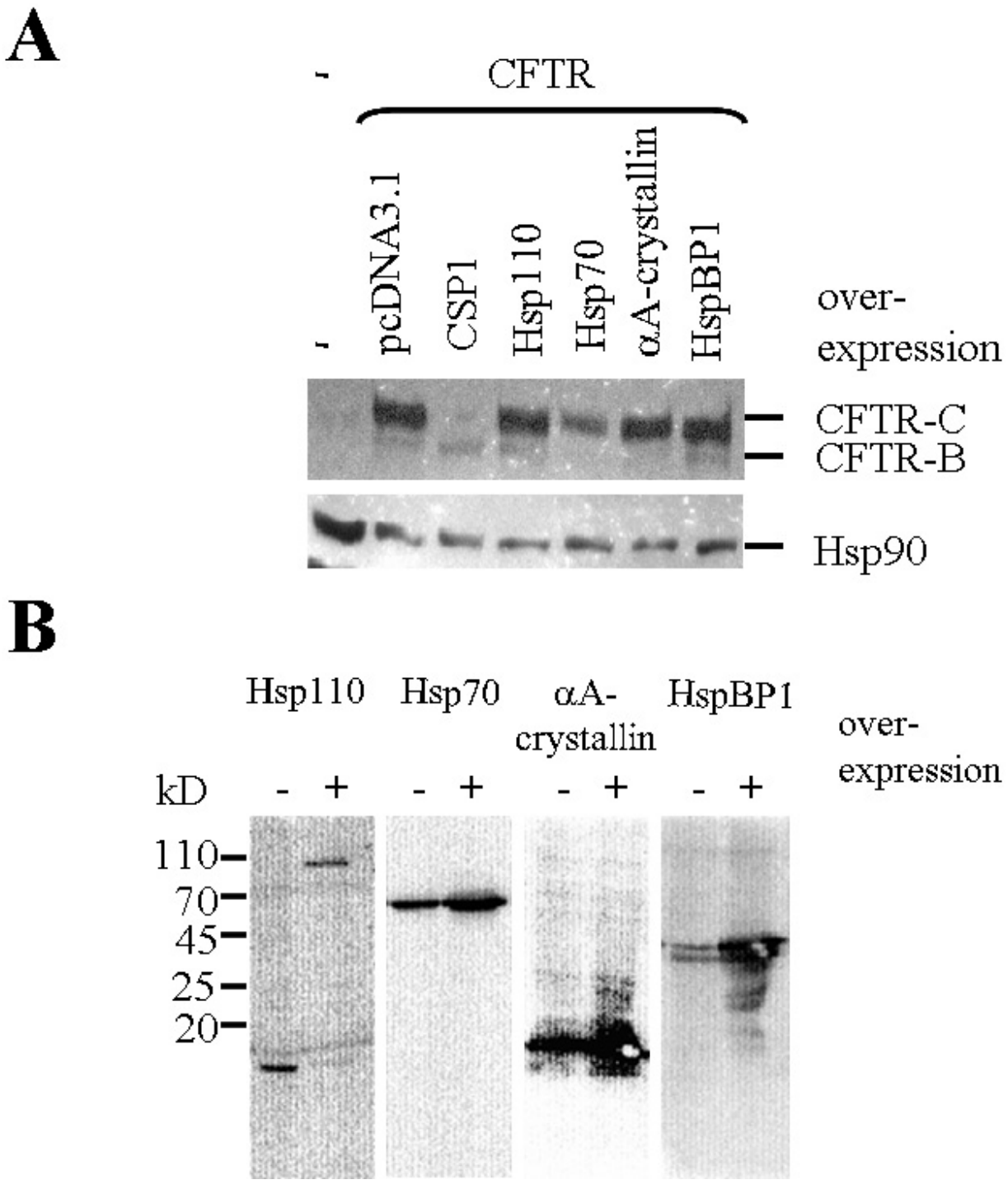

Figure 28: Steady-state expression levels of CFTR are decreased upon over-expression of Hsp70, and unchanged upon over-expression of Hsp110, αA-crystallin, and HspBP1.

1999; Boelens *et al.*, 2001; Ito *et al.*, 2002; den Engelsman *et al.*, 2003; Parcellier *et al.*, 2003; den Engelsman *et al.*, 2004). To this end, I co-transfected HEK293 cells with the CFTR expression vector and either the empty vector as a control or the αA-crystallin expression vector and performed pulse-chase immuno-precipitation experiments. Successful over-expression of αA-crystallin was confirmed by immuno-precipitation with anti-αA-crystallin antibodies (see Figure 29A). I also found that the maturation of CFTR from the immature, core-glycosylated form (CFTR B-band) to the mature, complex-glycosylated form (CFTR C-band) proceeded at equal rates in cultures transfected with the empty vector and those over-expressing αA-crystallin (see Figure 29A and B). Furthermore there is no difference in the disappearance of the B-band following over-expression of αA-crystallin (see Figure 29A and B). This suggests that the human sHsp αA-crystallin does not aid in the biogenesis of wild type CFTR, or that the levels of endogenous αA-crystallin or related chaperones are already saturating.

Since wild type CFTR when heterologously expressed in yeast is quantitatively degraded like the ΔF508-CFTR mutant is in mammalian cells (Zhang *et al.*, 2001), sHsps might only impact the biosynthesis of the mutant in mammalian cells. To explore this possibility I repeated the pulse-chase immuno-precipitation experiments in cells expressing the ΔF508-CFTR mutant. Consistent with the results on CFTR degradation obtained in the *hsp26Δhsp42Δ* mutant yeast, over-expression of the human sHsp, αA-crystallin, enhanced the proteolysis of the ΔF508-CFTR mutant compared to the vector control (see Figure 30A and B). This result implies that αA-crystallin impacts exclusively the ERAD of the ΔF508-CFTR mutant and, therefore, might be able to distinguish between the wild type and the mutant channel.

Figure 29: αA-crystallin over-expression has no effect on the biogenesis of wild type CFTR. A. HEK293 cells were transfected with 1.5 μg of pcDNA3.1-CFTR and 0.5 μg of pcDNA3.1 or pcDNA3.1-αA-crystallin. Rates of CFTR maturation and CFTR B-band degradation as well as αA-crystallin expression levels were determined by pulse-chase immuno-precipitation in HEK293 cells co-transfected with CFTR, and in cells containing a vector control or the αA-crystallin expressing vector. B. CFTR B-band degradation was determined from 3 independent sets of experiments and averaged. CFTR maturation was determined from 4 independent sets of experiments and averaged. All values were obtained after standardization to the levels detected at the beginning of the chase period (0 h). Closed blue circles represent immature/mature CFTR protein levels in HEK293 cells with the vector control, open purple circles represent immature/mature CFTR protein levels in HEK293 cells over-expressing αA-crystallin. Vertical bars indicate the standard errors of the mean.

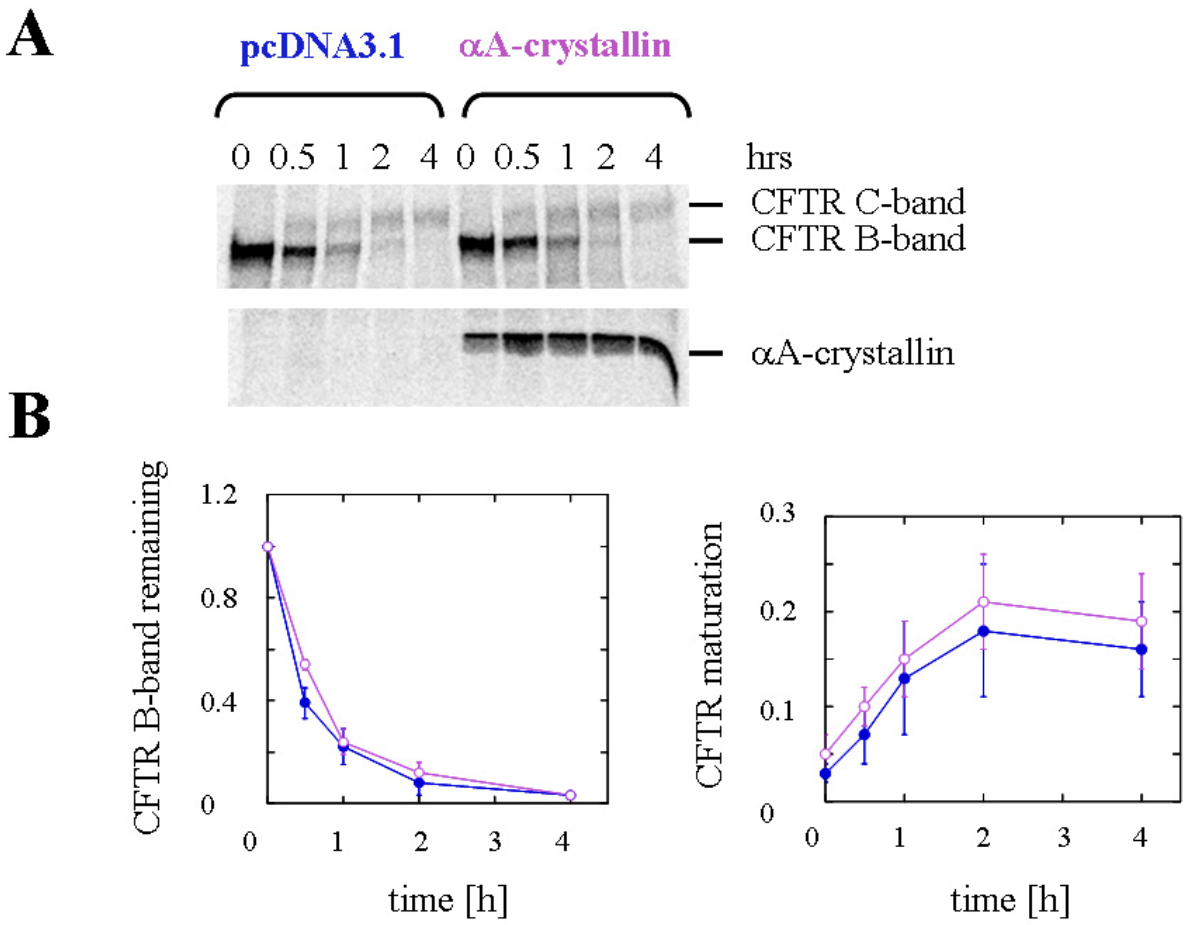

Figure 29: αA-crystallin over-expression has no effect on the biogenesis of wild type CFTR.

Figure 30: αA-crystallin over-expression accelerates the degradation of ΔF508-CFTR.

A. HEK293 cells were transfected with 1.5 μg of pcDNA3.1-ΔF508-CFTR and 0.5 μg of pcDNA3.1 or pcDNA3.1-αA-crystallin. Rates of ΔF508-CFTR degradation as well as αA-crystallin expression levels were determined by pulse-chase immuno-precipitation in each transfected HEK293 cell-type. B. ΔF508-CFTR degradation was determined from 4 independent sets of experiments and averaged. All values were obtained after standardization to the levels detected at the beginning of the chase period (0 h). Closed blue circles represent ΔF508-CFTR protein levels in HEK293 cells with the vector control, and open purple circles represent ΔF508-CFTR protein levels in HEK293 cells over-expressing αA-crystallin. Vertical bars indicate the standard errors of the mean. P: * = 0.0768, ** = 0.0001, ***= 0.003 , **** = 0.5

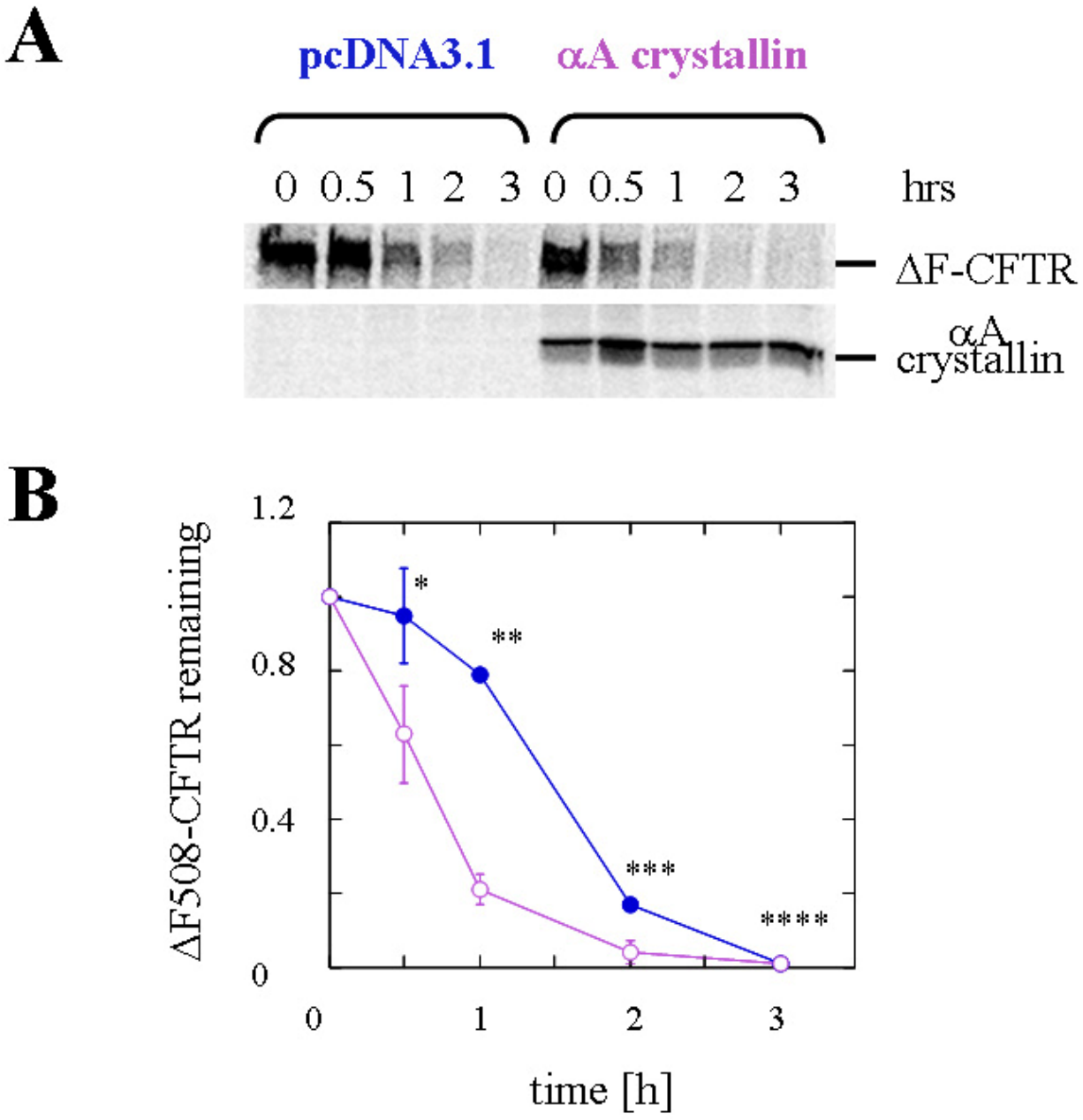

Figure 30: αA-crystallin over-expression accelerates the degradation of ΔF508-CFTR.

3.3.4. αA-crystallin prevents aggregation of the NBD1 of CFTR

Misfolding of a polypeptide can lead to its aggregation, and the NBD1 of CFTR is known to be aggregation prone (Qu and Thomas, 1996). During CFTR biogenesis, NBD1 is folded co-translationally while the post-translational folding of NBD2 depends on pre-folded NBD1 (Du *et al.*, 2005). It has previously been revealed that Hsp70 sustains NBD1 solubility but is also required for efficient degradation of CFTR (Strickland *et al.*, 1997; Meacham *et al.*, 1999; Meacham *et al.*, 2001). One model to account for these data is that Hsp70 maintains NBD1 solubility or unfolds the polypeptide to provide accessibility for proteasomal degradation. Since I found an involvement of sHsps in CFTR degradation, and sHsps have been demonstrated to associate with unfolded proteins and prevent their aggregation (Horwitz, 1992; Jakob *et al.*, 1993; Ehrnsperger *et al.*, 1997; Lee *et al.*, 1997; Haslbeck *et al.*, 1999; Biswas and Das, 2004; Haslbeck *et al.*, 2004), I wished to uncover if αA-crystallin inhibits NBD1 aggregation.

Toward this goal, I purified αA-crystallin from *E. coli* engineered to over-express the protein utilizing DEAE- and size-exclusion column chromatography (see Figure 31). The recombinant αA-crystallin was ~95% pure and its identity was confirmed by immunoblot analysis (see Figure 32A and B). At a molar ratio of 1:1, αA-crystallin suppressed the aggregation of CFTR NBD1 by ~80% (see Figure 33). The efficiency of αA-crystallin to abolish NBD1 aggregation was ATP-independent, and it should be noted that the ATP-dependence of sHsps action is still controversial. While some groups report no enhancement of activity upon addition of ATP

Figure 31: Purification of αA-crystallin.

A. Lysate from *E. coli* expressing αA-crystallin was loaded onto a DEAE column and proteins were separated with a linear 0-0.5M NaCl gradient and protein profiles of the fractions were assessed by SDS-PAGE and Coomassie Brilliant Blue staining. The indicated fractions (13-16) were pooled and concentrated. B. Concentrated eluate was further purified by size exclusion column chromatography. Indicated fractions (24-27; 28-30; 31-34) were pooled and dialyzed.

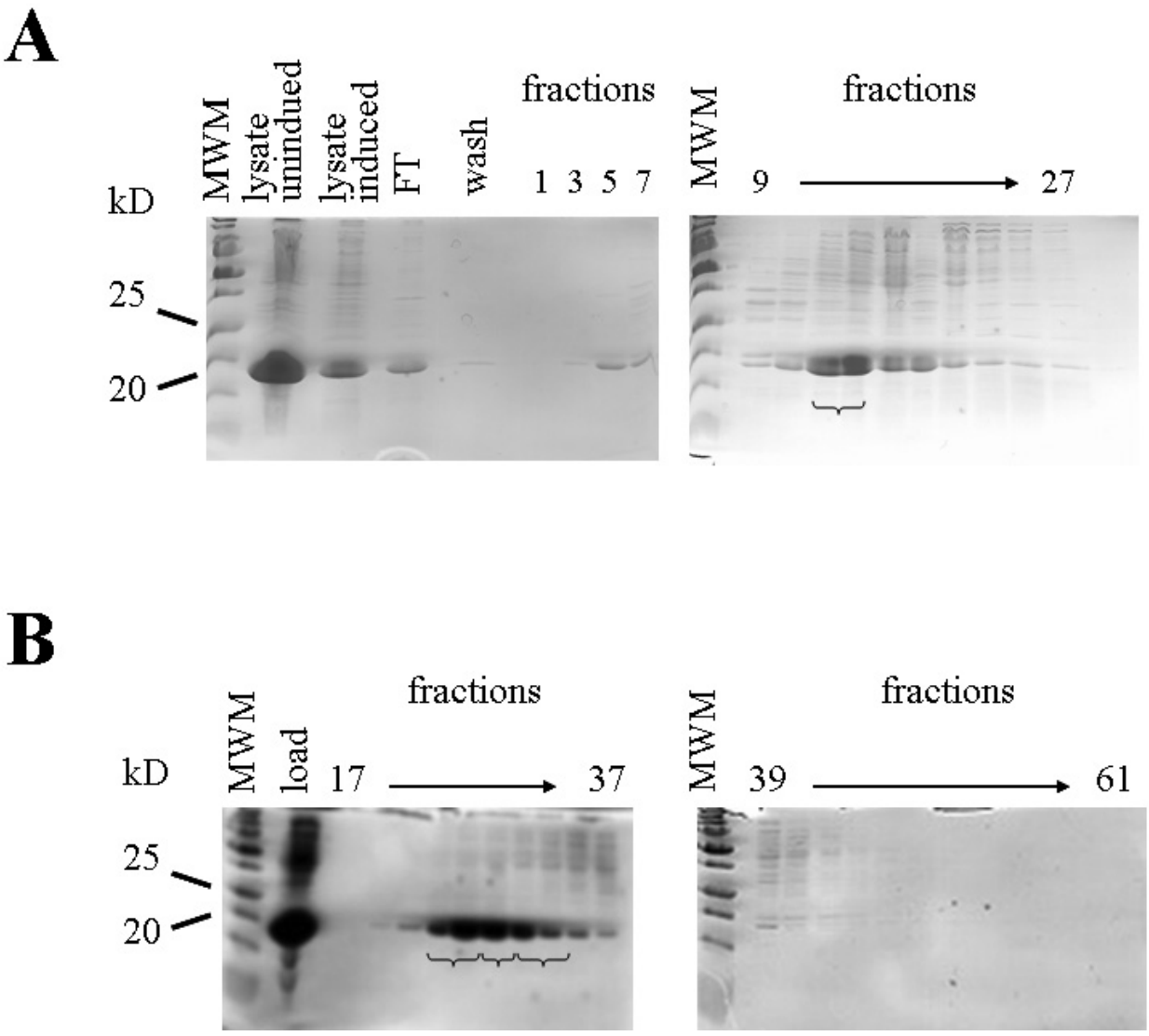

Figure 31: Purification of αA-crystallin.

Figure 32: αA-crystallin is 95 % pure.

A. Silver stained 15% SDS-PAGE of purified αA-crystallin. The pooled fractions 24-27 are 95% pure and were used for the in vitro aggregation experiments. B. Identity of the purified protein was verified by western blot analysis. αA-crystallin runs at a molecular weight of 18 kD. The higher molecular weight bands visible in the western blot might be αA-crystallin dimers and higher oligomers, which are known to exist (Narberhaus, 2002; Horwitz, 2003).

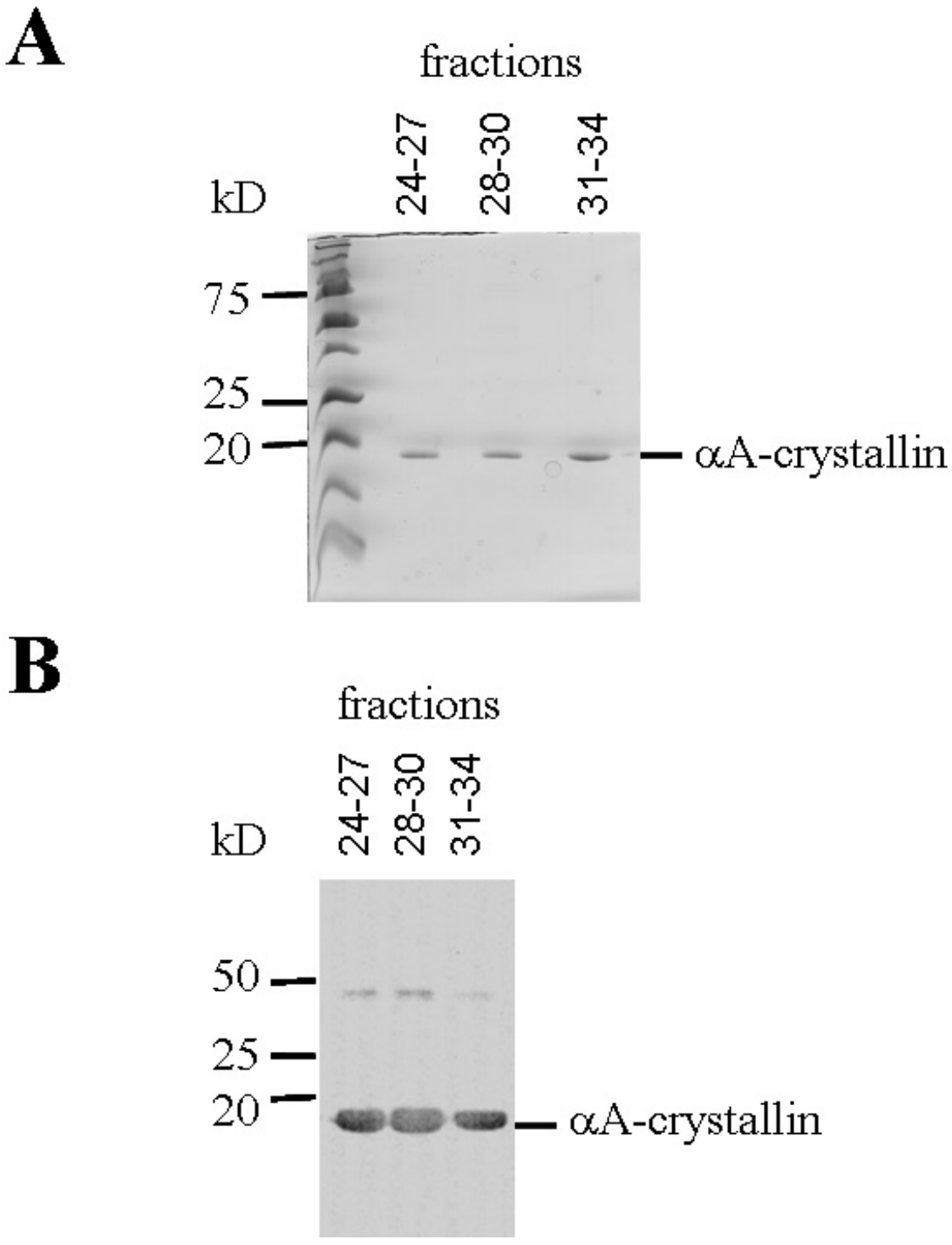

Figure 32: αA-crystallin is 95% pure.

Figure 33: αA-crystallin prevents NBD1 aggregation.

NBD1 aggregation was measured as a change in absorbance at 400 nm after its dilution out of denaturant and was determined in the presence and absence of αA-crystallin at a monomeric molar ratio of 1:1. The effect of 3.5mM ATP on the aggregation of NBD1 and the efficiency of αA-crystallin were also measured. Assays were performed at 37°C. Dark blue diamonds represent NBD1 aggregation alone, pink triangles represent NBD1 aggregation in the presence of αA-crystallin. Light blue circles depict NBD1 aggregation in the presence of ATP and purple squares depict NBD1 aggregation in the presence of αA-crystallin and ATP. NBD1=nucleotide binding domain 1, Apha-A=αA-crystallin.

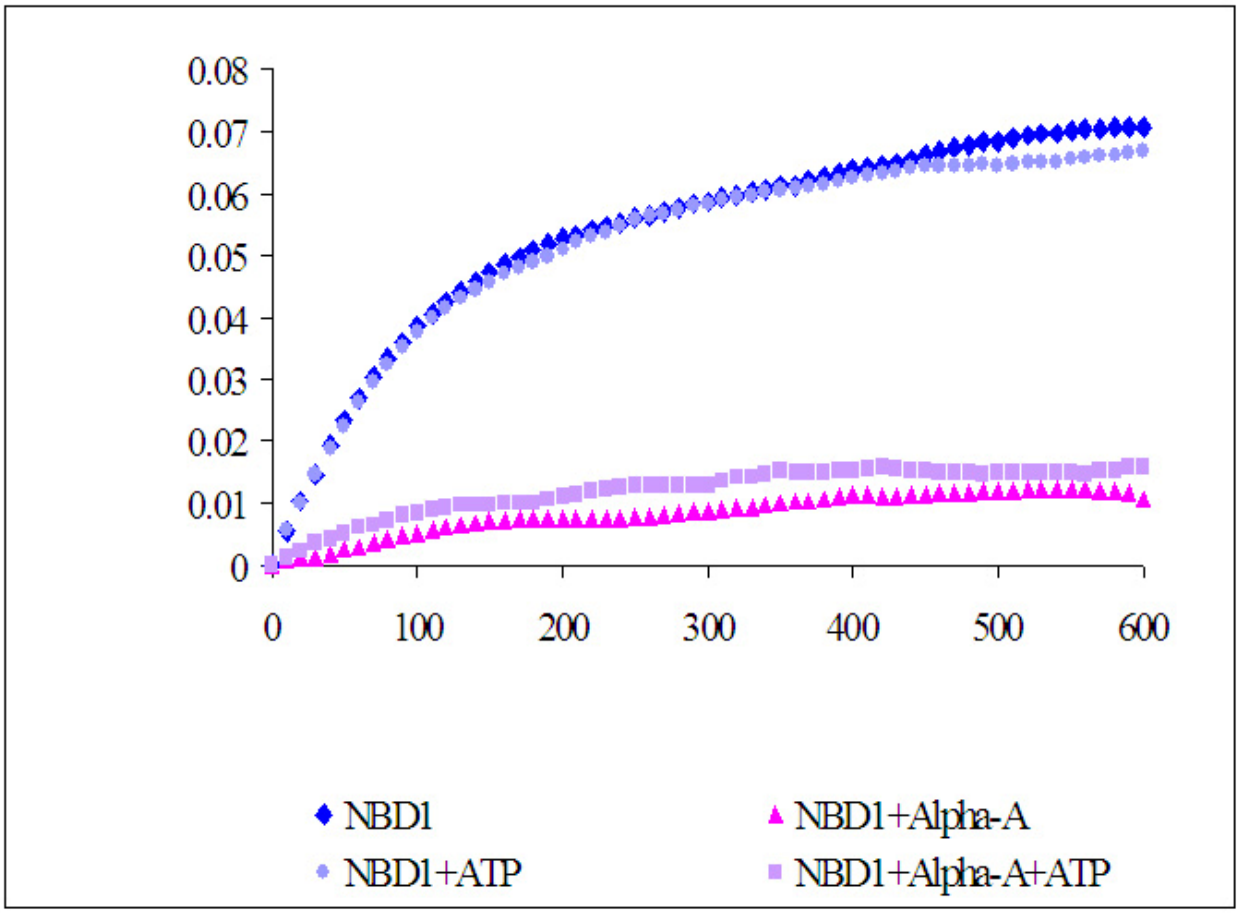

Figure 33: αA-crystallin prevents NBD1 aggregation.

(Lee *et al.*, 1995; Chang *et al.*, 1996; Ehrnsperger *et al.*, 1997; Veinger *et al.*, 1998), others claim an increase in efficiency in the presence of ATP, but not in the presence of nonhydrolyzable ATP analogs (Muchowski and Clark, 1998; Smykal *et al.*, 2000). A reduction of chaperone activity in the presence of ATP has also been described (Muchowski and Clark, 1998; Smykal *et al.*, 2000), and a recent study observed improved sHsp function even in the presence of nonhydrolyzable analogs (Biswas and Das, 2004). In any event, the results presented in Figure 37 could offer a putative explanation for the mechanism of sHsp action during ERAD.

3.4. DISCUSSION

In this Chapter, I describe the utilization of yeast to detect changes in transcript levels in response to the heterologous expression of CFTR via microarray analysis. The validation of this approach was provided by the identification of several genes known to play a role in CFTR maturation and degradation, such as *FES1*, *HSP82*, and *NPL4*. In addition, CFTR synthesis induced genes that are generally involved in protein biogenesis, trafficking, and degradation, as well as a number of uncharacterized ORFs. I was able to prove that for one of these candidates, Hsp26, the elevated mRNA level was significant: The deletion of the corresponding gene slows CFTR degradation, and the mammalian ortholog, αA-crystallin, also plays a role in the ERAD of ΔF508-CFTR.

The fold up-regulation of gene messages in response to CFTR expression in yeast was generally modest. Particularly, genes that may be involved in the control of CFTR biogenesis and degradation displayed a fold increase in mRNA levels ranging from ~1.4 to 1.8. Nevertheless, the results presented were based on 6 independent experiments and the up-regulation of several candidates was verified by northern blot analysis in which RNA from another set of independently transformed and grown cells was tested. Moreover, several of the induced transcripts correspond to proteins already known to affect CFTR biogenesis. Fes1p and its human ortholog, HspBP1, serve as nucleotide exchange factors for the cytoplasmic Hsp70 (Kabani *et al.*, 2002a; Kabani *et al.*, 2002b), and HspBP1 facilitates the Hsp70-dependent biosynthesis of CFTR (Alberti *et al.*, 2004). Hsp82, as well as its mammalian ortholog, Hsp90, facilitate CFTR biogenesis (Loo *et al.*, 1998; Youker *et al.*, 2004). Npl4p, which resides in a complex with Cdc48p and Ufd1p, catalyzes ERAD substrate retro-translocation from the ER and transfer to the proteasome (Bays and Hampton, 2002), and this complex facilitates CFTR degradation in yeast (Gnann *et al.*, 2004). Finally, it is important to note that we purposely chose to express CFTR from a moderate, constitutive promoter, rather than from a strong promoter, which might have given stronger induction of target genes. The reason for this choice is that we feared that strong induction of CFTR might lead to non-specific stresses.

Further characterization of one message identified in the microarray analysis, *HSP26*, revealed that deletion of this gene led to a modest stabilization of CFTR in yeast, but not of other tested ERAD substrates. This effect was even stronger in a yeast strain doubly mutated for *HSP26* and its homologue, *HSP42*. This finding is consistent with a recent study reporting a 90% overlap in substrate specificity for Hsp26 and Hsp42 (Haslbeck *et al.*, 2004). I was then able to confirm my

discovery by using mammalian cell culture systems, where ΔF508-CFTR, but not wild type CFTR degradation was enhanced upon over-expression of the mammalian ortholog, αA-crystallin. These results suggest that sHsps impact the ERAD of specific substrates, and αA-crystallin seems even to be able to distinguish between the wild type and ΔF508 mutant form of CFTR.

One mechanism to explain the sHsp control over proteolysis might be the prevention of substrate aggregation which may be required to preserve accessibility for ubiquitination and proteasome-mediated degradation. Indeed, αA-crystallin was able to suppress NBD1 aggregation *in vitro* at a molar (monomeric) ratio of 1:1 by 80%. This effect is stronger than the recently reported 5:1 molar ratio required for Hsp90 to decrease NBD1 aggregation by 60% (Youker *et al.*, 2004), but it is in line with other studies reporting a 1:1 molar ratio of sHsps to other substrates as being sufficient to nearly completely prevent aggregation (Horwitz, 1992; Jakob *et al.*, 1993; Chang *et al.*, 1996; Ehrnsperger *et al.*, 1997; Haslbeck *et al.*, 1999; Studer and Narberhaus, 2000). While suppression of aggregation may aid in efficiency of ERAD, there is also evidence that sHsps might regulate degradation more directly. For example, the interaction of sHsps with the ubiquitin-proteasome machinery provides an additional hypothesis to explain the enhanced degradation of ΔF508-CFTR in response to α-crystallin over-expression. Misfolded CFTR is targeted for ER-associated degradation via the ubiquitin-proteasome machinery (Jensen *et al.*, 1995; Ward *et al.*, 1995; Hohfeld *et al.*, 2001; Meacham *et al.*, 2001; Zhang *et al.*, 2001), and mutant CFTR that is artificially driven to the plasma membrane is ubiquitinated and thus rerouted for lysosomal degradation (Sharma *et al.*, 2004). Functional and physical interaction between sHsps and the 20S proteasome have been detected. While α-crystallin decreases peptide

hydrolyzing activities for some substrates, it protects the trypsin-like activity of the proteasome (Wagner and Margolis, 1995; Conconi *et al.*, 1998; Conconi *et al.*, 1999; Boelens *et al.*, 2001; Ito *et al.*, 2002). Hsp27 binds to the 26S proteasome and to a polyubiquitinated substrate (Parcellier *et al.*, 2003) and, αB-crystallin has been proposed to recruit the F-box protein, FBX4, an adaptor molecule for the ubiquitin ligase SCF, and to promote substrate ubiquitination (den Engelsman *et al.*, 2003; den Engelsman *et al.*, 2004). Intriguingly, one of the uncharacterized ORFs identified in my screen, *YJL149W,* encodes a cyclin-like F-box that interacts with the E3 ubiquitin-ligase, Skp-Cdc53-Hrt1. Together with my finding that the yeast sHsps, Hsp26 and Hsp42, and one of their mammalian orthologs, αA-crystallin, promote CFTR or ΔF508-CFTR degradation, respectively, and αA-crystallin keeps CFTR in a soluble state, the data suggest putative roles for sHsps in detecting misfolding of CFTR. I propose further that this provides maximal accessibility of CFTR for ubiquitination and/or degradation.

To further determine the mechanism by which sHsps regulate protein degradation I would first determine if the yeast Hsp26 and Hsp42 are also able to prevent aggregation of NBD1. In addition, a mutation of the conserved R116 to C in αA-crystallin causes cataracts in humans and diminishes its chaperone activity (Litt *et al.*, 1998; Andley *et al.*, 2002). An alignment of several sHsps identifies R159 in Hsp26 and R309 in Hsp42 as the corresponding, conserved residue (see Figure 34). Figure 35 represents the crystal structure of the wheat Hsp16.9, which presents the closest αA-crystallin ortholog with a solved crystal structure. R116 is shown in red and engages in an intermolecular salt bridge with E100 (depicted in blue) in Hsp16.9 to support dimerization.

Figure 34: Sequence alignment of 5 sHsps.

Sequence alignment of *Saccharomyces cerevisiae* Hsp26 and Hsp42, *Homo sapiens* αA-crystallin, *Triticum aestivum* Hsp16.9, *Methanococcus jannaschii* Hsp16.5. The red arrow indicates the conserved arginine in the α-crystallin domain.

Alignmet was created via the programs at:

http://searchlauncher.bcm.tmc.edu/multi-align/multi-align.html

http://www.ch.embnet.org/software/BOX_form.html.

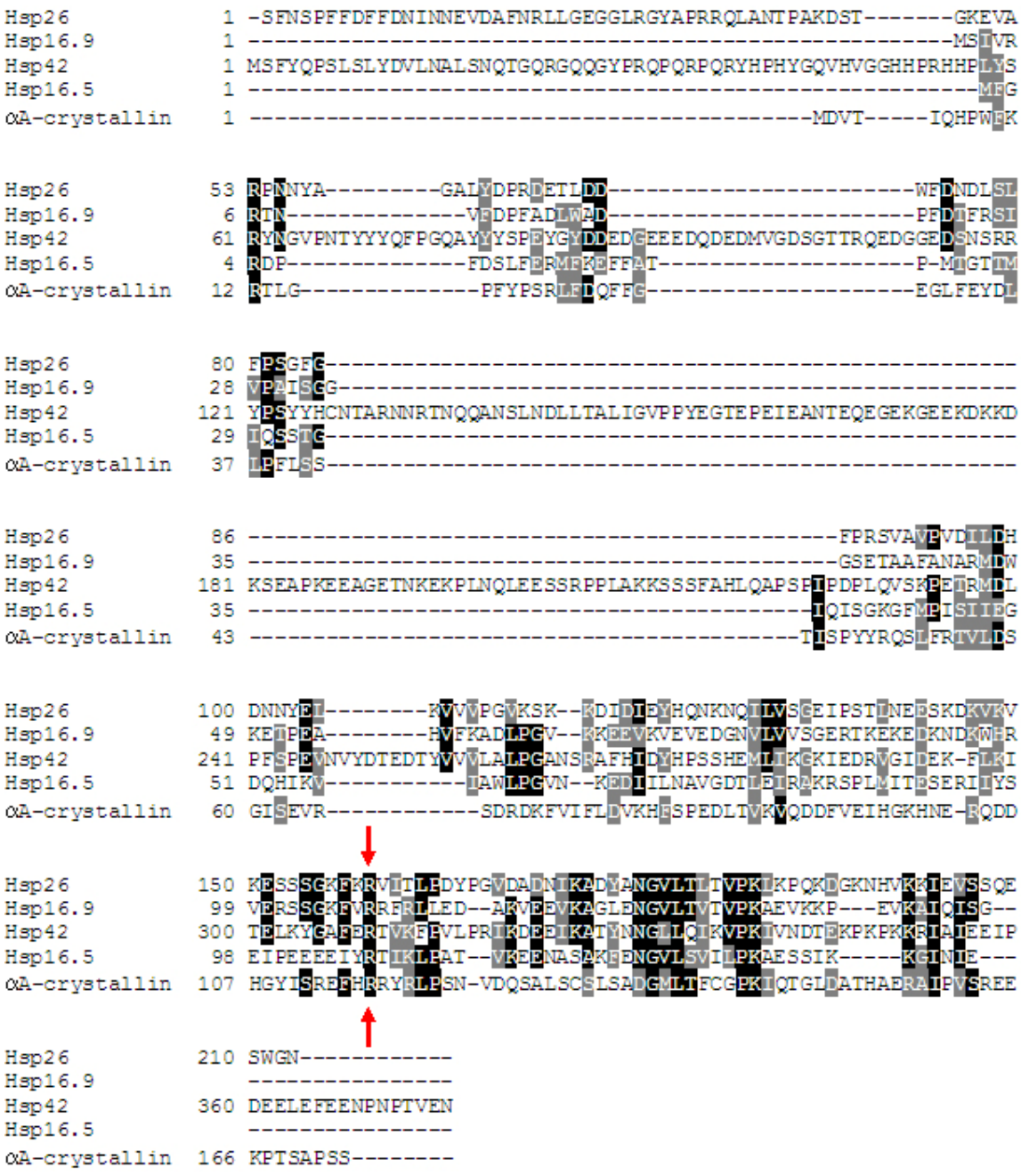

Figure 34: Sequence alignment of 5 sHsps.

Figure 35: Crystal structure of wheat Hsp16.9 dimer.

This figure depicts the tertiary structure of an Hsp16.9 dimer of the wheat *Triticum aestivum*. α-helices are represented in purple, extended β-sheets in yellow, turns in cyan, and coils in white. The position of the conserved R108 in the α-crystallin domain is illustrated in red, and the position of E100 in blue. The 42 N-terminal residues are depicted only for one of the monomers. (Van Monfort, et al., 2001, Nat Struct Biol 1025; modified with VMD (Visual Molecular Dynamics): Humphrey *et al.*, 1996).

Figure 35: Crystal structure of wheat Hsp16.9 dimer.

Although E100 is not conserved in αA-crystallin, R116 is still predicted to face the dimer interface and it might make possible variations in assembly modes (van Montfort *et al.*, 2001b; Guruprasad and Kumari, 2003). Particularly, since dimerization and oligomerization seem to play an important, but still largely ill-defined role in the regulation of sHsp activity (see Chapter 1.4), this residue should be mutated and its effects characterized. If the R to C mutants of αA-crystallin, Hsp26, and Hsp42 loose their ability to prevent NBD1 aggregation, it would then be important to test the impact of this mutation *in vivo* (e.g. effects on CFTR degradation and on other substrates). An alternative or parallel mechanism that sHsps might use to regulate ERAD that should be investigated is substrate poly-ubiquitination. If an impact on the level of CFTR ubiquitination is observed when αA-crystallin, Hsp26, and/or Hsp42 levels are altered, it will be important to examine effects on E3 ligase recruitment and activation.

The question also rises whether the observations described in this work are the result of a direct physical interaction between CFTR and the sHsps. Particularly, the observation that sHsps had no impact on Ste6p* degradation, despite the fact that CFTR and Ste6p are related members of the family of ABC transporters, raises the question if certain structural features might be required for association. If sHsps bind to the C-terminal part of CFTR, and maybe other ABC transporters, it would explain why Ste6p*, a C-terminal truncation mutant, might escape a sHsp quality control mechanism. Investigations of different Ste6p* and CFTR mutants might answer this question, and it might be worthwhile to map possible interaction sites.

A more indirect mechanism that might explain the results presented in this chapter might be provided by a role of the sHsps as mediators between CFTR and the cytoskeleton.

First, since intermediate filaments have been shown to play a role in CFTR biogenesis as well as to interact with small Hsps, the coordination of the intermediate filament-CFTR interaction could be an alternate mechanism by which α-crystallin effects CFTR maturation/degradation. In a recent study, Davezac *et al.* detected keratin 8 and keratin18 to be up-regulated in response to ΔF508-CFTR expression in HeLa cells. Moreover, knock-down of K18 by siRNA led to some ΔF508-CFTR maturation and its transport to the plasma membrane (Davezac *et al.,* 2004). Of interest, α-crystallins, as well as Hsp27, interact with various intermediate filaments and modulate their assembly and their interactions (Nicholl and Quinlan, 1994; Perng *et al.,* 1999; Perng *et al.,* 2004). The beaded filament of the eye lens is comprised of CP49 and filensin, two intermediate filament proteins, associated with α-crystallin. Most notably, CP49 and filensin show greatest sequence homology to type I and type II keratins, respectively, and CP49 is 39% identical to keratin 18 (Quinlan *et al.,* 1996). Also, Hsp27 has been shown to colocalize with keratin (Perng *et al.,* 1999). Finally, during apoptosis, K18 is cleaved at its C-terminus by caspase-9 and the caspase-9-activated caspases-3 and -7 (Schutte *et al.,* 2004). Caspase-3 activation in turn, can be inhibited by α-crystallin (Kamradt *et al.,* 2001; Kamradt *et al.,* 2002; Liu *et al.,* 2004a; Kamradt *et al.,* 2005). This evidence raises the question of a possible interaction between K18 and/or K8 and α-crystallin. Since we observed enhanced degradation of ΔF508-CFTR upon α-crystallin over-expression (see Figure 30), α-crystallin might interact with keratin/keratin filaments or induce rearrangement of intermediate filaments, and thus prevent their association with ΔF508-CFTR. This could abolish the stabilization of mutant CFTR by keratin and enhance its proteolysis. On the other hand, the fact that we did not observe an effect on wild type CFTR upon α-crystallin over-expression could be explained by a dual role of α-crystallin in CFTR biogenesis: In the case of wild type CFTR, α-crystallin might promote the

degradation of misfolded CFTR as well as the trafficking of properly folded CFTR out of the ER by coordinating CFTR interactions with keratins. Over-expression of α-crystallin would then enhance maturation as well as degradation, so that the net outcome might not yield an observable phenotype. Another explanation for the different effects of α-crystallin over-expression on wild type CFTR and ΔF508-CFTR would be that different keratins exert unique effects upon CFTR that might lead to its stabilization or destabilization. α-crystallin could be involved in the decision-making process that determines which keratin interacts with mutant and wild type CFTR.

Another cytoskeletal element linked to both α-crystallin and CFTR is actin. CFTR has been shown to exist in a multi-protein complex that includes E3KARP or EBP50/NHERF1, and ezrin at the apical plasma membrane. In addition to its function in regulating channel activity, this complex also connects CFTR to the cytoskeleton. This, in turn, could stabilize CFTR at the apical plasma membrane (Dransfield *et al.*, 1997; Hall *et al.*, 1998; Short *et al.*, 1998; Wang *et al.*, 1998; Sun *et al.*, 2000a; Sun *et al.*, 2000b). Interactions between small Hsps and the actin cytoskeleton have also been reported. The unphosphorylated, monomeric form of αB-crystallin, Hsp27, and yeast Hsp26 inhibit actin polymerization in vitro (Miron *et al.*, 1991; Benndorf *et al.*, 1994; Rahman *et al.*, 1995; Wieske *et al.*, 2001), over-expression of sHsps stabilized the actin cytoskeleton and organized cortical actin (Lavoie *et al.*, 1993a; Lavoie *et al.*, 1993b; Gu *et al.*, 1997; Piotrowicz and Levin, 1997). In addition, disorganization of the microfilament network was observed when αB-crystallin expression was reduced (Iwaki *et al.*, 1994), and a complex of αA-crystallin and αB-crystallin exhibited a stabilizing effect on actin filaments *in vitro* (Wang and Spector, 1996). The interactions between actin and sHsps seem to be dynamic and adjustable

to the needs of the cell, as inhibition of the proteasome causes the redistribution of sHsps to the actin cytoskeleton (Verschuure *et al.*, 2002). Hence, sHsps may help provide a network for CFTR interactions with actin and other proteins, which is vital for stability, activation, and mobility. Or, sHsps might even mediate interactions between the cytoskeleton and the CFTR regulatory complex. As suggested by some authors, actin-interaction might stabilize CFTR at the apical membrane (Sun *et al.*, 2000b) so that manipulation of the effects of sHsps on the actin cytoskeleton might even stabilize rescued ΔF508-CFTR at the apical plasma membrane.

Keratin and actin do not only interact with both CFTR and sHsps, but they also interact with each other. This offers additional complexity for a putative α-crystallin regulatory mechanism of CFTR. Intermediate filaments engage in various kinds of movements to coordinate assembly, disassembly, and subcellular organization, and although some of these activities are intrinsic to intermediate filaments, others are mediated via interactions with microtubules or actin-filaments, depending on the type of intermediate filament (Helfand *et al.*, 2004). In the case of keratins, the motile activities are mainly attributable to their interaction with actin-containing microfilaments, and possibly with actin-based motors like myosin (Helfand *et al.*, 2004). Interestingly, myosin VI seems to be involved in CFTR endocytosis (Swiatecka-Urban *et al.*, 2004). Since sHsps interact with intermediate filaments as well as with actin, they might help further to provide the crosstalk and organization of the cytoskeletal components required for CFTR transport to the plasma membrane, as well as for its endocytosis. Alternatively, they might mediate cytoskeleton-CFTR interaction directly.

In addition to *HSP26*, one uncharacterized ORF, *YBR075W*, that displayed only minimally elevated transcript levels in the microarray analysis has caught our interest. Computational analysis revealed that the gene product is a putative member of the M28 family of metalloproteases, and the closest human homolog is the uncharacterized KIAA1815 (http://hitsisb-sib.ch/cgi-bin/PFSCAN_pareser). The 976 amino acid protein may have 8 transmembrane segments that are predicted to span the ER membrane, and a ~36 kD soluble segment comprising the putative protease domain is calculated to reside within the ER lumen (http://psort.nibb.ac.jp/cgi-bin/runpsort.pl). An alignment of the putative protease domain of Ybr075Wp with those of *S. griseus* aminopeptidase and human Glutamate Carboxypeptidase II, both M28 metalloproteases, reveals conserved divalent cation (zinc)-coordinating residues in Ybr075Wp: H156, D168, E201, E/D226, H319 (see Figure 36) that in other proteases are known to impact protease activity (Speno *et al.*, 1999; Fundoiano-Hershcovitz *et al.*, 2004). Information about *YBR075W* from genome/proteome-wide screens is limited. On average, only 1 copy of *YBR075W* messanger RNA has been detected (http://web.wi.mit.edu/young/expression/transcriptome2.html), and Ybr075wp has been identified as ubiquitin-modified gene by mass spectrometry (Peng *et al.*, 2003).

To determine a potential involvement of this candidate in CFTR biogenesis I transformed yeast harboring a C-terminal truncation of YBR075Wp and the isogenic wild type strain with a plasmid expressing CFTR under the control of a constitutive promoter. Cycloheximide chase analysis uncovered compromised CFTR degradation in the *ybr075w* mutant yeast (see Figure 37). In contrast, CPY* degradation proceeded with equal efficiency in wild type and mutant yeast (see Figure 38). In addition, a general stress response was not induced in the truncation

Figure 36: Sequence alignment of the protease domains of 3 M28 metalloproteases.

Sequence alignment of *Saccharomyces cerevisiae* Ybr075Wp, *Streptomyces griseus* aminopeptidase and *Homo sapiens* Glutamate Carboxypeptidase II. The conserved divalent cation binding residues are denoted in red, and the red arrows indicate the identical positions in Ybr075Wp.

Alignmet was created via the programs at:

http://searchlauncher.bcm.tmc.edu/multi-align/multi-align.html

http://www.ch.embnet.org/software/BOX_form.html.

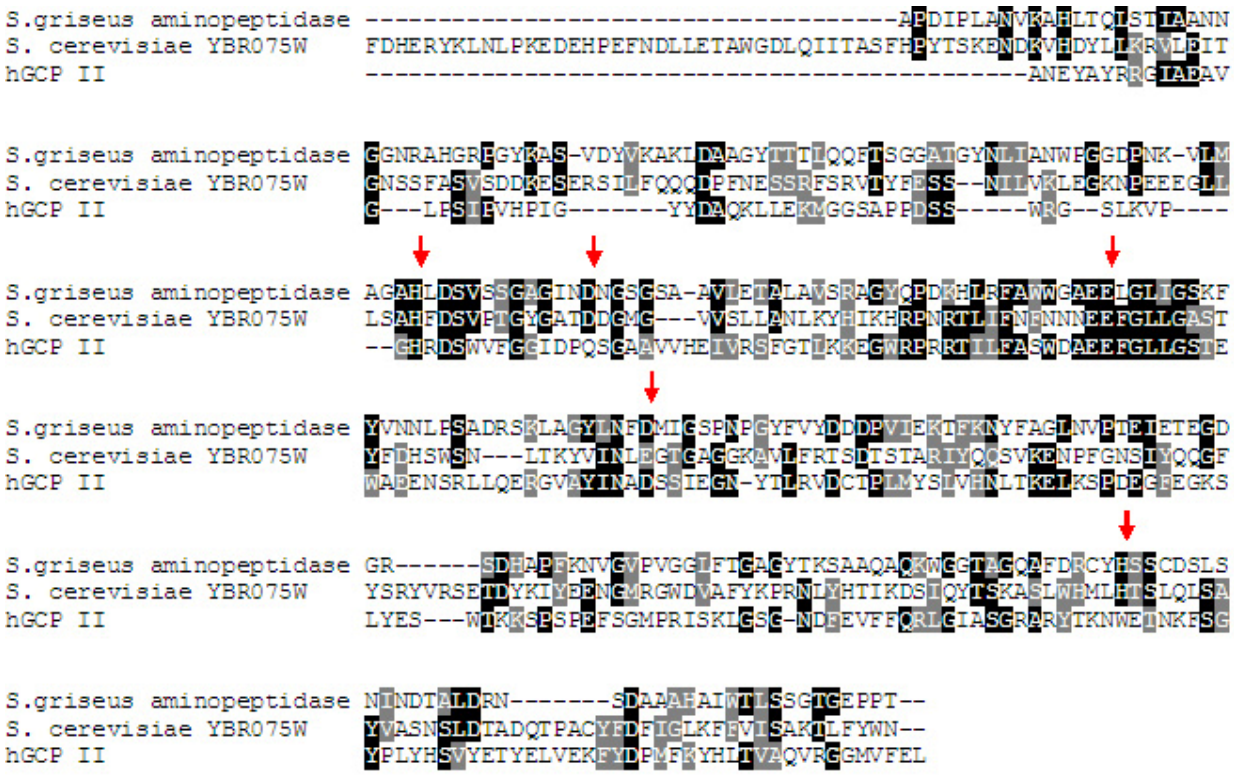

Figure 36: Sequence alignment of the protease domains of 3 M28 metalloproteases.

Figure 37: CFTR degradation is slowed in the *ybr075w* truncation mutant.

A. Rates of CFTR degradation were determined by cycloheximide chase experiments in *YBR075W* wild type yeast and in the *ybr075wΔ* C-terminal truncation mutant strain after addition of cycloheximide. Sec61p levels served as loading control. B. CFTR protein levels were quantified from 5 independent sets of experiments and averaged. All values were obtained after standardization to the levels detected directly after cycloheximide addition (0 min). Closed blue circles represent CFTR protein levels in *YBR075W* wild type cells, and open purple circles represent CFTR protein levels in *ybr075Δ* mutants. Vertical bars indicate the standard errors of the means. P: * = 0.0299, ** = 0.0464, ***= 0.0003, **** = 0.0005.

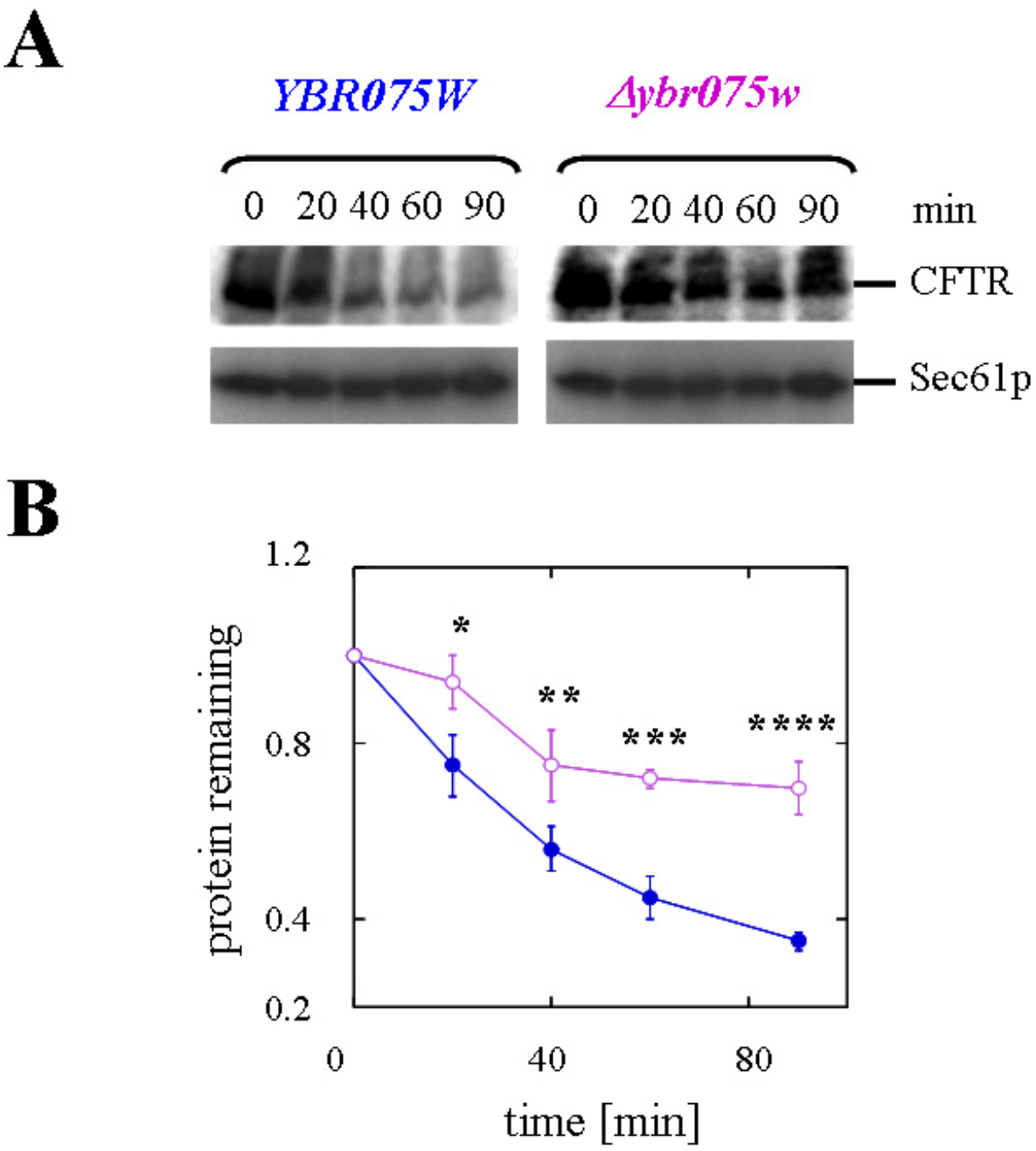

Figure 37: CFTR degradation is slowed in the *ybr075w* truncation mutant.

Figure 38: CPY* protein degradation is equally efficient in *YBR075W* wild type and *ybr075w* truncation strains.

A. Rates of CPY* degradation were determined by pulse-chase immuno-precipitation experiments in *YBR075W* wild type yeast and in the *ybr075wΔ* C-terminal truncation mutant strain after addition of cycloheximide. B. CPY* protein levels were quantified from 2 independent sets of experiments and averaged. All values were obtained after standardization to the levels detected directly after cycloheximide addition (0 min). Closed blue circles represent CPY* protein levels in *YBR075W* wild type cells, and open purple circles represent CPY* protein levels in *ybr075Δ* mutant yeast. Vertical bars indicate the range in the data.

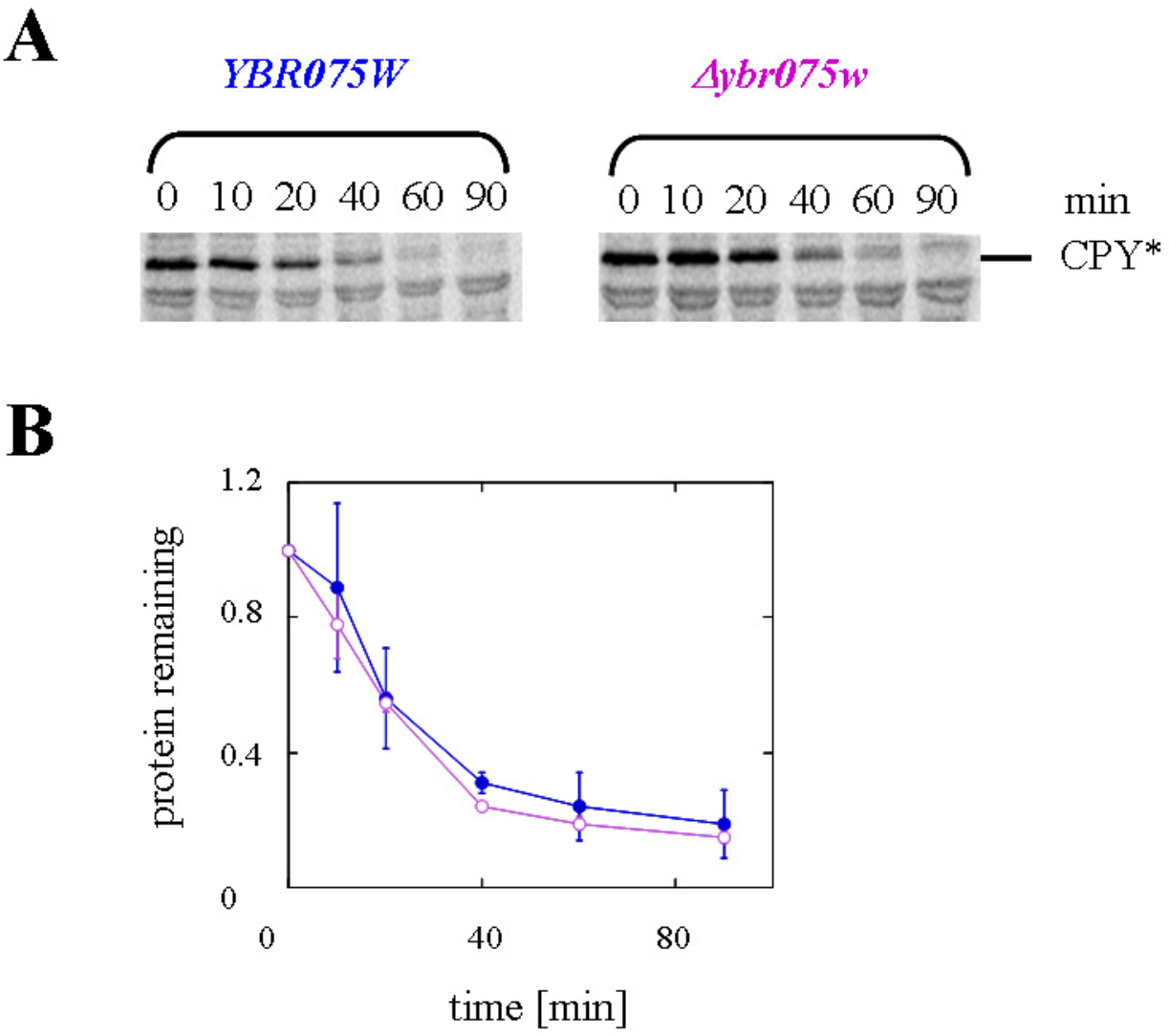

Figure 38: CPY* protein degradation is equally efficient in *YBR075W* wild type and *ybr075w* truncation strains.

mutant because levels of Kar2p were not elevated (see Figure 39). Therefore, Ybr075wp seems to impact ERAD directly and might degrade transmembrane and ER luminal segments left behind by the proteasome, similar to a sequential action of proteases described for the mitochondria (Kambacheld *et al.*, 2005), or it might provide a parallel or alternate pathway for quality control of membrane proteins.

To confirm the role of YBR075Wp in protein degradation, the putative protease activity should be verified through *in vitro* protease assays and functional investigation of mutations in active site residues (see above) might confirm Ybr075Wp as member of the M28 protease family. Determination of Ybr075W's subcellular localization and substrate specificity would then be essential to corroborate the computational prediction of this protein as a new ER resident protease that plays a role in ERAD.

Figure 39: The Stress response is not induced in the *ybr075w* truncation mutant.

Kar2p and Sec61p protein levels in the *YBR075W* wild type and *ybr075w* truncation mutant strain were determined by immuno-precipitation. Results of two independent experiments are displayed. The proteins in the *YBR075W* wild type strain are denoted as "*WT*" in blue, and the proteins in the *ybr075w* truncation mutant are denoted as "*Δ*" in purple.

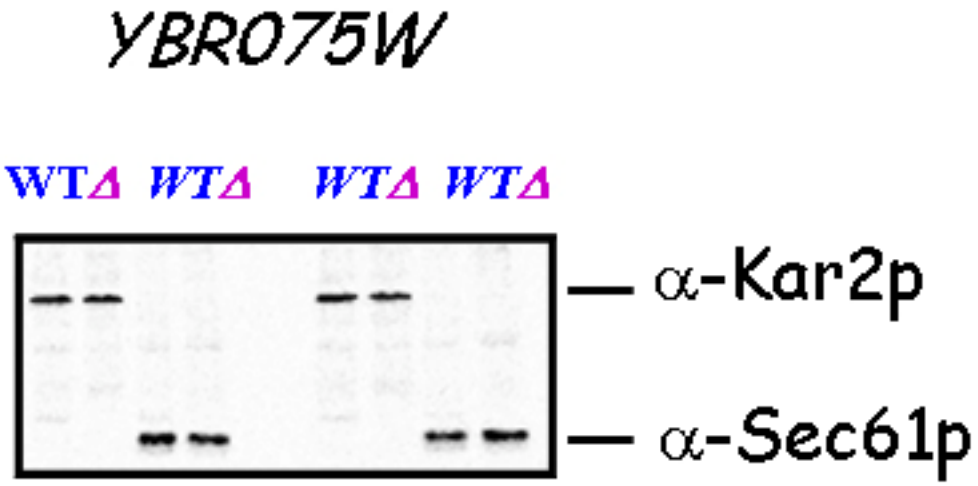

Figure 39: The Stress response is not induced in the *ybr075w* truncation mutant.

In summary, the microarray analysis of the transcriptional response of yeast to heterologous expression of CFTR has provided me with at least 2 genes that affect CFTR degradation in yeast. Prior to this study the impact of these proteins on CFTR biogenesis or ERAD was unknown. I also began to characterize the gene products and was able to show that sHsp function in ERAD is conserved. In addition, there are a large number of interesting up-regulated genes that will provide an avenue of future research. Together, my results validate the use of a genomic approach in yeast to investigate proteins related to human diseases, and I suggest that this attack might be of great value to examine the cause of other protein quality control diseases.

4. CONCLUSION

Chaperone requirements for the folding and degradation of soluble, sectretory proteins and integral membrane proteins have been studied in detail and are distinct from each other (see above) (Plemper *et al.*, 1997; Strickland *et al.*, 1997; Brodsky *et al.*, 1999; Meacham *et al.*, 1999; Hill and Cooper, 2000; Choo-Kang and Zeitlin, 2001; Meacham *et al.*, 2001; Nishikawa *et al.*, 2001; Zhang *et al.*, 2001; Farinha *et al.*, 2002; Kabani *et al.*, 2003; Taxis *et al.*, 2003; Alberti *et al.*, 2004; Huyer *et al.*, 2004; Youker *et al.*, 2004). However, the chaperone requirements for the biogenesis, folding, and degradation of distinct cytoplasmic polypeptides is still rather poorly defined (Schneider *et al.*, 1996; Brodsky *et al.*, 1998; Kim *et al.*, 1998b; Kampinga *et al.*, 2003). My results on the biogenesis on FFLux in yeast (see Chapter 2) and CFTR (see Chapter 3) suggest some overlap in the chaperone requirements between cytoplasmic substrates and integral membrane protein substrates with prominent cytosolic domains (see Table 8). For example, I found that the yeast Hsp70, Ssa1p, and its NEF, Fes1p, facilitate FFLux folding in yeast (Chapter 2), consistent with the involvement of their mammalian orthologs, Hsp70 and HspBP1, in the maturation of CFTR (Strickland *et al.*, 1997; Meacham *et al.*, 1999; Farinha *et al.*, 2002; Alberti *et al.*, 2004). In addition, I found that αA-crystallin prevents the aggregation of the first NBD of CFTR, one of its cytoplasmic domains, and αA-crystallin and other sHsps are known to keep numerous cytoplasmic polypeptides soluble (Narberhaus, 2002). Further evidence in the literature indicates that Hsp70 and Hsp90 can solubilize cytoplasmic client proteins and CFTR

Table 8: Chaperone action on cytoplasmic and integral membrane substrate proteins.

Hsp		Function	Cytoplasmic soluble substrate	Integral membrane substrate
Yeast	**mammalian**			
Sse1p	Hsp110	Prevention of aggregation	Goeckeler *et al*., 2002 Oh *et al*., 1999	-
		Protein maturation	-	Appendix, this study
Hsp82	Hsp90	Translation	Ahner *et al*.,2005; Chapter 2, this study	-
		Folding/maturation	Schneider *et al*., 1996 Wegele *et al*., 2004	Youker *et al*., 2004 Loo *et al*., 1998
		Prevention of aggregation	Wiech *et al*., 1992 Wegele *et al*., 2004	Youker *et al*., 2004
		Protein degradation	Immamura *et al.*, 1998 Murata *et al*., 2001 Connell *et al.*, 2001	Fuller *et al*., 2000
Ssa1p	Hsp70	RNA stability/degradation	Ahner *et al*., 2005 Chapter 2, this study Barnes, 1998 Duttagupta *et al*., 2003	-
		Translation	General effect, specific substrates not examined	
		Folding/maturation	Ahner *et al*., 2005 Chapter 2, this study Kim *et al*., 1998 Luders *et al*.,, 2000 Wegele *et al*., 2004	Farinha *et al*., 2002 Meacham *et al*., 1999 Strickland *et al*., 1997
		Prevention of aggregation	Kim *et al*., 1998 Luders *et al*.,, 2000 Wegele *et al*., 2004	Meacham *et al*., 1999 Strickland *et al*., 1997
		Protein degradation	Murata *et al*., 2001	Zhang *et al*., 2001 Meacham *et al*., 2001
Hsp26/ Hsp42	αA-crystallin	Prevention of aggregation	Narberhaus, 2002	Chapter 3, this study
		Protein degradation	-	Chapter 3, this study
Fes1p	HspBP1	Translation	General effect, specific substrates not examined	
		Folding/Maturation	Ahner *et al.*, 2005 Chapter 2, this study	Alberti *et al*., 2004

NBD1 (Wiech *et al.*, 1992; Strickland *et al.*, 1997; Kim *et al.*, 1998b; Meacham *et al.*, 1999; Luders *et al.*, 2000; Youker *et al.*, 2004), that Hsp70 and Hsp90 are involved in the degradation of cytoplasmic and transmembrane proteins (Imamura *et al.*, 1998; Fuller and Cuthbert, 2000; Connell *et al.*, 2001; Meacham *et al.*, 2001; Murata *et al.*, 2001; Zhang *et al.*, 2001; Huyer *et al.*, 2004), and that Hsp90 aids in the folding of diverse cytoplasmic proteins as well as in the folding of CFTR (Loo *et al.*, 1998; Wegele *et al.*, 2004; Youker *et al.*, 2004). Finally, Hsp110 has been reported to prevent denatured FFLux from aggregating, and the slight increase in wild type CFTR maturation upon Hsp110 over-expression that I report in the Appendix might have arisen from a similar phenomenon (Oh *et al.*, 1999; Goeckeler *et al.*, 2002). To this end, it will be interesting to reveal if sHsps are involved in the degradation of FFLux or other cytoplasmic proteins, consistent with their role in CFTR degradation (see also Table 8).

Despite the observed similarity in chaperone requirements between cytoplasmic and transmembrane proteins, my findings also emphasize specificity in Hsp function. A chaperone does not only recognize its substrates but it also needs to "decide" which function to exert on a client protein. This decision depends on the substrate polypeptide and on the interaction with co-chaperones. For example, although Ssa1p and Fes1p have been implicated in protein translation, neither of them affects FFLux translation: instead, both likely collaborate to help FFLux folding (see Table 8; Horton *et al.*, 2001; Kabani *et al.*, 2002a). In addition, while Ssa1p also impacts FFLux biogenesis at several other levels, Fes1p does not (see Capter 2.3.). The fact that I uncovered multiple, functionally distinct involvements of Ssa1p during the biosynthesis of one substrate but the Ssa1p cofactor Fes1p was only required for one of these functions, leads to several questions: Does Ssa1p interact with a different cofactor or different cofactors to support

each function? Is there a default function of Ssa1p when it acts on its own and does association with a distinct cofactor induce a specific change in function? For example, Ssa1p might keep a polypeptide soluble and hence accessible for cofactor-mediated functions, such as ubiquitination, degradation, folding, and maturation. How do different cofactors compete for chaperone interaction? And, what is the mechanism utilized by the co-chaperones that alters chaperone function?

For example, two mammalian co-chaperones, the E3 ubiquitin ligase CHIP, and the NEF Bag-1, associate simultaneously with Hsc70, and this protein complex promotes substrate ubiquitination and degradation; however, the nucleotide release factor for Hsc70, HspBP1, competes with Bag-1 for Hsc70 binding and inhibits CHIP-mediated ubiquitination of CFTR by the chaperone complex, but does not impact the CHIP-regulated half-life of the glucocorticoid receptor (Alberti *et al.*, 2004). Therefore, Hsc70 function is dependent on Hsc70-co-chaperone interaction, co-chaperone-combinations, and the substrate.

In fact, yeast contain two known nucleotide exchange factors for the cytoplasmic Hsp70, Ssa1p, the Bag-1 ortholog, Snl1 (Sondermann *et al.*, 2002), and the HspBP1 ortholog, Fes1p (Kabani *et al.*, 2002b), which I found to be involved in Ssa1p-catalyzed FFLux folding (see Chapter 2.3.). Hence, it should be worthwhile to investigate a putative involvement of Snl1p in FFLux biogenesis and a possible cooperation between this Bag-1 ortholog and Ssa1p in FFLux biosynthesis and maturation. It should be mentioned though that a yeast ortholog of CHIP has not been identified to date, so that an Hsp70-Snl1p interaction in yeast might lead to different effects than the action of their mammalian counterparts. Also, because different cofactors might

bind to different domains of a chaperone, an investigation of mutated chaperones might only reveal allele specific effects.

Additional evidence for the specificity of Hsp action originates from the observation that the presence of a mutation within a protein might change the impact of the chaperone: whereas the biogenesis of wild type CFTR was unaffected by αA-crystallin over-expression, ΔF508-CFTR degradation was enhanced (see Chapter 3.3.). Moreover, two structurally related transmembrane ERAD substrates, CFTR and Ste6p*, with homology limited to their NBDs (see Chapter 3.3.; and Kuchler *et al.*, 1989), are degraded by the same proteolytic machinery in yeast, and efficient proteolysis of both requires the yeast Hsp70, Ssa1p (Huyer *et al.*, 2004). In contrast, I found that sHsps impact only the degradation of CFTR but not the proteolysis of Ste6p* (see Chapter 3.3.). Hence, sHsps either differentiate between these integral membrane substrates whereas Ssa1p does not, or sHsps might recognize the C-terminus of Ste6p, which is deleted in mutant Ste6p*, to associate with this substrate (see Chapter 3.3.). These data suggest that the Ssa1p interaction site resides in a different segment of the protein.

Together, these results indicate a high complexity of the chaperone network. To gain a better understanding of the decision processes it will be necessary to determine the chaperone and co-chaperone requirements for numerous protein substrates and different mutant variants of each substrate.

APPENDIX A

THE ROLE OF HSP110 IN CFTR MATURATION AND DEGRADATION

Introduction

Hsp110s comprise a subfamily of the Hsp70 family of chaperones, and homology between the two groups resides mostly in the N-terminal nucleotide-binding site (Easton *et al.*, 2000). Mammalian Hsp110 and the yeast Hsp110 ortholog, Sse1p, retain denatured proteins in a folding competent conformation, but are unable to catalyze the refolding process, and they interact with and are required for the function of the Hsp90 complex (Oh *et al.*, 1997; Brodsky *et al.*, 1999; Liu *et al.*, 1999; Oh *et al.*, 1999; Goeckeler *et al.*, 2002). In contrast to the Hsp70s, the substrate specificity of this class of chaperones has not been characterized.

It was previously shown that the deletion of the yeast *HSP110* did not affect CFTR biogenesis or degradation (Youker *et al.*, 2004). But, this result could not rule out that redundancy in chaperone function might have compensated for the loss of Hsp110. Also, the functions of the yeast and mammalian Hsp110 might not be entirely conserved. In addition, a previous report on a microarray analysis on the transcriptional response of IB3-1 cells (a bronchial epithelial cell line that expresses ΔF508-CFTR) to 4-phenylbutyrate (PBA) reported an up-regulation of HSP110 (Wright *et al.*, 2004). PBA has been demonstrated to impact the expression levels of many molecular chaperones, and it induces ΔF508-CFTR maturation and restores ion conductance of the mutant channel (Rubenstein *et al.*, 1997; Rubenstein and Zeitlin, 1998, 2000; Zeitlin *et al.*, 2002). These data raised the question whether the effect of PBA is at least in part mediated through Hsp110 up-regulation. Therefore, I tested the effect of Hsp110 over-expression

on the biogenesis of wild type CFTR and on ΔF508-CFTR in HEK293 cells. My preliminary data suggest that elevated Hsp110 levels are insufficient to induce maturation of ΔF508-CFTR maturation.

Materials and Methods

Mammalian cell culture, plasmids, and transient transfection

HEK293 (human embryonic kidney) cells were cultured in Dulbecco's modified Eagel's medium (DMEM; Sigma) with 10% fetal bovine serum (Invitrogen), 4mM L-gutamine (Sigma), and penicillin-streptomycin (GibcoBRL) at 37°C in a humidified environment containing 5% CO_2.
The Hsp110 encoding gene in the pBacPAKHis-1 vector (kindly provided by J.R. Subjeck, Roswell Park Cancer Institute, Buffalo, New York) was sub-cloned into pcDNA3.1 (kindly provided by R. Hughey, University of Pittsburgh) as described in chapter 3.2.2., and the CFTR and ΔF508-CFTR genes in pcDNA3.1 were kindly provided by R.A. Frizzell, University of Pittsburgh.

For all experiments, HEK293 cells were grown in 60-mm dishes and transiently transfected with the indicated pcDNA3.1 expression plasmids aided by Lipofectamine 2000 (Invitrogen). After 24h, cells were subjected to pulse-chase analysis as described previously (Zhang *et al.*, 2002a)

with minor modifications (described in Chapter 3.2.7.). P-values were calculated via the program at http://faculty.vassar.edu/lowry/t_ind_stats.html.

Immunoblot analysis

Protein extracts were prepared as described (Zhang *et al.*, 2002a) with minor modifications (described in Chapter 3.2.7.) and were concentrated ~4-fold with microcon YM-30 filters (Amicon). Samples were loaded onto 12.5% SDS-polyacrylamide gels, and after electrophoresis, the proteins were transferred to nitrocellulose (Schleicher and Schuell, pore diameter of 0.2µm). The primary antibodies used were raised against Hsp90 and Hsp110 (Stressgen). To detect the primary antibody, horse-radish peroxidase-conjugated secondary antibodies (anti-rabbit and anti-rat (Amersham)) were used. The complexes were visualized using the enhanced chemiluminescence detection kit (Pierce) and quantified using Kodak 1D software (v3.6; Kodak).

Results

To assess the impact of Hsp110 on CFTR biogenesis, I co-transfected HEK293 cells with the CFTR expression vector and either the empty vector as a control or the Hsp110 expression

vector and performed pulse-chase immuno-precipitation experiments. Successful over-expression of Hsp110 was confirmed by western blot analysis (see Figure 40A). I found that the efficiency of CFTR maturation from the immature, core-glycosylated form (CFTR B-band) to the mature, complex-glycosylated form (CFTR C-band) was slightly increased in cultures transfected with the Hsp110 over-expression vector (see Figure 40A and B). There was no difference in the disappearance of the B-band following over-expression of Hsp110 (see Figure 40A and B). These preliminary data suggest that the human Hsp110 might aid in the maturation of wild type CFTR. To explore the possibility that Hsp110 might similarly affect the biogenesis of ΔF508-CFTR I repeated the pulse-chase immuno-precipitation experiments in cells expressing the ΔF508-CFTR mutant. Successful over-expression of Hsp110 was confirmed by western blot analysis, and Hsp90 served as a loading control (see Figure 41A). In preliminary experiments, I did not observe an increase in ΔF508-CFTR maturation upon Hsp110 over-expression (no C-band could be detected), and the degradation of the B-band proceeded with equal efficiency in HEK293 cells, independent of Hsp110 protein levels (see Figure 41A and B).

Discussion

I observed that the over-expression of Hsp110 caused a small increase in the efficiency of wild type CFTR maturation, but processing of the ΔF508-CFTR mutant protein was unaffected. Although these results are preliminary, they suggest a role for Hsp110 in at least wild type CFTR

Figure 40: Hsp110 over-expression slightly increases the efficiency of wild type CFTR maturation. A. HEK293 cells were transfected with 1.5 μg of pcDNA3.1-CFTR and 1.5 μg of pcDNA3.1 or pcDNA3.1-Hsp110. Rates of CFTR maturation and CFTR B-band degradation were determined by pulse-chase immuno-precipitation in HEK293 cells co-transfected with CFTR, and in cells containing a vector control or the Hsp110 expressing vector. Hsp110 expression levels were assessed by western blot analysis. B. CFTR B-band degradation and CFTR maturation were determined from 3 independent sets of experiments and averaged. All values were obtained after standardization to the levels detected at the beginning of the chase period (0 h). Closed blue circles represent immature/mature CFTR protein levels in HEK293 cells with the vector control, and open purple circles represent immature/mature CFTR protein levels in HEK293 cells over-expressing Hsp110. Vertical bars indicate the standard errors of the mean. P: * = 0.024, ** = 0.0228.

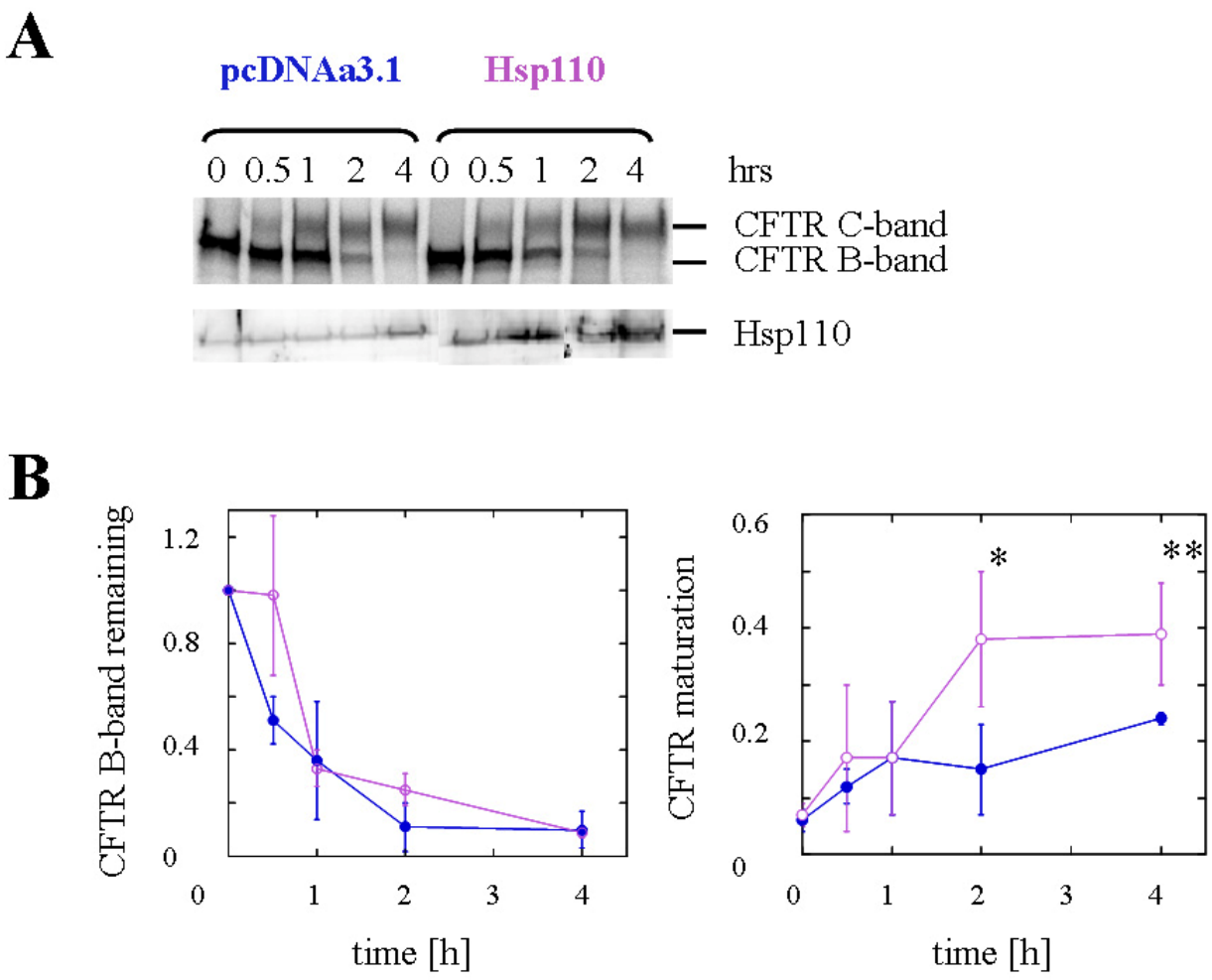

Figure 40: Hsp110 over-expression slightly increases the efficiency of wild type CFTR maturation.

Figure 41: Hsp110 over-expression has no effect on the degradation of ΔF508-CFTR.

A. HEK293 cells were transfected with 1.5 μg of pcDNA3.1-ΔF508-CFTR and 1.5 μg of pcDNA3.1 or pcDNA3.1-HSP110. Rates of ΔF508-CFTR degradation were determined by pulse-chase immuno-precipitation in each transfected HEK293 cell-type. Hsp110 and Hsp90 (as a loading control) expression levels were assessed by western blot analysis B. ΔF508-CFTR degradation was determined from 3 independent sets of experiments and averaged. All values were obtained after standardization to the levels detected at the beginning of the chase period (0 h). Closed blue circles represent ΔF508-CFTR protein levels in HEK293 cells with the vector control, and open purple circles represent ΔF508-CFTR protein levels in HEK293 cells over-expressing Hsp110. Vertical bars indicate the standard errors of the mean.

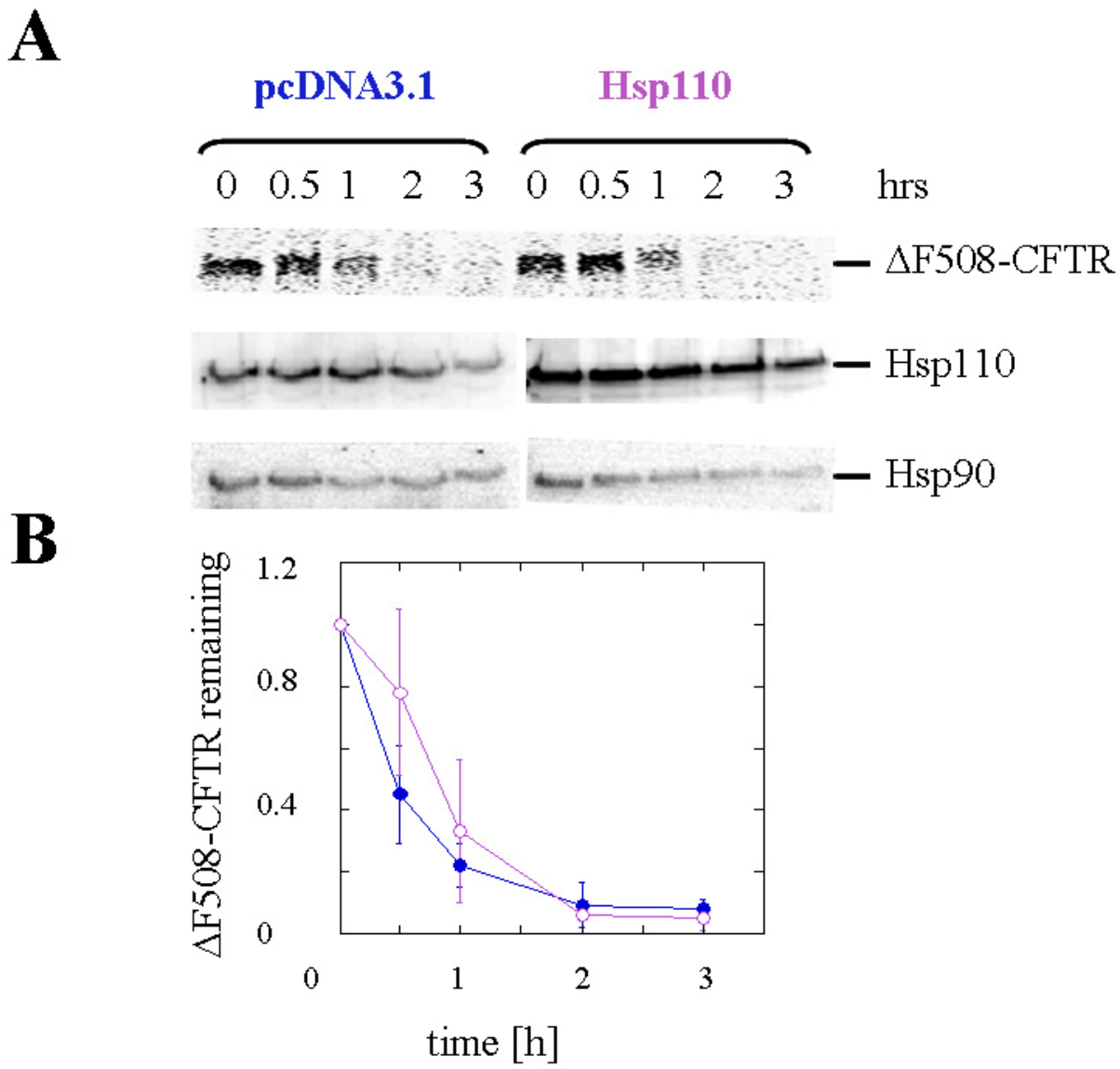

Figure 41: Hsp110 over-expression has no effect on the degradation of ΔF508-CFTR.

maturation. The fact that I did not detect any maturation of the ΔF508-CFTR mutant protein might tell us that Hsp110 alone does not mediate the PBA-induced restoration of ΔF508-CFTR trafficking and function, or Hsp110 might be necessary but not sufficient for this mechanism (Rubenstein *et al.*, 1997; Rubenstein and Zeitlin, 1998, 2000; Zeitlin *et al.*, 2002). Also, the heterologous over-expression of ΔF508-CFTR and the cell line chosen might interfere with a putative impact of Hsp110 on ΔF508-CFTR biogenesis. Careful repetition of the experiments, the use of a physiological relevant system, and simultaneous manipulation of other chaperones/factors might aid in solving this question.

BIBLIOGRAPHY

Ahner, A., and Brodsky, J.L. (2004). Checkpoints in ER-associated degradation: excuse me, which way to the proteasome? Trends Cell Biol *14*, 474-478.

Alberti, S., Bohse, K., Arndt, V., Schmitz, A., and Hohfeld, J. (2004). The cochaperone HspBP1 inhibits the CHIP ubiquitin ligase and stimulates the maturation of the cystic fibrosis transmembrane conductance regulator. Mol Biol Cell *15*, 4003-4010.

Andley, U.P., Patel, H.C., and Xi, J.H. (2002). The R116C mutation in alpha A-crystallin diminishes its protective ability against stress-induced lens epithelial cell apoptosis. J Biol Chem *277*, 10178-10186.

Arndt, K.M., Ricupero-Hovasse, S., and Winston, F. (1995). TBP mutants defective in activated transcription in vivo. EMBO J *14*, 1490-1497.

Atencio, D.P., and Yaffe, M.P. (1992). MAS5, a yeast homolog of DnaJ involved in mitochondrial protein import. Mol Cell Biol *12*, 283-291.

Ausubel, F.M., Brent, R., Kingston, R. E., Moore, D. D., Seidmann, J. G., Smith, J. G., and Struhl, K. (1988). Current protocols in molecular biology. Greene Publishing Associates and Wiley-Interscience: New York.

Barlowe, C., Orci, L., Yeung, T., Hosobuchi, M., Hamamoto, S., Salama, N., Rexach, M.F., Ravazzola, M., Amherdt, M., and Schekman, R. (1994). COPII: a membrane coat formed by Sec proteins that drive vesicle budding from the endoplasmic reticulum. Cell *77*, 895-907.

Barnes, C.A. (1998). Upf1 and Upf2 proteins mediate normal yeast mRNA degradation when translation initiation is limited. Nucleic Acids Res *26*, 2433-2441.

Barnes, C.A., MacKenzie, M.M., Johnston, G.C., and Singer, R.A. (1995). Efficient translation of an SSA1-derived heat-shock mRNA in yeast cells limited for cap-binding protein and eIF-4F. Mol Gen Genet *246*, 619-627.

Barnes, C.A., Singer, R.A., and Johnston, G.C. (1993). Yeast prt1 mutations alter heat-shock gene expression through transcript fragmentation. EMBO J *12*, 3323-3332.

Barr, F.A., and Short, B. (2003). Golgins in the structure and dynamics of the Golgi apparatus. Curr Opin Cell Biol *15*, 405-413.

Bays, N.W., and Hampton, R.Y. (2002). Cdc48-Ufd1-Npl4: stuck in the middle with Ub. Curr Biol *12*, R366-371.

Becker, J., Walter, W., Yan, W., and Craig, E.A. (1996). Functional interaction of cytosolic hsp70 and a DnaJ-related protein, Ydj1p, in protein translocation in vivo. Mol Cell Biol *16*, 4378-4386.

Beelman, C.A., Stevens, A., Caponigro, G., LaGrandeur, T.E., Hatfield, L., Fortner, D.M., and Parker, R. (1996). An essential component of the decapping enzyme required for normal rates of mRNA turnover. Nature *382*, 642-646.

Benharouga, M., Haardt, M., Kartner, N., and Lukacs, G.L. (2001). COOH-terminal truncations promote proteasome-dependent degradation of mature cystic fibrosis transmembrane conductance regulator from post-Golgi compartments. J Cell Biol *153*, 957-970.

Benndorf, R., Hayess, K., Ryazantsev, S., Wieske, M., Behlke, J., and Lutsch, G. (1994). Phosphorylation and supramolecular organization of murine small heat shock protein HSP25 abolish its actin polymerization-inhibiting activity. J Biol Chem *269*, 20780-20784.

Bertrand, C.A., and Frizzell, R.A. (2003). The role of regulated CFTR trafficking in epithelial secretion. Am J Physiol Cell Physiol *285*, C1-18.

Biswas, A., and Das, K.P. (2004). Role of ATP on the interaction of alpha-crystallin with its substrates and its implications for the molecular chaperone function. J Biol Chem *279*, 42648-42657.

Blond-Elguindi, S., Cwirla, S.E., Dower, W.J., Lipshutz, R.J., Sprang, S.R., Sambrook, J.F., and Gething, M.J. (1993). Affinity panning of a library of peptides displayed on bacteriophages reveals the binding specificity of BiP. Cell *75*, 717-728.

Boelens, W.C., Croes, Y., and de Jong, W.W. (2001). Interaction between alphaB-crystallin and the human 20S proteasomal subunit C8/alpha7. Biochim Biophys Acta *1544*, 311-319.

Bohen, S.P., and Yamamoto, K.R. (1993). Isolation of Hsp90 mutants by screening for decreased steroid receptor function. Proc Natl Acad Sci U S A *90*, 11424-11428.

Bonifacino, J.S., and Glick, B.S. (2004). The mechanisms of vesicle budding and fusion. Cell *116*, 153-166.

Bonifacino, J.S., and Lippincott-Schwartz, J. (2003). Coat proteins: shaping membrane transport. Nat Rev Mol Cell Biol *4*, 409-414.

Bonifacino, J.S., and Traub, L.M. (2003). Signals for sorting of transmembrane proteins to endosomes and lysosomes. Annu Rev Biochem *72*, 395-447.

Bova, M.P., Yaron, O., Huang, Q., Ding, L., Haley, D.A., Stewart, P.L., and Horwitz, J. (1999). Mutation R120G in alphaB-crystallin, which is linked to a desmin-related myopathy, results in an irregular structure and defective chaperone-like function. Proc Natl Acad Sci U S A *96*, 6137-6142.

Brachmann, C.B., Davies, A., Cost, G.J., Caputo, E., Li, J., Hieter, P., and Boeke, J.D. (1998). Designer deletion strains derived from Saccharomyces cerevisiae S288C: a useful set of strains and plasmids for PCR-mediated gene disruption and other applications. Yeast *14*, 115-132.

Braun, B.C., Glickman, M., Kraft, R., Dahlmann, B., Kloetzel, P.M., Finley, D., and Schmidt, M. (1999). The base of the proteasome regulatory particle exhibits chaperone-like activity. Nat Cell Biol *1*, 221-226.

Brehmer, D., Rudiger, S., Gassler, C.S., Klostermeier, D., Packschies, L., Reinstein, J., Mayer, M.P., and Bukau, B. (2001). Tuning of chaperone activity of Hsp70 proteins by modulation of nucleotide exchange. Nat Struct Biol *8*, 427-432.

Briknarova, K., Takayama, S., Brive, L., Havert, M.L., Knee, D.A., Velasco, J., Homma, S., Cabezas, E., Stuart, J., Hoyt, D.W., Satterthwait, A.C., Llinas, M., Reed, J.C., and Ely, K.R. (2001). Structural analysis of BAG1 cochaperone and its interactions with Hsc70 heat shock protein. Nat Struct Biol *8*, 349-352.

Brodsky, J.L., Goeckeler, J., and Schekman, R. (1995). BiP and Sec63p are required for both co- and posttranslational protein translocation into the yeast endoplasmic reticulum. Proc Natl Acad Sci U S A *92*, 9643-9646.

Brodsky, J.L., Lawrence, J.G., and Caplan, A.J. (1998). Mutations in the cytosolic DnaJ homologue, YDJ1, delay and compromise the efficient translation of heterologous proteins in yeast. Biochemistry *37*, 18045-18055.

Brodsky, J.L., and Schekman, R. (1993). A Sec63p-BiP complex from yeast is required for protein translocation in a reconstituted proteoliposome. J Cell Biol *123*, 1355-1363.

Brodsky, J.L., Werner, E.D., Dubas, M.E., Goeckeler, J.L., Kruse, K.B., and McCracken, A.A. (1999). The requirement for molecular chaperones during endoplasmic reticulum- associated

protein degradation demonstrates that protein export and import are mechanistically distinct. J Biol Chem *274*, 3453-3460.

Butler, J.S. (2002). The yin and yang of the exosome. Trends Cell Biol *12*, 90-96.

Caldwell, S.R., Hill, K.J., and Cooper, A.A. (2001). Degradation of endoplasmic reticulum (ER) quality control substrates requires transport between the ER and Golgi. J Biol Chem *276*, 23296-23303.

Caplan, A.J. (1999). Hsp90's secrets unfold: new insights from structural and functional studies. Trends Cell Biol *9*, 262-268.

Caplan, A.J., Cyr, D.M., and Douglas, M.G. (1992). YDJ1p facilitates polypeptide translocation across different intracellular membranes by a conserved mechanism. Cell *71*, 1143-1155.

Caplan, A.J., and Douglas, M.G. (1991). Characterization of YDJ1: a yeast homologue of the bacterial dnaJ protein. J Cell Biol *114*, 609-621.

Carson, M.R., Travis, S.M., and Welsh, M.J. (1995). The two nucleotide-binding domains of cystic fibrosis transmembrane conductance regulator (CFTR) have distinct functions in controlling channel activity. J Biol Chem *270*, 1711-1717.

Caspers, G.J., Leunissen, J.A., and de Jong, W.W. (1995). The expanding small heat-shock protein family, and structure predictions of the conserved "alpha-crystallin domain". J Mol Evol *40*, 238-248.

Chang, Z., Primm, T.P., Jakana, J., Lee, I.H., Serysheva, I., Chiu, W., Gilbert, H.F., and Quiocho, F.A. (1996). Mycobacterium tuberculosis 16-kDa antigen (Hsp16.3) functions as an oligomeric structure in vitro to suppress thermal aggregation. J Biol Chem *271*, 7218-7223.

Chapman, R., Sidrauski, C., and Walter, P. (1998). Intracellular signaling from the endoplasmic reticulum to the nucleus. Annu Rev Cell Dev Biol *14*, 459-485.

Chappell, T.G., Konforti, B.B., Schmid, S.L., and Rothman, J.E. (1987). The ATPase core of a clathrin uncoating protein. J Biol Chem *262*, 746-751.

Cheetham, M.E., and Caplan, A.J. (1998). Structure, function and evolution of DnaJ: conservation and adaptation of chaperone function. Cell Stress Chaperones *3*, 28-36.

Chen, C.Y., and Shyu, A.B. (1995). AU-rich elements: characterization and importance in mRNA degradation. Trends Biochem Sci *20*, 465-470.

Chen, Y.A., and Scheller, R.H. (2001). SNARE-mediated membrane fusion. Nat Rev Mol Cell Biol *2*, 98-106.

Cheng, S.H., Gregory, R.J., Marshall, J., Paul, S., Souza, D.W., White, G.A., O'Riordan, C.R., and Smith, A.E. (1990). Defective intracellular transport and processing of CFTR is the molecular basis of most cystic fibrosis. Cell *63*, 827-834.

Chirico, W.J., Waters, M.G., and Blobel, G. (1988). 70K heat shock related proteins stimulate protein translocation into microsomes. Nature *332*, 805-810.

Choo-Kang, L.R., and Zeitlin, P.L. (2001). Induction of HSP70 promotes DeltaF508 CFTR trafficking. Am J Physiol Lung Cell Mol Physiol *281*, L58-68.

Christianson, T.W., Sikorski, R.S., Dante, M., Shero, J.H., and Hieter, P. (1992). Multifunctional yeast high-copy-number shuttle vectors. Gene *110*, 119-122.

Collart, M.A.O., S. (1993). Preparation of Yeast RNA.

Conconi, M., Djavadi-Ohaniance, L., Uerkvitz, W., Hendil, K.B., and Friguet, B. (1999). Conformational changes in the 20S proteasome upon macromolecular ligand binding analyzed with monoclonal antibodies. Arch Biochem Biophys *362*, 325-328.

Conconi, M., Petropoulos, I., Emod, I., Turlin, E., Biville, F., and Friguet, B. (1998). Protection from oxidative inactivation of the 20S proteasome by heat-shock protein 90. Biochem J *333*, 407-415.

Connell, P., Ballinger, C.A., Jiang, J., Wu, Y., Thompson, L.J., Hohfeld, J., and Patterson, C. (2001). The co-chaperone CHIP regulates protein triage decisions mediated by heat-shock proteins. Nat Cell Biol *3*, 93-96.

Coughlan, C.M., and Brodsky, J.L. (2003). Yeast as a model system to investigate protein conformational diseases. Methods Mol Biol *232*, 77-90.

Cyr, D.M., Lu, X., and Douglas, M.G. (1992). Regulation of Hsp70 function by a eukaryotic DnaJ homolog. J Biol Chem *267*, 20927-20931.

Dabir, D.V., Trojanowski, J.Q., Richter-Landsberg, C., Lee, V.M., and Forman, M.S. (2004). Expression of the small heat-shock protein alphaB-crystallin in tauopathies with glial pathology. Am J Pathol *164*, 155-166.

Dai, R.M., and Li, C.C. (2001). Valosin-containing protein is a multi-ubiquitin chain-targeting factor required in ubiquitin-proteasome degradation. Nat Cell Biol *3*, 740-744.

Davezac, N., Tondelier, D., Lipecka, J., Fanen, P., Demaugre, F., Debski, J., Dadlez, M., Schrattenholz, A., Cahill, M.A., and Edelman, A. (2004). Global proteomic approach unmasks involvement of keratins 8 and 18 in the delivery of cystic fibrosis transmembrane conductance regulator (CFTR)/deltaF508-CFTR to the plasma membrane. Proteomics *4*, 3833-3844.

de Jong, W.W., Caspers, G.J., and Leunissen, J.A. (1998). Genealogy of the alpha-crystallin--small heat-shock protein superfamily. Int J Biol Macromol *22*, 151-162.

den Engelsman, J., Bennink, E.J., Doerwald, L., Onnekink, C., Wunderink, L., Andley, U.P., Kato, K., de Jong, W.W., and Boelens, W.C. (2004). Mimicking phosphorylation of the small heat-shock protein alphaB-crystallin recruits the F-box protein FBX4 to nuclear SC35 speckles. Eur J Biochem *271*, 4195-4203.

den Engelsman, J., Keijsers, V., de Jong, W.W., and Boelens, W.C. (2003). The small heat-shock protein alpha B-crystallin promotes FBX4-dependent ubiquitination. J Biol Chem *278*, 4699-4704.

Denning, G.M., Anderson, M.P., Amara, J.F., Marshall, J., Smith, A.E., and Welsh, M.J. (1992). Processing of mutant cystic fibrosis transmembrane conductance regulator is temperature-sensitive. Nature *358*, 761-764.

Deshaies, R.J., Koch, B.D., Werner-Washburne, M., Craig, E.A., and Schekman, R. (1988). A subfamily of stress proteins facilitates translocation of secretory and mitochondrial precursor polypeptides. Nature *332*, 800-805.

Dransfield, D.T., Bradford, A.J., Smith, J., Martin, M., Roy, C., Mangeat, P.H., and Goldenring, J.R. (1997). Ezrin is a cyclic AMP-dependent protein kinase anchoring protein. EMBO J *16*, 35-43.

Du, K., Sharma, M., and Lukacs, G.L. (2005). The DeltaF508 cystic fibrosis mutation impairs domain-domain interactions and arrests post-translational folding of CFTR. Nat Struct Mol Biol *12*, 17-25.

Dunckley, T., and Parker, R. (1999). The DCP2 protein is required for mRNA decapping in Saccharomyces cerevisiae and contains a functional MutT motif. EMBO J *18*, 5411-5422.

Duttagupta, R., Vasudevan, S., Wilusz, C.J., and Peltz, S.W. (2003). A yeast homologue of Hsp70, Ssa1p, regulates turnover of the MFA2 transcript through its AU-rich 3' untranslated region. Mol Cell Biol *23*, 2623-2632.

Easton, D.P., Kaneko, Y., and Subjeck, J.R. (2000). The hsp110 and Grp1 70 stress proteins: newly recognized relatives of the Hsp70s. Cell Stress Chaperones *5*, 276-290.

Eaton, P., Fuller, W., Bell, J.R., and Shattock, M.J. (2001). AlphaB crystallin translocation and phosphorylation: signal transduction pathways and preconditioning in the isolated rat heart. J Mol Cell Cardiol *33*, 1659-1671.

Ehrnsperger, M., Graber, S., Gaestel, M., and Buchner, J. (1997). Binding of non-native protein to Hsp25 during heat shock creates a reservoir of folding intermediates for reactivation. EMBO J *16*, 221-229.

Ehrnsperger, M., Lilie, H., Gaestel, M., and Buchner, J. (1999). The dynamics of Hsp25 quaternary structure. Structure and function of different oligomeric species. J Biol Chem *274*, 14867-14874.

Ellgaard, L., and Helenius, A. (2003). Quality control in the endoplasmic reticulum. Nat Rev Mol Cell Biol *4*, 181-191.

Farinha, C.M., Nogueira, P., Mendes, F., Penque, D., and Amaral, M.D. (2002). The human DnaJ homologue (Hdj)-1/heat-shock protein (Hsp) 40 co-chaperone is required for the in vivo stabilization of the cystic fibrosis transmembrane conductance regulator by Hsp70. Biochem J *366*, 797-806.

Fewell, S.W., Travers, K.J., Weissman, J.S., and Brodsky, J.L. (2001). The action of molecular chaperones in the early secretory pathway. Annu Rev Genet *35*, 149-191.

Flaherty, K.M., DeLuca-Flaherty, C., and McKay, D.B. (1990). Three-dimensional structure of the ATPase fragment of a 70K heat-shock cognate protein. Nature *346*, 623-628.

Fliss, A.E., Benzeno, S., Rao, J., and Caplan, A.J. (2000). Control of estrogen receptor ligand binding by Hsp90. J Steroid Biochem Mol Biol *72*, 223-230.

Flynn, G.C., Pohl, J., Flocco, M.T., and Rothman, J.E. (1991). Peptide-binding specificity of the molecular chaperone BiP. Nature *353*, 726-730.

Frydman, J. (2001). Folding of newly translated proteins in vivo: the role of molecular chaperones. Annu Rev Biochem *70*, 603-647.

Fu, L., and Sztul, E. (2003). Traffic-independent function of the Sar1p/COPII machinery in proteasomal sorting of the cystic fibrosis transmembrane conductance regulator. J Cell Biol *160*, 157-163.

Fuller, W., and Cuthbert, A.W. (2000). Post-translational disruption of the delta F508 cystic fibrosis transmembrane conductance regulator (CFTR)-molecular chaperone complex with geldanamycin stabilizes delta F508 CFTR in the rabbit reticulocyte lysate. J Biol Chem *275*, 37462-37468.

Fundoiano-Hershcovitz, Y., Rabinovitch, L., Langut, Y., Reiland, V., Shoham, G., and Shoham, Y. (2004). Identification of the catalytic residues in the double-zinc aminopeptidase from Streptomyces griseus. FEBS Lett *571*, 192-196.

Gadsby, D.C., and Nairn, A.C. (1999). Control of CFTR channel gating by phosphorylation and nucleotide hydrolysis. Physiol Rev *79*, S77-S107.

Gallie, D.R. (1998). A tale of two termini: a functional interaction between the termini of an mRNA is a prerequisite for efficient translation initiation. Gene *216*, 1-11.

Garnier, C., Lafitte, D., Tsvetkov, P.O., Barbier, P., Leclerc-Devin, J., Millot, J.M., Briand, C., Makarov, A.A., Catelli, M.G., and Peyrot, V. (2002). Binding of ATP to heat shock protein 90: evidence for an ATP-binding site in the C-terminal domain. J Biol Chem *277*, 12208-12214.

Gautschi, M., Mun, A., Ross, S., and Rospert, S. (2002). A functional chaperone triad on the yeast ribosome. Proc Natl Acad Sci U S A *99*, 4209-4214.

Gelman, M.S., Kannegaard, E.S., and Kopito, R.R. (2002). A principal role for the proteasome in endoplasmic reticulum-associated degradation of misfolded intracellular cystic fibrosis transmembrane conductance regulator. J Biol Chem *277*, 11709-11714.

Geoffrey, A.e.a. (1997). The yeast genome directory. Nature *387*, 1-107.

Gething, M.J. (1999). Role and regulation of the ER chaperone BiP. Semin Cell Dev Biol *10*, 465-472.

Glickman, M.H., and Ciechanover, A. (2002). The ubiquitin-proteasome proteolytic pathway: destruction for the sake of construction. Physiol Rev *82*, 373-428.

Glickman, M.H., Rubin, D.M., Fried, V.A., and Finley, D. (1998). The regulatory particle of the Saccharomyces cerevisiae proteasome. Mol Cell Biol *18*, 3149-3162.

Gnann, A., Riordan, J.R., and Wolf, D.H. (2004). Cystic fibrosis transmembrane conductance regulator degradation depends on the lectins Htm1p/EDEM and the Cdc48 protein complex in yeast. Mol Biol Cell *15*, 4125-4135.

Goeckeler, J.L., Stephens, A., Lee, P., Caplan, A.J., and Brodsky, J.L. (2002). Overexpression of Yeast Hsp110 Homolog Sse1p Suppresses ydj1-151 Thermosensitivity and Restores Hsp90-dependent Activity. Mol Biol Cell *13*, 2760-2770.

Greenberg, M.E., Shyu, A.B., and Belasco, J.G. (1990). Deadenylylation: a mechanism controlling c-fos mRNA decay. Enzyme *44*, 181-192.

Grenert, J.P., Sullivan, W.P., Fadden, P., Haystead, T.A., Clark, J., Mimnaugh, E., Krutzsch, H., Ochel, H.J., Schulte, T.W., Sausville, E., Neckers, L.M., and Toft, D.O. (1997). The amino-terminal domain of heat shock protein 90 (hsp90) that binds geldanamycin is an ATP/ADP switch domain that regulates hsp90 conformation. J Biol Chem *272*, 23843-23850.

Gu, J., Emerman, M., and Sandmeyer, S. (1997). Small heat shock protein suppression of Vpr-induced cytoskeletal defects in budding yeast. Mol Cell Biol *17*, 4033-4042.

Gunderson, K.L., and Kopito, R.R. (1995). Conformational states of CFTR associated with channel gating: the role ATP binding and hydrolysis. Cell *82*, 231-239.

Guo, P.X., and Moss, B. (1990). Interaction and mutual stabilization of the two subunits of vaccinia virus mRNA capping enzyme coexpressed in Escherichia coli. Proc Natl Acad Sci U S A *87*, 4023-4027.

Guruprasad, K., and Kumari, K. (2003). Three-dimensional models corresponding to the C-terminal domain of human alphaA- and alphaB-crystallins based on the crystal structure of the small heat-shock protein HSP16.9 from wheat. Int J Biol Macromol *33*, 107-112.

Gusarova, V., Caplan, A.J., Brodsky, J.L., and Fisher, E.A. (2001). Apoprotein B degradation is promoted by the molecular chaperones hsp90 and hsp70. J Biol Chem *276*, 24891-24900.

Haley, D.A., Bova, M.P., Huang, Q.L., McHaourab, H.S., and Stewart, P.L. (2000). Small heat-shock protein structures reveal a continuum from symmetric to variable assemblies. J Mol Biol *298*, 261-272.

Haley, D.A., Horwitz, J., and Stewart, P.L. (1998). The small heat-shock protein, alphaB-crystallin, has a variable quaternary structure. J Mol Biol *277*, 27-35.

Hall, R.A., Ostedgaard, L.S., Premont, R.T., Blitzer, J.T., Rahman, N., Welsh, M.J., and Lefkowitz, R.J. (1998). A C-terminal motif found in the beta2-adrenergic receptor, P2Y1 receptor and cystic fibrosis transmembrane conductance regulator determines binding to the Na+/H+ exchanger regulatory factor family of PDZ proteins. Proc Natl Acad Sci U S A *95*, 8496-8501.

Haslbeck, M., Braun, N., Stromer, T., Richter, B., Model, N., Weinkauf, S., and Buchner, J. (2004). Hsp42 is the general small heat shock protein in the cytosol of Saccharomyces cerevisiae. EMBO J *23*, 638-649.

Haslbeck, M., Walke, S., Stromer, T., Ehrnsperger, M., White, H.E., Chen, S., Saibil, H.R., and Buchner, J. (1999). Hsp26: a temperature-regulated chaperone. EMBO J *18*, 6744-6751.

Helfand, B.T., Chang, L., and Goldman, R.D. (2004). Intermediate filaments are dynamic and motile elements of cellular architecture. J Cell Sci *117*, 133-141.

Henics, T., Nagy, E., Oh, H.J., Csermely, P., von Gabain, A., and Subjeck, J.R. (1999). Mammalian Hsp70 and Hsp110 proteins bind to RNA motifs involved in mRNA stability. J Biol Chem *274*, 17318-17324.

Higgins, C. (1989). Transport proteins. Export-import family expands. Nature *340*, 342.

Higgins, C.F., Gallagher, M.P., Mimmack, M.L., and Pearce, S.R. (1988). A family of closely related ATP-binding subunits from prokaryotic and eukaryotic cells. Bioessays *8*, 111-116.

Hill, K., and Cooper, A.A. (2000). Degradation of unassembled Vph1p reveals novel aspects of the yeast ER quality control system. EMBO J *19*, 550-561.

Hiller, M.M., Finger, A., Schweiger, M., and Wolf, D.H. (1996). ER degradation of a misfolded luminal protein by the cytosolic ubiquitin-proteasome pathway. Science *273*, 1725-1728.

Hohfeld, J., Cyr, D.M., and Patterson, C. (2001). From the cradle to the grave: molecular chaperones that may choose between folding and degradation. EMBO Rep *2*, 885-890.

Hoover, H.E., Thuerauf, D.J., Martindale, J.J., and Glembotski, C.C. (2000). alpha B-crystallin gene induction and phosphorylation by MKK6-activated p38. A potential role for alpha B-crystallin as a target of the p38 branch of the cardiac stress response. J Biol Chem *275*, 23825-23833.

Horton, L.E., James, P., Craig, E.A., and Hensold, J.O. (2001). The yeast hsp70 homologue Ssa is required for translation and interacts with Sis1 and Pab1 on translating ribosomes. J Biol Chem *276*, 14426-14433.

Horwitz, J. (1992). Alpha-crystallin can function as a molecular chaperone. Proc Natl Acad Sci U S A *89*, 10449-10453.

Horwitz, J. (2003). Alpha-crystallin. Exp Eye Res *76*, 145-153.

Humphrey, W., Dalke, A., and Schulten, K. (1996). VMD: visual molecular dynamics. J Mol Graph *14*, 33-38, 27-38.

Hundley, H., Eisenman, H., Walter, W., Evans, T., Hotokezaka, Y., Wiedmann, M., and Craig, E. (2002). The in vivo function of the ribosome-associated Hsp70, Ssz1, does not require its putative peptide-binding domain. Proc Natl Acad Sci U S A *99*, 4203-4208.

Huyer, G., Piluek, W.F., Fansler, Z., Kreft, S.G., Hochstrasser, M., Brodsky, J.L., and Michaelis, S. (2004). Distinct machinery is required in saccharomyces cerevisiae for the endoplasmic

reticulum-associated degradation of a multispanning membrane protein and a soluble lumenal protein. J Biol Chem *279*, 38369-38378.

Ikuma, M., and Welsh, M.J. (2000). Regulation of CFTR Cl- channel gating by ATP binding and hydrolysis. Proc Natl Acad Sci U S A *97*, 8675-8680.

Imamura, T., Haruta, T., Takata, Y., Usui, I., Iwata, M., Ishihara, H., Ishiki, M., Ishibashi, O., Ueno, E., Sasaoka, T., and Kobayashi, M. (1998). Involvement of heat shock protein 90 in the degradation of mutant insulin receptors by the proteasome. J Biol Chem *273*, 11183-11188.

Ito, H., Kamei, K., Iwamoto, I., Inaguma, Y., Garcia-Mata, R., Sztul, E., and Kato, K. (2002). Inhibition of proteasomes induces accumulation, phosphorylation, and recruitment of HSP27 and alphaB-crystallin to aggresomes. J Biochem (Tokyo) *131*, 593-603.

Iwaki, T., Iwaki, A., Tateishi, J., and Goldman, J.E. (1994). Sense and antisense modification of glial alpha B-crystallin production results in alterations of stress fiber formation and thermoresistance. J Cell Biol *125*, 1385-1393.

Jacobs, J.S., Anderson, A.R., and Parker, R.P. (1998). The 3' to 5' degradation of yeast mRNAs is a general mechanism for mRNA turnover that requires the SKI2 DEVH box protein and 3' to 5' exonucleases of the exosome complex. EMBO J *17*, 1497-1506.

Jacobson, A., and Peltz, S.W. (1996). Interrelationships of the pathways of mRNA decay and translation in eukaryotic cells. Annu Rev Biochem *65*, 693-739.

Jakob, C.A., Bodmer, D., Spirig, U., Battig, P., Marcil, A., Dignard, D., Bergeron, J.J., Thomas, D.Y., and Aebi, M. (2001). Htm1p, a mannosidase-like protein, is involved in glycoprotein degradation in yeast. EMBO Rep *2*, 423-430.

Jakob, U., Gaestel, M., Engel, K., and Buchner, J. (1993). Small heat shock proteins are molecular chaperones. J Biol Chem *268*, 1517-1520.

Jensen, T.J., Loo, M.A., Pind, S., Williams, D.B., Goldberg, A.L., and Riordan, J.R. (1995). Multiple proteolytic systems, including the proteasome, contribute to CFTR processing. Cell *83*, 129-135.

Jilling, T., and Kirk, K.L. (1997). The biogenesis, traffic, and function of the cystic fibrosis transmembrane conductance regulator. Int Rev Cytol *172*, 193-241.

Johnson, A.E., and van Waes, M.A. (1999). The translocon: a dynamic gateway at the ER membrane. Annu Rev Cell Dev Biol *15*, 799-842.

Kaarniranta, K., Holmberg, C.I., Helminen, H.J., Eriksson, J.E., Sistonen, L., and Lammi, M.J. (2000). Protein synthesis is required for stabilization of hsp70 mRNA upon exposure to both hydrostatic pressurization and elevated temperature. FEBS Lett *475*, 283-286.

Kabani, M., Beckerich, J.M., and Brodsky, J.L. (2002a). Nucleotide exchange factor for the yeast Hsp70 molecular chaperone Ssa1p. Mol Cell Biol *22*, 4677-4689.

Kabani, M., Kelley, S.S., Morrow, M.W., Montgomery, D.L., Sivendran, R., Rose, M.D., Gierasch, L.M., and Brodsky, J.L. (2003). Dependence of endoplasmic reticulum-associated degradation on the peptide binding domain and concentration of BiP. Mol Biol Cell *14*, 3437-3448.

Kabani, M., McLellan, C., Raynes, D.A., Guerriero, V., and Brodsky, J.L. (2002b). HspBP1, a homologue of the yeast Fes1 and Sls1 proteins, is an Hsc70 nucleotide exchange factor. FEBS Lett *531*, 339-342.

Kalin, N., Claass, A., Sommer, M., Puchelle, E., and Tummler, B. (1999). DeltaF508 CFTR protein expression in tissues from patients with cystic fibrosis. J Clin Invest *103*, 1379-1389.

Kambacheld, M., Augustin, S., Tatsuta, T., Muller, S., and Langer, T. (2005). Role of the Novel Metallopeptidase MoP112 and Saccharolysin for the Complete Degradation of Proteins Residing in Different Subcompartments of Mitochondria. J Biol Chem *280*, 20132-20139.

Kampinga, H.H., Kanon, B., Salomons, F.A., Kabakov, A.E., and Patterson, C. (2003). Overexpression of the cochaperone CHIP enhances Hsp70-dependent folding activity in mammalian cells. Mol Cell Biol *23*, 4948-4958.

Kamradt, M.C., Chen, F., and Cryns, V.L. (2001). The small heat shock protein alpha B-crystallin negatively regulates cytochrome c- and caspase-8-dependent activation of caspase-3 by inhibiting its autoproteolytic maturation. J Biol Chem *276*, 16059-16063.

Kamradt, M.C., Chen, F., Sam, S., and Cryns, V.L. (2002). The small heat shock protein alpha B-crystallin negatively regulates apoptosis during myogenic differentiation by inhibiting caspase-3 activation. J Biol Chem *277*, 38731-38736.

Kamradt, M.C., Lu, M., Werner, M.E., Kwan, T., Chen, F., Strohecker, A., Oshita, S., Wilkinson, J.C., Yu, C., Oliver, P.G., Duckett, C.S., Buchsbaum, D.J., LoBuglio, A.F., Jordan, V.C., and Cryns, V.L. (2005). The small heat shock protein alpha B-crystallin is a novel inhibitor of TRAIL-induced apoptosis that suppresses the activation of caspase-3. J Biol Chem *280*, 11059-11066.

Kanelakis, K.C., Morishima, Y., Dittmar, K.D., Galigniana, M.D., Takayama, S., Reed, J.C., and Pratt, W.B. (1999). Differential effects of the hsp70-binding protein BAG-1 on glucocorticoid receptor folding by the hsp90-based chaperone machinery. J Biol Chem *274*, 34134-34140.

Kappe, G., Franck, E., Verschuure, P., Boelens, W.C., Leunissen, J.A., and de Jong, W.W. (2003). The human genome encodes 10 alpha-crystallin-related small heat shock proteins: HspB1-10. Cell Stress Chaperones *8*, 53-61.

Kartner, N., Augustinas, O., Jensen, T.J., Naismith, A.L., and Riordan, J.R. (1992). Mislocalization of delta F508 CFTR in cystic fibrosis sweat gland. Nat Genet *1*, 321-327.

Kato, K., Ito, H., Kamei, K., Inaguma, Y., Iwamoto, I., and Saga, S. (1998). Phosphorylation of alphaB-crystallin in mitotic cells and identification of enzymatic activities responsible for phosphorylation. J Biol Chem *273*, 28346-28354.

Keenan, R.J., Freymann, D.M., Stroud, R.M., and Walter, P. (2001). The signal recognition particle. Annu Rev Biochem *70*, 755-775.

Keller, G., Ray, E., Brown, P.O., and Winge, D.R. (2001). Haa1, a protein homologous to the copper-regulated transcription factor Ace1, is a novel transcriptional activator. J Biol Chem *276*, 38697-38702.

Kelley, W.L. (1998). The J-domain family and the recruitment of chaperone power. Trends Biochem Sci *23*, 222-227.

Kerem, B., Rommens, J.M., Buchanan, J.A., Markiewicz, D., Cox, T.K., Chakravarti, A., Buchwald, M., and Tsui, L.C. (1989). Identification of the cystic fibrosis gene: genetic analysis. Science *245*, 1073-1080.

Kim, K.K., Kim, R., and Kim, S.H. (1998a). Crystal structure of a small heat-shock protein. Nature *394*, 595-599.

Kim, S., Schilke, B., Craig, E.A., and Horwich, A.L. (1998b). Folding in vivo of a newly translated yeast cytosolic enzyme is mediated by the SSA class of cytosolic yeast Hsp70 proteins. Proc Natl Acad Sci U S A *95*, 12860-12865.

Kimura, Y., Yahara, I., and Lindquist, S. (1995). Role of the protein chaperone YDJ1 in establishing Hsp90-mediated signal transduction pathways. Science *268*, 1362-1365.

Kiser, G.L., Gentzsch, M., Kloser, A.K., Balzi, E., Wolf, D.H., Goffeau, A., and Riordan, J.R. (2001). Expression and degradation of the cystic fibrosis transmembrane conductance regulator in Saccharomyces cerevisiae. Arch Biochem Biophys *390*, 195-205.

Knittler, M.R., Dirks, S., and Haas, I.G. (1995). Molecular chaperones involved in protein degradation in the endoplasmic reticulum: quantitative interaction of the heat shock cognate protein BiP with partially folded immunoglobulin light chains that are degraded in the endoplasmic reticulum. Proc Natl Acad Sci U S A *92*, 1764-1768.

Knop, M., Finger, A., Braun, T., Hellmuth, K., and Wolf, D.H. (1996). Der1, a novel protein specifically required for endoplasmic reticulum degradation in yeast. EMBO J *15*, 753-763.

Kopito, R.R. (1999). Biosynthesis and degradation of CFTR. Physiol Rev *79*, S167-173.

Kostova, Z., and Wolf, D.H. (2003). For whom the bell tolls: protein quality control of the endoplasmic reticulum and the ubiquitin-proteasome connection. EMBO J *22*, 2309-2317.

Kreda, S.M., Mall, M., Mengos, A., Rochelle, L., Yankaskas, J., Riordan, J.R., and Boucher, R.C. (2005). Characterization of wild-type and {delta}f508 cystic fibrosis transmembrane regulator in human respiratory epithelia. Mol Biol Cell *16*, 2154-2167.

Kuchler, K., Sterne, R.E., and Thorner, J. (1989). Saccharomyces cerevisiae STE6 gene product: a novel pathway for protein export in eukaryotic cells. EMBO J *8*, 3973-3984.

LaGrandeur, T.E., and Parker, R. (1998). Isolation and characterization of Dcp1p, the yeast mRNA decapping enzyme. EMBO J *17*, 1487-1496.

Lam, Y.A., Lawson, T.G., Velayutham, M., Zweier, J.L., and Pickart, C.M. (2002). A proteasomal ATPase subunit recognizes the polyubiquitin degradation signal. Nature *416*, 763-767.

Lander, E.S., Linton, L.M., Birren, B., Nusbaum, C., Zody, M.C., Baldwin, J., Devon, K., Dewar, K., Doyle, M., FitzHugh, W., Funke, R., Gage, D., Harris, K., Heaford, A., Howland, J., Kann, L., Lehoczky, J., LeVine, R., McEwan, P., McKernan, K., Meldrim, J., Mesirov, J.P., Miranda, C., Morris, W., Naylor, J., Raymond, C., Rosetti, M., Santos, R., Sheridan, A., Sougnez, C., Stange-Thomann, N., Stojanovic, N., Subramanian, A., Wyman, D., Rogers, J., Sulston, J., Ainscough, R., Beck, S., Bentley, D., Burton, J., Clee, C., Carter, N., Coulson, A., Deadman, R., Deloukas, P., Dunham, A., Dunham, I., Durbin, R., French, L., Grafham, D., Gregory, S., Hubbard, T., Humphray, S., Hunt, A., Jones, M., Lloyd, C., McMurray, A., Matthews, L., Mercer, S., Milne, S., Mullikin, J.C., Mungall, A., Plumb, R., Ross, M., Shownkeen, R., Sims, S., Waterston, R.H., Wilson, R.K., Hillier, L.W., McPherson, J.D., Marra, M.A., Mardis, E.R., Fulton, L.A., Chinwalla, A.T., Pepin, K.H., Gish, W.R., Chissoe, S.L., Wendl, M.C., Delehaunty, K.D., Miner, T.L., Delehaunty, A., Kramer, J.B., Cook, L.L., Fulton, R.S., Johnson, D.L., Minx, P.J., Clifton, S.W., Hawkins, T., Branscomb, E., Predki, P., Richardson, P., Wenning, S., Slezak, T., Doggett, N., Cheng, J.F., Olsen, A., Lucas, S., Elkin, C., Uberbacher, E., Frazier, M., Gibbs, R.A., Muzny, D.M., Scherer, S.E., Bouck, J.B., Sodergren, E.J., Worley, K.C., Rives, C.M., Gorrell, J.H., Metzker, M.L., Naylor, S.L., Kucherlapati, R.S., Nelson, D.L., Weinstock, G.M., Sakaki, Y., Fujiyama, A., Hattori, M., Yada, T., Toyoda, A., Itoh, T., Kawagoe, C., Watanabe, H., Totoki, Y., Taylor, T., Weissenbach, J., Heilig, R., Saurin, W., Artiguenave, F., Brottier, P., Bruls, T., Pelletier, E., Robert, C., Wincker, P., Smith, D.R., Doucette-Stamm, L., Rubenfield, M., Weinstock, K., Lee, H.M., Dubois, J., Rosenthal, A., Platzer, M., Nyakatura, G., Taudien, S., Rump, A., Yang, H., Yu, J., Wang, J., Huang, G., Gu, J., Hood, L., Rowen, L., Madan, A., Qin, S., Davis, R.W., Federspiel, N.A., Abola, A.P., Proctor, M.J., Myers, R.M., Schmutz, J., Dickson, M., Grimwood, J., Cox, D.R., Olson, M.V., Kaul, R., Raymond, C., Shimizu, N., Kawasaki, K., Minoshima, S., Evans, G.A., Athanasiou, M., Schultz,

R., Roe, B.A., Chen, F., Pan, H., Ramser, J., Lehrach, H., Reinhardt, R., McCombie, W.R., de la Bastide, M., Dedhia, N., Blocker, H., Hornischer, K., Nordsiek, G., Agarwala, R., Aravind, L., Bailey, J.A., Bateman, A., Batzoglou, S., Birney, E., Bork, P., Brown, D.G., Burge, C.B., Cerutti, L., Chen, H.C., Church, D., Clamp, M., Copley, R.R., Doerks, T., Eddy, S.R., Eichler, E.E., Furey, T.S., Galagan, J., Gilbert, J.G., Harmon, C., Hayashizaki, Y., Haussler, D., Hermjakob, H., Hokamp, K., Jang, W., Johnson, L.S., Jones, T.A., Kasif, S., Kaspryzk, A., Kennedy, S., Kent, W.J., Kitts, P., Koonin, E.V., Korf, I., Kulp, D., Lancet, D., Lowe, T.M., McLysaght, A., Mikkelsen, T., Moran, J.V., Mulder, N., Pollara, V.J., Ponting, C.P., Schuler, G., Schultz, J., Slater, G., Smit, A.F., Stupka, E., Szustakowski, J., Thierry-Mieg, D., Thierry-Mieg, J., Wagner, L., Wallis, J., Wheeler, R., Williams, A., Wolf, Y.I., Wolfe, K.H., Yang, S.P., Yeh, R.F., Collins, F., Guyer, M.S., Peterson, J., Felsenfeld, A., Wetterstrand, K.A., Patrinos, A., Morgan, M.J., de Jong, P., Catanese, J.J., Osoegawa, K., Shizuya, H., Choi, S., and Chen, Y.J. (2001). Initial sequencing and analysis of the human genome. Nature *409*, 860-921.

Laroia, G., Cuesta, R., Brewer, G., and Schneider, R.J. (1999). Control of mRNA decay by heat shock-ubiquitin-proteasome pathway. Science *284*, 499-502.

Lavoie, J.N., Gingras-Breton, G., Tanguay, R.M., and Landry, J. (1993a). Induction of Chinese hamster HSP27 gene expression in mouse cells confers resistance to heat shock. HSP27 stabilization of the microfilament organization. J Biol Chem *268*, 3420-3429.

Lavoie, J.N., Hickey, E., Weber, L.A., and Landry, J. (1993b). Modulation of actin microfilament dynamics and fluid phase pinocytosis by phosphorylation of heat shock protein 27. J Biol Chem *268*, 24210-24214.

Lawson, B., Brewer, J.W., and Hendershot, L.M. (1998). Geldanamycin, an hsp90/GRP94-binding drug, induces increased transcription of endoplasmic reticulum (ER) chaperones via the ER stress pathway. J Cell Physiol *174*, 170-178.

Lee, C., Schwartz, M.P., Prakash, S., Iwakura, M., and Matouschek, A. (2001). ATP-dependent proteases degrade their substrates by processively unraveling them from the degradation signal. Mol Cell *7*, 627-637.

Lee, G.J., Pokala, N., and Vierling, E. (1995). Structure and in vitro molecular chaperone activity of cytosolic small heat shock proteins from pea. J Biol Chem *270*, 10432-10438.

Lee, G.J., Roseman, A.M., Saibil, H.R., and Vierling, E. (1997). A small heat shock protein stably binds heat-denatured model substrates and can maintain a substrate in a folding-competent state. EMBO J *16*, 659-671.

Lee, R.J., Liu, C.W., Harty, C., McCracken, A.A., Latterich, M., Romisch, K., DeMartino, G.N., Thomas, P.J., and Brodsky, J.L. (2004). Uncoupling retro-translocation and degradation in the ER-associated degradation of a soluble protein. EMBO J *23*, 2206-2215.

Lenk, U., Yu, H., Walter, J., Gelman, M.S., Hartmann, E., Kopito, R.R., and Sommer, T. (2002). A role for mammalian Ubc6 homologues in ER-associated protein degradation. J Cell Sci *115*, 3007-3014.

Leroux, M.R., Ma, B.J., Batelier, G., Melki, R., and Candido, E.P. (1997). Unique structural features of a novel class of small heat shock proteins. J Biol Chem *272*, 12847-12853.

Letourneur, F., Gaynor, E.C., Hennecke, S., Demolliere, C., Duden, R., Emr, S.D., Riezman, H., and Cosson, P. (1994). Coatomer is essential for retrieval of dilysine-tagged proteins to the endoplasmic reticulum. Cell *79*, 1199-1207.

Lewis, H.A., Buchanan, S.G., Burley, S.K., Conners, K., Dickey, M., Dorwart, M., Fowler, R., Gao, X., Guggino, W.B., Hendrickson, W.A., Hunt, J.F., Kearins, M.C., Lorimer, D., Maloney, P.C., Post, K.W., Rajashankar, K.R., Rutter, M.E., Sauder, J.M., Shriver, S., Thibodeau, P.H.,

Thomas, P.J., Zhang, M., Zhao, X., and Emtage, S. (2004). Structure of nucleotide-binding domain 1 of the cystic fibrosis transmembrane conductance regulator. EMBO J *23*, 282-293.

Lilley, B.N., and Ploegh, H.L. (2004). A membrane protein required for dislocation of misfolded proteins from the ER. Nature *429*, 834-840.

Lindner, R.A., Carver, J.A., Ehrnsperger, M., Buchner, J., Esposito, G., Behlke, J., Lutsch, G., Kotlyarov, A., and Gaestel, M. (2000). Mouse Hsp25, a small shock protein. The role of its C-terminal extension in oligomerization and chaperone action. Eur J Biochem *267*, 1923-1932.

Litt, M., Kramer, P., LaMorticella, D.M., Murphey, W., Lovrien, E.W., and Weleber, R.G. (1998). Autosomal dominant congenital cataract associated with a missense mutation in the human alpha crystallin gene CRYAA. Hum Mol Genet *7*, 471-474.

Liu, B., Bhat, M., and Nagaraj, R.H. (2004a). AlphaB-crystallin inhibits glucose-induced apoptosis in vascular endothelial cells. Biochem Biophys Res Commun *321*, 254-258.

Liu, C.W., Corboy, M.J., DeMartino, G.N., and Thomas, P.J. (2003). Endoproteolytic activity of the proteasome. Science *299*, 408-411.

Liu, C.W., Millen, L., Roman, T.B., Xiong, H., Gilbert, H.F., Noiva, R., DeMartino, G.N., and Thomas, P.J. (2002). Conformational remodeling of proteasomal substrates by PA700, the 19 S regulatory complex of the 26 S proteasome. J Biol Chem *277*, 26815-26820.

Liu, J.P., Schlosser, R., Ma, W.Y., Dong, Z., Feng, H., Lui, L., Huang, X.Q., Liu, Y., and Li, D.W. (2004b). Human alphaA- and alphaB-crystallins prevent UVA-induced apoptosis through regulation of PKCalpha, RAF/MEK/ERK and AKT signaling pathways. Exp Eye Res *79*, 393-403.

Liu, X.D., Morano, K.A., and Thiele, D.J. (1999). The yeast Hsp110 family member, Sse1, is an Hsp90 cochaperone. J Biol Chem *274*, 26654-26660.

Loayza, D., Tam, A., Schmidt, W.K., and Michaelis, S. (1998). Ste6p mutants defective in exit from the endoplasmic reticulum (ER) reveal aspects of an ER quality control pathway in Saccharomyces cerevisiae. Mol Biol Cell *9*, 2767-2784.

Loo, M.A., Jensen, T.J., Cui, L., Hou, Y., Chang, X.B., and Riordan, J.R. (1998). Perturbation of Hsp90 interaction with nascent CFTR prevents its maturation and accelerates its degradation by the proteasome. EMBO J *17*, 6879-6887.

Loo, T.W., and Clarke, D.M. (1997). Correction of defective protein kinesis of human P-glycoprotein mutants by substrates and modulators. J Biol Chem *272*, 709-712.

Luders, J., Demand, J., Papp, O., and Hohfeld, J. (2000). Distinct isoforms of the cofactor BAG-1 differentially affect Hsc70 chaperone function. J Biol Chem *275*, 14817-14823.

Luirink, J., and Sinning, I. (2004). SRP-mediated protein targeting: structure and function revisited. Biochim Biophys Acta *1694*, 17-35.

Lukacs, G.L., Mohamed, A., Kartner, N., Chang, X.B., Riordan, J.R., and Grinstein, S. (1994). Conformational maturation of CFTR but not its mutant counterpart (delta F508) occurs in the endoplasmic reticulum and requires ATP. EMBO J *13*, 6076-6086.

Luo, Y., Mao, X., Deng, L., Cong, P., and Shuman, S. (1995). The D1 and D12 subunits are both essential for the transcription termination factor activity of vaccinia virus capping enzyme. J Virol *69*, 3852-3856.

Ma, T., Vetrivel, L., Yang, H., Pedemonte, N., Zegarra-Moran, O., Galietta, L.J., and Verkman, A.S. (2002). High-affinity activators of cystic fibrosis transmembrane conductance regulator

(CFTR) chloride conductance identified by high-throughput screening. J Biol Chem *277*, 37235-37241.

Mao, Y.W., Liu, J.P., Xiang, H., and Li, D.W. (2004). Human alphaA- and alphaB-crystallins bind to Bax and Bcl-X(S) to sequester their translocation during staurosporine-induced apoptosis. Cell Death Differ *11*, 512-526.

Marcu, M.G., Chadli, A., Bouhouche, I., Catelli, M., and Neckers, L.M. (2000). The heat shock protein 90 antagonist novobiocin interacts with a previously unrecognized ATP-binding domain in the carboxyl terminus of the chaperone. J Biol Chem *275*, 37181-37186.

McCarty, J.S., Buchberger, A., Reinstein, J., and Bukau, B. (1995). The role of ATP in the functional cycle of the DnaK chaperone system. J Mol Biol *249*, 126-137.

McCarty, N.A. (2000). Permeation through the CFTR chloride channel. J Exp Biol *203*, 1947-1962.

McClellan, A.J., and Brodsky, J.L. (2000). Mutation of the ATP-binding pocket of SSA1 indicates that a functional interaction between Ssa1p and Ydj1p is required for post-translational translocation into the yeast endoplasmic reticulum. Genetics *156*, 501-512.

McClellan, A.J., Endres, J.B., Vogel, J.P., Palazzi, D., Rose, M.D., and Brodsky, J.L. (1998). Specific molecular chaperone interactions and an ATP-dependent conformational change are required during posttranslational protein translocation into the yeast ER. Mol Biol Cell *9*, 3533-3545.

McCracken, A.A., and Brodsky, J.L. (2003). Evolving questions and paradigm shifts in endoplasmic-reticulum-associated degradation (ERAD). Bioessays *25*, 868-877.

Meacham, G.C., Lu, Z., King, S., Sorscher, E., Tousson, A., and Cyr, D.M. (1999). The Hdj-2/Hsc70 chaperone pair facilitates early steps in CFTR biogenesis. EMBO J *18*, 1492-1505.

Meacham, G.C., Patterson, C., Zhang, W., Younger, J.M., and Cyr, D.M. (2001). The Hsc70 co-chaperone CHIP targets immature CFTR for proteasomal degradation. Nat Cell Biol *3*, 100-105.

Merck, K.B., Groenen, P.J., Voorter, C.E., de Haard-Hoekman, W.A., Horwitz, J., Bloemendal, H., and de Jong, W.W. (1993). Structural and functional similarities of bovine alpha-crystallin and mouse small heat-shock protein. A family of chaperones. J Biol Chem *268*, 1046-1052.

Merlie, J.P., and Lindstrom, J. (1983). Assembly in vivo of mouse muscle acetylcholine receptor: identification of an alpha subunit species that may be an assembly intermediate. Cell *34*, 747-757.

Milarski, K.L., and Morimoto, R.I. (1989). Mutational analysis of the human HSP70 protein: distinct domains for nucleolar localization and adenosine triphosphate binding. J Cell Biol *109*, 1947-1962.

Miron, T., Vancompernolle, K., Vandekerckhove, J., Wilchek, M., and Geiger, B. (1991). A 25-kD inhibitor of actin polymerization is a low molecular mass heat shock protein. J Cell Biol *114*, 255-261.

Molinari, M., Calanca, V., Galli, C., Lucca, P., and Paganetti, P. (2003). Role of EDEM in the release of misfolded glycoproteins from the calnexin cycle. Science *299*, 1397-1400.

Morrison, L.E., Hoover, H.E., Thuerauf, D.J., and Glembotski, C.C. (2003). Mimicking phosphorylation of alphaB-crystallin on serine-59 is necessary and sufficient to provide maximal protection of cardiac myocytes from apoptosis. Circ Res *92*, 203-211.

Muchowski, P.J., Bassuk, J.A., Lubsen, N.H., and Clark, J.I. (1997). Human alphaB-crystallin. Small heat shock protein and molecular chaperone. J Biol Chem *272*, 2578-2582.

Muchowski, P.J., and Clark, J.I. (1998). ATP-enhanced molecular chaperone functions of the small heat shock protein human alphaB crystallin. Proc Natl Acad Sci U S A *95*, 1004-1009.

Muhlrad, D., Decker, C.J., and Parker, R. (1994). Deadenylation of the unstable mRNA encoded by the yeast MFA2 gene leads to decapping followed by 5'-->3' digestion of the transcript. Genes Dev *8*, 855-866.

Muhlrad, D., Decker, C.J., and Parker, R. (1995). Turnover mechanisms of the stable yeast PGK1 mRNA. Mol Cell Biol *15*, 2145-2156.

Muhlrad, D., and Parker, R. (1994). Premature translational termination triggers mRNA decapping. Nature *370*, 578-581.

Mukai, H., Kuno, T., Tanaka, H., Hirata, D., Miyakawa, T., and Tanaka, C. (1993). Isolation and characterization of SSE1 and SSE2, new members of the yeast HSP70 multigene family. Gene *132*, 57-66.

Murata, S., Minami, Y., Minami, M., Chiba, T., and Tanaka, K. (2001). CHIP is a chaperone-dependent E3 ligase that ubiquitylates unfolded protein. EMBO Rep *2*, 1133-1138.

Nakatsukasa, K., Nishikawa, S., Hosokawa, N., Nagata, K., and Endo, T. (2001). Mnl1p, an alpha -mannosidase-like protein in yeast Saccharomyces cerevisiae, is required for endoplasmic reticulum-associated degradation of glycoproteins. J Biol Chem *276*, 8635-8638.

Narberhaus, F. (2002). Alpha-crystallin-type heat shock proteins: socializing minichaperones in the context of a multichaperone network. Microbiol Mol Biol Rev *66*, 64-93; table of contents.

Nelson, R.J., Ziegelhoffer, T., Nicolet, C., Werner-Washburne, M., and Craig, E.A. (1992). The translation machinery and 70 kd heat shock protein cooperate in protein synthesis. Cell *71*, 97-105.

Ng, D.T., Spear, E.D., and Walter, P. (2000). The unfolded protein response regulates multiple aspects of secretory and membrane protein biogenesis and endoplasmic reticulum quality control. J Cell Biol *150*, 77-88.

Nicholl, I.D., and Quinlan, R.A. (1994). Chaperone activity of alpha-crystallins modulates intermediate filament assembly. EMBO J *13*, 945-953.

Nishikawa, S.I., Fewell, S.W., Kato, Y., Brodsky, J.L., and Endo, T. (2001). Molecular chaperones in the yeast endoplasmic reticulum maintain the solubility of proteins for retrotranslocation and degradation. J Cell Biol *153*, 1061-1070.

Norkina, O., Kaur, S., Ziemer, D., and De Lisle, R.C. (2004). Inflammation of the cystic fibrosis mouse small intestine. Am J Physiol Gastrointest Liver Physiol *286*, G1032-1041.

Oda, Y., Hosokawa, N., Wada, I., and Nagata, K. (2003). EDEM as an acceptor of terminally misfolded glycoproteins released from calnexin. Science *299*, 1394-1397.

Oh, H.J., Chen, X., and Subjeck, J.R. (1997). Hsp110 protects heat-denatured proteins and confers cellular thermoresistance. J Biol Chem *272*, 31636-31640.

Oh, H.J., Easton, D., Murawski, M., Kaneko, Y., and Subjeck, J.R. (1999). The chaperoning activity of hsp110. Identification of functional domains by use of targeted deletions. J Biol Chem *274*, 15712-15718.

Okiyoneda, T., Harada, K., Takeya, M., Yamahira, K., Wada, I., Shuto, T., Suico, M.A., Hashimoto, Y., and Kai, H. (2004). Delta F508 CFTR pool in the endoplasmic reticulum is increased by calnexin overexpression. Mol Biol Cell *15*, 563-574.

Palmer, E.A., Kruse, K.B., Fewell, S.W., Buchanan, S.M., Brodsky, J.L., and McCracken,A.A. (2003). Differential requirements of novel A1PiZ degradation deficient (*ADD*) genes in ER-associated protein degradation. J Cell Sci *116*, 2361-2373.

Parcellier, A., Schmitt, E., Gurbuxani, S., Seigneurin-Berny, D., Pance, A., Chantome, A., Plenchette, S., Khochbin, S., Solary, E., and Garrido, C. (2003). HSP27 is a ubiquitin-binding protein involved in I-kappaBalpha proteasomal degradation. Mol Cell Biol *23*, 5790-5802.

Parker, R., Herrick, D., Peltz, S.W., and Jacobson, A. (1991). Measurement of mRNA decay rates in Saccharomyces cerevisiae. Methods Enzymol *194*, 415-423.

Peng, J., Schwartz, D., Elias, J.E., Thoreen, C.C., Cheng, D., Marsischky, G., Roelofs, J., Finley, D., and Gygi, S.P. (2003). A proteomics approach to understanding protein ubiquitination. Nat Biotechnol *21*, 921-926.

Perng, M.D., Cairns, L., van den, I.P., Prescott, A., Hutcheson, A.M., and Quinlan, R.A. (1999). Intermediate filament interactions can be altered by HSP27 and alphaB-crystallin. J Cell Sci *112*, 2099-2112.

Perng, M.D., Wen, S.F., van den, I.P., Prescott, A.R., and Quinlan, R.A. (2004). Desmin aggregate formation by R120G alphaB-crystallin is caused by altered filament interactions and is dependent upon network status in cells. Mol Biol Cell *15*, 2335-2346.

Pfund, C., Lopez-Hoyo, N., Ziegelhoffer, T., Schilke, B.A., Lopez-Buesa, P., Walter, W.A., Wiedmann, M., and Craig, E.A. (1998). The molecular chaperone Ssb from Saccharomyces cerevisiae is a component of the ribosome-nascent chain complex. EMBO J *17*, 3981-3989.

Pickart, C.M. (2004). Back to the future with ubiquitin. Cell *116*, 181-190.

Pind, S., Riordan, J.R., and Williams, D.B. (1994). Participation of the endoplasmic reticulum chaperone calnexin (p88, IP90) in the biogenesis of the cystic fibrosis transmembrane conductance regulator. J Biol Chem *269*, 12784-12788.

Piotrowicz, R.S., and Levin, E.G. (1997). Basolateral membrane-associated 27-kDa heat shock protein and microfilament polymerization. J Biol Chem *272*, 25920-25927.

Plemper, R.K., Bohmler, S., Bordallo, J., Sommer, T., and Wolf, D.H. (1997). Mutant analysis links the translocon and BiP to retrograde protein transport for ER degradation. Nature *388*, 891-895.

Pratt, W.B., and Toft, D.O. (2003). Regulation of signaling protein function and trafficking by the hsp90/hsp70-based chaperone machinery. Exp Biol Med (Maywood) *228*, 111-133.

Preiss, T., and Hentze, M.W. (1998). Dual function of the messenger RNA cap structure in poly(A)-tail- promoted translation in yeast. Nature *392*, 516-520.

Prince, L.S., Karp, P.H., Moninger, T.O., and Welsh, M.J. (2001). KGF alters gene expression in human airway epithelia: potential regulation of the inflammatory response. Physiol Genomics *6*, 81-89.

Prodromou, C., Panaretou, B., Chohan, S., Siligardi, G., O'Brien, R., Ladbury, J.E., Roe, S.M., Piper, P.W., and Pearl, L.H. (2000). The ATPase cycle of Hsp90 drives a molecular 'clamp' via transient dimerization of the N-terminal domains. EMBO J *19*, 4383-4392.

Prodromou, C., Roe, S.M., O'Brien, R., Ladbury, J.E., Piper, P.W., and Pearl, L.H. (1997). Identification and structural characterization of the ATP/ADP-binding site in the Hsp90 molecular chaperone. Cell *90*, 65-75.

Qian, X., Hou, W., Zhengang, L., and Sha, B. (2002). Direct interactions between molecular chaperones heat-shock protein (Hsp) 70 and Hsp40: yeast Hsp70 Ssa1 binds the extreme C-terminal region of yeast Hsp40 Sis1. Biochem J *361*, 27-34.

Qu, B.H., Strickland, E.H., and Thomas, P.J. (1997). Localization and suppression of a kinetic defect in cystic fibrosis transmembrane conductance regulator folding. J Biol Chem *272*, 15739-15744.

Qu, B.H., and Thomas, P.J. (1996). Alteration of the cystic fibrosis transmembrane conductance regulator folding pathway. J Biol Chem *271*, 7261-7264.

Quinlan, R.A., Carte, J.M., Sandilands, A., and Prescott, A.R. (1996). The beaded filament of the eye lens: an unexpected key to intermediate filament structure and function. Trends Cell Biol *6*, 123-126.

Rahman, D.R., Bentley, N.J., and Tuite, M.F. (1995). The Saccharomyces cerevisiae small heat shock protein Hsp26 inhibits actin polymerisation. Biochem Soc Trans *23*, 77S.

Ramirez, C.V., Vilela, C., Berthelot, K., and McCarthy, J.E. (2002). Modulation of eukaryotic mRNA stability via the cap-binding translation complex eIF4F. J Mol Biol *318*, 951-962.

Rapoport, T.A., Matlack, K.E., Plath, K., Misselwitz, B., and Staeck, O. (1999). Posttranslational protein translocation across the membrane of the endoplasmic reticulum. Biol Chem *380*, 1143-1150.

Richter-Landsberg, C., and Bauer, N.G. (2004). Tau-inclusion body formation in oligodendroglia: the role of stress proteins and proteasome inhibition. Int J Dev Neurosci *22*, 443-451.

Richter, K., and Buchner, J. (2001). Hsp90: chaperoning signal transduction. J Cell Physiol *188*, 281-290.

Riordan, J.R. (1999). Cystic fibrosis as a disease of misprocessing of the cystic fibrosis transmembrane conductance regulator glycoprotein. Am J Hum Genet *64*, 1499-1504.

Riordan, J.R. (2005). Assembly of functional CFTR chloride channels. Annu Rev Physiol *67*, 701-718.

Riordan, J.R., Rommens, J.M., Kerem, B., Alon, N., Rozmahel, R., Grzelczak, Z., Zielenski, J., Lok, S., Plavsic, N., Chou, J.L., and et al. (1989). Identification of the cystic fibrosis gene: cloning and characterization of complementary DNA. Science *245*, 1066-1073.

Robinson, J.S., Klionsky, D.J., Banta, L.M., and Emr, S.D. (1988). Protein sorting in Saccharomyces cerevisiae: isolation of mutants defective in the delivery and processing of multiple vacuolar hydrolases. Mol Cell Biol *8*, 4936-4948.

Romisch, K. (1999). Surfing the Sec61 channel: bidirectional protein translocation across the ER membrane. J Cell Sci *112*, 4185-4191.

Rose, M.D., Winston, F., and Hieter, P. (1990). Methods in Yeast Genetics: A Laboratory Course Manual. Cold Spring Habor Laboratory Press: Cold Spring Habor, NY.

Ross, A.F., Rapuano, M., Schmidt, J.H., and Prives, J.M. (1987). Phosphorylation and assembly of nicotinic acetylcholine receptor subunits in cultured chick muscle cells. J Biol Chem *262*, 14640-14647.

Rubenstein, R.C., Egan, M.E., and Zeitlin, P.L. (1997). In vitro pharmacologic restoration of CFTR-mediated chloride transport with sodium 4-phenylbutyrate in cystic fibrosis epithelial cells containing delta F508-CFTR. J Clin Invest *100*, 2457-2465.

Rubenstein, R.C., and Zeitlin, P.L. (1998). A pilot clinical trial of oral sodium 4-phenylbutyrate (Buphenyl) in deltaF508-homozygous cystic fibrosis patients: partial restoration of nasal epithelial CFTR function. Am J Respir Crit Care Med *157*, 484-490.

Rubenstein, R.C., and Zeitlin, P.L. (2000). Sodium 4-phenylbutyrate downregulates Hsc70: implications for intracellular trafficking of DeltaF508-CFTR. Am J Physiol Cell Physiol *278*, C259-267.

Rudiger, S., Schneider-Mergener, J., and Bukau, B. (2001). Its substrate specificity characterizes the DnaJ co-chaperone as a scanning factor for the DnaK chaperone. EMBO J *20*, 1042-1050.

Sales, K., Brandt, W., Rumbak, E., and Lindsey, G. (2000). The LEA-like protein HSP 12 in Saccharomyces cerevisiae has a plasma membrane location and protects membranes against desiccation and ethanol-induced stress. Biochim Biophys Acta *1463*, 267-278.

Sanders, S.L., Whitfield, K.M., Vogel, J.P., Rose, M.D., and Schekman, R.W. (1992). Sec61p and BiP directly facilitate polypeptide translocation into the ER. Cell *69*, 353-365.

Sato, S., Ward, C.L., Krouse, M.E., Wine, J.J., and Kopito, R.R. (1996). Glycerol reverses the misfolding phenotype of the most common cystic fibrosis mutation. J Biol Chem *271*, 635-638.

Schmid, D., Baici, A., Gehring, H., and Christen, P. (1994). Kinetics of molecular chaperone action. Science *263*, 971-973.

Schneider, C., Sepp-Lorenzino, L., Nimmesgern, E., Ouerfelli, O., Danishefsky, S., Rosen, N., and Hartl, F.U. (1996). Pharmacologic shifting of a balance between protein refolding and degradation mediated by Hsp90. Proc Natl Acad Sci U S A *93*, 14536-14541.

Schutte, B., Henfling, M., Kolgen, W., Bouman, M., Meex, S., Leers, M.P., Nap, M., Bjorklund, V., Bjorklund, P., Bjorklund, B., Lane, E.B., Omary, M.B., Jornvall, H., and Ramaekers, F.C. (2004). Keratin 8/18 breakdown and reorganization during apoptosis. Exp Cell Res *297*, 11-26.

Schwartz, D.C., and Parker, R. (1999). Mutations in translation initiation factors lead to increased rates of deadenylation and decapping of mRNAs in Saccharomyces cerevisiae. Mol Cell Biol *19*, 5247-5256.

Schwartz, D.C., and Parker, R. (2000). mRNA decapping in yeast requires dissociation of the cap binding protein, eukaryotic translation initiation factor 4E. Mol Cell Biol *20*, 7933-7942.

Sharma, M., Benharouga, M., Hu, W., and Lukacs, G.L. (2001). Conformational and temperature-sensitive stability defects of the delta F508 cystic fibrosis transmembrane conductance regulator in post-endoplasmic reticulum compartments. J Biol Chem *276*, 8942-8950.

Sharma, M., Pampinella, F., Nemes, C., Benharouga, M., So, J., Du, K., Bache, K.G., Papsin, B., Zerangue, N., Stenmark, H., and Lukacs, G.L. (2004). Misfolding diverts CFTR from recycling to degradation: quality control at early endosomes. J Cell Biol *164*, 923-933.

Shearstone, J.R., and Baneyx, F. (1999). Biochemical characterization of the small heat shock protein IbpB from Escherichia coli. J Biol Chem *274*, 9937-9945.

Shirayama, M., Kawakami, K., Matsui, Y., Tanaka, K., and Toh-e, A. (1993). MSI3, a multicopy suppressor of mutants hyperactivated in the RAS-cAMP pathway, encodes a novel HSP70 protein of Saccharomyces cerevisiae. Mol Gen Genet *240*, 323-332.

Shomura, Y., Dragovic, Z., Chang, H.C., Tzvetkov, N., Young, J.C., Brodsky, J.L., Guerriero, V., Hartl, F.U., and Bracher, A. (2005). Regulation of Hsp70 function by HspBP1: structural analysis reveals an alternate mechanism for Hsp70 nucleotide exchange. Mol Cell *17*, 367-379.

Short, D.B., Trotter, K.W., Reczek, D., Kreda, S.M., Bretscher, A., Boucher, R.C., Stutts, M.J., and Milgram, S.L. (1998). An apical PDZ protein anchors the cystic fibrosis transmembrane conductance regulator to the cytoskeleton. J Biol Chem *273*, 19797-19801.

Shuman, S. (1990). Catalytic activity of vaccinia mRNA capping enzyme subunits coexpressed in Escherichia coli. J Biol Chem *265*, 11960-11966.

Smykal, P., Masin, J., Hrdy, I., Konopasek, I., and Zarsky, V. (2000). Chaperone activity of tobacco HSP18, a small heat-shock protein, is inhibited by ATP. Plant J *23*, 703-713.

Sondermann, H., Ho, A.K., Listenberger, L.L., Siegers, K., Moarefi, I., Wente, S.R., Hartl, F.U., and Young, J.C. (2002). Prediction of novel Bag-1 homologs based on structure/function analysis identifies Snl1p as an Hsp70 co-chaperone in Saccharomyces cerevisiae. J Biol Chem *277*, 33220-33227.

Sondermann, H., Scheufler, C., Schneider, C., Hohfeld, J., Hartl, F.U., and Moarefi, I. (2001). Structure of a Bag/Hsc70 complex: convergent functional evolution of Hsp70 nucleotide exchange factors. Science *291*, 1553-1557.

Soti, C., Racz, A., and Csermely, P. (2002). A Nucleotide-dependent molecular switch controls ATP binding at the C-terminal domain of Hsp90. N-terminal nucleotide binding unmasks a C-terminal binding pocket. J Biol Chem *277*, 7066-7075.

Speno, H.S., Luthi-Carter, R., Macias, W.L., Valentine, S.L., Joshi, A.R., and Coyle, J.T. (1999). Site-directed mutagenesis of predicted active site residues in glutamate carboxypeptidase II. Mol Pharmacol *55*, 179-185.

Stanton, B.A. (1997). Cystic fibrosis transmembrane conductance regulator (CFTR) and renal function. Wien Klin Wochenschr *109*, 457-464.

Stebbins, C.E., Russo, A.A., Schneider, C., Rosen, N., Hartl, F.U., and Pavletich, N.P. (1997). Crystal structure of an Hsp90-geldanamycin complex: targeting of a protein chaperone by an antitumor agent. Cell *89*, 239-250.

Stirling, C.J., Rothblatt, J., Hosobuchi, M., Deshaies, R., and Schekman, R. (1992). Protein translocation mutants defective in the insertion of integral membrane proteins into the endoplasmic reticulum. Mol Biol Cell *3*, 129-142.

Strickland, E., Hakala, K., Thomas, P.J., and DeMartino, G.N. (2000). Recognition of misfolding proteins by PA700, the regulatory subcomplex of the 26 S proteasome. J Biol Chem *275*, 5565-5572.

Strickland, E., Qu, B.H., Millen, L., and Thomas, P.J. (1997). The molecular chaperone Hsc70 assists the in vitro folding of the N-terminal nucleotide-binding domain of the cystic fibrosis transmembrane conductance regulator. J Biol Chem *272*, 25421-25424.

Studer, S., and Narberhaus, F. (2000). Chaperone activity and homo- and hetero-oligomer formation of bacterial small heat shock proteins. J Biol Chem *275*, 37212-37218.

Sun, F., Hug, M.J., Bradbury, N.A., and Frizzell, R.A. (2000a). Protein kinase A associates with cystic fibrosis transmembrane conductance regulator via an interaction with ezrin. J Biol Chem *275*, 14360-14366.

Sun, F., Hug, M.J., Lewarchik, C.M., Yun, C.H., Bradbury, N.A., and Frizzell, R.A. (2000b). E3KARP mediates the association of ezrin and protein kinase A with the cystic fibrosis transmembrane conductance regulator in airway cells. J Biol Chem *275*, 29539-29546.

Swiatecka-Urban, A., Boyd, C., Coutermarsh, B., Karlson, K.H., Barnaby, R., Aschenbrenner, L., Langford, G.M., Hasson, T., and Stanton, B.A. (2004). Myosin VI regulates endocytosis of the cystic fibrosis transmembrane conductance regulator. J Biol Chem *279*, 38025-38031.

Tarun, S.Z., Jr., and Sachs, A.B. (1996). Association of the yeast poly(A) tail binding protein with translation initiation factor eIF-4G. EMBO J *15*, 7168-7177.

Taxis, C., Hitt, R., Park, S.H., Deak, P.M., Kostova, Z., and Wolf, D.H. (2003). Use of modular substrates demonstrates mechanistic diversity and reveals differences in chaperone requirement of ERAD. J Biol Chem *278*, 35903-35913.

Tharun, S., and Parker, R. (2001). Targeting an mRNA for decapping: displacement of translation factors and association of the Lsm1p-7p complex on deadenylated yeast mRNAs. Mol Cell *8*, 1075-1083.

Thrower, J.S., Hoffman, L., Rechsteiner, M., and Pickart, C.M. (2000). Recognition of the polyubiquitin proteolytic signal. EMBO J *19*, 94-102.

Travers, K.J., Patil, C.K., Wodicka, L., Lockhart, D.J., Weissman, J.S., and Walter, P. (2000). Functional and genomic analyses reveal an essential coordination between the unfolded protein response and ER-associated degradation. Cell *101*, 249-258.

Tsai, B., Ye, Y., and Rapoport, T.A. (2002). Retro-translocation of proteins from the endoplasmic reticulum into the cytosol. Nat Rev Mol Cell Biol *3*, 246-255.

Tusher, V.G., Tibshirani, R., and Chu, G. (2001). Significance analysis of microarrays applied to the ionizing radiation response. Proc Natl Acad Sci U S A *98*, 5116-5121.

Van Montfort, R., Slingsby, C., and Vierling, E. (2001a). Structure and function of the small heat shock protein/alpha-crystallin family of molecular chaperones. Adv Protein Chem *59*, 105-156.

van Montfort, R.L., Basha, E., Friedrich, K.L., Slingsby, C., and Vierling, E. (2001b). Crystal structure and assembly of a eukaryotic small heat shock protein. Nat Struct Biol *8*, 1025-1030.

Varga, K., Jurkuvenaite, A., Wakefield, J., Hong, J.S., Guimbellot, J.S., Venglarik, C.J., Niraj, A., Mazur, M., Sorscher, E.J., Collawn, J.F., and Bebok, Z. (2004). Efficient intracellular processing of the endogenous cystic fibrosis transmembrane conductance regulator in epithelial cell lines. J Biol Chem *279*, 22578-22584.

Vashist, S., Kim, W., Belden, W.J., Spear, E.D., Barlowe, C., and Ng, D.T. (2001). Distinct retrieval and retention mechanisms are required for the quality control of endoplasmic reticulum protein folding. J Cell Biol *155*, 355-368.

Vashist, S., and Ng, D.T. (2004). Misfolded proteins are sorted by a sequential checkpoint mechanism of ER quality control. J Cell Biol *165*, 41-52.

Vasudevan, S., and Peltz, S.W. (2001). Regulated ARE-mediated mRNA decay in Saccharomyces cerevisiae. Mol Cell *7*, 1191-1200.

Veinger, L., Diamant, S., Buchner, J., and Goloubinoff, P. (1998). The small heat-shock protein IbpB from Escherichia coli stabilizes stress-denatured proteins for subsequent refolding by a multichaperone network. J Biol Chem *273*, 11032-11037.

Vergani, P., Lockless, S.W., Nairn, A.C., and Gadsby, D.C. (2005). CFTR channel opening by ATP-driven tight dimerization of its nucleotide-binding domains. Nature *433*, 876-880.

Verma, R., Chen, S., Feldman, R., Schieltz, D., Yates, J., Dohmen, J., and Deshaies, R.J. (2000). Proteasomal proteomics: identification of nucleotide-sensitive proteasome-interacting proteins by mass spectrometric analysis of affinity-purified proteasomes. Mol Biol Cell *11*, 3425-3439.

Verschuure, P., Croes, Y., van den, I.P.R., Quinlan, R.A., de Jong, W.W., and Boelens, W.C. (2002). Translocation of small heat shock proteins to the actin cytoskeleton upon proteasomal inhibition. J Mol Cell Cardiol *34*, 117-128.

Vicart, P., Caron, A., Guicheney, P., Li, Z., Prevost, M.C., Faure, A., Chateau, D., Chapon, F., Tome, F., Dupret, J.M., Paulin, D., and Fardeau, M. (1998). A missense mutation in the alphaB-crystallin chaperone gene causes a desmin-related myopathy. Nat Genet *20*, 92-95.

Vilela, C., Velasco, C., Ptushkina, M., and McCarthy, J.E. (2000). The eukaryotic mRNA decapping protein Dcp1 interacts physically and functionally with the eIF4F translation initiation complex. EMBO J *19*, 4372-4382.

Voges, D., Zwickl, P., and Baumeister, W. (1999). The 26S proteasome: a molecular machine designed for controlled proteolysis. Annu Rev Biochem *68*, 1015-1068.

Wagner, B.J., and Margolis, J.W. (1995). Age-dependent association of isolated bovine lens multicatalytic proteinase complex (proteasome) with heat-shock protein 90, an endogenous inhibitor. Arch Biochem Biophys *323*, 455-462.

Wall, D., Zylicz, M., and Georgopoulos, C. (1994). The NH2-terminal 108 amino acids of the Escherichia coli DnaJ protein stimulate the ATPase activity of DnaK and are sufficient for lambda replication. J Biol Chem *269*, 5446-5451.

Walter, J., Urban, J., Volkwein, C., and Sommer, T. (2001). Sec61p-independent degradation of the tail-anchored ER membrane protein Ubc6p. EMBO J *20*, 3124-3131.

Wang, K., and Spector, A. (1996). alpha-crystallin stabilizes actin filaments and prevents cytochalasin-induced depolymerization in a phosphorylation-dependent manner. Eur J Biochem *242*, 56-66.

Wang, S., Raab, R.W., Schatz, P.J., Guggino, W.B., and Li, M. (1998). Peptide binding consensus of the NHE-RF-PDZ1 domain matches the C-terminal sequence of cystic fibrosis transmembrane conductance regulator (CFTR). FEBS Lett *427*, 103-108.

Wang, T.F., Chang, J.H., and Wang, C. (1993). Identification of the peptide binding domain of hsc70. 18-Kilodalton fragment located immediately after ATPase domain is sufficient for high affinity binding. J Biol Chem *268*, 26049-26051.

Wang, X., Matteson, J., An, Y., Moyer, B., Yoo, J.S., Bannykh, S., Wilson, I.A., Riordan, J.R., and Balch, W.E. (2004). COPII-dependent export of cystic fibrosis transmembrane conductance regulator from the ER uses a di-acidic exit code. J Cell Biol *167*, 65-74.

Ward, C.L., and Kopito, R.R. (1994). Intracellular turnover of cystic fibrosis transmembrane conductance regulator. Inefficient processing and rapid degradation of wild-type and mutant proteins. J Biol Chem *269*, 25710-25718.

Ward, C.L., Omura, S., and Kopito, R.R. (1995). Degradation of CFTR by the ubiquitin-proteasome pathway. Cell *83*, 121-127.

Wegele, H., Muller, L., and Buchner, J. (2004). Hsp70 and Hsp90--a relay team for protein folding. Rev Physiol Biochem Pharmacol *151*, 1-44.

Wiech, H., Buchner, J., Zimmermann, R., and Jakob, U. (1992). Hsp90 chaperones protein folding in vitro. Nature *358*, 169-170.

Wieske, M., Benndorf, R., Behlke, J., Dolling, R., Grelle, G., Bielka, H., and Lutsch, G. (2001). Defined sequence segments of the small heat shock proteins HSP25 and alphaB-crystallin inhibit actin polymerization. Eur J Biochem *268*, 2083-2090.

Wilson, T., and Treisman, R. (1988). Removal of poly(A) and consequent degradation of c-fos mRNA facilitated by 3' AU-rich sequences. Nature *336*, 396-399.

Wilusz, C.J., Wormington, M., and Peltz, S.W. (2001). The cap-to-tail guide to mRNA turnover. Nat Rev Mol Cell Biol *2*, 237-246.

Wong, B.R., Parlati, F., Qu, K., Demo, S., Pray, T., Huang, J., Payan, D.G., and Bennett, M.K. (2003). Drug discovery in the ubiquitin regulatory pathway. Drug Discov Today *8*, 746-754.

Wright, J.M., Zeitlin, P.L., Cebotaru, L., Guggino, S.E., and Guggino, W.B. (2004). Gene expression profile analysis of 4-phenylbutyrate treatment of IB3-1 bronchial epithelial cell line demonstrates a major influence on heat-shock proteins. Physiol Genomics *16*, 204-211.

Xiong, X., Chong, E., and Skach, W.R. (1999). Evidence that endoplasmic reticulum (ER)-associated degradation of cystic fibrosis transmembrane conductance regulator is linked to retrograde translocation from the ER membrane. J Biol Chem *274*, 2616-2624.

Xu, Y., Clark, J.C., Aronow, B.J., Dey, C.R., Liu, C., Wooldridge, J.L., and Whitsett, J.A. (2003). Transcriptional adaptation to cystic fibrosis transmembrane conductance regulator deficiency. J Biol Chem *278*, 7674-7682.

Yan, W., Schilke, B., Pfund, C., Walter, W., Kim, S., and Craig, E.A. (1998). Zuotin, a ribosome-associated DnaJ molecular chaperone. EMBO J *17*, 4809-4817.

Yang, H., Shelat, A.A., Guy, R.K., Gopinath, V.S., Ma, T., Du, K., Lukacs, G.L., Taddei, A., Folli, C., Pedemonte, N., Galietta, L.J., and Verkman, A.S. (2003). Nanomolar affinity small molecule correctors of defective Delta F508-CFTR chloride channel gating. J Biol Chem *278*, 35079-35085.

Yang, Y., Janich, S., Cohn, J.A., and Wilson, J.M. (1993). The common variant of cystic fibrosis transmembrane conductance regulator is recognized by hsp70 and degraded in a pre-Golgi nonlysosomal compartment. Proc Natl Acad Sci U S A *90*, 9480-9484.

Ye, Y., Meyer, H.H., and Rapoport, T.A. (2003). Function of the p97-Ufd1-Npl4 complex in retrotranslocation from the ER to the cytosol: dual recognition of nonubiquitinated polypeptide segments and polyubiquitin chains. J Cell Biol *162*, 71-84.

Ye, Y., Shibata, Y., Yun, C., Ron, D., and Rapoport, T.A. (2004). A membrane protein complex mediates retro-translocation from the ER lumen into the cytosol. Nature *429*, 841-847.

Yoo, J.S., Moyer, B.D., Bannykh, S., Yoo, H.M., Riordan, J.R., and Balch, W.E. (2002). Non-conventional trafficking of the cystic fibrosis transmembrane conductance regulator through the early secretory pathway. J Biol Chem *277*, 11401-11409.

Youker, R.T., Walsh, P., Beilharz, T., Lithgow, T., and Brodsky, J.L. (2004). Distinct roles for the Hsp40 and Hsp90 molecular chaperones during cystic fibrosis transmembrane conductance regulator degradation in yeast. Mol Biol Cell *15*, 4787-4797.

Young, J.C., and Hartl, F.U. (2000). Polypeptide release by Hsp90 involves ATP hydrolysis and is enhanced by the co-chaperone p23. EMBO J *19*, 5930-5940.

Younger, J.M., Ren, H.Y., Chen, L., Fan, C.Y., Fields, A., Patterson, C., and Cyr, D.M. (2004). A foldable CFTR{Delta}F508 biogenic intermediate accumulates upon inhibition of the Hsc70-CHIP E3 ubiquitin ligase. J Cell Biol *167*, 1075-1085.

Zeitlin, P.L., Diener-West, M., Rubenstein, R.C., Boyle, M.P., Lee, C.K., and Brass-Ernst, L. (2002). Evidence of CFTR function in cystic fibrosis after systemic administration of 4-phenylbutyrate. Mol Ther *6*, 119-126.

Zhang, F., Kartner, N., and Lukacs, G.L. (1998). Limited proteolysis as a probe for arrested conformational maturation of delta F508 CFTR. Nat Struct Biol *5*, 180-183.

Zhang, H., Peters, K.W., Sun, F., Marino, C.R., Lang, J., Burgoyne, R.D., and Frizzell, R.A. (2002a). Cysteine string protein interacts with and modulates the maturation of the cystic fibrosis transmembrane conductance regulator. J Biol Chem *277*, 28948-28958.

Zhang, S., Williams, C.J., Hagan, K., and Peltz, S.W. (1999a). Mutations in VPS16 and MRT1 stabilize mRNAs by activating an inhibitor of the decapping enzyme. Mol Cell Biol *19*, 7568-7576.

Zhang, S., Williams, C.J., Wormington, M., Stevens, A., and Peltz, S.W. (1999b). Monitoring mRNA decapping activity. Methods *17*, 46-51.

Zhang, Y., Michaelis, S., and Brodsky, J.L. (2002b). CFTR expression and ER-associated degradation in yeast. Methods Mol Med *70*, 257-265.

Zhang, Y., Nijbroek, G., Sullivan, M.L., McCracken, A.A., Watkins, S.C., Michaelis, S., and Brodsky, J.L. (2001). Hsp70 molecular chaperone facilitates endoplasmic reticulum-associated protein degradation of cystic fibrosis transmembrane conductance regulator in yeast. Mol Biol Cell *12*, 1303-1314.

Zhong, T., and Arndt, K.T. (1993). The yeast SIS1 protein, a DnaJ homolog, is required for the initiation of translation. Cell *73*, 1175-1186.

Zhu, X., Zhao, X., Burkholder, W.F., Gragerov, A., Ogata, C.M., Gottesman, M.E., and Hendrickson, W.A. (1996). Structural analysis of substrate binding by the molecular chaperone DnaK. Science *272*, 1606-1614.

Ziegelhoffer, T., Lopez-Buesa, P., and Craig, E.A. (1995). The dissociation of ATP from hsp70 of Saccharomyces cerevisiae is stimulated by both Ydj1p and peptide substrates. J Biol Chem *270*, 10412-10419.

Zou, J., Guo, Y., Guettouche, T., Smith, D.F., and Voellmy, R. (1998). Repression of heat shock transcription factor HSF1 activation by HSP90 (HSP90 complex) that forms a stress-sensitive complex with HSF1. Cell *94*, 471-480.